UNIVERSITY OF LONDON

IMPERIAL COLLEGE OF SCIENCE AND TECHNOLOGY

DEPARTMENT OF ELECTRICAL ENGINEERING

A POWER SYSTEM SIMULATOR FOR TRANSIENT STABILITY STUDIES

Thesis submitted for the degree of

Doctor of Philosophy in Engineering

by

Asif Mahmood Hassan

May , 1969.

ABSTRACT

A Power System Simulator has been developed which uses a network analyser and an analogue computer. This simulation is dynamic so that transient stability studies and automatic control investigations can be carried out.

With the growth in the size of power systems it is becoming increasingly difficult to achieve maximum economy and security by operating them manually. Automation up to various degrees is being applied at all levels of operation and more integrated schemes using process control computers are being developed.

As a result of these advances in automation the role of the operator is shifting from carrying out routine checks on the plant performance to monitoring and guiding the control action of the computers.

Before a new scheme is applied to a real system, a laboratory trial of it may give useful information to the designer and experience to the future operators. System

constraints, set by stability considerations, can also be determined with safety. Evidently the need arises for a system simulator in which all parts of the system are adequately represented.

Because of its importance, investigations have been concentrated on simulating a synchronous machine and associated regulating and governing systems.

The choice of the mathematical model was made by considering the need for economy in making and running the system simulator, the availability of data and the flexibility and speed of simulation to be achieved. Park's equations for the synchronous machine were simplified and found suitable as the basis of this mathematical model.

The simulator uses a network analyser of the direct impedance type working at mains frequency. The mathematical model chosen enables the machine to be represented as a voltage variable in magnitude and phase behind a fixed reactance. Rotor angle is defined as the phase of this voltage with respect to the system reference voltage. The magslip - I-pot combination conventionally used for generator

representation is driven by servo-mechanisms on command from the analogue computer. D. C. servo-mechanisms of high follow-up accuracy and rapid response have been developed and the wholly electronic instrumentation can respond to transient changes in 20 m-secs.

Overall accuracy is shown to be good by comparing the simulator performance with the solution of the equations of the mathematical model on a digital computer. Error in most cases is less than 3%.

Inadequacies of the mathematical model have been discussed with reference to the real system tests and studies of the works appearing in the literature.

It is found that this simulation technique promotes a clear understanding of the dynamics of the power system.

ACKNOWLEDGMENTS

The work described in this thesis was carried out under the supervision of Dr. M. J. Short. The author wishes to express his gratitude for his help and guidance at all stages of work, especially in organising the writing of the thesis. His encouragement of personal initiative and keen interest in the results the author regards very highly.

Many thanks are due to Mr. K. Patel for his valuable assistance, in developing many electronic devices.

Thanks are also due to Mr. Hardie for his help in laboratory work.

The author also appreciates the financial support of the Attock Oil Co. Ltd. (Pakistan Oil Fields), West Pakistan University of Engineering and Technology, Lahore and the Department of Scientific and Industrial Research (U. K.). Almost all the laboratory apparatus was purchased from the D. S. I. R. grant, which has made this work possible.

CONTENTS

		Page
Abstract		3
Acknowledgments		5
Contents		6
List of Symbols and Abbreviations		
CHAPTER 1		
INTRODUCTION		
1.1	Power System Operation	17
1.2	Manual Control in System Operation	18
1.3	Automatic Control	20
	1.3.1 National Control	20
	1.3.2 Grid Control Centres	23
	1.3.3 Generating Stations	26
1.4	Role of the Power System Simulator	30
1.5	Simulation Techniques	36
	1.5.1 Network Analyser	37
	1.5.2 Micro Machine System	38
	1.5.3 Analogue Computers	42
	1.5.4 Digital Computers	44
	1.5.5 Hybrid Simulators	47

1.6 Adopted Scheme for System Simulation 55

CHAPTER 2

SYNCHRONOUS MACHINE THEORY AND BASIC SIMULATION TECHNIQUE

2.1 Fundamental Synchronous Machine Equations 61

2.1.1. Vector Diagram for Balanced Steady State Operation at Synchronous Speed 69

2.1.2 Sign Conventions for the Generators 74

2.1.3 Vector Diagram for the Transient State 78

2.1.4 Constant Voltage behind Direct Axis Transient Reactance. 83

2.1.5 Variable Voltage behind Quadrature Axis Synchronous Reactance. 85

2.2 Elements of Power System Simulator 86

2.2.1 Network Analyser 86

2.2.2 Generator Units 89

(a) Magslip 89

(b) I-Pot 94

2.2.3 Load Units 97

2.3 Automatic Solution of Swing Equation for a Single Machine connected to an Infinite Bus-bar, through Two Parallel Transmission Circuits 99

2. 3. 1 Simulation of Inertia and Damping by using Acceleration and Speed Feed-back 103

2. 3. 2 Simulation of Inertia and Damping on the Analogue Computer 116

2. 3. 3 Design of Velodyne 117

2. 3. 4 Calibration of

(i) Inertia 122

(ii) Damping 127

2. 3. 5 Compenstion for the delays due to Power Measurement and Velodyne System 129

2. 3. 6 Checking the Calibration for Inertia and Damping 136

2. 3. 7 Check Problem 142

2. 3. 8 Accuracy and Flexibility of Simulation 149

2. 3. 9 Digital Computer Program 158

2. 3. 10 Summary 161

CHAPTER 3

SPECIAL PURPOSE EQUIPMENT

3. 1 Servo Amplifiers 162

3. 1. 1 Commercially Available Servo Amplifiers 163

3. 1. 2 Performance of Single Stage Cathode Coupled Long Tailed Pair 166

	3.1.3 Modifications of SA 61 Amplifier	167
3.2	Stabilised Power Supplies	170
	3.2.1 +350V, 750 mA.	171
	3.2.2 -250V, 60 mA	173
3.3	Constant Current Supplies for Armatures of Servo-motors	175
	3.3.1 1.5 Amps. Constant Current Supply	177
	3.3.2 0.48Amps. Constant Current Supply	181
	3.3.3 Heat Sinks	181
	Electronic Metering Equipment	185
3.4	Load Angle Measurement	186
	3.4.1 General	187
	3.4.2 Requirement of a Load Angle Meter	187
	3.4.3 Principle of Operation	189
3.5	Electronic Wattmeters	
	3.5.1 General	194
	3.5.2 I Cos ϕ Meter (Wattmeter 1)	203
	.1 Principle of Operation	204
	.2 Circuit Details	204
	3.5.3 Wattmeter 2	213
	.1 Principle of Operation	213
	.2 Circuit Details	215
3.6	Current Component Resolver	222

3.7	Voltage Measurement	222
	3.7.1 General	225
	3.7.2 Principle of Operation	
	3.7.3 Circuit Details	
	.1 Voltage behind the Machine Reactance	225
	.2 Machine Terminal Voltage	228
3.8	SQ-10 a Operational Amplifiers	231
3.9	Fault Relay	238
3.10	Network Analyser Impedance Unit.	243

CHAPTER 4

MORE ACCURATE SIMULATION

4.1	Including Transient Saliency	250
	4.1.1 I-Pot Position Control Mechanism	252
	4.1.2 Time Scaling	254
	4.1.3 Test Problem	262
4.2	Including the Effects of Variable Flux Linkages	266
	4.2.1 A Note on Per Unit (p.u.) System	268
	4.2.2 Test Problem	269
4.3	Automatic Voltage Regulators	269
	4.3.1 Proportional Voltage Regulators	271
	4.3.2 Test Problem	274

4.4	Governors	266
	4.4.1 A Simple Speed Governor	277
	4.4.2 Test Problem	281
4.5	Effects on Generator Stability Studies with Accurate Simulation	281
4.6	Faults near to the Synchronous Machine	287

CHAPTER 5

CRITICISM OF SYNCHRONOUS MACHINE ANALYSIS AND FULL SCALE TESTS

5.1	Need for Full Scale Tests	292
5.2	Comparison with Goldington Test	295
5.3	Synchronous Machine Theory with Damper Windings	303
5.4	Incremental Excitation due to Increase in Stator Current	308
5.5	Incremental Excitation due to increase in Field Voltage	312
5.6	Incremental Excitation under Slip Conditions	
5.7	Neglected Terms	316
5.8	Other Neglected Factors	322
	(a) Asymmetric Currents	322
	(b) Saturation	324

CHAPTER 6

CONCLUSIONS 327

6.1 Summary of Discussions and Conclusions 330

6.2 Suggestions for Improvements and Furthur Work

6.2.1 Damping Characteristics 337

6.2.2 Substitution of Electronic Amplitude Modulator for I-Pot Servo 338

6.2.3 Extensions 340

6.2.4 Load Representations 341

6.2.5 Induction Motors 344

6.3 Other Uses of the Simulator 351

6.3.1 Teaching and Training Aid 351

6.3.2 Self Balancing Load Flow Analyser 352

6.3.3 Dynamic Security Assessor 353

APPENDIX I 355

REFERENCES 363

LIST OF SYMBOLS AND ABBREVIATIONS

v	Instantaneous value of the voltage
$''$	Transformed Axis voltage
V	R.M.S. voltage
$\overrightarrow{V}$	Voltage vector
E	Electromotive Force
i	Instantaneous value of the current
$''$	Transformed Axis current
I	RMS current
$\overrightarrow{I}$	Current vector
r, R	Resistance
L	Inductance
l	Leakage inductance
L_m, M	Mutual Inductance
c, C	Capacitance
x, X	Reactance
z, Z	Impedance
ϕ	Flux
ψ	Flux linkages
t	Time
(t)	Function of time
p	Laplace's transform operator
(p)	Function in Laplace's operator

H	Inertia constant
K_d	Damping coefficient
δ	Load angle
f	Torque
w, w_s	Angular speed (synchronous)
ω	Instantaneous angular speed
k, K	Constant
s	Slip
Ω	Ohm
$\mho$	Mho
τ, T	Time constant
c/s, Hz	Cycles per second
J	Inertia
G_m	Amplifier conductance
ξ'	Incremental excitation
n	Gear ratio
j	Imaginary quantity

Subscripts

d	Direct axis quantities
q	Quadrature axis quantities
o	Zero sequence quantities
a, b, c	Phase quantities
e	Electrical quantities
m	Mechanical quantities

i, I	Induced quantities
1, 2	Primary and secondary quantities
g	Tacho-generator or governor quantity
ps	Steam power
pe	Electrical power
k	Damper windings quantities
a	Armature quantities or accelerating quantities

Superscript

'	Transient values or increments
''	Subtransient values

Abbreviations

A.V.R.	Automatic Voltage Regulator
C.E.G.B.	Central Electricity Generating Board
N.A.	Network analyser
I-Pot	Inductive potentiometer

For anydeparture from these notations or wherever duplication has appeared in this list, the symbols are locally defined.

CHAPTER 1

INTRODUCTION

This chapter briefly reviews the rapid advancements which recent years have seen in the operation of a large power system. As more and more integrated control is being developed, the operator's task is shifting from routine checks on the plant performance to feeding into the controller the limits within which the system has to operate and to take over the control in case of emergency. Before any control scheme is put into field application a laboratory trial is essential where a simulated power system is controlled. Also the operational limits can be derermined in the laboratory. In the later part of the chapter the role of the simulator is discussed and the broad objectives for an adequate simulator are laid down. Effort has then been made to discuss the salient features of the simulation techniques which have been developed over the past twenty years. In the end, some important aspects of the power system simulator, which is the subject of this thesis, have been included.

1.1 POWER SYSTEM OPERATION ;

The operation of a large power system under a unified control requires one to predict the load demand at all times and then allocate generation to all the stations within the system to meet this demand. This allocation is made to keep the cost of generation minimum and the system secure. A system is considered secure when loss of any one item in the generation sources and transmission network does not cause loss of load or tripping of any other item due to subsequent overload. Apart from the criteria of ECONOMY & SECURITY, the system organisation has the obligation to maintain the frequency and the voltage within the statutory limits.

Different tasks in the operation can be listed as follows :

(i) Controlling the available generators and interconnecting networks to meet the existing and the anticipated demand.

(ii) Governing of the turbines to maintain the correct frequency and suitable sharing of the loads.

(iii) Regulating the excitation of the alternators

to maintain correct voltage and suitable sharing of VARS.

(iv) Continuous assessment of and safeguarding the ability of the system to withstand faults.

(v) Systematic loading of the plant to achieve maximum economy of operation.

The order of priorities in ordering how generators should be loaded is system security, maximum economy, maintenance of frequency and voltage.

1.2 MANUAL CONTROL IN SYSTEM OPERATION :

For the facility of organisation the tasks listed above are performed at several different levels. This division applies both to manual as well as automatic control. The C.E.G.B. in England and Wales has three hierarchical levels; National Control Centre, Area Grid Control Centres and the Generating Stations. A detail of the control arrangements and organization involved in the Central Electricity Generating Board (C.E.G.B.) system is given by Short. (Ref. 1) It has been reported in a recent paper by Pulseford (Ref. 2) that to relieve the congestion in communication and display at the area control level the task of at least some of these centres will be divided into two or three sub-centres in

1969. These centres will be known as ' District Control Centres'. Control is achieved for the most part manually -- on the basis of information fed by telemetric links and telephone instructions, and also by the action of governors and automatic voltage regulators. Estimates of the expected loads are passed from the regional or area grid control centres to the national control along with the incremental and decremental cost of unit generation. The national control orders inter-area transfers for the reasons of system security and of national minimum generating cost. The grid control centres then order plant to be ready for loading and give instructions for loading it to give the most economic generation with-in the area, taking the inter-area transfer into account and keeping the system in the area secure. In order to meet the changing load imposed by the consumer on the supply system, provisions must be made some hours ahead to meet the major changes of the loads; boilers must be brought up to temperature and pressure; turbine generators warmed up and then loaded up at a controlled rate. Some, at least, of the generating sets running must be capable of moment to moment changes of output, if load is to be matched by generation while keeping the frequency constant.

1.3 AUTOMATIC CONTROL :

For a large, complex and expanding system like the C. E. G. B. the necessity of automatic assistance was realised quite long ago and the study of the various aspects of automatic control was well in progress in late 50's and early 60's. Recently automation started appearing at different levels in different forms. In the following sub-sections a brief review of progress is given.

1.3.1 NATIONAL CONTROL :

At the national control level security assessment is the only field which has received attention for automation. Around 1964-65 a mixed analogue and digital equipment called a super-grid security assessor was installed which has recently been replaced completely by a digital computer security assessment programme.

The Supergrid Security Assessor is an analogue model of the network and a small special purpose digital computer fed with on line information as regards switch positions and actual

line flows. In the analogue model, resistors proportional to the line reactances are used. The configuration of the lines in the model can be switched by means of relays to make it the same as that of the real grid system. The power flow conditions are not reproduced in the analogue, instead it carries currents representing power flows following the loss of a line in the super grid system. To simulate the outage of a line, the corresponding line in the analogue is open circuited and a fixed current is injected in series with the break. The distribution of the injected current among the lines will represent proportionally. the distribution of power in the grid following a line outage. Invoking the principle of superposition, the total new power resulting from the redistribution due to loss of the line is calculated. The value of this power flow is compared with 75% and 100% of the preset limits and information displayed if either figure is exceeded. The display is in the form of semigeographical lay-out of the major lines of the network and overloads shown in the form of coloured lights. Printed information is also available. This consists of a list of those lines which if lost will cause overloads, lines which will be overloaded, and power flows in those lines.

The assumptions of the linearity of the system on which this assessor is based are met only under the conditions of

small disturbances on a stable system. The limits are based on thermal ratings. Thermal limits and system linearity are invalid bases for security assessment when the system is being operated near the synchronous stability limit.

The assessor uses the information about network and loading configuration prevalent at the instant when a security check is being made. There is no provision for predicting the network configuration and load a few hours ahead.

Assessment of the system security by a digital computer at the national control level of the C. E. G. B. is an extension of the programme primarily developed for use at the Grid Control Centres. This programme solves D. C. approximations of the A. C. network equations. Loss of a single circuit and double circuit line in the super-grid network is considered to estimate a new power flow pattern. Security constraints are the upper limits on the permissible real power flow in each line.

Looking ahead, a computer at the national control level will take up the job of inter-area transfer for economy ...

and making the security checks. This will be based on the expected loads and network configuration supplied by the computers at the grid control centres. This would leave the annual co-ordination of the fuel allocation and plant maintenance and switching activities to be performed manually.

1.3.2 GRID CONTROL CENTRES :

The C.E.G.B. has very recently completed a four and a half year experiment in which 31 generating sets in the S.W. region were controlled from the grid control centre at Keynsham. The details of this scheme have been discussed in a series of papers at a colloquium arranged by the Institution of Electrical Engineers. (Refs. 3, 4, 5, 6, 7, 8)

At the start of the introduction of automatic control at the grid control centre, only automatic load despatching has received priority. This is in the area where benefits in terms of improved security and possibly economic operation were most likely to accrue. Automatic switching of the network had no obvious advantages and presented several complex

problems for its successful operation. Similarly, voltage control has been excluded, as the optimisation of the reactive power flows is not considered rewarding.

The control aspects at the present moment entail predicting future load demand, preparing and revising a schedule of target output for minimum operating costs and instructing the plant to give such outputs in accordance with the schedule.

Automatic load prediction is the most difficult and at the same time most rewarding aspect of automation. The load prediction is made using the past records including those of the last few hours and the past three months. Other factors such as temperature, day light, T. V. programmes, day of the week etc. etc. may also be added if required. A man can predict only peak loads for certain periods but with the help pf the computer prediction can be made at very short intervals and three to four hours in advance. Therefore, closer matching of the economically despatched load to the actual demand, than was possible with manual efforts, can be achieved.

Arising from the load prediction is plant ordering - warning to the stations to get boilers and sets ready for loading. Generating schedules are prepared and instructions are passed on to the individual generating sets. Complex calculations can be made, given the information about cost of generation at each station and of losses in the lines, to determine how the predicted load can be supplied at the lowest cost.

Security is tackled by the computer looking at the system as it is to be half and one hour ahead and checking the effect of removing each line and each generator in turn to show whether it will result in an insecure system. Any element which will cause overloading of any other is displayed and the appropriate action has to be decided by the operator. This was initially done by changing the generator limits and asking for a new calculation.

Control of frequency is achieved by the frequency control loop on the generator.

1.3.3 GENERATING STATIONS :

The computer at the grid control centre carries out generator scheduling, from the economic point of view, every half hour and five minutes. The scheduling is completely worked out for the moment which is $\frac{3}{4}$ hour ahead. The security of the system is also checked. If the security is satisfactory the computer eventually predicts the load for five minutes ahead and works out the generating schedule that will meet it. At the five minutes interval it sends instruction to the machine controller giving the MW output that will be required at the end of the five minute interval. When the controller has received the instructions, it compares the value demanded for five minutes ahead with the current generation and interpolates to give a linear rate of change of load between those times and thus provides continuous loading instructions. Actual generation and demanded generation are compared from moment to moment and pulses passed to the speeder motor to change the steam valve position to control this. The half hour estimates of loading are also fed to the machine controller and should the five minute instruction fail to reach the

machine controller, a linear interpolation based on a half hour estimate can be inserted. An auxilliary control loop detects frequency deviation from 50 c/s. The frequency error is converted into the power error required to maintain a certain frequency - power droop characteristic, and fed into the power error channel. A number of protective features, like a rate limiter and a device to detect the sticking of the governor valve, are also included. The power error is finally converted into a series of pulses which are passed on to speeder motor and the control is excercised through the normal hydraulic servo-system. The machine controller is an electromechanical system and has been designed with the consideration that the control requirements are kept to the minimum and that it should penetrate the minimum distance in to the power station. The equipment seems to be quite complex and was not trouble free.

In any future installation the machine controller will take the form of a small special purpose digital computer or on a large sized station only a few extra sub-routines on an already installed computer for control purposes.

Whilst to date the various generating unit closed- loop controls have not been sufficiently well integrated to be classed as comprehensive, the situation is changing rapidly. Closed - loop systems are being developed which can adequately control a boiler/turbine unit over a wider load spectrum than was previously possible and can control the pressure raising procedure on a boiler. The rapid development in power generation coupled with parallel developments in instrumentation, electronics, data reduction and data processing, has given rise to a reappraisal of operational and control philosophy and methods of increasing plant efficiency. The rethinking has led to the concept of a comprehensive fully integrated scheme for the automatic supervision and control of major generating sets. The plant is continuously supervised by a system which is always alert and capable of instant action. Precise control and supervision of the operational procedure eliminates the possibility of error through human fallibility and also increases the plant life. With more routine tasks being performed by the computer the operating staff can concentrate on optimum operation and rapid correction of

abnormalities and faults. Thermal stresses and shocks to the vulnerable parts of the plant are minimised by constant repeatable start up procedures, which lead to better and more consistent machine performance and to a reduction in outage and maintenance periods.

The 4x500 MW Fawley Station, due to start generating sometime this year, will have four process computers for the four sets. The direct communication of computers with the plant consists of 1200 analogue inputs and 1750 digital inputs. There are 900 outputs from the control loops. The computer has a self checking routine for its own health and the correct functioning of the data and control circuits. The computer controls the alarm display as well.

In case of failure of the computer, the plant can be controlled manually, and for this purpose the control system is duplicated.

On command to start up from cold, the first contacts are closed by the computer to start pump motors and

the like, and as each part of the plant responds so the signals to the computer modify. If the correct logic sequence is followed, the computer initiates the next control operation and so on until the command has been obeyed.

If a fault develops, or if some part of the plant does not respond to a command, the computer will digress to a subroutine which will restore conditions or shut down all or part of the plant. The display system keeps up a running report of the plant and so presents to the operator only that information which he needs at a given instant.

Generating stations have up till now received the maximum priority in automatizing the control and operation of the system. In future, we will see more and more comprehensive schemes developed on the lines explained above.

1.4 RCLE CF POWER SYSTEM SIMULATOR :

As power systems are growing in size and complexity, economic operation is becoming impossible

to achieve manually. In the recent past many new automatic control devices and computational aides have been provided to achieve this and also to relieve the operator of routine tasks.

In a fully computerised control the role of the operator is to monitor the computer's control action, to guide its actions by feeding it the appropriate data, and to use it as an aid in studying problems which require an element of manual decision.

The data referred to above consists of constraints on the generators and the network, i. e. maximum and minimum permissable output of each station, maximum possible rate of increase or decrease of each station, and maximum spare capacity. The network constraints are the limits on the real power flow.

Before a new control scheme is applied to the real system a laboratory trial of it may give very useful experience although the ultimate worth of any scheme can only be assessed in the actual field trials. Also the operational

limits, like maximum rate of loading, can safely be determined on the laboratory model.

As the new control devices are becoming operative the study of synchronous machine stability is also needing reappraisal. The old operational chart providing for a 10% stability margin might have to be changed.

More integrated control of turbine and boiler may increase the capability of the alternator to pick up load more rapidly than was possible before. Under such circumstances there may be a possibility of revising the policy of providing a very large generating capacity only as a spinning reserve.

Preliminary investigations of applying a power and a frequency control loop to the synchronous generator at Imperial College were done on the analogue computer and are reported in detail in Ref. 1. The synchronous machine in this study was only represented by a second order complex transfer function relating electrical output to the mechanical output from the prime mover. No provision was made for the representation of electrical quantities like voltages, currents and power factors.

In this method no interconnection between the generators was possible. Need arose for a more comprehensive machine representation.

Before different techniques for simulating a power system are reviewed it will be in order to lay down the major objectives in the light of what has been said above.

The model should be able to simulate the system statically and dynamically so that studies of transient stability and automatic control investigations, relevent to load/frequency control, load despatching, system optimisation, voltage/VAR control, can be carried out.

Adequate representation of every part of the system - boiler, governor, valves, turbine, machine electrodynamics, voltage regulators, transmission network and load characteristics, is needed.

Flexibility in simulating significant parameters of all the plant items is most desirable as this will allow different types of turbo-generator designs to be represented in a composite system.

The model should be suitable for extension to a multi-machine system. Although during the initial investigations an infinite busbar reference is very helpful, the model should be ultimately capable of running free of the fixed references and follow variations in frequency according to the deficiency or excess of total generation over total load.

An easy method of setting up the initial conditions is very desirable.

The model should have the same time scale and frequency as the full scale system. This will enable designers to make interface equipment between the model and the control computer very similar to the actual. For a fully computerised control the efficacy of the computer routines in monitoring all the points and issuing a correct instruction can only be judged when the simulator is working on real time.

The choice of the mathematical model for the machines on the system will ultimaltely determine the overall accuracy which can be achieved on a simulator. It is clearly

impracticable if not impossible to include in the simulation all the details of the component parts. The passion for accuracy has to be balanced against economy in making and running the simulator on the one hand and the avilability of data on the other hand. Since the behaviour of the synchronous machine is of utmost importance in any study the present investigations are restricted to the synchronous machine and the associated regulating and the governing system. Some effects, if they are truly negligble, are to be excluded from representation completly. Simplification and approximation have to be adopted in those where the calculations are very difficult to make or when complex or expensive analogue components are needed. Some effects have to be approximated if all the data required for an accurate representation is not available. Whatever the choice of the mathematical model, it is desirable to keep the target accuracy of the component parts of the simulator as near to the 1% figure as possible. The deficiencies in the mathematical model ultimately have to be made up by comparison with actual full scale tests and the requirements which will finally be determined from the economic implication of certain types of studies. Simpler mathematical models can be used for example,

when a simulator is needed only as a teaching or training aid and for testing a computer programme for control purposes. When optimisation in economic operation is limited by stability considerations, need arises for more accurate determination of the stability limits. This would require the overall error in the simulation to be less than 1 %. This may require very sophisticated mathematical models or adjustments in various parameters to bring the individual machine performance as near as possible to the results obtained from actual tests, if available, when subjected to various types of disturbances.

1.5 SIMULATION TECHNIQUES :

Because of the difficulties of tests on an actual system and the very complex computations required in the case of a purely theoretical approach, engineers have been developing system simulators for design and development studies. The following sections will briefly review the techniques and their relative merits and the particular area of investigations where these are most useful.

1.5.1 NETWORK ANALYSERS :

Before large sized digital computers became available, network analysers were recognised to be very important tools for studies related to the planning, modification and extensions of the power system. Initially, the D.C. network analyser was generally considered to be quite adequate, and was very cheap to construct, but it very quickly was replaced by A.C. analysers as there was no provision for representing the relative voltage phase difference of the generating sources on a D.C. network analyser, and study of the problems of stability required both the magnitude and phase for complete representation.

The network analyser represents the transmission system by interconnections of the equivalent circuits of their component parts with all the voltages, currents and impedances converted to values which are proportional to the actual values. The representation is steady state. Generally only the balanced conditions are considered and so a polyphase system is represented by an equivalent single phase system. For studies relating to unbalanced faults application of

symmetrical components theory reduces the system to an equivalent single phase, but with an appropriate shunt at the point of the fault. At the area control levels, network analysers are still quite widely used for load flow studies.

The network analyser gives an accurate, very flexible and most economic representation of the transmission network. For transient stability studies the network analyser is a useful tool for determining the power output of each generator on the system. The generator representation is usually simplified to a constant voltage behind the transient reactance and numerical techniques of integration are used to solve the rotor swing equation. (see also section 2.1.4). The rotor settings are then made manually.

1.5.2. MICRO - MACHINE SYSTEM :

Micro machines are specially designed alternators and the guiding design principle is to get all the parameters on p.u. basis same as on the actual full scale system. The parameters simulated are synchronous and transient reactances and time constants, resistances of all the circuits and

the inertia constant. A micro-alternator is bigger in physical dimensions than an ordinary machine of similar ratings. This is done to keep p.u. resistance low. The available area for copper on the rotor is limited and to make the field time constant equal to that o f the bigger machine an auxilliary feed back loop, ' Time Constant Regulator,' is used, which compensatesfor the resistance. The arrangement is fully described by Alford. (Ref. 9)

The inertia constant can be changed by mounting different fly-wheels.

For transmission lines, air cored reactors and shunt capacitors in nominal $\overline{\Pi}$ configuration are used. The micro alternator is driven by a separately excited D. C. motor. Very recently the armature has been supplied from a Thyristor bridge which use s speed signals to control the firing angle s to simulate the turbine torque - speed characteristics.

The power system laboratories at Imperial College have two micro alternators with changeable rotors to provide a range of parameters. A resume of micro-machine studies at I. C. is given by Adkins. (Ref. 10) A more recent

installation includesa micro alternator with divided rotor windings and a specially designed induction motor which may be called a micro induction-motor.

Developments in power system design studies with the help of micro-machines in the Soviet Union are described in another paper by Dr. Adkins. (Ref. 11)

Micro-machines provide the most realistic simulation techniques and even help to formulate the exact mathematical model for the generator.

The micro-machines have been found to give a higher loss torque compared to that calculated during a short period just after the fault. (Ref. 12) This has been attributed to the slow response of the time constant regulator loop. (see section 5. 7) Work is being done to replace the present scheme, which includes a D. C. exciter with split field, by a completely electronic scheme.

The eddy currents effects in the solid turbine generator rotor are very poorly simulated by a solid rotor of

a micro machine., (Ref. 13) because this phenomenon is so much dependent on the physical dimensions. The same is true of the saturation characteristics. Micro-machines in U.S.S.R. are of 30 KW rating compared to I.C. or French machine rating of 2 KW. The Soviet machines, are, therefore, likely to simulate eddy currents and saturation effects more near to those in large machines.

In those areas of operation of the synchronous machine where either the detailed knowledge is not available, or the available analytical techniques cannot take into account the complexity of the equations formulated, a micro-machine system is the only tool available. Also, where the risks involved in the full scale tests in terms of damage to the equipment are high, a micro-machine system can help to assess the behaviour of a large machine and protective devices can be designed.

A micro-machine system is not very flexible where a large system using plants with widely different characteristics and parameters is to be simulated. Cost of the machines as well as that of the auxilliary equipment is very high. In a large sized micro-machine system the difficulties and hazards encountered in operation under abnormal conditions are almost of the

same magnitude as the actual system.

1.5.3 ANALOGUE COMPUTERS :

Once the mathematical equations describing any physical system or process have been formulated and if the equations are such that the classical methods of solution are not applicable because of non linearities, analogue computers can be employed.

When the physical system can be divided into several interconnecting sub-systems, each of which can be defined seperately as a mathematical equation or equations, the analogue computer offers a great advantage in enabling several variables to be monitored simultaneously. When repeated solutions of the same set of equations are required with some or all the parameters changed analogue computers lend speed, ease and economy. The most suitable application of the analogue computer is for the solution of integro-differential equations with time as an independent variable and most of the co-efficients as constants.

The synchronous machine equations when expressed in Park's transformed variables are amenable

to solution by analogue computers, (Refs. 14, 15, 16) both in the simplified form or in full detail. (Ref. 17) Thermo-dynamics of the boiler turbine system, governor equations and various elements in the automatic voltage regulators can be included with great ease and flexibility. Non-linearities like dead bands and limits can be included quite easily. Analogue computers have been widely used for studies of the effects of AVR's and Governors. (Ref. 18) The equations for the transmission lines have also to be converted in to the axes quantities. When a multi-machine case is considered interconnections (Ref. 19, 20) present the biggest obstacle in attempting to analyse the system on the analogue computer. Equations for every machine in the system are written within its own reference frame (Direct and Quadrature Axes) and then a common refrence frame has to be selected to which all the machines must be referred. The transformation from one reference frame to the common requires the use of four sine and four cosine function generators for each machine.

Apart from considerable expense on account of the function generators, solution of the network equations presents considerable difficulties due to oscillations in the loops.

1.5.4 DIGITAL COMPUTERS :

Digital computers offer the most flexible and , in accuracy, unparalleled, techniques of simulating any physical system which can be described in mathematical or even in numerical or graphical form. Digital computers are being used intensively for a wide variety of power system problems.

Early studies of the transient stability problem (Refs. 21, 22, 23, 24, 25) on the digital computer go through the same computational steps as on a network analyser and hand calculations. A system load balance is first obtained using the digital load flow programme. (Ref. 26) Following this loads are automatically converted to fixed impedances and transient reactance is inserted between the bus representing the generator terminal voltage and a new bus. Initial components of these voltages at these new buses are calculated on the basis of generator reactance and terminal conditions determined from the load flow studies, and acceleration constants calculated from the moment of inertia of each machine are read into the computer.

Following a system disturbance or a switching operation involving a change in the acceleration of one or more of the generators or a loss of generation, a new system load balance is established. This is followed by numerical integration for the solution of the equation of motion of the machine rotors to determine the change in the angle during a small time interval. The voltage angles behind the transient reactances are then adjusted in accordance with this calculation, (the voltage magnitude being held constant) and a new load balance is obtained. This procedure is continued, alternating between load balance and the calculation of the change of angle. As the nature of the system changed it was considered desirable to accept the limitations of this approach because of the simplifying assumptions involved. More recent digital computer programmes(Ref. 27, 28, 30) included the effects of flux decay, transient saliency, automatic voltage regulators and governors. Approximate methods were developed to include the D. C. braking torque and saturation. These techniques are all oriented towards a network analyser approach.

Still more recently digital computer programmes have been developed (Refs. 29, 31) which are

more closely based on Park's equations and provide a very detailed representation of synchronous machines. The passion for developing digital computer simulators at the present moment is limited because all the data is not available and the accurate representation of eddy current damping effects is very difficult. (see section 5.1.) Even when simplified digital computer simulations techniques, discussed by Olive (Ref. 27) and Day and Parton (Ref. 38) are applied to a large system, the computational process proves to be quite slow largely because of the serial nature of the digital computer operations.

A simulation technique which makes it possible to solve the equations for every part of the system simultaneously and continuously has many attractions for studies involving control by a small process control computer. This type of control requires many points to be monitored simultaneously and the control instructions so adjusted as to get correcting action within the most desirable time limit.

1.5.5 HYBRID SIMULATORS :

The idea of coupling some computing aid to the network analyser for solving the electro-mechanical differential equation of the synchronous machine goes back to the time when the network analyser installation became popular for load flow and advanced planning studies. The problem is not one of concept but of constructing instrumenting and computing systems which would fulfill the operation and economic requirements of desired N.A. services.

Mortlock (Ref. 32) describes the use of potentiometers for carrying out the steps in the numerical integration and how the angle settings are done manually. Watkins (Ref. 33) described an automatic computer which performed all the operations in the step by step method automatically. Power was measured by watt-meter which produced a signal proportional to the power. Increments of angle were calculated by a computing device and a summator gave the angle to be set on the computer.

A paper by Adamson, Barnes & Nellist (Ref. 34)

described the method of construction and mode of operation of an automatic step by step computer. The watt-meter is a dynamometer type but a servo is so arranged as to provide the moving coil a torque restoring its position to the null conditions. The servo-mechanism also drives a potentiometer which gives the measure of the electrical power output. A combination of transmitter and differential magslip are connected in the form of summators and perform the integration required as well as setting the magslip rotor of the network analyser generating unit. The watt-meter is common to all machines and a master controller connects this wattmeter in turn to control other operations sequentially.

Boast and Rector(Ref. 35) designed a special purpose computer in which the analogue of the swing equation is set up by an L-R-C circuit in which the charge on the capacitors is analogous to δ (generator load angle), and L and R to inertia and damping coefficient. Constant mechanical input power is represented by a constant voltage but the output power is given as a function of δ by photoformer. The relationship between the output power and δ is obtained from

the network analyser as also the conditions before the fault.

Kaneff (Ref. 36) developed a simulator in which a machine unit is a variable frequency oscillator. Under steady conditions its frequency is synchronised to a Master Oscillator at 10 Kc/s. The voltage to represent the machine (voltage behind the D-axis transient reactance) is set at the output stage of this oscillator. The operational principle is that during a disturbance the power supplied by the prime-mover must be equal to the electrical power output plus the power going into or taken from the machine rotor. A wattmeter measures the electrical power output and a differential amplifier controls the flow of energy into an energy store. This energy store is a condenser and the stored energy is proportional to the square of the voltage on the condenser. The energy stored in the machine rotor is proportional to the square of the instantaneous frequency and by analogy the voltage across the condenser represents the instantaneous frequency. The control of frequency in the machine simulator is obtained from a reactance tube in which the control of frequency proportional to the signal applied to the control grid can be obtained. The oscillator under steady conditions is to be highly stabilised and

a very sophisticated synchronising circuit was used. Multi-electrode valves were used for multiplication of voltage and current even for a simple case in which voltage is kept constant. The angle metering circuit, strictly speaking, records the sine of the angle. Kaneff recognised the difficulties of synchronising to a master oscillator and suggested a phase modulation process in which separate machine oscillators will not be needed.

A second paper by Kaneff (Ref. 37) used the same operational principle as explained above but the control of frequency was obtained from a velodyne circuit driving a magslip unit. The wattmeter in this case is a special three element dynamometer type giving a torque proportional to accelerating torque. Three elements respectively produce torque proportional to mechanical, electrical and rate of change in the stored energy. The deflection of the shaft is converted to a D. C. voltage by photo-electric devices.

A paper by Shen and Packer (Ref. 38) mainly concentrated on making an electrical analogue for

studying hunting phenomena but also suggests the principle of cascaded phase shifters for machine representation. This consists of a number of R-C phase shifters but resistance is taken from the plate characteristics of a vacuum tube in which case resistance can be changed by applying the potential to the control grid. To avoide non-linearities a phase shift of 30° is obtained from one circuit.

Shen and Lisser (Ref. 39) developed this further and reported a machine simulator. The power measurement was done by using the square law portion of the curve of anode current - grid voltage characteristics. Recording of the swing curve was made using intensity modulation on a CRO.

Beckey and Shott (Ref. 40) used mechanical integrators for solving the swing equation and setting of the magslip rotor but the power from the N.A. was measured on an ordinary wattmeter and the needle reading was converted into proportional shaft movment manually.

Van Ness (Ref. 41) proposed rotor angle control by means of a precision servo-mechanism and a wattmeter which gives a D. C. signal proportional to electrical output. His wattmeter used a wave chopping principle to measure the current component in phase with the voltage. Filters had to be used causing delay in the power measurement and the simulator had to work on a slower time base.

Van Ness and Peterson (Ref. 43) later designed a fully electronic simulator. A phase modulation circuit ' Phantastron ' was used. This circuit receives pulses and sends them out after a delay which can be continuously controlled.

Adamson, Barnes and Nellist (Ref. 34) in the second half of their paper suggested a direct analogue of the alternator driven by a velodyne circuit and used a power measuring technique similar to one used by Van Ness.

Corless and Aldred (Ref. 42) also designed an electronic power system simulator which gave the facility

of both amplitude as well as phase modulation. Phase modulation is obtained by a phantastron and amplitude modulation from conventional envelope modulators.

Dineley's (Ref. 43) computer also consists of high frequency oscillators and phase and amplitude modulation. This paper provides no details of the modulation techniques but these are likely to be similar to those of Corless and Aldred.

Kusko and Heller (Ref. 44) produced a generator simulator in which the acceleration power was measured as the speed of the watt-hour meter disc. The speed of the disk is picked up by photo electric devices and a servo-mechanism sets a variac so that variac output is proportional to the number of revolutions of the disc. This voltage is fed into another watt-hour meter the current coil of which is fed from a constant current source. Another servo-mechanism controls the shaft movement of the magslip proportional to the number of revolutions of the disc on the 2nd watt-hour meter. The simulator's five minutes are equal to one second on the actual system.

Richardson and Wane (Ref. 46) applied servo-mechanisms to the Bonville Power Administration Network Analyser, in which the magslips could be run continuously by velodyne circuits to change the frequency in sympathy with the excess or deficiency of generation and individual governor characteristics. The governor consisted of a simple exponential lag function with a gain setting for varying the droop. The simulator time was 120 times slower than the real time.

Bain (Ref. 47) developed a simulator which is similar to that of the Bonville Power Administration but he later replaced the generator unit by an electronic oscillator with variable frequency. A signal proportional to the change in the rotor speed following a disturbance is obtained from the analogue computing amplifier which is then used to control the speed of the magslip or in its modified form, the frequency of the variable frequency oscillator. These controls, however, are both open loop and the accuracy of the system in following up the command signal can only be poor. The variable frequency oscillator in the model is Wien-bridge type and the variation of the frequency is obtained by switching portions of the resistive branches in and out of the bridge circuit. The pulses controlling

the switching in-and-out period are'mark-space' modulated by the control signal. The multiplier used for power measurement uses the ' mark-space ' modulation of the square pulses proportional to one signal and amplitude modulation proportional to the other signal. Signal proportional to the real power output of the generator can only be obtained after filtering the multiplier output. Bain's model is only suitable for studies of events,for example, load scheduling and frequency control, which take longer than 5 to 10 seconds and cannot simulate fast disturbances; in fact the control loops have been heavily damped with the deliberate intention of suppressing transient instability among the generators.

1.6. ADOPTED SCHEME FOR SYSTEM SIMULATION :

Pending developments in computer graphics, a network analyser is the only available tool to give a physical feel of the behaviour of the network. Combined with economy and flexibility it is evidently the best choice for basic investigations.

Auxilliaries to the turbo-generator, such as

AVR and Governor, as also the thermodynamics of boiler and turbine unit, could be best represented by cascaded simple transfer function blocks for which the analogue computer is most suitable. This gives ease of programming and flexibility in changing the parameters.

The analogue computer can also provide the control signals to the servo-mechanisms.

Network analyser frequency of 50 c/s and the simulation of the dynamics in real time were considered desirable features (see section 1.4). At this frequency a conjugate analyser is more economic and I.C. Power Systems Laboratory possessed one, but the distortion on the current wave was considerable. (see section 3.10) A direct analyser was therefore used and for the usual Q-factor of aerial lines was not found too difficult to design.

For solving the electro-dynamic equations of the machine, an analogue computer is used in conjunction with D.C. servo-mechanisms driving the magslip - I-pot combination used on the analyser for generator representation. The phase modulation processes described above (section 1.5.5) are

discontinuous and therefore network analyser frequency has to be kept high compared to the rate of change of phase angle. Phase shifting by cascaded resistance tube introduces distortion and the output of the phantastron circuit is square wave form. Filters are, therefore, used to extract the fundamental frequency voltage wave. In the adopted scheme the magslip is driven by velodyne servos and the arrangement can give smooth and continuous phase modulation. The speed of response required is well within the capability of the electro-mechanical servos for an inertia representation of 3 to 5 seconds of H-constant.

Amplitude modulation from the I-pot position control presents considerable difficulties because of the slow response speed coupled with the iterative nature of the solution for the machine voltage equations (see section 4.1.2.) Position control servo-mechanisms introduce error only at the instant of step change in the armature current, especially due to short circuits, etc. When the demagnetising component of the armature current suddenly goes up the field current has to rise to keep the the flux linkages with the field circuit constant. The voltage proportional to field current E_i and the voltage behind the Q-axis synchronous reactance E_{qd} which is used for simulating

the generator equations undergo step changes. (see section 2.1.3 and 4.1.2) Changes in E_{qd} because of the decay of flux linkages or the AVR action are normally slow because of the large field time constant and the I-pot positioning servo-mechanisms can follow these changes quite well. Developments in more accurate simulation techniques were continued with simulator time slower than the actual time. Slowing down the time on the simulator has a disadvantage in that the R-C combinations for the time constants of AVR and Governor loops are not easily obtained from the more common values for these components. For one or two machines which are nearest to the fault location the I-pot positioning servo-mechanism will have to be replaced by an electronic amplitude modulator.

Developments in instrumenting and metering techniques have been carried to an ultimate in the response speed which is 20 m-secs., or time for one cycle of the network analyser frequency. In the turbo-generator dynamic response changes faster than that are not likely to be of interest. The output of all the instruments is in terms of a proportional D.C. voltage with low ripple component and would be suitable for digitisation if a small process computer is used for an overall

computer control of a multimachine simulator.

In summary the objectives listed in section 1.4 with associated requirements of accuracy and flexibility can be best achieved by combining an analogue computer, simulating the thermodynamic equations of the steam system and turbine and also the electro-dynamic equations of the synchronous machine, with a network analyser simulating the transmission network. For each machine a magslip and I-pot combination, conventionally used for generator representation on the network analyser, will be coupled to D.C. servo-mechanisms. These servo-mechanisms will follow the command from the analogue computer. It is possible to achieve 1 % overall accuracy on a modern analogue computer. Also it is possible to obtain a network analyser capable of representing line units to 1% accuracy. For the interconnecting equipment the need is to develop high grade servo-mechanisms with both static and dynamic accuracy of 1 % and instrumentation for power, voltage, current and angle measurement.

CHAPTER 2

SYNCHRONOUS MACHINE THEORY & BASIC SIMULATION TECHNIQUE

The most important type of machine in any study of the Power System is the synchronous machine. This chapter deals first briefly with the synchronous machine theory and an account of assumptions underlying the development of the theory, and then the conventional simplifications to describe the machine behaviour under large disturbances. (Section 2.1) These simplified equations provide the essential principles for the simulation of the synchronous machine. The simulator in its basic form will then be described (Sections 2.2 and 2.3) and the results obtained with it will be compared with solution of the equations from a digital computer.

The details of the electronic circuitry employed in the simulator are discussed in Chapter 3.

Inclusions of such factors as Transient Saliency, changes in flux linkages, excitation regulation is left for a later chapter

2.1 FUNDAMENTAL SYNCHRONOUS MACHINE EQUATIONS

Before the growth of power systems into their present size the performance of the machine was largely judged in terms of its steady-state characteristics. The emergence of stability problems in power systems is largely responsible for more detailed study of the transient characteristics ofthe machine and the present state of this knowledge has arisen as a result.

Blondel attacked the problem of the variable character of the air-gap of the conventional salient pole machine by resolving the armature m.m.f. and fluxes into two components - one in line with the poles (direct axis), and the other in quadrature there to (quadrature axis). This concept was then used by Doherty & Nickle (ref. 48, 49) for defining several new constants of the synchronous machine such as transient and sub-transient reactances.

A classical application of this concept is the derivation of the general equations of synchronous machines derived by Park. A comprehensive account of the equations of the synchronous machine in the reference-frame adopted by Park and covering all modes of operation

has been given by Adkins.(ref. 50).

Three fundamental assumptions are made in deriving the basic equations. These assumptions form the Park's (ref. 51, 52) definition of an 'Ideal Machine' and are as follows.

(i) That the stator windings are sinusoidally distributed around the air-gap as far as the mutual effects between them and the rotor are concerned, i.e. harmonics in the M.M.F. wave round the air-gap are neglected.

(ii) That saturation is not present and that the self and mutual inductances vary sinusoidally as the rotor moves and are of the form $(L_s + L_m \text{ Cos } 2\theta)$ and $\left[-M_s + L_m \text{ Cos } 2(\theta - 60^\circ)\right]$ respectively where L_s, M_s and L_m are constant.(ref. 53)

(iii) That the effects of hysteresis and eddy currents are negligible.

The starting point for the derivation of the basic equations is that the machine consists of several inductively coupled circuits. The instantaneous terminal voltage of anyone of these circuits is written in the form $v = ri + \frac{d\psi}{dt}$ where i is the current and $\frac{d\psi}{dt}$ is the rate of change of flux linkages.

Flux linkages are then written in the form of the product of self and mutual inductances and the instantaneous values of the currents. All the inductances are time varying quantities. The solution for currents is then sought assuming that the voltages are known functions of time.

The resulting differential equations are too complicated to handle and therefore currents, voltages and flux linkages are replaced by a set of fictitious currents, voltages and flux linkages such that the equations involving circuits and their time-derivatives have constant co-efficients. Such a substitution was first used by Park and is known after his name as "Park's Transformation" the equations can now be solved for the new variables as functions of time and from the results the actual quantities can be found by using the inverse transformation.

No method is available to apply these equations to the network-analyser and therefore a number of further simplifying assumptions are made which are discussed in this section as well as subsequent sections. Most of the

recently developed digital computer programs are also based on similar simplifying assumptions. This approach alone is well suited for handling a practical sized power-system.

In what is discussed below, Park's two-reaction theory of the machine is simplified to an extent as to make it suitable for the network-analyser approach. A three phase machine, without the damper winding, is considered.

The theory applies equally to a salient pole or non-salient pole machine. The inadequacy due to neglecting the damper winding is partially offset by approximating it to a damping torque proportional to slip. (The word 'partial' is used because it only corrects for positive sequence damping torque. Some approximate methods are also available to represent the D.C. braking torque and the negative sequence torque.) Dampers neglected, the machine has four windings, the field winding and the three armature phase windings.

Park's transformation may be regarded as a purely mathematical process, but when the transformation is applied, the resulting equations for the flux linkages

in terms of the new variables are differential equations with constant co-efficients, and suggest a physical interpretation of the transformation.

The axes currents i_d & i_q can be defined as currents in fictitious coils, located on the axes, having the same number of turns as the phase coils, and which would set up the same M.M.F. wave as the actual currents i_a, i_b, i_c. So in fact three actual coils can be replaced by a system of two axis coils and are shown in fig. 2.1. The usual convention for the signs are also shown in this figure.

The equations for the flux linkages are :

$$\begin{aligned} \psi_d &= L_d\, i_d + M_{df}\, i_f \\ \psi_q &= L_q\, i_q \\ \psi_o &= L_o\, i_o \\ \psi_f &= L_f\, i_f + M_{df}\, i_f \end{aligned} \qquad 2.1.1.$$

where the subscripts d & q refer to the axis coils and f the field coil.

i_o in the transformed variable is identical with the zero-sequence current in the theory of symmetrical components, except that it is an instantaneous value of

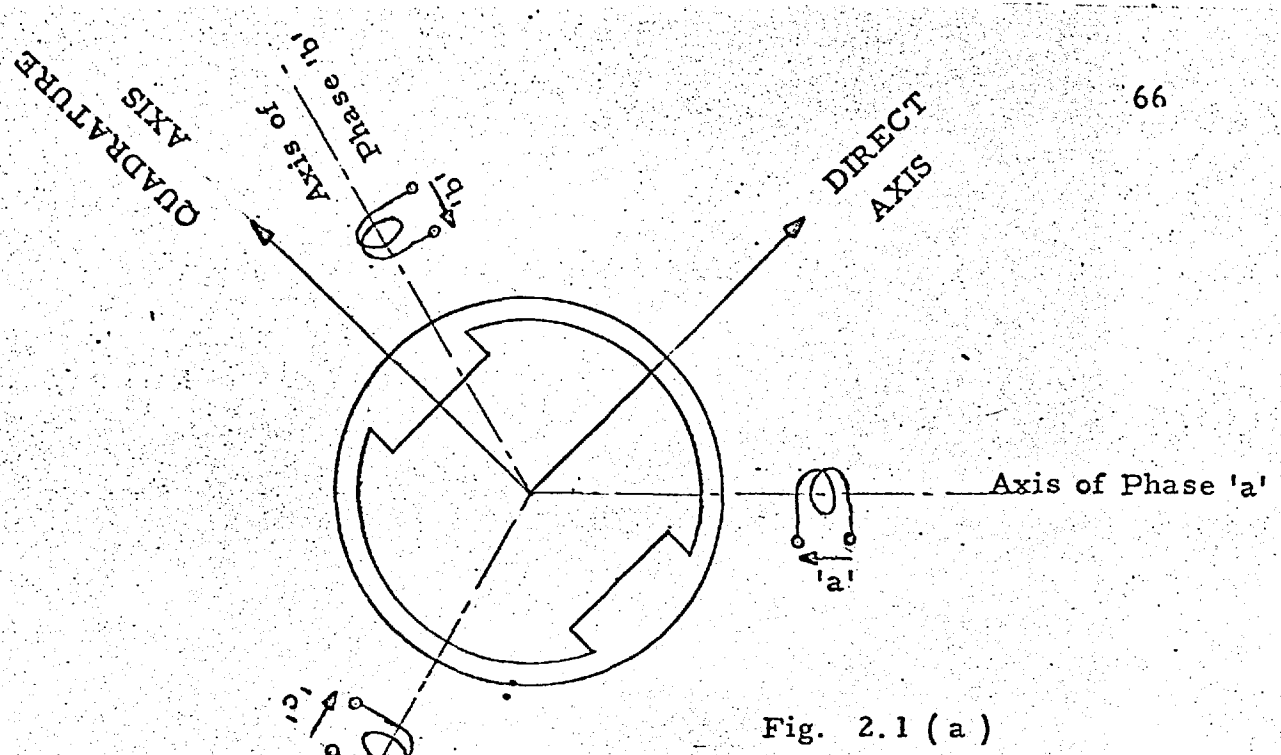

Fig. 2.1 (a)

Idealised Synchronous Machine

Showing Three Phase Coils

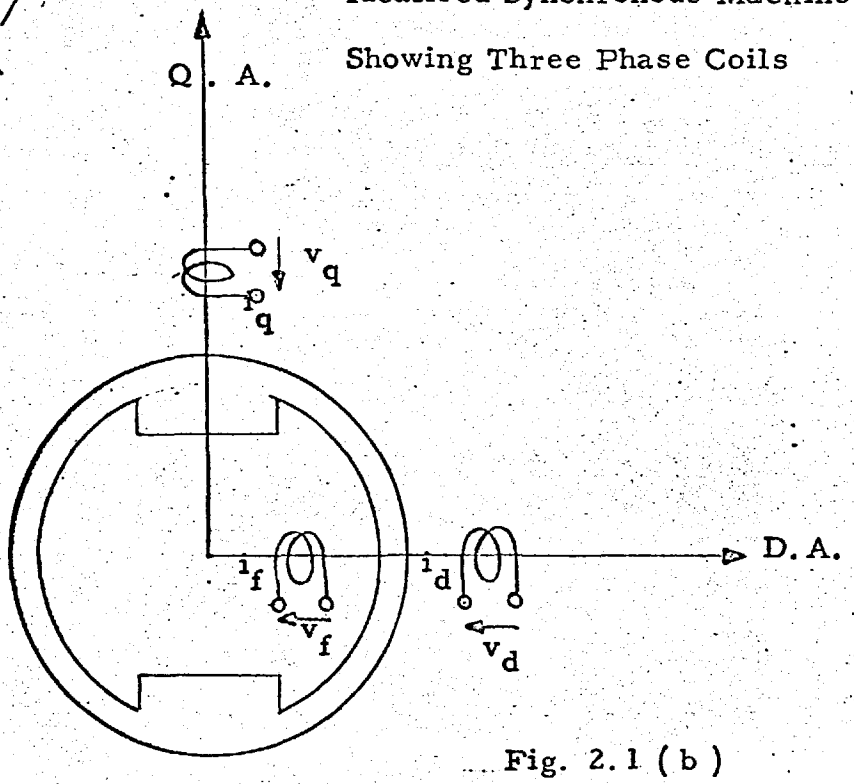

Fig. 2.1 (b)

Three Phase Coils Replaced

By Two Axis Coils.

current, which may vary with time in any manner. This current gives no space fundamental air gap flux.

The armature voltage equations can be written, by first writing down the terms as if all the coils are ordinary stationary coils and then adding to it the rotational voltage terms. The signs for these terms are determined by considering the torque produced by the interaction of the fields set up by the current in the windings and is explained in fig. 2.2.

The axis voltage equations are

$$v_d = ri_d + p\psi_d - \omega\psi_q$$
$$v_q = ri_q + p\psi_q + \omega\psi_d \qquad 2.7.2.a$$

The zero-sequence voltage and field voltage equations have no rotational voltage terms and are

$$v_o = ri_o + p\psi_o$$
$$v_f = r_f i_f + p\psi_f \qquad 2.7.2.b$$

The electrical torque is given by the following equation

$$fe = \frac{w}{2}(\psi_q i_d - \psi_d i_q) \qquad 2.1.3.a$$

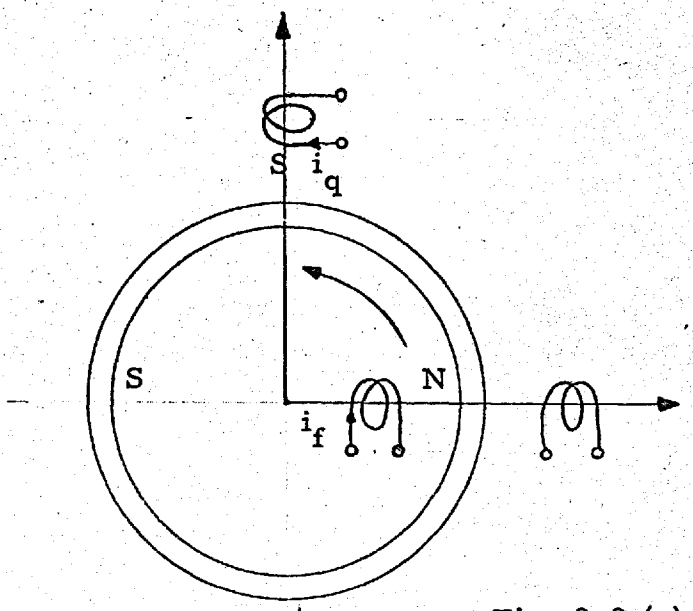

Fig. 2.2 (a)

Torque due to Positive i_f and Postive i_q, in the Positive Direction of Rotation (Motoring Action)

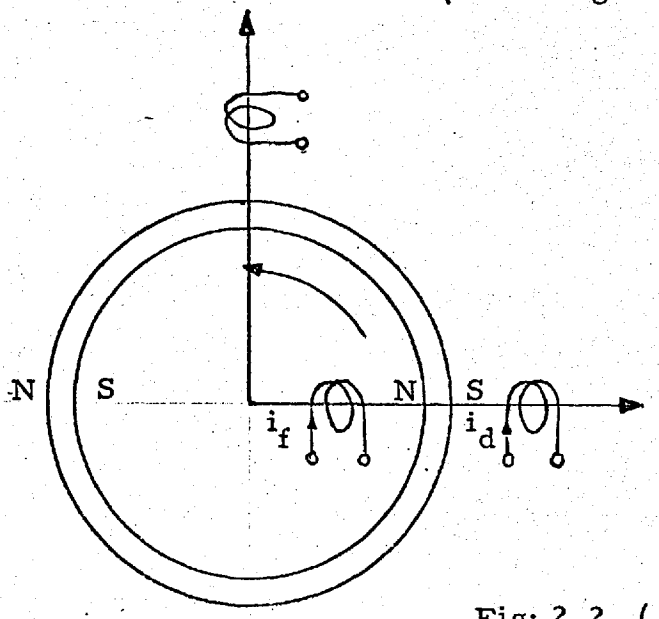

Fig: 2.2. (b)

Torque due to Positive i_f and Positive i_d in the Negative Direction of Rotation (Generating Action)

The mechanical input torque is related to the electrical torque by the following equation.

$$fm = fe + \frac{2H}{w} \cdot p\omega + \frac{Kd}{w}(\omega - \omega) \qquad 2.1.3.b$$

The term $\frac{Kd}{w} \cdot \omega$ has been introduced to partially compensate for neglecting the damper windings.

2.1.1. VECTOR DIAGRAM FOR BALANCED STEADY-STATE OPERATION AT SYNCHRONOUS SPEED

If the field is excited with a constant current and the machine is running steadily at synchronous speed, i.e.

$$i_f = I_f$$

and

$$\omega = w$$

$$v_o = i_o = o$$

Also if zero time is taken when the direct axis is in alignment with that of phase 'a' and if the armature currents be steady and of positive sequence.

$$\begin{aligned} i_a &= I_{max} \text{ Cos } (wt+\beta) \\ i_b &= I_{max} \text{ Cos } (wt+\beta-120^o) \\ i_c &= I_{max} \text{ Cos } (wt+\beta+120^o) \end{aligned} \qquad 2.1.4.$$

Applying Park's transformation

$$i_d = I_{max} \cos\beta = \sqrt{2}\, I_d = \text{constant}$$
$$i_q = I_{max} \sin\beta = \sqrt{2}\, I_q = \text{constant} \qquad 2.1.5.$$

where I_d & I_q are resolved components of current in phase 'a'.

Also if v_d and v_q are the transformed axes components the voltage applied to the phase 'a'

$$V_a = v_d \cos wt - v_q \sin wt \qquad 2.1.6.a$$

If V_d and V_q are the resolved components of voltage applied to phase 'a'

$$V_a = R_e \left[\sqrt{2}\, (V_d + j\, V_q)\, e^{jwt} \right]$$
$$= \sqrt{2}\, (V_d \cos wt - V_q \sin wt) \qquad 2.1.6.b$$

comparing equations 2.1.6.a and b

$$v_d = \sqrt{2}\, V_d$$
$$v_q = \sqrt{2}\, V_q \qquad 2.1.7.$$

From eq = ns 2.1.1. and 2.1.2., voltages in terms of Park's variablesare :

$$v_d = ri_d - w\,(L_q i_q) = ri_d - x_q i_q$$

$$v_q = ri_q + w(L_d i_d + M_{fd} i_f) = ri_q + x_d i_d + wM_{fd} i_f$$

and therefore

$$\vec{V} = \frac{1}{\sqrt{2}}\left[v_d + j\, v_q \right]$$

$$\frac{1}{\sqrt{2}}\left[ri_d - x_q i_q + (ri_q + x_d i_d + wM_{fd}\, i_f) \right]$$

$$= r\,(I_d + jI_q) - x_q I_q + j\, x_d I_d + j\,\frac{w M_{fd}}{\sqrt{2}}\, I_f$$

$\frac{jwM_{fd}}{\sqrt{2}}\, I_f = \vec{E}_I$ = No load voltage proportional to the field current.

$$\vec{V} = r\vec{I} - x_q I_q + x_d I_d + \vec{E}_I \qquad 2.1.8.$$

The vector diagram corresponding to this equation is shown in fig. 2.3.a. The angle between the terminal voltage $\vec{V}$ and the Q-axis is known as the load angle and is denoted by δ.

For most transient stability studies the stator resistance can be neglected and the vector diagram is simplified to one shown in fig. 2.3.b. This vector diagram corresponds to the motoring conditions with lagging current.

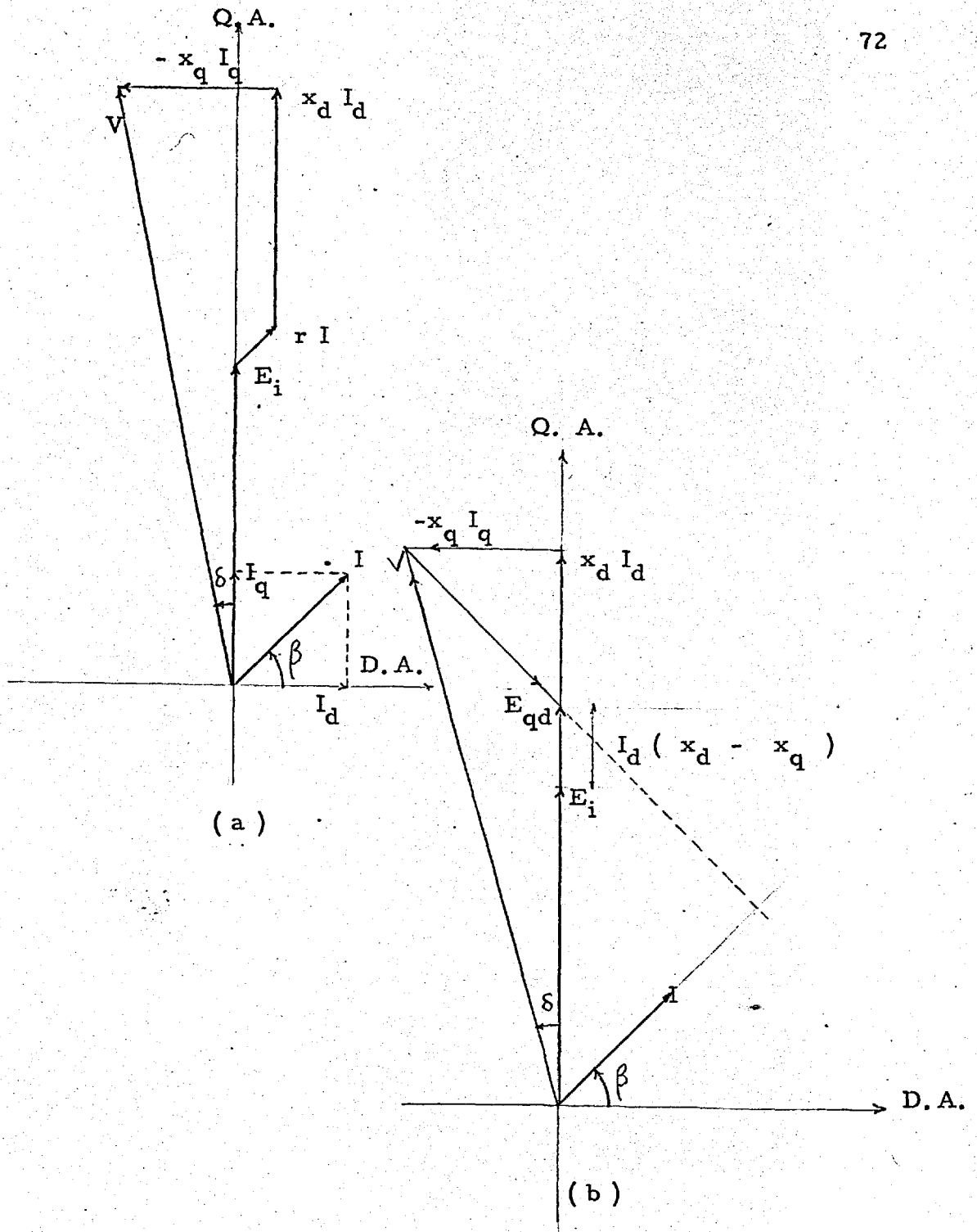

FIG : 2.3

VECTOR DIAGRAM FOR BALANCED STEADY-STATE OPERATION AT SYNCHRONOUS SPEED.

If a vector $j x_q \vec{I}$ is subtracted from the terminal voltage $\vec{V}$ a vector $\vec{E}_{qd}$ is obtained which also lies on the quadrature axis. The relation of E_{qd} with E_I is shown below :

From eq = n 2.1.8.

$$\vec{V} = \vec{E}_I + j x_d I_d - x_q I_q$$

$$= \vec{E}_I + j(I_d + j I_q) x_q + j(x_d - x_q) I_d$$

$$= \vec{E}_I + j(x_d - x_q) \vec{I}_d + j x_q \vec{I}$$

$$\vec{V} = \vec{E}_{qd} + j x_q \vec{I} \qquad 2.1.9.$$

$$E_{qd} = E_I + (x_d - x_q) I_d$$

Vectors $\vec{I}_d$ and $\vec{I}_q$ can be written in symbolic notation as I_d and $j I_q$ where I_d & I_q are the magnitudes.

From eq=n. 2.1.3.a the electrical torque is given by

$$fe = \frac{w}{2}\left[\psi_q i_d - \psi_d i_q\right]$$

$$= \frac{w}{2}\left[L_q i_q i_d - (M_{fd} i_f + L_d i_d) i_q\right]$$

$$= wL_q \frac{iq}{\sqrt{2}} \frac{id}{\sqrt{2}} - \left(\frac{wM_{fd}}{\sqrt{2}} i_f + wL_d \frac{i_d}{\sqrt{2}}\right) \frac{i_q}{\sqrt{2}}$$

$$= x_q I_q I_d - \left(\frac{wM_{fd}}{\sqrt{2}} I_f + x_d I_d\right) I_q$$

$$= - \left[E_I + (x_d - x_q) I_d\right] I_q$$

$$= - E_{qd} I_q \qquad 2.1.10.$$

In the case of a round rotor machine where $x_d = x_q$ and therefore $E_{qd} = E_I$, the steady state conditions can be simulated on the network analyser by a voltage E_I behind x_d, direct axis synchronous reactance.

In the case of a salient pole machine simulation is possible by a variable voltage E_{qd} behind x_q, the quadrature axis synchronous reactance.

In the derivation of the equations for steady-state synchronous operations transformed axes currents and the resolved components of the phase currents are related by a constant. This applies only to the steady state conditions but in general the only way to calculate the phase values from the axes values is to apply the Park's Transformation equations.

2.1.2. SIGN CONVENTIONS FOR GENERATORS

In developing a general theory of machines the circuit equations are so established that positive power means the power consumed and therefore eq = n 2.1.8. bears the same sign convention

$$V = E + Z\ I \qquad 2.1.11.$$

In dealing with generators the convention on signs is usually taken so that eq = n 2.1.1. becomes

$$E = V + Z\ I \qquad 2.1.12.$$

This can be done by changing the sign of I (i.e. both of I_d and I_q) without changing the sign of I_f. The equations 2.1.1., 2.1.2. and 2.1.3. will be modified to

$$\begin{aligned}
\psi_d &= M_{fd} i_f - L_d i_d \\
\psi_q &= L_q i_q \qquad\qquad 2.1.13. \\
\psi_f &= L_{ff} i_f - M_{fd} i_d
\end{aligned}$$

$$\begin{aligned}
v_d &= -\ r i_d + p\psi_d - \partial\psi_q \\
v_q &= -\ r i_q + p\psi_q + \partial\psi_d \qquad\qquad 2.1.14. \\
v_o &= -\ r i_o + p\psi_o \\
v_f &= r_f i_f + p\psi_f
\end{aligned}$$

With the change in sign positive I_d is demagnetising current and positive I_q represents generated current.

The electrical torque

$$fe = \frac{w}{2}\left[\psi_d i_q - \psi_q i_d\right] \qquad 2.1.15.$$

For steady state operation at synchronous speed and under balanced conditions, (discussed in section 2.1.1.) :-

$$V_d = - rI_d + x_q I_q$$

$$V_q = - rI_q - x_d I_d + \vec{E}_i$$

$$\vec{V} = V_d + jV_q$$

$$= - \vec{rI} - jx_d I_d + x_q I_q + \vec{E}_i$$

or neglecting resistance

$$\vec{V} = E_i - jx_d I_d + x_q I_q \qquad 2.1.16.$$

The vector diagram is shown in fig. 2.4 The quadrature axis is shown horizontal as is customary in the conventional books on Electrical Machinery.

If a vector $x_q \vec{I}$ is added to the terminal voltage a vector $\vec{E}_{qd}$ is obtained which lies on the quadrature axis. This can be shown in the same way as discussed for the synchronous motor case in section 2.1.1.

The expression for the electrical torque also similar to the case of a motor in section 2.1.1., except for the change in sign, is

$$fe = \left[E_i - (x_d - x_q) I_d\right] I_q$$

$$= E_{qd} \times I_q \qquad 2.1.17.$$

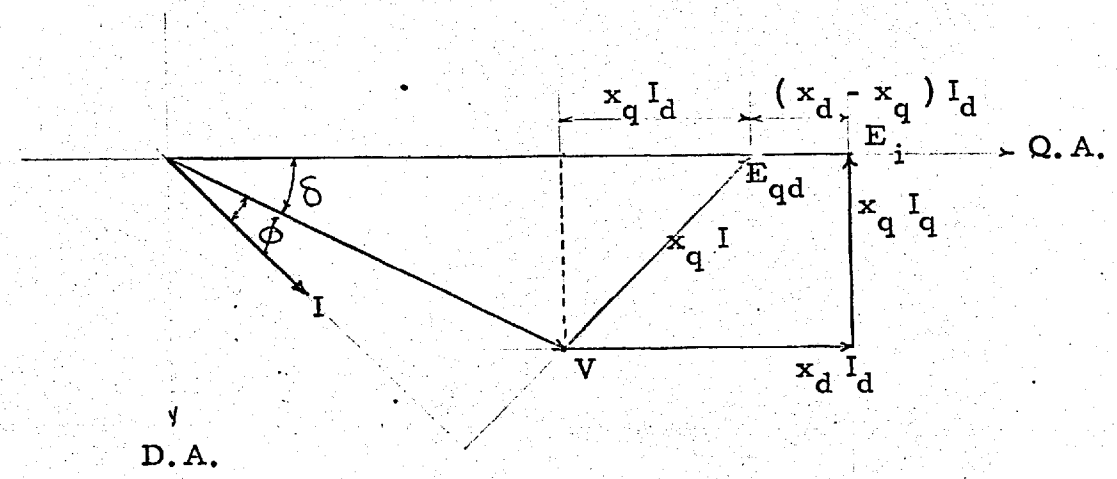

FIG : 2.4

STEADY STATE VECTOR DIAGRAM

FOR A SYNCHRONOUS GENERATOR

2.1.3. VECTOR DIAGRAM FOR THE TRANSIENT STATE

Vector diagrams discussed in section 2.1.1. and 2.1.2. are applicable only when the changes in the armature current are very slow in which case the field current I_f and the fictitious induced voltage proportional to the field current E_i remains constant. The terminal voltage varies because of the changing synchronous impedance drop.

The vector diagram for the machines under transient conditions can be constructed if it is assumed:-

(i) That under the conditions of rapidly changing currents such as caused by switching, faults, or swinging of the machines, the terms $p\psi_d$ and $p\psi_q$ in the voltage equations are negligible compared to the rotational voltages $\partial\psi_d$ and $\partial\psi_q$ in the equations for axis voltages. The assumption is fair except for short circuits very near to the terminals of the machine. This assumption also enables one to use the terms effective or R.M.S. value of voltages or currents for the varying components of the alternating quantities denoted by symbols V_d, V_q and I_d, I_q.

(ii) That during the swinging of the machine the speed is assumed constant at w radians/sec. This is a fair assumption for all the disturbances which do not lead to the instability of the machine.

With these assumptions and the well known fact that the flux linkages with an inductive circuit having zero resistance cannot change whatever may occur in other mutually coupled circuits, the study of transient phenomena in synchronous machines can be very much facilitated. The theorem known as the "constant flux linkage theorem" due to Doherty is frequently used.

Since it is ψ_f which remains constant during changes of the type described above, a new fictitious voltage is defined proportional to the field flux linkages and denoted by E'_q which will also remain constant during the change of armature current.

$$E'_q = \frac{wM_{fd}}{\sqrt{2}} \times \frac{\psi_f}{L_{ff}} \qquad 2.1.18.$$

A relationship will now be derived between E'_q & E_I. An expression for the direct axis transient reactance in terms of the direct axis synchronous reactance and the

field & D-axis mutual reactance is considered first.

According to the definition (ref. 53,54,55) of the transient reactance, it is the initial value of the ratio (ψ_a/i_a) when three phase balanced positive currents are suddenly applied to the stator, when the field is shorted, and the field structure is so rotated that the direct axis is in line with the axis of phase A.

Under these conditions

$i_d = \sqrt{2}\ I.1$ (where 1 is unit step)

i_q & i_o are both equal to zero.

From equation 2.1.1. $\psi_f = M_{fd}\, i_d + L_{ff} i_f = o$

$$i_f = -\frac{M_{fd}}{L_{ff}}\, i_d$$

$$\psi_d = L_d i_d + M_{fd} i_f$$

$$= L_d i_d - \frac{M_{fd}^2}{L_{ff}}\, i_d$$

Applying inverse transformation

$$\psi_a = \frac{1}{\sqrt{2}} \left[L_d i_d - \frac{M_{fd}^2}{L_{ff}}\, i_d \right] \text{Cos wt}$$

$$i_a = \frac{1}{\sqrt{2}}\, i_d \text{ Cos wt}$$

$$L_d' = \frac{\psi_a}{i_a} = L_d - \frac{M_{fd}^2}{L_{ff}} \qquad 2.1.19.$$

Combining eq=n 2.1.18. with expression for E_i

$$E_i - E'_q = \frac{wM_{fd}}{\sqrt{2}} i_f - \frac{wM_{fd}}{\sqrt{2}} \frac{\psi_f}{L_{ff}}$$

substituting the relation for ψ_f from (eq =n 2.1.10)

$$E_i - E'_q = \frac{wM_{fd}}{\sqrt{2}} i_f - \frac{wM_{fd}}{\sqrt{2}} \left[L_{ff} i_f - M_{fd} i_d \right] / L_{ff}.$$

$$= \frac{w M_{fd}^2}{\sqrt{2}\, L_{ff}} i_d$$

$$= w(L_d - L'_d) \frac{i_d}{2} \quad \text{(from 2.1.19)}$$

$$= (x_d - x'_d) I_d$$

This result can be arranged as

$$E_i - x_d I_d = E'_q - x'_d I_d \qquad 2.1.20.$$

substituting this relationship in Eq=n 2.1.16.a and neglecting armature resistance.

$$V_d = x_q I_q$$

$$V_q = -x_d I_d + E_i$$

$$= - x'_d I_d + E'_q$$

$$\vec{V} = V_d + j V_q = \vec{E'_q} + x_q I_q - j x'_d I_d$$

or $$\vec{V} = \vec{E'_q} - j x_d \vec{I_d} - j x_q \vec{I_q} \qquad 2.1.21.$$

The vector diagram corresponding to this equation is shown in fig. 2.5.a.

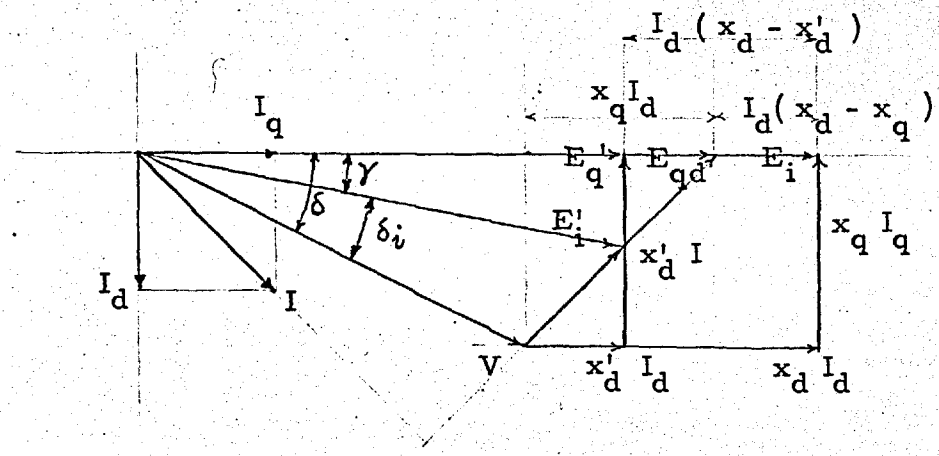

(a)

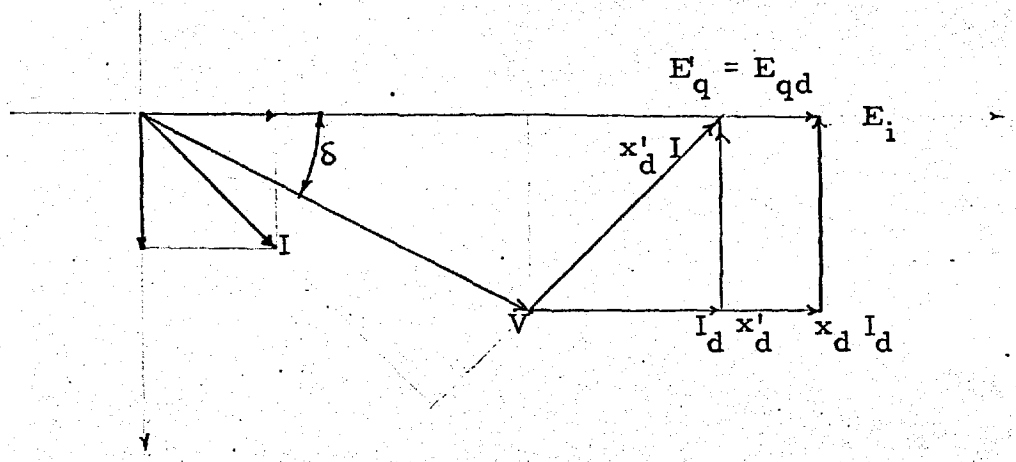

(b)

FIG: 2. 5.

VECTOR DIAGRAM FOR SYNCHRONOUS GENERATOR

UNDER TRANSIENT CONDITIONS

(a) $x'_a = x_q$

(b) $x'_d = x_q$

The electrical torque

$$fe = \frac{w}{2}\left[\psi_d i_q - \psi_q i_d\right]$$

now $$\psi_d = M_{fd} i_f - L_d i_d$$

$$= \frac{M_{fd}}{L_{ff}}(\psi_f + M_{fd} i_d) - L_d i_d$$

$$\psi_q = - L_q i_q$$

$$fe = \frac{w}{2}\left[\left(\frac{M_{fd}\psi_f}{L_{ff}} + \frac{M_{fd}^2}{L_{ff}} i_d - L_d i_d \right) i_q - (-L_q i_q) i_d \right]$$

$$= E'_q I_q + (x_d - x'_d) I_d I_q - x_d I_d I_q + x_q I_q I_d$$

$$= \left[E'_q + (x_q - x'_d) I_d\right] I_q = E_{qd} * I_q \qquad 2.1.22.$$

2.1.4. CONSTANT VOLTAGE BEHIND D.A. TRANSIENT REACTANCE

A generator simulation by constant voltage behind direct axis transient reactance is possible if it is assumed that $x'_d = x_q$.

substituting this condition in equation 2.1.21.

$$\vec{V} = \vec{E'_q} - j x'_d \vec{I}_d - j x'_d \vec{I}_q$$

$$= \vec{E'_q} - j (\vec{I}_d + \vec{I}_q) x'_d$$

$$= \vec{E'_q} - j \vec{I} x'_d \qquad 2.1.23$$

The vector diagram corresponding to this equation is shown in Fig. 2.5.b.

From Eq=n 2.1.22

$$fe = E'q * Iq \qquad 2.1.24$$

This method was first applied to the A.C. Network Analyser. Combined with the assumption of constant power input, the accelerating power is found by subtracting from it the electrical power output which is metered on the network analyser. This is assumed constant for a small period of time and the new position of the rotor is determined from the mechanical equation 2.1.3.b in which torques fm & f_e can be replaced by power P_m and P_e since w is assumed constant during the disturbance.

$$P_m - P_e = \frac{2H}{w} p^2 \gamma + \frac{Kd}{w}(\eta - \omega)$$

and $$\delta = \frac{1}{p}\gamma$$

these two are often combined in one

$$P_m - P_e \frac{2H}{w} p^2 \delta + \frac{Kd}{w} p \delta \qquad 2.1.24.$$

In early developments of the digital computer program the same method was used.

Actually $x'_d \neq x_q$ in which case the initial conditions and the position of the Q-axis are determined from the vector diagram of fig. 2.5.a. A vector E'_i is obtained

such that

$$E_i = V + j\ x_d \vec{I}$$

This voltage is kept constant during the period of the swing.

The inertia of the machine is then associated with the vector E_i' for the computation of the swing curve. The position of the quadrature axis is obtained by adding angle γ (angle between E_i& Q-axis) which remains constant.

2.1.5. VARIABLE VOLTAGE BEHIND Q-AXIS SYNCHRONOUS REACTANCE

This is a more general case and is described by equations 2.1.17 and vector diagram of Fig. 2.5.a.

To represent constant field flux linkage, E_q' is obtained on the quadrature axis and is held constant throughout the study interval. In order to maintain E_q' constant with varying armature current and the machine voltage E_{qd} is changed as given by the relation $E_{qd} = E_q' + I_d (x_q - x_d')$.

This method makes it possible to represent the machine reactance by a single reactive unit which in this case is quadrature axis synchronous reactance.

Electrical Torque fe = $E_{qd}.I_q$ as shown in section 2.1.3. and can be measured on the network analyser.

The two fundamental configurations for the generator simulation (secton 2.1.4. & 2.1.5.) are sufficient for the description of the elements of the power system simulator. Therefore, consideration for including the flux decay and excitation regulation is left until a later chapter.

2.2. ELEMENTS OF POWER SYSTEM SIMULATOR

Central to the design of the simulator is a network-analyser and the equations for the generators and loads are so manipulated as to make the use of a network analyser possible. In the following section a brief description of the network analyser is given and then the design of the Electro-mechanical actuating mechanisms for the generating units to make an automatic solution of the simplified generator swing equation.

2.2.1. NETWORK ANALYSER

A brief description of network analysers is given in section 1.5.1. of Chapter 1.

The Power system laboratory at Imperial College

has the facility of the use of an 'A.C. Conjugate Impedance Analyser' operating at 50 c/s. It was initially intended to use this for the transmission network representation, static loads and generators, transformers and motor impedances. For reasons described in section 3.10 this idea had to be abandoned in favour of a direct impedance type analyser but still operating at mains-frequency. The idea of mains frequency operation was retained because it offers the facility that the network analyser excitation supply can be derived directly from the mains.

It has been reported (ref. 56) recently that loads and the transmission line may contribute to the damping of the synchronous machine oscillations depending upon both steady state and oscillation frequencies. A closer simulation of these effects can be made using base frequency of 50c/s and solving the machine equations on real time base.

The C.E.G.B. maintains, as a statutory obligation, the system frequency between 49.5 & 50.5 c/s which was considered adequate for the basic design and development of the simulator. In fact the variation of the

frequency on the C.E.G.B. is much less than the statutory limits.

The design of the basic impedance unit used in the network analyser is discussed in section 3.10.

The representation on the network analyser of a transmission system is done by converting all voltages, currents and impedances to values which are proportional to the actual values. Generally the information is all recorded in terms of the units of base quantities.

Base values used are

voltage	25 volts
current	2.5 mA
Impedance	10,000 Ω
Power	62.5mVA
Admittance	100 μ℧
Frequency	50 c/s

2.2.2. GENERATOR UNITS

The generator units which provide sources of e.m.f, independently variable in both phase and magnitude, each consists of a magslip transmitter and auto-transformer (Inductive Potentiometer). The magslip is used to control the phase shift while the I-pot controls the voltage magnitude. Different reactances are used in series to get the required simulation.

2.2.2.a MAGSLIP

The name 'magslip' is synonymously used with synchros, selsyns, asynn, autosyn and telesyn, etc. They all describe transducer of rotary induction type which are extensively used in servo-mechanism (ref.57) and data-transmission (ref.58)

Physically a magslip resembles a small dynamo-electric machine (fig.2.6) having a wound rotor and a wound stator. The position of the rotor winding relative to the stationary stator winding determines the voltage induced in one when an alternating voltage is applied to the other and provides an indication of their relative position.

The basic form of the magslip called the control magslip is shown in fig. 2.6. The unit consists of three star connected windings, These windings are distributed to give a sinusoidal distribution of flux when energised and they have axes 120^{o} apart in the manner of a three phase machine. The rotor carries a single coil. Connections to the rotor are through brushes and slip rings. If the rotor is excited from an a.c. supply an alternating magnetic field is set up in the magslip in the direction of the rotor axis. This field links up with the stator winding in varying degrees depending upon relative angles between the rotor axis and each stator winding axis. As a consequence e.m.f.'s of different magnitudes are induced in the three windings on the stator, but they are all in phase. This magslip is called a transmitter magslip. If the stator windings of this magslip are connected to another magslip called the receiver magslip, a magnetic field is set up whose direction corresponds to the direction of the field in the transmitter. The rotor has an e.m.f. induced in it and the servo-mechanism motor moves the rotor to an angle where there is no coupling. The alignment of the

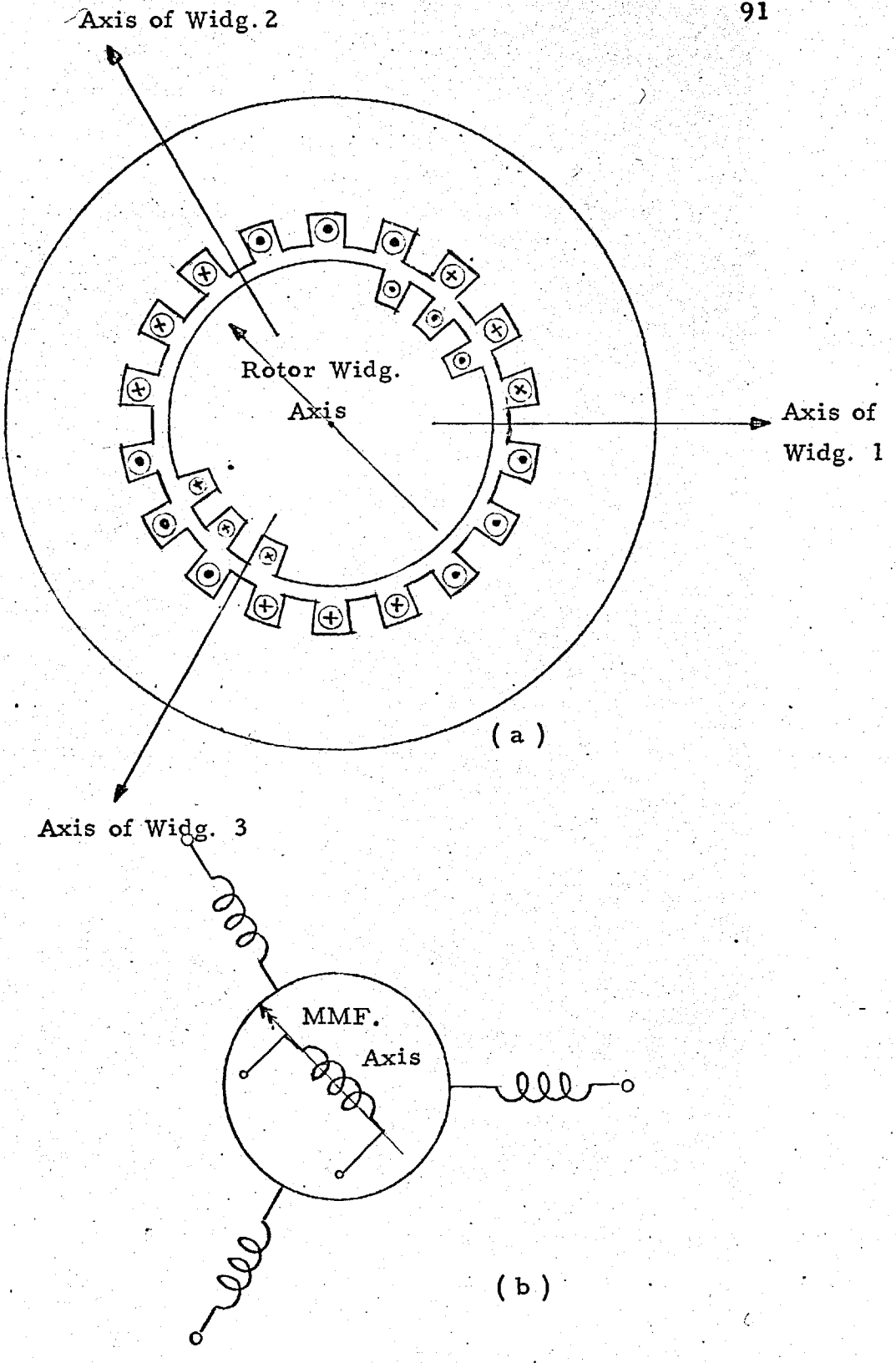

FIG : 2.6

TRANSMITTER MAGSLIP

(a) SECTIONAL VIEW (b) SCHEMATIC

input and output shafts corresponds to the position where the rotor is at right angles to its stator field.

It was hoped that this type of magslip might be suitable for the role of phase shifter. When a three phase A.C. voltage is applied to the stator of the magslip it produces a rotating field and because the rotor is not made of thin laminations it produces a high induction motor torque. For its more usual application the rotor only links a pulsating field.

Another type of magslip, also available in the Laboratory, is called the resolver magslip. Its winding arrangement is shown in fig. 2.7. This magslip has two windings on it and was found not to produce induction torque. The military requirements for high accuracy position control has given us a high precision variable phase source. These magslips are capable of indicating 1/10th of a degree.

The resolver magslip provides an extra facility of providing an A.C. voltage at 90^{o} phase difference which was found useful for the development of several measuring

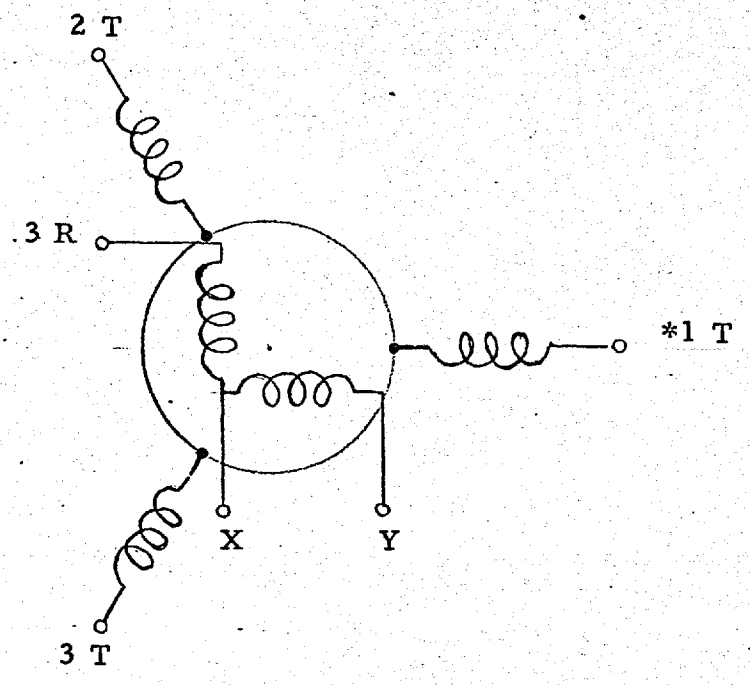

FIG: 2.7

WINDING SCHEMATIC OF

A RESOLVER MAGSLIP

circuits described in Chapter 3.

The sinusoidal wave form obtained from the rotor is good. Harmonic contents are 0.7% of 3rd 1.1% of the 5th and 0.5% of the 7th.

Electrical data for the magslip used is

STATOR : Three-phase star connected

voltage rating 50 volts

Impedance 30 + 140

ROTOR : Two-phase 'L' connected

Voltage rating 50 volts

Impedance 20 + j 100

The voltages given are line to line but the magslip could be run at 50 volts phase allowing extra heating. The voltage rating of the magslip necessitated selection of 25 volts as the base voltage.

2.2.2.b I-POT

The I-Pot is a precision wound auto transformer carrying a toroidal winding on a mu-metal core. The output derived from the moving contact is linearly proportional to the angle of rotation. The I-Pot used for voltage setting purposes was developed by admiralty designated No. 1 Mk. 1. The winding is of enamelled

copper wire accurately spaced on a former in which slots have been cut every $\frac{1}{4}^{o}$ for location of the winding turn. The moving contact consists of a carbon roller mounted on a castor which bears on a suitabletrack on the winding from which the insulation has been removed. A 340^{o} rotation is possible by this contact arm.Soldering lugs provided at the top are marked as shown in fig. 2.8.

The I-Pot is admirably suited for our purpose. It takes negligibly small current for magnetisation. Frequency range is 50 c/s to 2000 c/s and the maximum voltage is 55 volts. Output current is of the order of 500 mA. An auto transformer gives lower output impedance compared to the equivalent two winding transformer.

The base voltage of 25 volts was selected considering the maximum voltage rating of the magslip.

Some important considerations for selecting the base current value are :

(i) The burden of the metering circuits should be small compared to the unit current.

(ii) The leakage impedances of the magslip and the I-Pot should be very small compared to the unit impedance which is given by Base .Voltage/Base Current.

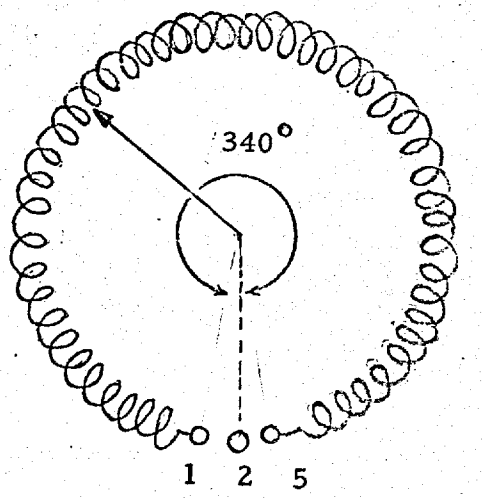

FIG : 2. 8

INDUCTIVE POTENTIOMETER

(iii) The magnitude of the current at which the reactance core starts saturating.

Choosing 2.5 mA as the base current was found to satisfy most of these conditions. All the circuits for instrumentation were designed to have input impedance of 10M Ω . The leakage impedances of the magslip and the I-pot were around 1% of the base impedance. The core used for reactance unit could take up to 4 units of current.

2.2.3. LOAD UNITS

Synchronous motors are represented in the same way as the generators. The synchronous motor load is often a negligible proportion of the total load.

Induction motor loads are often the most difficult to represent on the Network Analyser especially when the concentrations of the induction motors are such that their transient behaviour has a significant effect upon system stability limits. Where the induction motors are not expected to lose stability a steady state equivalent circuit of the induction motor might be a good compromise. In this case the secondary resistance (r_2/s), where s is the slip is changed during the swing period so as to

keep the power at the pre-fault level. Possibilities of more adequate representation of induction motors will be discussed in the concluding chapter.

In the absence of adequate information for the loads the following representations can be used for the period of the study.

(i) Constant Impedance

(ii) Constant Power (active & reactive)

(iii) Constant current (active & reactive)

These methods are used only for convenience.

In the first case an impedance unit needs to be connected between the load bus-bar and the neutral point. This method leads to optimistic results.

For constant active and reactive power an auto transformer will be used between the load node and the impedance unit to keep the voltage across the load unit constant. This leads to pessimistic results and the assumptions become markedly absurd when the voltage actually falls considerably during the period of short circuits.

The third-method which is sometimes used during

a step by step process of transient stability study on the network analyser is quite difficult to adopt during automatic solutions.

For any general representation a voltage source variable in phase and magnitude, as in the case of a generator, may be adopted for other types of representation.

2.3. AUTOMATIC SOLUTION OF SWING EQUATION FOR A SINGLE MACHINE CONNECTED TO AN INFINITE BUS-BAR THROUGH TWO PARALLEL TRANSMISSION CIRCUITS :

The starting point in all stability studies is the consideration of a single machine connected through a reactive tie line to an infinite bus-bar. This is of value for general investigations or for a remote generator connected through a long transmission line to a large system. The infinite bus-bar assumption reduces the analytical complexity and helps to assess the accuracy of the simulation at each stage during its development.

Several simplifying assumptions discussed in section 1 of this chapter are essential to reduce the system to a black-box concept of a constant voltage behind

the direct-axis transient reactance. The vector diagram shown in fig. 2.5 and equations derived in section 2.1.4. are the easiest to simulate on the analyser for automatic solution.

A reactance equal to the sum of the transient reactance of the synchronous machine and the transmission line reactance is connected to the two generator units at the two ends. For the infinite bus bar representation the magslip is locked in any position and any desired value of the voltage is selected by appropriate setting on the I-Pot. These two settings will not be changed during the period of the transient swing.

Similarly the magnitude of the voltage for the generator for the present simple case can be set by hand, and the rotor of the generator magslip is moved so as to give A.C. voltage in advance of the reference or infinite bus-bar, the power being fed into this bus. The angle of advance is the generator load angle δ .

Any difference between turbine torque and the electromagnetic torque has to satisfy the torque balance

equation 2.1.3.b. As the change in speed from the synchronous speed w is negligible, the torque balance equation is often written as a power balance equation:-

$$P_m - P_e = \frac{2H}{w} p^2\delta + \frac{K_d}{w} p\delta$$

An electronic wattmeter gives a D.C. signal proportional to the power output. A D.C. signal proportional to the input power is also obtained from the wiper of a potentiometer. The difference of the two signals is used to drive a split field D.C. servo motor which, through reduction gearing, drives the magslip rotor. (fig. 2.9.)

Both magslip and I-pot are driven by D.C. servo-mechanisms. The following balance sheet favoured the use of D.C. servo-mechanisms.

ADVANTAGES :

(i) High output from a D.C. servo-motor of a smaller frame size because there are no slip losses.

(ii) D.C. motors can be driven from a small D.C. Amplifier, compared to the size of an A.C. Amplifier for equal rating of A.C. motor.

(iii) A variety of stabilising techniques are

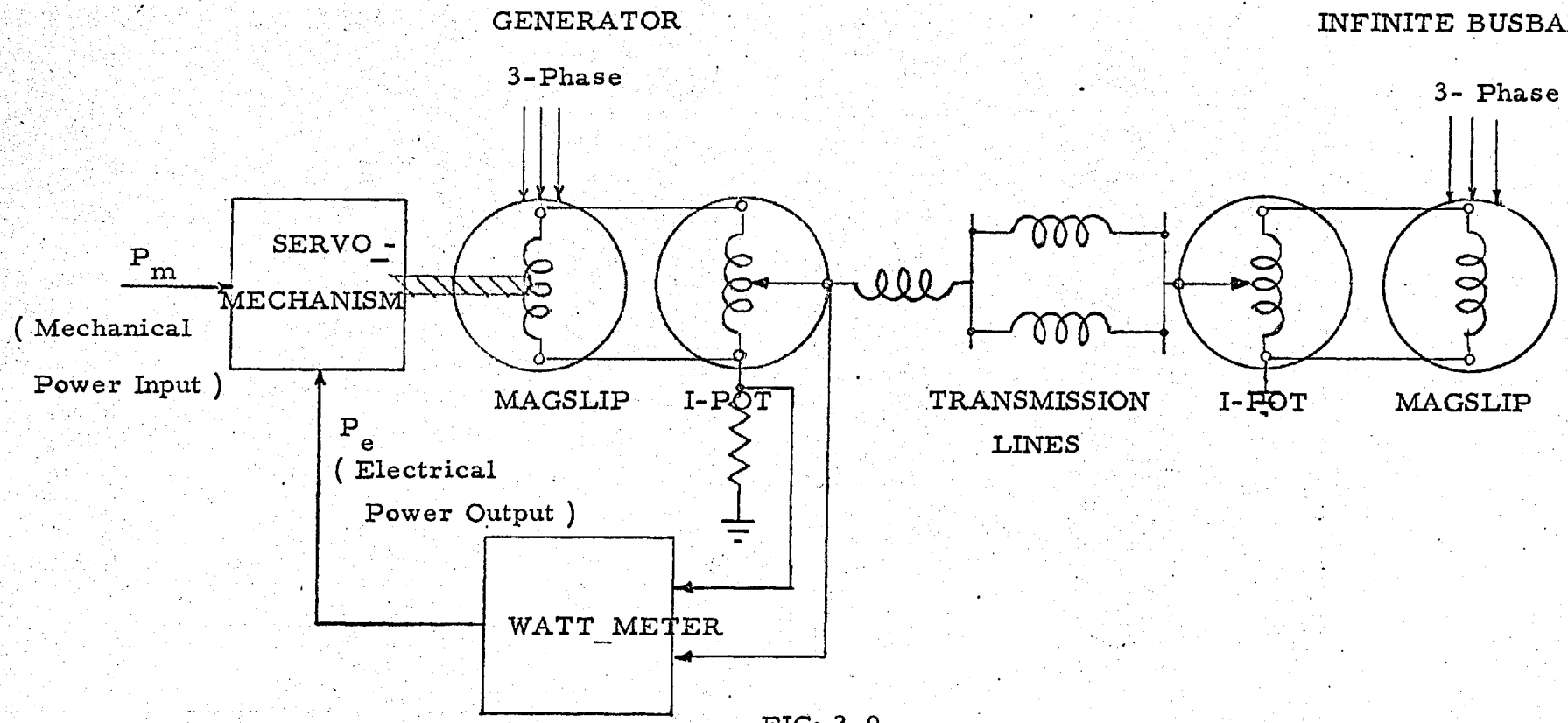

FIG: 2.9

SET-UP FOR A SIMPLE STABILITY PROBLEM

available which are easier to design.

(iv) Residual voltages are negligibly small.

(v) D.C. motors are more efficient for a variable speed application.

DISADVANTAGES

(i) D.C. amplifiers are more unreliable and have to be carefully designed to avoid drift problems and non-linearities.

(ii) Commutator require maintenance and replacement to ensure reliable brush performance.

(iii) Commutator and brushes occupy a large part of the motor.

(iv) Hysteresis, non-linearity and highly inductive field offer considerable stabilization problem.

Two schemes are described in the following sections for representing the inertia and damping.

2.3.1. SIMULATION OF INERTIA AND DAMPING BY USING ACCELERATION & SPEED FEEDBACK

The split field D.C. servo-motor produces a torque proportional to the signal applied at the input of the servo-amplifier. The torque accelerates the motor shaft

and the load shaft. If now a signal proportional to the acceleration is deducted from the accelerating signal, the system will behave as though it has a very large inertia. Similarly a negative speed feed-back will introduce a damping effect.

The scheme shown in fig. 2.10a has been suggested in ref. 1 and for reasons of avoiding interacting terms in the summation process by passive impedance elements the scheme shown in fig. 2.10b was tried. Only the summation and differentiation is being done on the analogue computing elements at this stage.

The transfer function for the computing element in the feed back path

$$V_3 = \frac{pC_1R_2}{(1+pC_2R_2)} V_1 + \frac{R_2}{R_1(1+pC_2R_2)} V_2$$

If the highest frequency of the tacho-generator signal is such that $2\pi f \cdot C_2R_2 \ll 1$ the transfer function can be simplified to

$$V_3 = p\, C_1R_2\ V_1 + \frac{R_2}{R_1}\ V_2$$

In fact a small trimmer capacitor C_2 in parallel

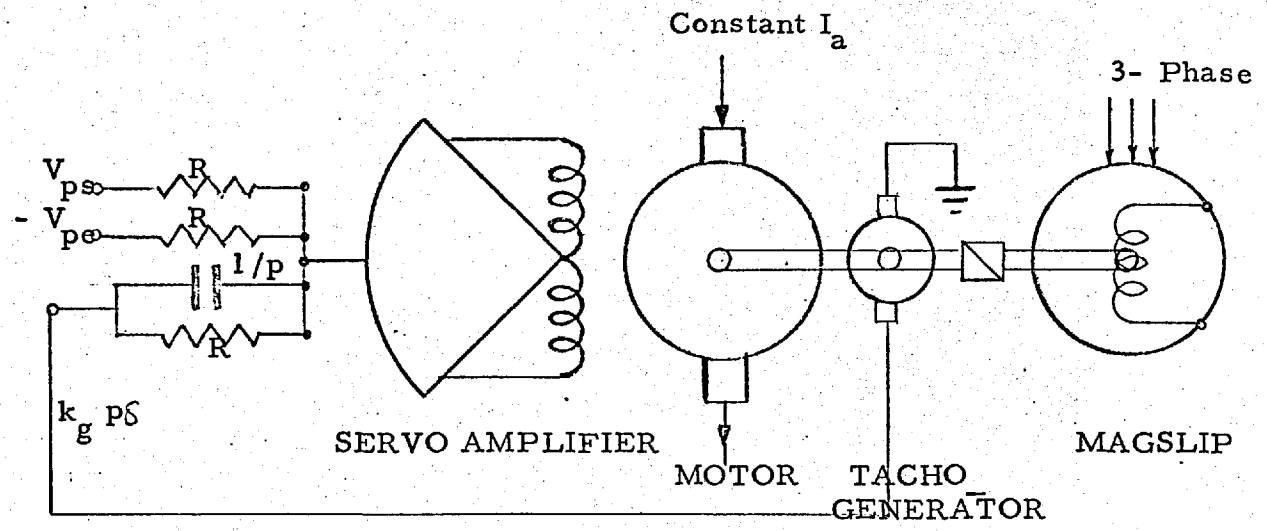

(a)

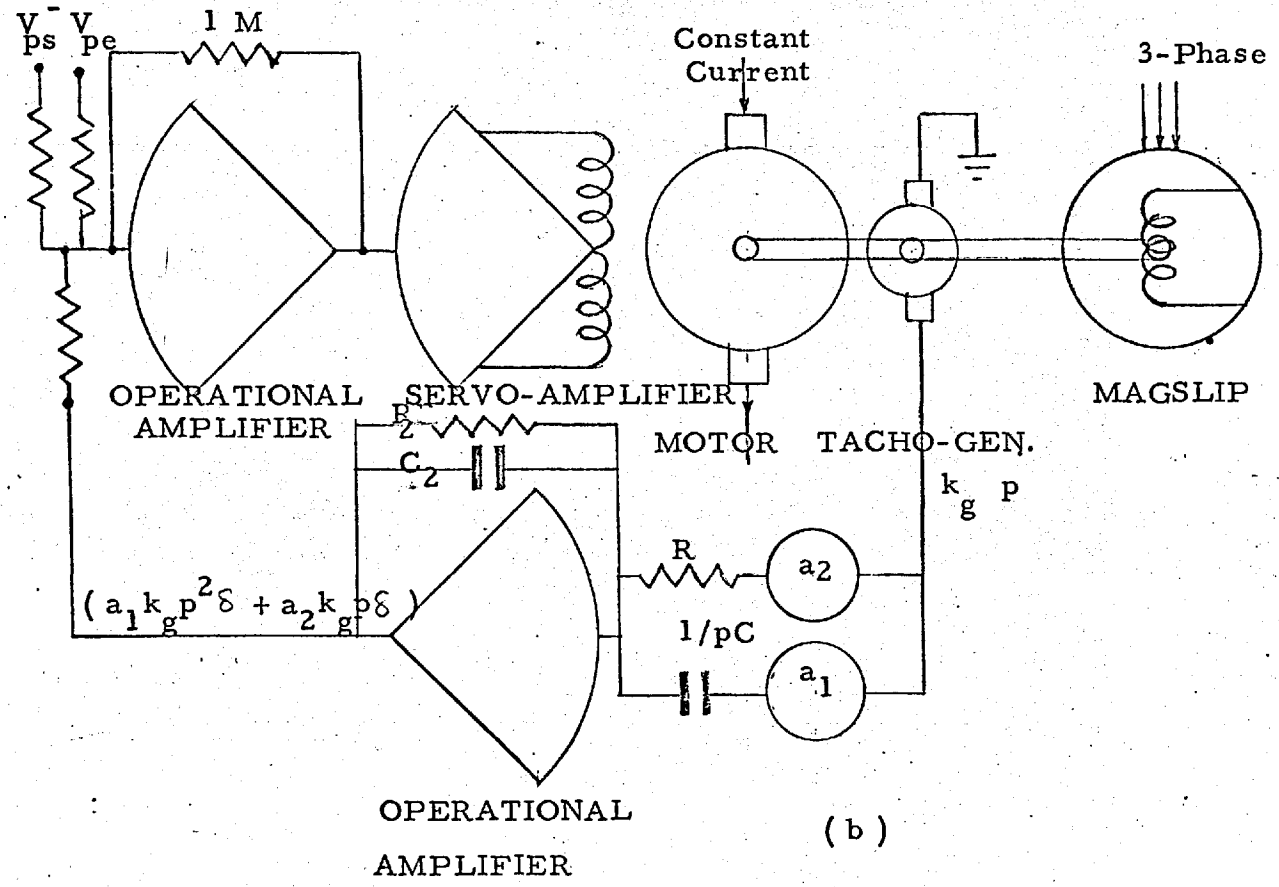

(b)

FIG: 2.10

SIMULATION OF INERTIA AND DAMPING

with the feed back resistor R_2 reduces the high frequency noise.

For the values of the components given in fig.2.10b :

$$V_3 = pV_1 + V_2$$

If kg is the tacho-generator constant (volts/speed) a_1 & a_2 are the fractions of tacho-output fed to the amplifier.

$$V_3 = (a_1 nkg\ p^2\delta + a_2 nkg\ p\delta)$$

$p\delta$ is the speed of the magslip shaft and n is motor-magslip reduction ratio. The input to the servo-amplifier

$$Vg = (V_{ps} - V_{pe}) + (ank_g\ p^2\delta + a_2 nk_g\ p\delta)$$

$$= (V_{ps} - V_{pe}) + (ak'_g\ p^2\delta + a_2 k'_g\ p\delta)$$

where V_{ps} is the steam power input, V_{pe} is the signal from the electronic wattmeter proportional to the signal applied to the servo amplifier and if the motor armature current is kept constant, the torque produced is proportional to the field current.

$$I_f = \frac{G_m \cdot V_g}{(1 + p\,T_f)}$$

$$f_a = J_m\ p^2\delta + K_{dm}\ p\delta = K_a\ I_f$$

where G_m is the gain of the amplifier

T_f is the motor-field time constant

f_a is the accelerating torque

J_m is the motor and magslip inertia seen from the magslip shaft

K_{dm} is the frictional torque coefficient seen from the magslip shaft.

Combining these two equations

$$V_g = \frac{(1 + pT_f)}{K_a G_m} \left[J_m p^2\delta + K_{dm} p\delta \right] \quad \ldots\ldots 2.3.2.$$

Combining 2.3.1 and 2.3.2.

$$(V_{ps} - V_{pe}) + a_1 K'_g p^2\delta + a_2 k'_g p\delta =$$

$$\frac{(1+p T_f)}{K_a G_m} \left[J_m p^2\delta + K_{dm} p\delta \right]$$

$$\left[a_1 k'_g + \frac{(1 + p T_f)}{K_a G_m} \cdot J_m \right] p^2\delta + \left[a_2 k'_g + \frac{(1+pT_f)}{K_a G_m} K_{dm} \right] p\delta$$

$$= - (V_{ps} - V_{pe})$$

If G_m is sufficiently large and T_f is small which is the case for most servo amplifiers and motors, terms like $\frac{(1 + p T_f)}{K_a G_m} J_m$ and $\frac{(1 + p T_f)}{K_a G_m} \cdot K_{dm}$ can be neglected.

Then

$$a_1 k\acute{g} \cdot p^2\delta + a_2 kg \cdot p\delta = -(Vps-Vpe) \quad 2.3.3.$$

Comparing eq=n 2.3.3. with the torque balance equation 2.1.24 but replacing the torques by power since speed is assumed constant.

$$P_m - P_e = \frac{2H}{w} p^2\delta + \frac{K_d}{w} p\delta$$

$$\frac{2H}{w} = a_1 k\acute{g}$$

$$\& \quad \frac{K_d}{w} = a_2 k\acute{g}$$

a_1 & a_2 being the pot-settings, provide the facility of varying the feed back and so different inertia and damping constants to be simulated.

Several practical difficulties were experienced in the implementation of this scheme.

The acceleration signal is obtained by differentiating the voltage from a D.C. Tacho-generator. The output of the tacho-generator is in fact rectified A.C. and at very low speeds contains a very large ripple component. Because of the property of the differentiating circuits for amplifying the high frequency signals, a very large ripple component is given out by the differentiator. Under these conditions the servo motor failed to pick up

speed smoothly even for step inputs of accelerating torques.

Possibilities were explored for the use of an A.C. tacho (also known as an induction generator). The control winding of the induction generator is supplied from a 400c/s A.C. The output of the device also has a frequency of 400c/s but amplitude is proportional to the speed. Since the swing frequency of the synchronous generator is very small compared to 400 c/s, it is possible to extract an acceleration signal after rectification and differentiation. During this speculative stage the operation of the induction generator under D.C. excitation was being examined by the author and the possibility arose of using the induction generator as an acceleration transducer. It was later found that the device has in fact, already, been used for this purpose.(ref. 59) The operating principle is described with reference to fig. 2.11.

A d.c. current in one winding produces flux proportional to the current. When the rotor accelerates flux is produced at an angle 90° to the main flux and thus links with the second winding and induces in it a voltage proportional to the acceleration. The following

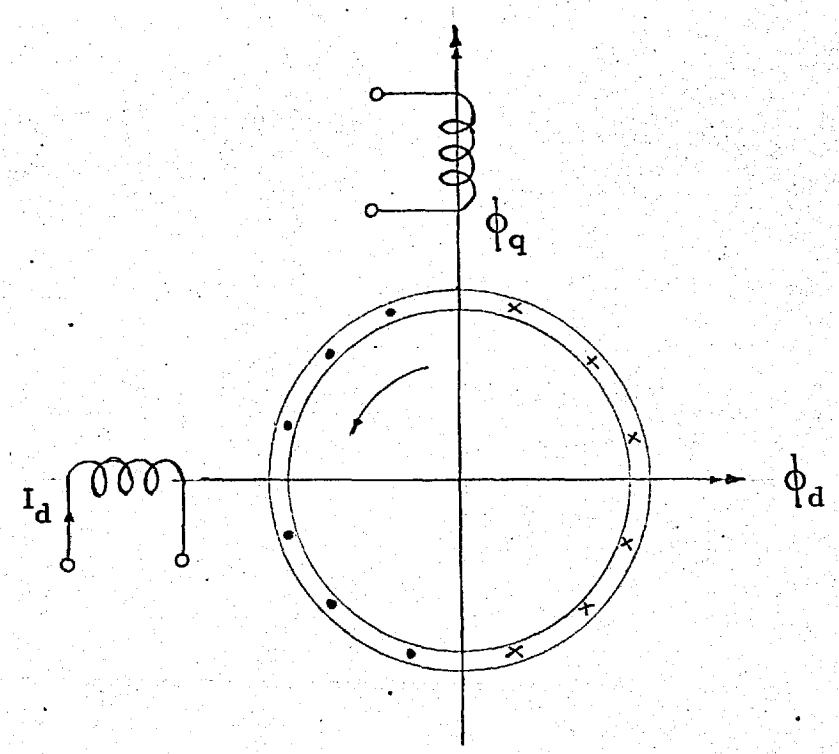

FIG: 2. 11

INDUCTION GENERATOR AS

ACCELERATION TRANSDUCER

equations eloquently explain the process.

$$\phi_d = K_1 I_d$$

$$\phi_q = K_2 w \phi_d = K_1 K_2 w I_d$$

$$\frac{d\phi_q}{dt} = K_1 K_2 I_d \frac{dw}{dt}$$

$$E_q = K_3 \frac{d\phi_q}{dt} = K_1 K_2 K_3 \frac{dw}{dt}$$ (type 11M248)

A 2 phase drag cup induction motor made by VACTRIC CONTROL EQUIPMENT LTD. was available in the laboratory and was found to be a reliable accelerometer, provided that a noise-free D.C. amplifier stage is provided close to the output terminals. This device was tried in the scheme shown in fig. 2.12. The system behaved better under step accelerating conditions compared with the scheme of fig. 2.10. But this scheme was still unsatisfactory for small signal conditions for the reasons discussed below.

It was assumed in the derivation of equation 2.3.2. that the torque developed is proportional to the current in the field and that the torque speed characteristics of the motor are linear. Unfortunately the motor showed considerable hysteresis effect and non-linearity in the

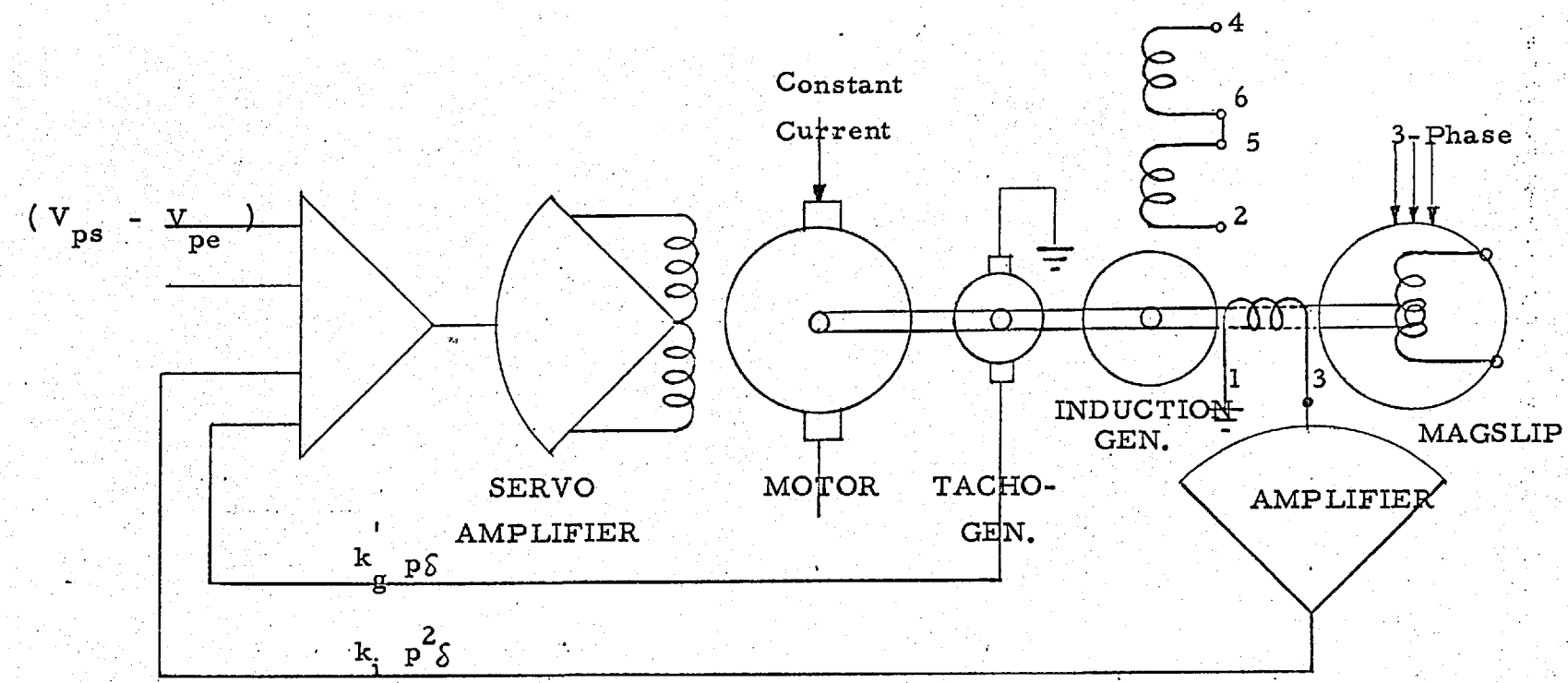

FIG: 2. 12

SIMULATION OF INERTIA AND DAMPING

USING TACHO-GEN. AND INDUCTION GEN.

torque speed characteristic due to static friction. If the steady speed is measured as a function of the control field current I_f the curve shown in fig. 2.13.b is obtained. This characteristic shows an unacceptable non-linearity.

The effects of the non linearity in a system can be reduced if it has a very high open loop gain and a large proportion of the controlled variable is fed back. The elementary text book treatment on servo-mechanisms which mainly deal with position or speed control does not clearly emphasise this point, because in fact the open loop gain in the former case is infinite and in the second case is very high. In the type of mechanism which has been discussed above we are in fact trying to control the acceleration and such a system has zero steady-state gain, Although this system looked promising when discussed qualitatively and supported by mathematical treatment, the assumption of linearity in the torque versus field current characteristic was fatal.

The system shown in Fig. 2.10b gave good results when a steady speed bias is provided to the motor and the accelerating signals are superimposed. The speed bias

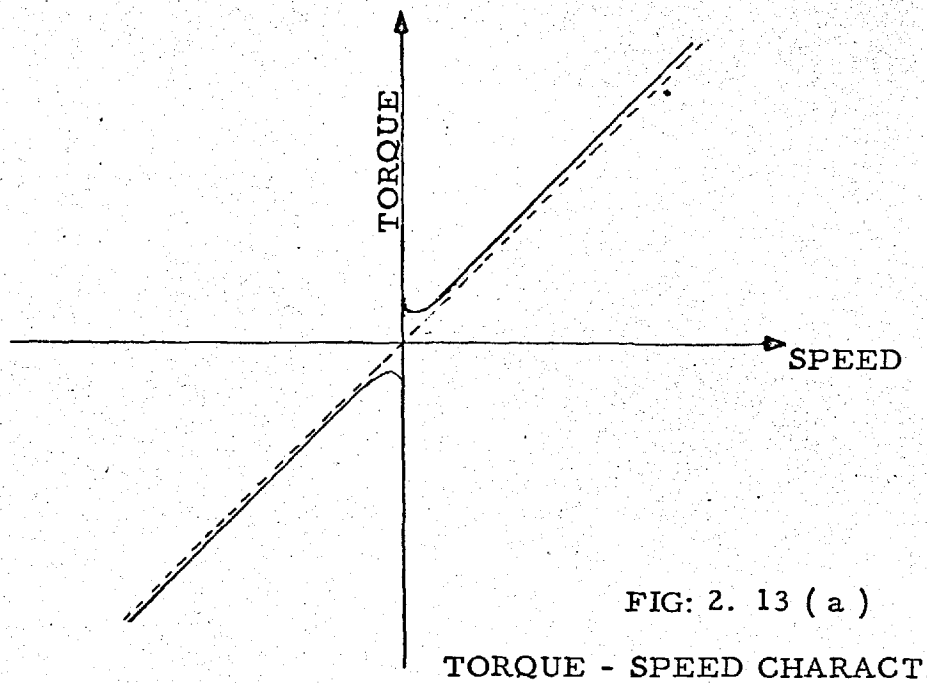

FIG: 2. 13 (a)

TORQUE - SPEED CHARACTERISTIC

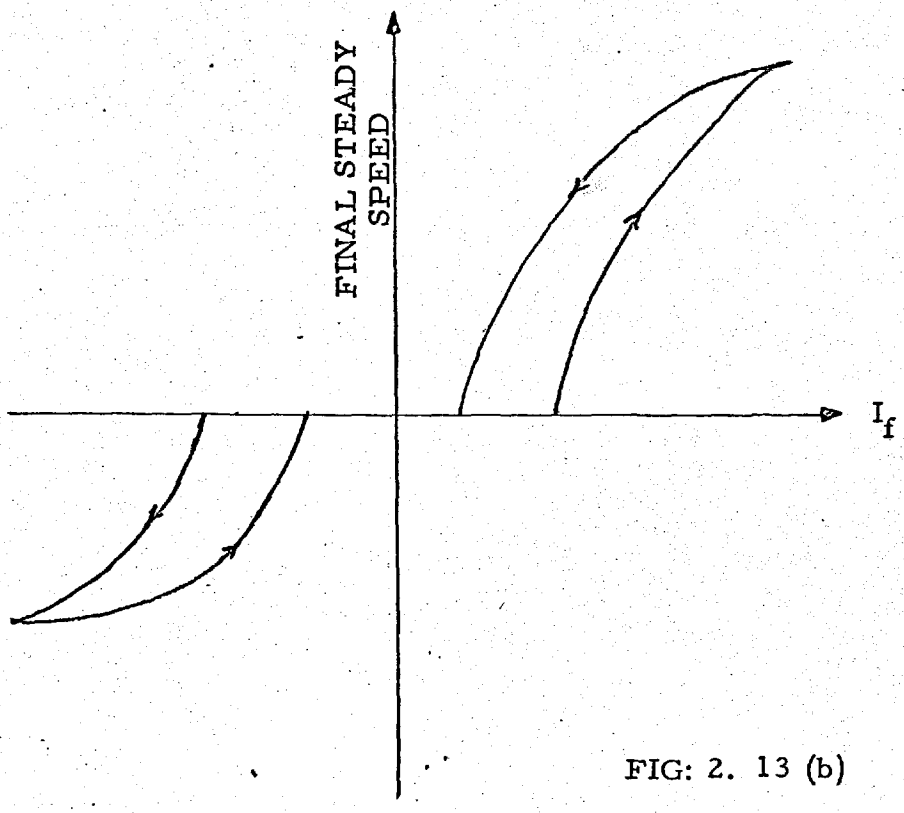

FIG: 2. 13 (b)

CONTROL FIELD CURRENT - FINAL STEAI
SPEED

SHOWING NON- LINEARITIES IN THE
SERVO-MOTOR

given was enough not to cause the motor to go through a zero speed condition. The possibility at this stage was explored of exciting the magslips from a 48 c/s supply enabling the system to be run with a steady speed, but had to be abandoned for the following reasons.

(i) Additional requirement of a 3-phase supply af 48 c/s for the magslip with high frequency stability.

(ii) The simulation of zero-speed of magslip rotor for the synchronous speed of the machine has the great merit, that provided with suitable power input signals and excitation level, or the terminal voltage, all the machines in the simulator can be brought in use, while the scheme for giving a steady speed bias will require the machine to be run up to the correct speed, connected to the system, and then gradually loaded, in much the same way as the machine is synchronised in an actual system.

(iii) Continuous running of the motor will, of course, shorten the life of the motor. Commutator and brush troubles have been reported in C.E.R.L. model.(ref. 47.)

2.3.2. SIMULATION OF INERTIA AND DAMPING ON THE ANALOGUE COMPUTER

From the discussion in section 2.3.1. it is abundantly clear that the problems of non-linearities can be completely eliminated if the magslip drive controls the speed and not the acceleration. The mechanical equation governing the rotational motion of the magslip rotor can be solved on the analogue computer in terms of the speed and the output signal used to control the servo-mechanism. A speed control servo-mechanism is more commonly known as Velodyne.

The equation

$$P_m - P_e = \frac{2H}{w} p^2\delta + \frac{K_d}{w} p\delta$$

$$= M p^2\delta + K_d' p\delta$$

can be arranged as

$$p\delta = \frac{1}{M}\int (P_a - K_d' \cdot p\delta)\ dt$$

The magslip in following this speed signal will automatically perform the second integration. In fact an accurate velodyne is used as a mechanical integrator.

2.3.3. DESIGN OF VELODYNE

A few essential points about the design of the velodyne are included in this section.

The determining factor for the selection of the gear ratio from the motor shaft to the magslip shaft is the limit on the acceleration of the motor shaft. The maximum acceleration of the rotor will be dependent upon the lowest inertia of the machine to be simulated.

A ratio of three was selected. For the convenience of lay-out on the base plate and cutting down the friction due to metallic gear wheels, timing belts and gear system was used.

Ever-shed and Vignoles split field D.C. servo-motor generator type F.B.A1/A1/BD having the highest ratio of the total torque/frictional torque is used for the drive. The field is excited from a specially developed servo-amplifier which is a modification of servo-amplifier type S A 61 (see section 3.1.3.) The armature of the motor is supplied with constant current supply of 1.5 amps. Details of this power supply are given in section 3.3.

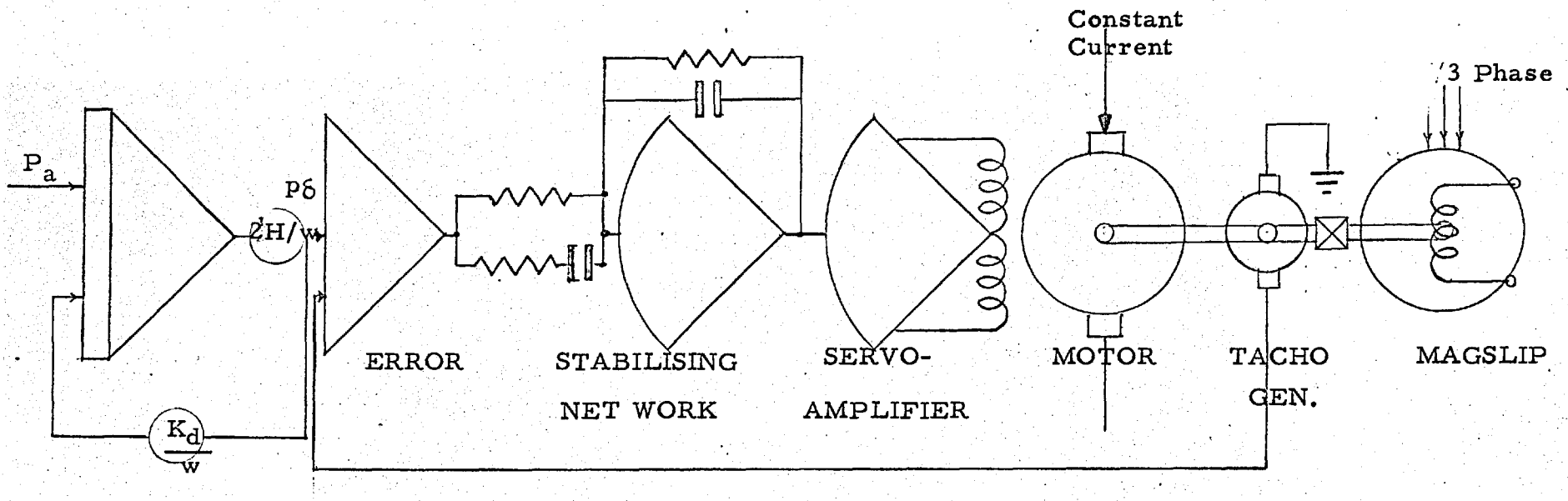

VELODYNE

FIG: 2. 14

SIMULATION OF INERTIA AND DAMPING USING ANALOGUE COMPUTER AND VELODYNE

Open loop frequency response of the velodyne system was investigated with the help of a Solartron Transfer Function Analyser with 1% negative feed-back. The Nyquist diagram and the corresponding pole-zero pattern is shown in fig. 2.15. The system seems to have a transfer function of the type $\frac{K}{(1+pT_1)\ (1+pT_2)}$. The following values were estimated from the open loop frequency response K = 700 T_1 = 0.08 secs. = T_2. The two time constants are due to inertia/friction and the field winding. The 180° line pattern is also shown in fig. 2.16. The system is inherently stable one.

For our purpose, obviously the most desirable position for the closed loop poles is on the negative real axis far removed from the origin. The velodyne will in this case have a response which is (i) non-oscillatory (ii) has very small output lag.

The forward path pole-zero pattern is modified to give a single zero (fig. 2.17)

The gain can then be adjusted to have the closed loop poles at the desired position. For a double pole at -500 an open loop gain of 2800 is needed.

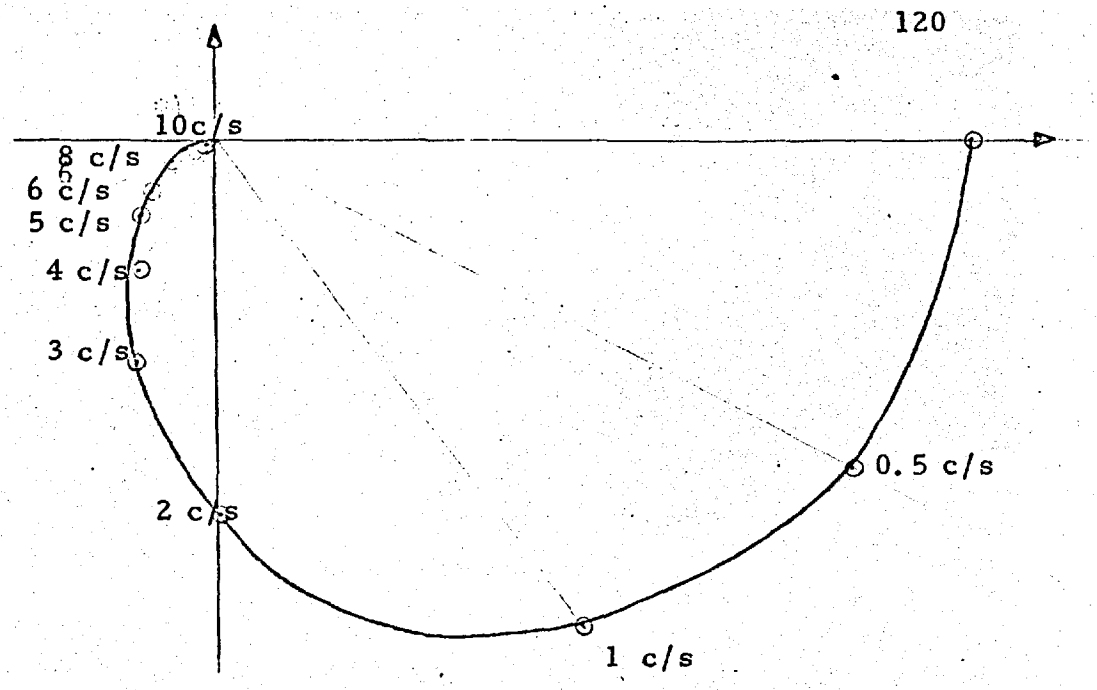

FIG: 2. 15 OPEN LOOP FREQUENCY RESPONSE CURVE

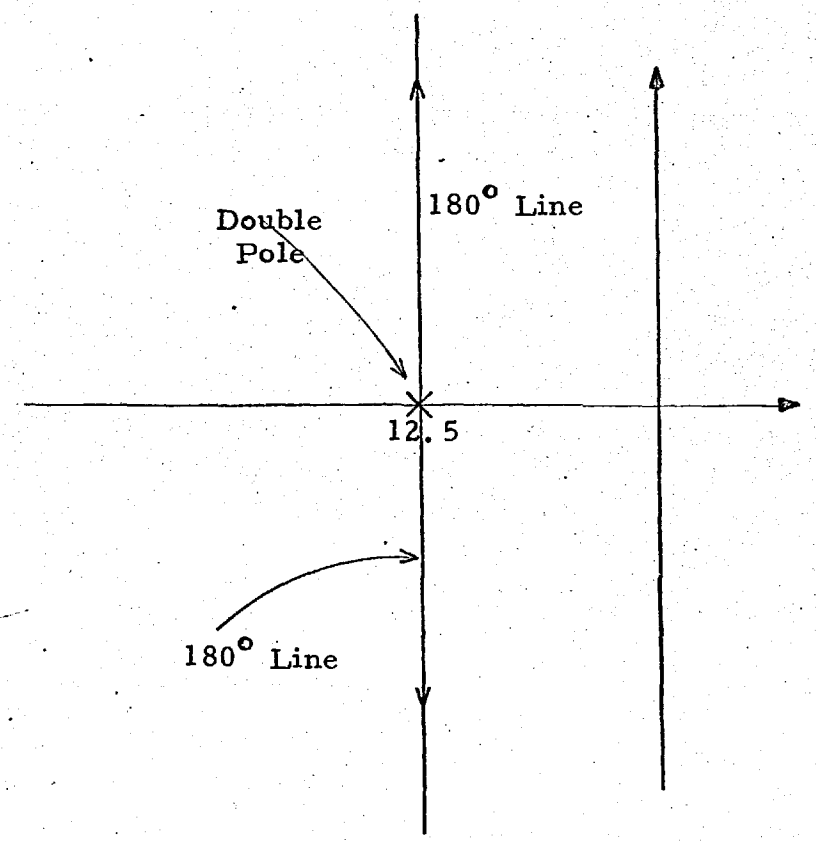

FIG: 2. 16 p-PLANE PLOT OF OPEN LOOP TRANSFER FUNCTION

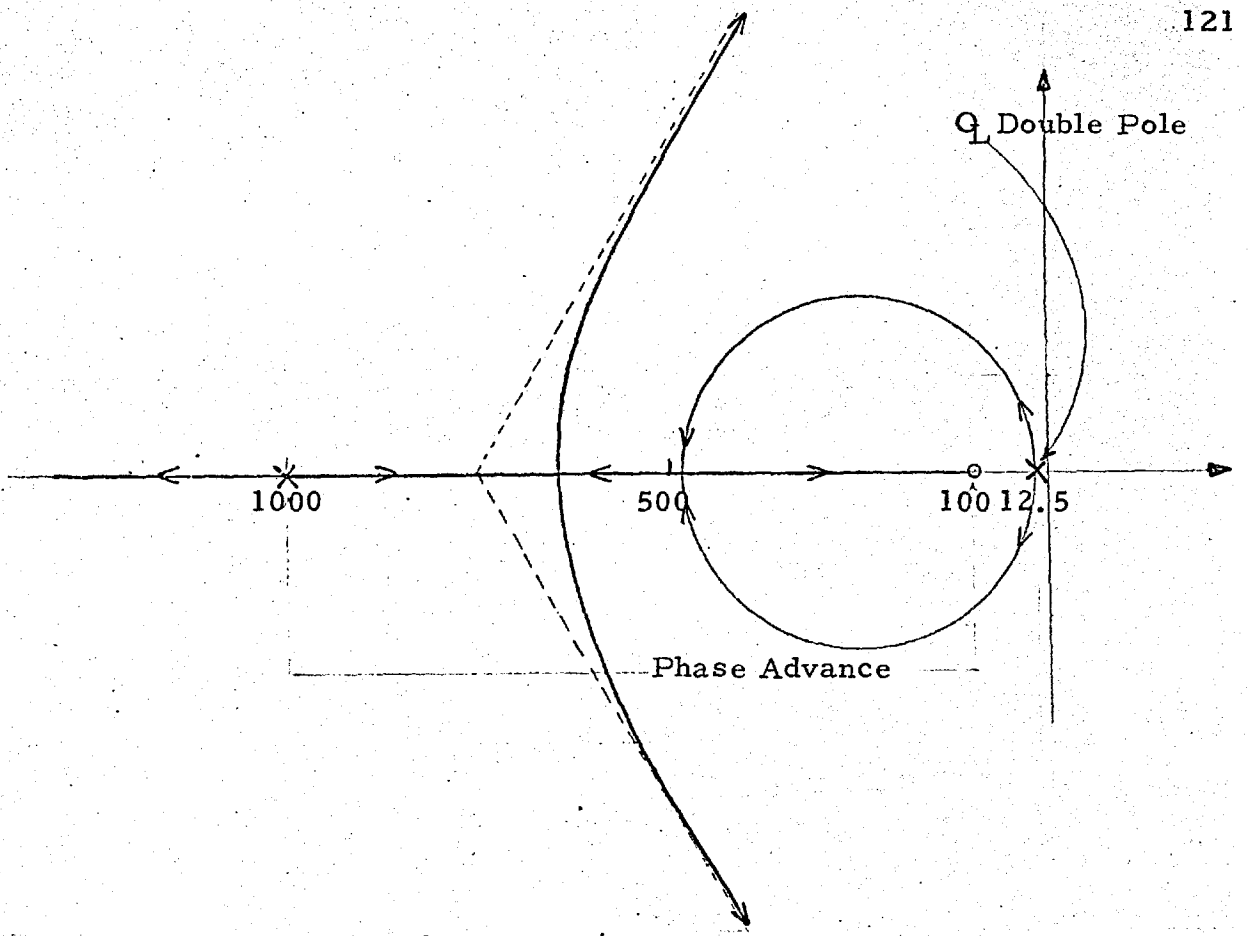

FIG: 2. 17 180° LINE PATTERN MODIFIED BY PHASE ADVANCE

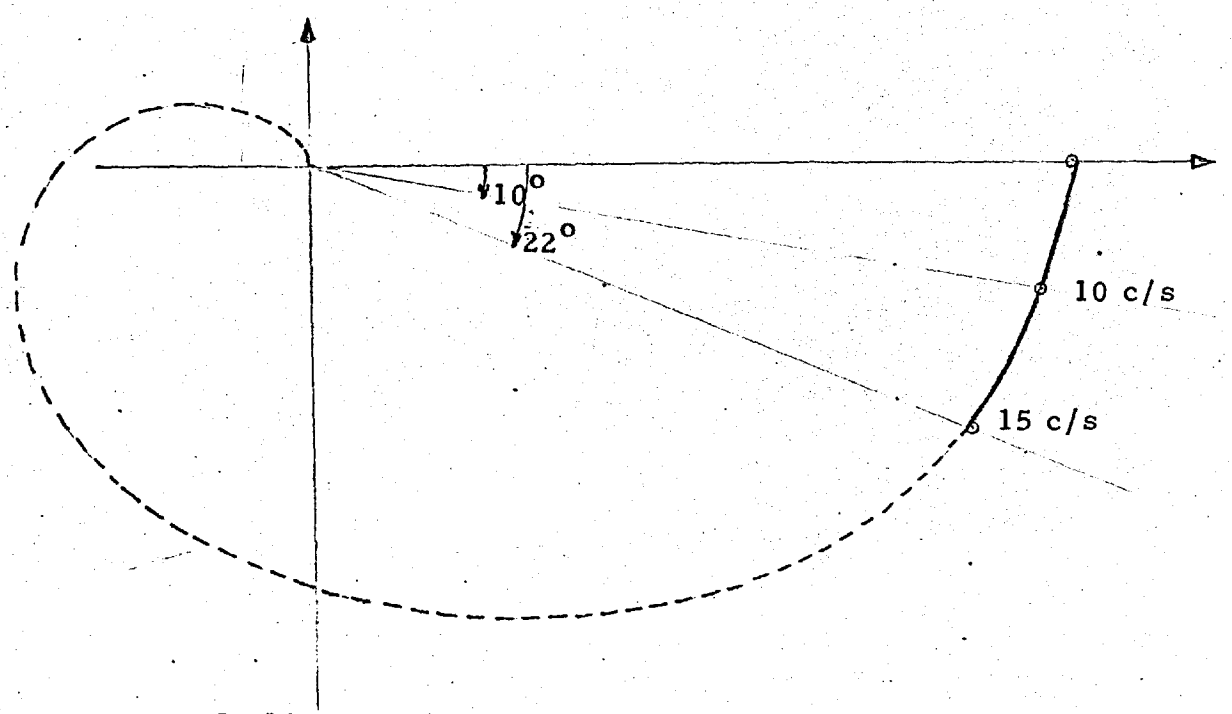

FIG : 2. 18 CLOSED LOOP FREQUENCY RESPONSE OF VELODYNE

The closed loop response can now be checked by the help of a T.F.A. The results are shown in fig. 2.18. Because of the unbalance in the field windings at high frequency the closed loop frequency response could not be checked beyond about 17 c/s. Closed loop response of the velodyne system is shown for very small signals at low frequency (1c/s), ramp input and step input in figs. 2.19; 2.20; 2.21.

2.3.4. CALIBRATION

(i) INERTIA : The moment of inertia of the machine in the p.u. system, is expressed by the inertia constant, denoted by H and defined by the following relation.

$$H = \frac{\text{Stored energy at the synchronous speed in KW-SEC}}{\text{Rated KVA}}$$

In the p.u. system, unit power is defined equal to that given by rated KVA at unity power factor. So H is in fact p.u. stored energy. It has the dimension of time and its value is given in seconds.

The relation between the moment of inertia and the H-constant is derived as follows :

If fa is the accelerating torque, J moment of

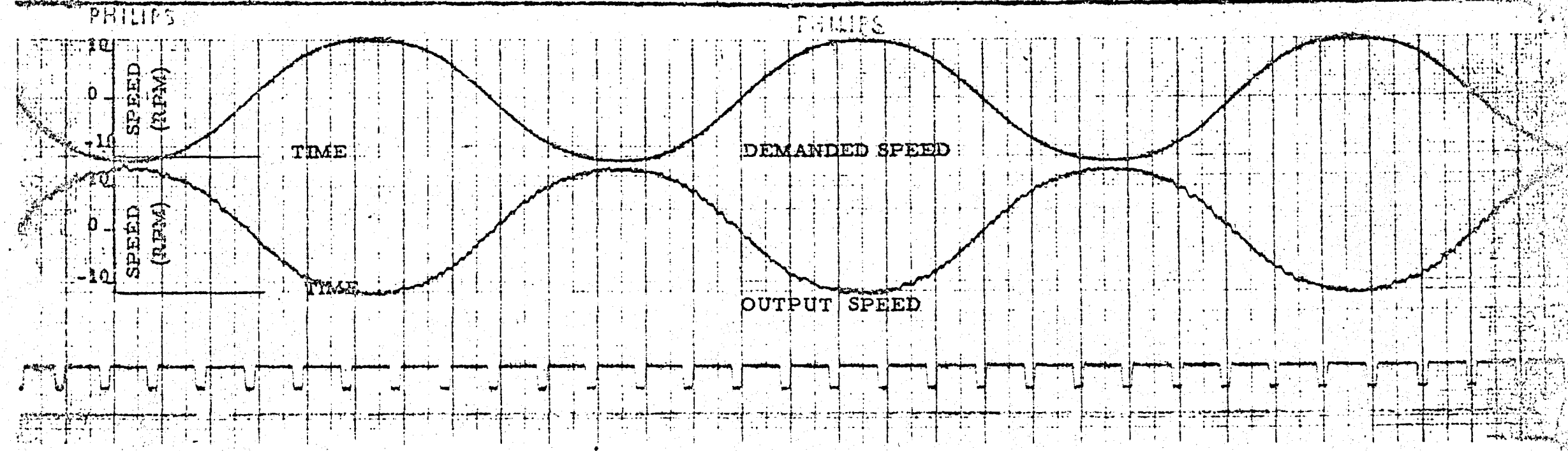

FIG : 2.19

VELODYNE CLOSED LOOP RESPONSE TO

SMALL LOW FREQUENCY SIGNALS

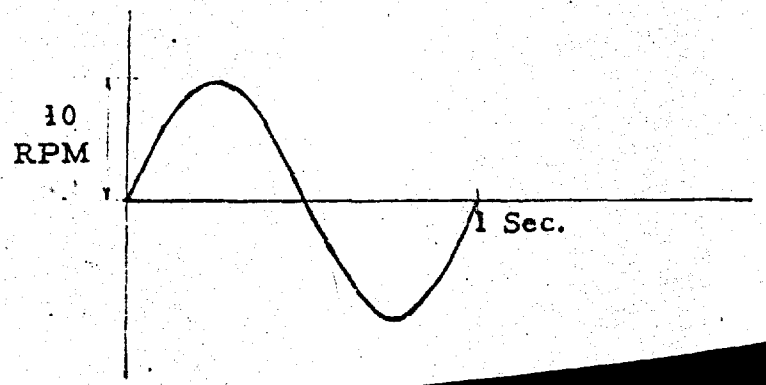

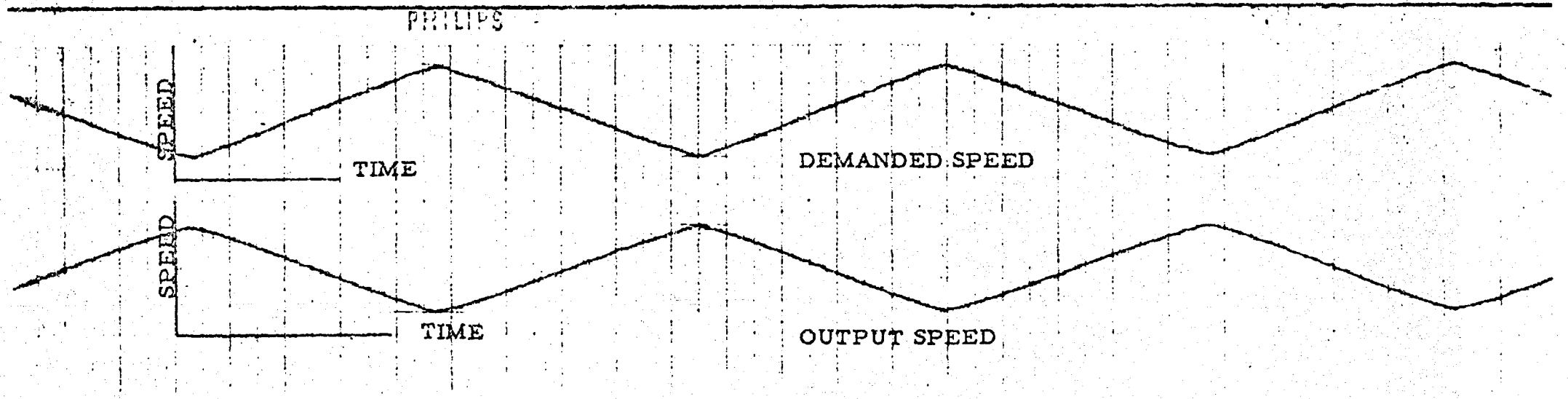

FIG : 2. 20

VELODYNE CLOSED LOOP RESPONSE

TO RAMP INPUT SIGNALS

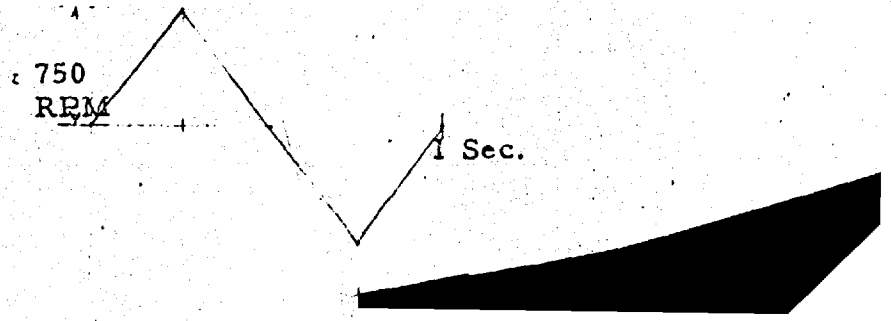

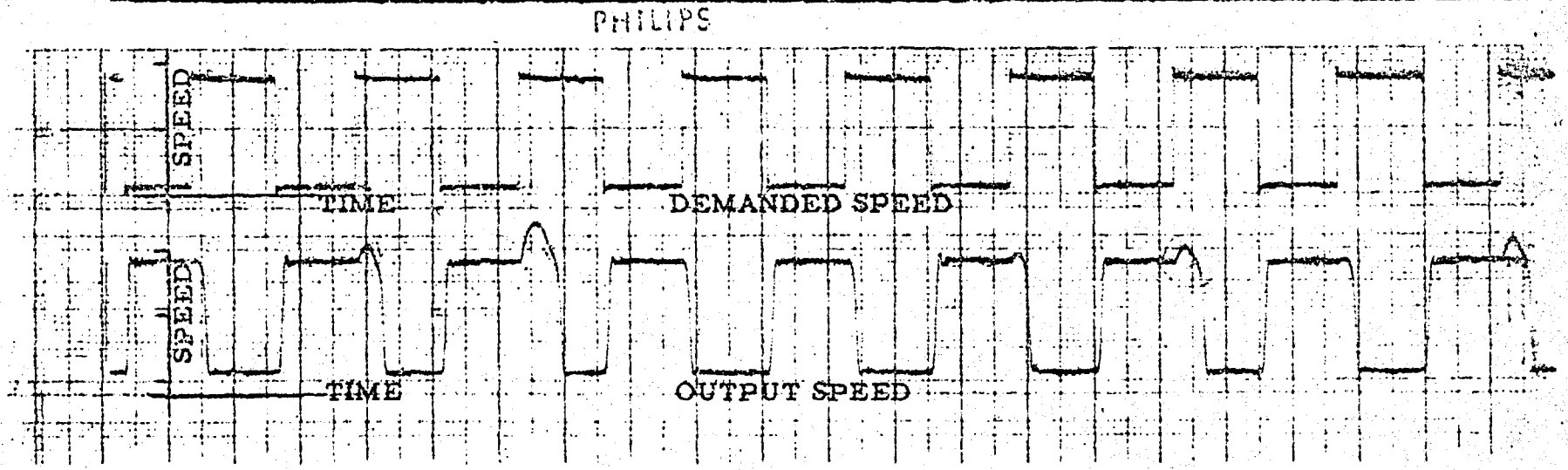

FIG: 2. 21

VELODYNE CLOSED LOOP RESPONSE

TO STEP INPUT SIGNALS

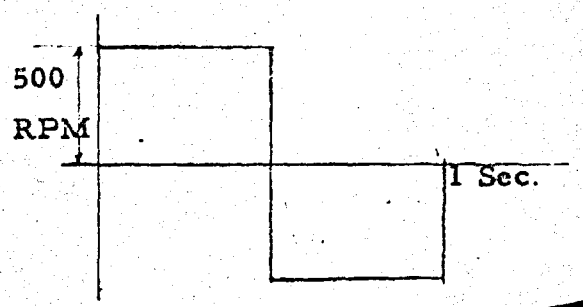

inertia of the rotor, and V the rotational speed then the following relation is true in any consistent dimensional units.

$$fa = J. \frac{d\omega}{dt} \qquad 2.3.1.$$

If the rotor of the machine be accelerated uniformly from rest to the rated speed w in one second the torque from eq=n 2.3.1. will be equal to Jw.

The stored energy is that produced by the power corresponding to the mean speed, i.e. $^{w}/2$

$$\text{Stored energy} = \tfrac{1}{2} Jw^2$$

In the p.u. system, unit torque is defined as the torque which produces unit power at the nominal speed w and the unit of energy is given by unit power acting for one second. In the p.u. system the stored energy is given by $\frac{1}{2}$ Jw

From the definition of H

$$H = \tfrac{1}{2} Jw$$

and $$J = \frac{2H}{w}$$

Eq=n 2.3.1. can be written as

$$f_a = \frac{2H}{w} \cdot \frac{d\omega}{dt}$$

Now if a unit accelerating torque is applied the rotor will reach the rated speed w in 2H seconds. If Vpe (volts) is the output from the electronic wattmeter for 1 unit power, the output of the integrator after 2H seconds will be 2H Vpe (volts) and this is equal to the rated speed w. If the tacho-generator output is G (volts) at the magslip rotor speed of w then $\frac{G}{2HVpe}$ of the integrator output will be fed into the velodyne system.

DAMPING

Due to the characteristics of the prime-mover generator and transmission system, oscillations due to disturbances are often damped. Prime-mover torque increases due to the decrease in speed. The damper winding, during the swing, act very much like an induction motor operating in the straight line portion of the torque-slip characteristic. Recent investigations have shown that transmission lines and loads also contribute to the positive damping. In a simplified case like the one we are discussing at the moment, the damping represented is to account approximately for the action of the damper winding.

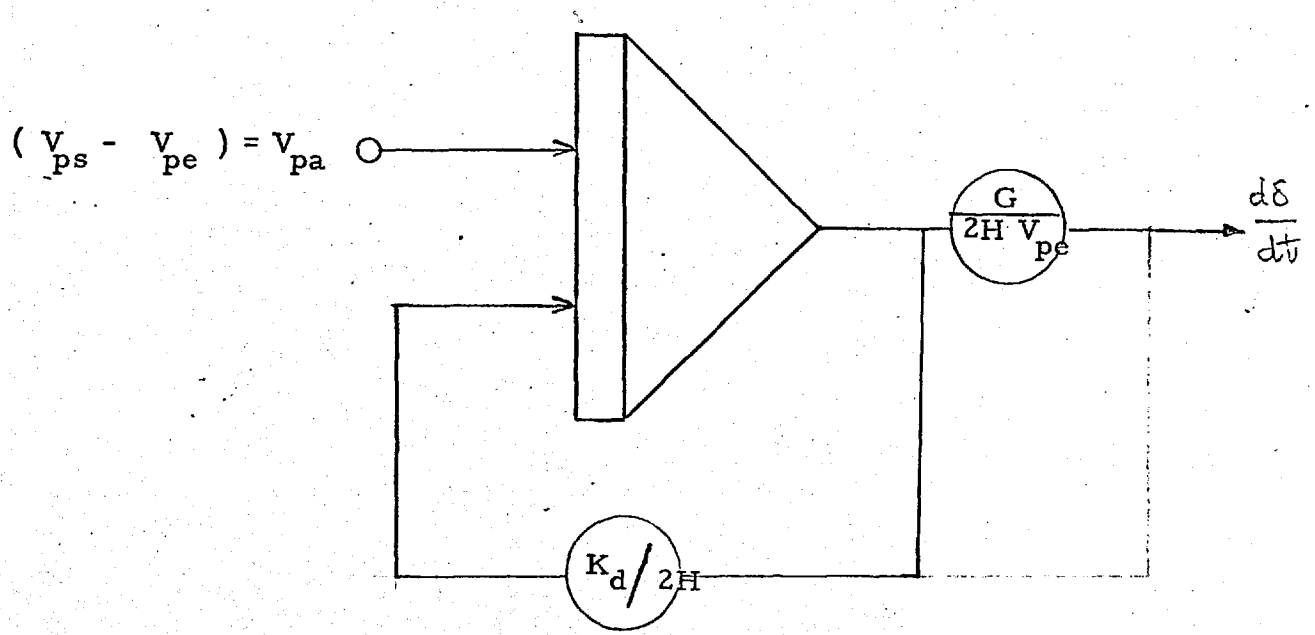

FIG: 2. 22

POTENTIOMETER SETTINGS FOR

INERTIA CONSTANT

AND

DAMPING COEFFICIENT

Damping in the p.u. system is represented by a damping co-efficient denoted by K_d and is equal to the p.u. change in torque due to 1 p.u. slip.

Since the base speed w at the integrator output is 2H x Vpe volts p.u. slip is given by $\frac{\text{O/P of the integrator}}{2H \times Vpe}$

The p.u. change in torque is $\frac{K_d \times \text{O/P of the integrator}}{2H \times Vpe.}$

Converted into volts at the integrator input change in torque (in volts) = $\frac{K_d \times \text{O/P of the integrator}}{2H \times Vpe} \times Vpe.$

$$= \frac{K_d}{2H}$$

This arrangement is shown in fig. 2.2.2.

2.3.5. COMPENSATION FOR THE DELAYS DUE TO POWER MEASUREMENT AND VELODYNE SYSTEM

The closed loop response of the velodyne system is represented in the pole zero diagram of fig. 2.17. The system experimentally checked showed very little phase shift up to 10c/s. The swing frequency is much lower.

The electronic wattmeter used is described completely in section 3.5.2. At first sight this

appears to be a device which measures power every cycle of the A.C. wave and was expected to introduce delays negligible for our purpose.

It was found on completing the analogue that these delays introduce inaccuracies in the inertia and damping simulation and in fact for low values of the damping coefficient the machine simulator hunts. At this stage it was decided to look into the delays due to the power measuring technique more carefully and compensation provided for that.

The electronic wattmeter is essentially a "SAMPLE & ZERO ORDER HOLD DEVICE" (see section 3.5.2.) At the instant when the voltage is passing through its peak the current has the instantaneous value $I \cdot \cos\phi$. (It is proportional to power for constant voltage). This value is sampled and held constant until the next peak when the previous sample is destroyed and the new value is sampled. Since the device does not interpolate the measured power in between the two sampling periods it is called a zero order hold device. The output of this device is shown in fig. 2.23. and mathematically expressed as a series.(ref.75

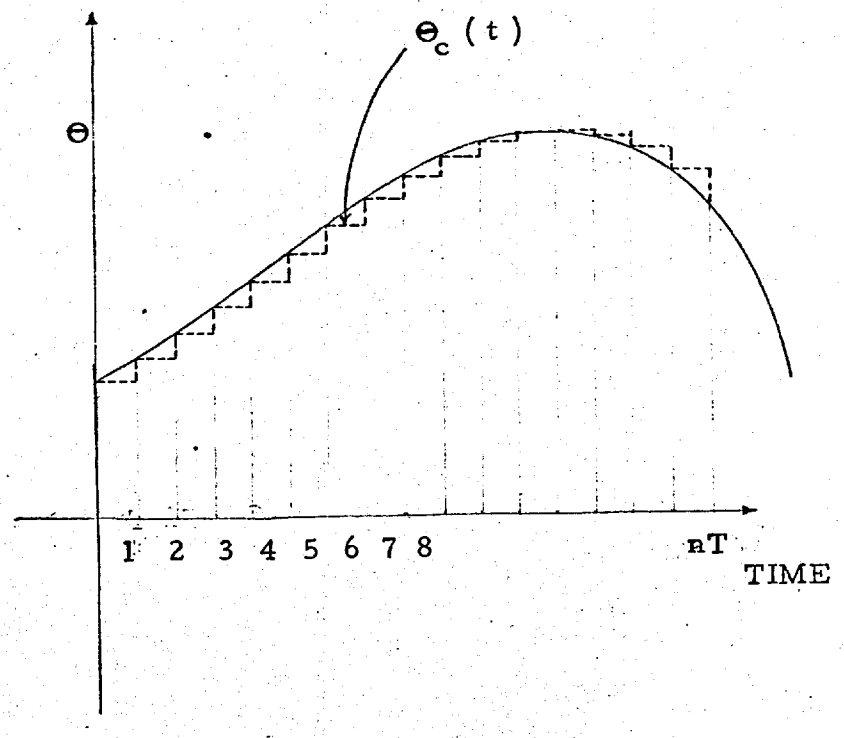

FIG: 2. 23

OUT PUT OF A SAMPLE & ZERO ORDER HOLD DEVICE

$\theta_c(t) = a\ U_T(0) + a_1 U_T(T) + a_2(2T) + \ldots a_n(nT)$

where a_0, a_1, $a_2 \ldots a_n$ are the values of the input wave at the instant of sampling and $U_T(nT)$ if the unit square wave lasting from t = nT to t = (n + 1) T where T is the sampling period.

Laplace's Transform of $U_T(nT)$ is $(\frac{1 - e^{-pT}}{p})e^{-npt}$

$$\theta_c(t) = (\frac{1 - e^{-pT}}{p})\quad a_o + a_1 e^{-pT} + a_2 e^{-2pT} + \ldots.$$

$$\ldots a_n e^{-npT}$$

$$= C(p)\ \bar{\theta}*$$

$\bar{\theta}* = a_o + a_1 e^{-pT} + a_2 e^{-2pT} + \ldots a_n e^{-npT}$ is an impulse modulated form of θ (input) and contains all the information θ (t) has.

The Laplace Transform of the zero order hold device is given by $(\frac{1 - e^{-pT}}{p})$ and denoted as C (p).

Frequency response of the hold device is

$$C(jw) = \frac{1 - e^{-jwT}}{jw}$$

$$= \frac{2 \text{ Sin } wT/2}{w} \angle - wT/2$$

$$= T. \frac{\text{Sin } wT/2}{wT/2} \angle - wT/2$$

$$= T. \angle - wT/2 \quad (\because \text{For small values of } \frac{\text{Sin } wT/2}{wT/2} \quad 1.)$$

The device behaves as if there is a finite lag of $T/2$ which in our case is 10 m - sec.

A simpler approach to the problem and giving a better physical picture is to use a Fourier Analysis to the stepped output of the device (ref. 76) Only the fundamental component is of importance.

If the input to the zero-order hold device is D Sin wt and the first sample is taken at wt = ϕ and n is the number of samples/cycle then $\theta c(t)$ which is stepped can be written as

$$\theta c\ (t) = D \text{ Sin } \left[\phi + (m-1)\ \frac{2\pi}{n}\right] \text{where } m = 1, 2, 3 \ldots n$$

The co-efficients of the fundamental components of the Fourier Series are given by the formulae

$$A_1 = \frac{1}{\pi} \int_{\phi}^{2\pi+\phi} \theta_c(t) \text{ Cos wt dwt}$$

$$B_1 = \frac{1}{\pi} \int_{\phi}^{2\pi+\phi} \theta_c(t) \text{ Sin wt dwt}$$

and are found to be

$$A_1 = \frac{nD}{\pi} \text{ Sin}^2 \left(\frac{\pi}{n}\right) \text{ \& } B_1 = \frac{nD}{\pi} \text{ Sin } \left(2\pi/n\right)$$

The magnitude of the fundamental component is given by

$$\sqrt{A_1^2 + B_1^2} = \frac{nD}{\pi} \sqrt{\text{Sin}^4\left(\frac{\pi}{n}\right) + \tfrac{1}{4} \text{ Sin}^2\left(2\pi/n\right)}$$

$$= D\ \frac{\text{Sin } \pi/n}{\pi/n} \qquad 2.3.2.$$

If π/n is small $\frac{\text{Sin } (\pi/n)}{\pi/n} \longrightarrow 1$

and the phase difference

$$= \tan^{-1} (-A1/B1) = \tan^{-1} \frac{-2\text{Sin}^2 \pi/n}{\text{Sin } (2\pi/n)}$$

$$= - \pi/n \qquad 2.3.3.$$

combining equations 2.3.2. & 2.3.3.

the output is given by D Sin (wt - π/n)

Where the machine swing frequency is of the order of 1c/s and there are 50 samples/second (π/n) is of the order of $180/50 = 3.6^{o}$.

From the discussion above it follows that if we can introduce a phase-advance in the power measuring circuit of the type $(1+pT_a)$ where T_a is 10 m.sec. it will effectively neutralise the effect of the delay in the power measuring circuit. In fact T_a slightly higher than 10 m-sec. say 12 m-sec. was used. This can compensate lag due to the velodyne system. This phase advance can be introduced by the standard circuit shown in fig. 2.2.4.

After providing this compensation the machine simulator behaved perfectly satisfactorily and the potentiometer settings for the calibration of inertia and the damping co-efficient could then be correctly worked out by the formulae given in section 2.3.4.

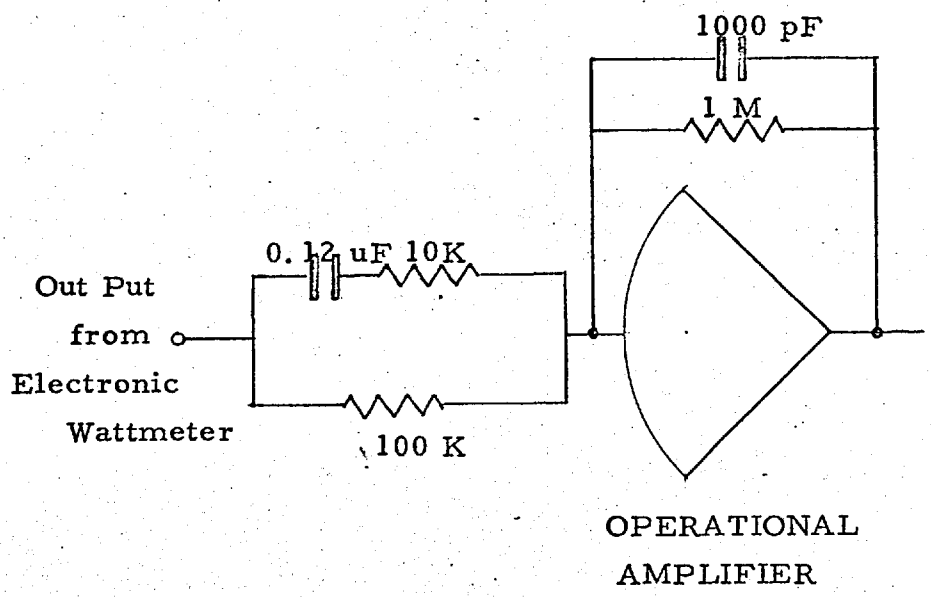

FIG: 2. 24

PHASE ADVANCE IN THE
POWER MEASURING LOOP

2.3.6. CHECKING THE CALIBRATION FOR INERTIA AND DAMPING

The settings for inertia and damping can be very effectively checked by recording the rotor oscillations of small amplitude around a point of equilibrium. The power angle curve for small displacements in angle can be considered as a straight line tangent to the curve at the equilibrium point. The swing equation in this case becomes a second order linear differential equation.

$$\frac{2H}{w}\frac{d^2\delta}{dt^2} + \frac{K_d}{w}\frac{d\delta}{dt} = T_s(\delta_m - \delta)$$

where T_s is the slope of the power - angle curve at the point of equilibrium.

$T_s \delta_m$ - is the mechanical input torque.

Initially $\delta_m = \delta = \delta_o$

Now consider a change in input torque of $Ts\,\delta'_m$ and if δ' is the change of load angle from the equilibrium position δ_o

$$\frac{2H}{w} \times \frac{d^2\delta}{dt^2} + \frac{K_d}{w}\frac{d\delta}{dt} = Ts\,(\overline{\delta_m + \delta'_m} - \overline{\delta_o + \delta'})$$

where $\delta = \delta_o + \delta'$ is instantaneous load angle.

The differential equation can now be converted in the form of increments in δ.

$$\frac{2H}{w} \times \frac{d^2\delta'}{dt^2} + \frac{K_d}{w}\frac{d\delta'}{dt} = Ts\,(\delta'_m - \delta')$$

$$\frac{2H}{w} \times \frac{d^2\delta}{dt^2} + \frac{K_d}{w}\frac{d\delta}{dt} + Ts\delta' = Ts\,\delta'_m \qquad 2.3.4$$

If the impulse $T_s\delta'_m$ is approximated by differentiating a step then transforming 2.3.4. in Laplaces' operator.

$$\frac{2H}{w} p^2\delta' + \frac{K_d}{w} p\,\delta' + T_s\delta' = T_s\delta'_m$$

$$\delta'(p) = \frac{Ts\delta'_m}{\frac{2H}{w}p^2 + \frac{K_d}{w}p + T_s} = \frac{\delta'_m}{\frac{2H}{T_s w}p^2 + \frac{K_d}{T_s w}p + 1} \qquad 2.3.5.$$

The roots of the denominator of 2.3.5. for an underdamped case are given by

$$-\frac{K_d}{4H} + j\sqrt{\frac{wTs}{2H} - \frac{K_d^2}{16H^2}} = \alpha \pm j\beta$$

then $\delta'(t) = \mathcal{L}^{-1}\,\frac{\delta_m}{(p+\alpha)^2 + \beta^2}$

$$\delta(t) = \frac{\delta m}{\beta} e^{-\alpha t} \sin \beta t \qquad 2.3.6.$$

where $\alpha = -\frac{K_d}{4H}$ & $\beta = \sqrt{\frac{wTs}{2H} - \frac{K_d^2}{16H^2}}$

The impulse response looks like the wave form given in fig.2.25.

If δ_1 and δ_2 are two successive peaks at the time interval ΔT then from 2.3.6.

$$\log e \frac{\delta 1}{\delta 2} = \alpha . \Delta T \qquad 2.3.7.$$

The frequency of the oscillations and the decrement can both be checked against the values calculated from equation 2.3.6. Calculation of the decrement, though, is a bit inaccurate.

The network of the check problem (section 2.3.5.) was used to assess the accuracy of the inertia and damping simulation.

Table 2.1. shows the calculated and observed values of oscillation frequency of generator simulator following an impulse in the mechanical input torque. At least five complete cycles of oscillations were recorded

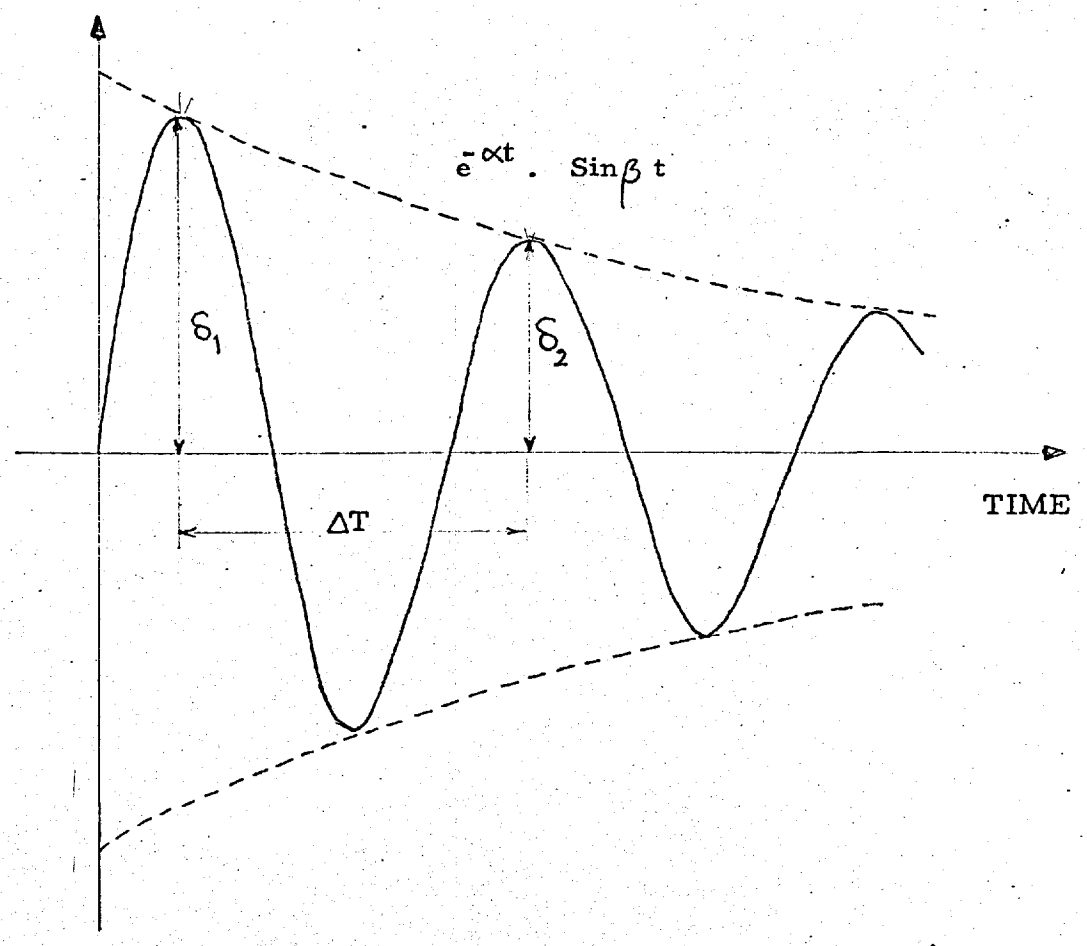

FIG: 2. 25

IMPULSE RESPONSE OF A

SECOND ORDER SYSTEM

following the impulse and the test repeated three to four times. The time period of oscillations recorded in the table is that of the first swing. (successive oscillations are observed to have the same T) The results show that in most cases the error is less than 1%.

TABLE 2.1.

Initial Load Angle δ_o	$T_s = T_{MAX}\cos\delta_o$ Slope of P-S curve at δ_o	$W_s = \sqrt{T_s \frac{\pi f}{H} - (\frac{Kd}{4H})^2}$ (Angular Frequency)	$T = \frac{2\pi}{w_s}$ (Time Period)	T(OBS) (Secs.)
H=3 $K_{d/w}$ = 6				
10^o	1.708	9.44	0.665	.66
20^o	1.63	9.22	0.681	.67
30^o	1.50	8.85	0.709	.70
40	1.33	8.33	0.754	.76
50	1.09	7.54	0.833	.84
60	0.867	6.72	0.935	1.0
70	0.593	5.55	1.13	1.2
H=2 $K_{d/w}$ = 3				
20^o	1.63	11.3	0.55	0.55
30^o	1.5	10.85	0.58	0.58
40^o	1.33	10.21	0.616	0.62
60^o	0.867	8.25	0.788	0.8
H=5 $K_{d/w}$ = 6				
10	1.708	7.32	0.858	0.87
20	1.63	7.15	0.878	0.89
30	1.5	6.86	0.916	0.92
40	1.33	6.46	0.972	1.03
60	0.8675	5.21	1.205	1.24

2.3.7. CHECK PROBLEM

The network conditions of fig. 2.26 were simulated and the rotor angle following the outage of Line A was recorded.

Several combinations of inertia constant H and the damping co-efficient $K_{d/w}$ were assigned to the generator. The values are shown below.

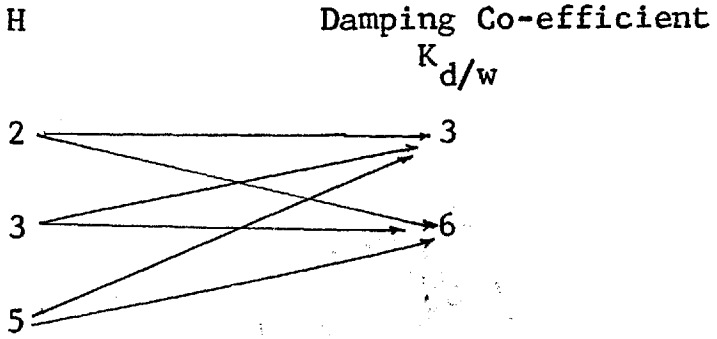

The swing curves are shown in figs. 2.27 to 2.30

Another series of tests with the values of H & $\frac{K_d}{w}$ as given above were performed on the simulator where the loss of line was followed by reclosing the line after 10 cycles or 0.2 seconds. The fault relay arrangement is described in section 3.9.

The reclosing of the line, presented the problem of the current wave form becoming asymmetric. The

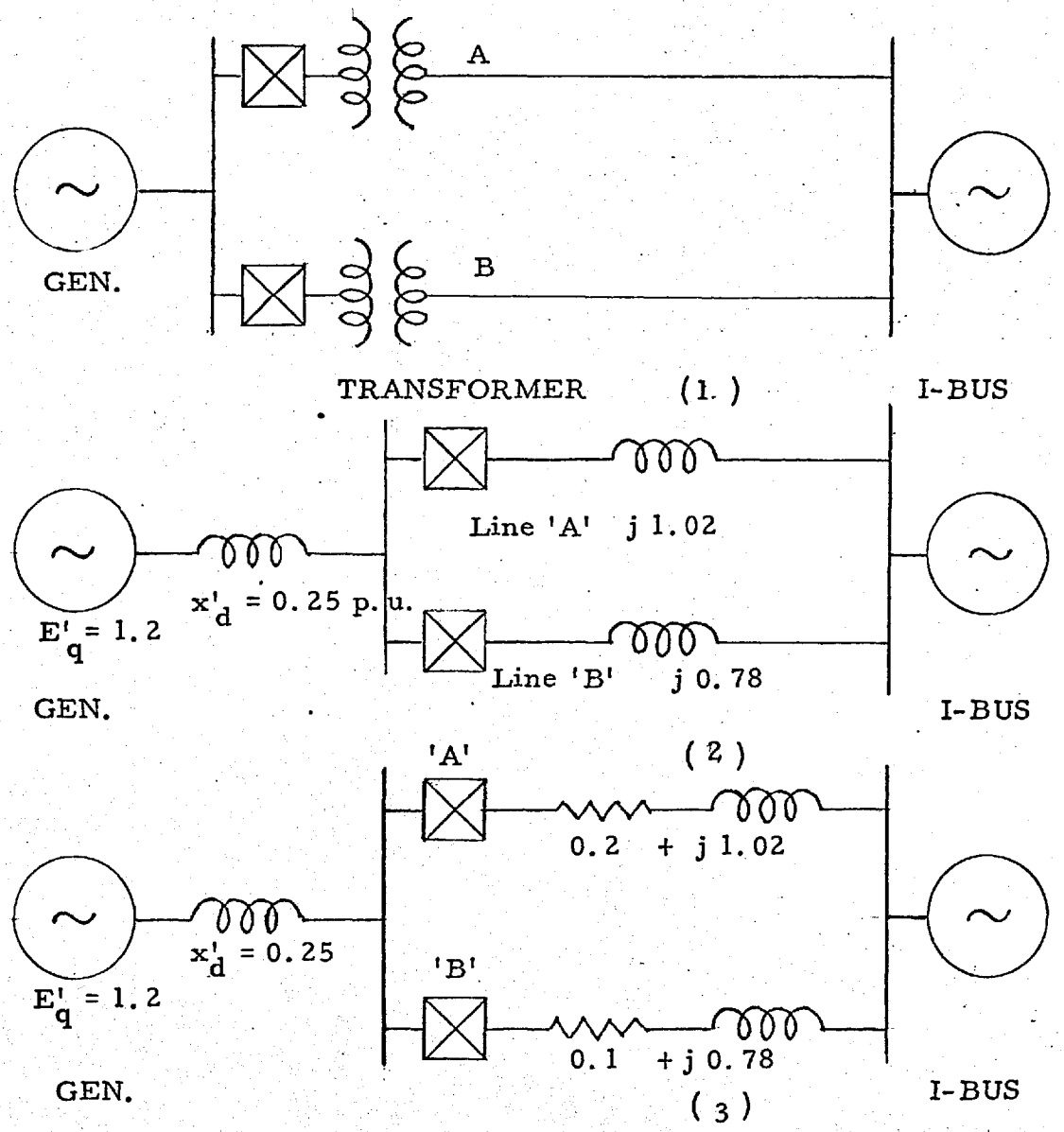

FIG: 2. 26

(1) LINE DIAGRAM FOR THE TEST PROBLEM

(2) LINE DATA NEGLECTING RESISTANCE

(3) LINE DATA INCLUDING RESISTANCE

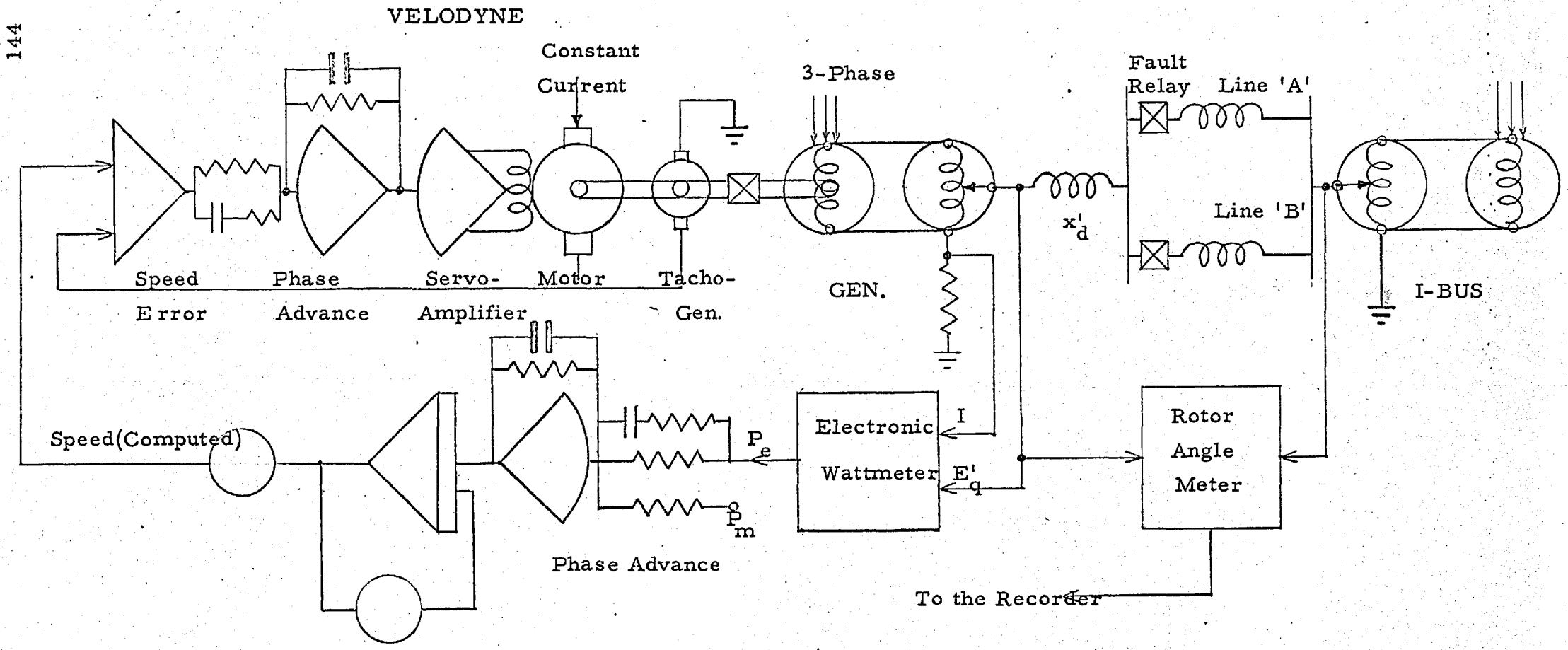

FIG: 2. 26 (a) COMPLETED SIMULATOR

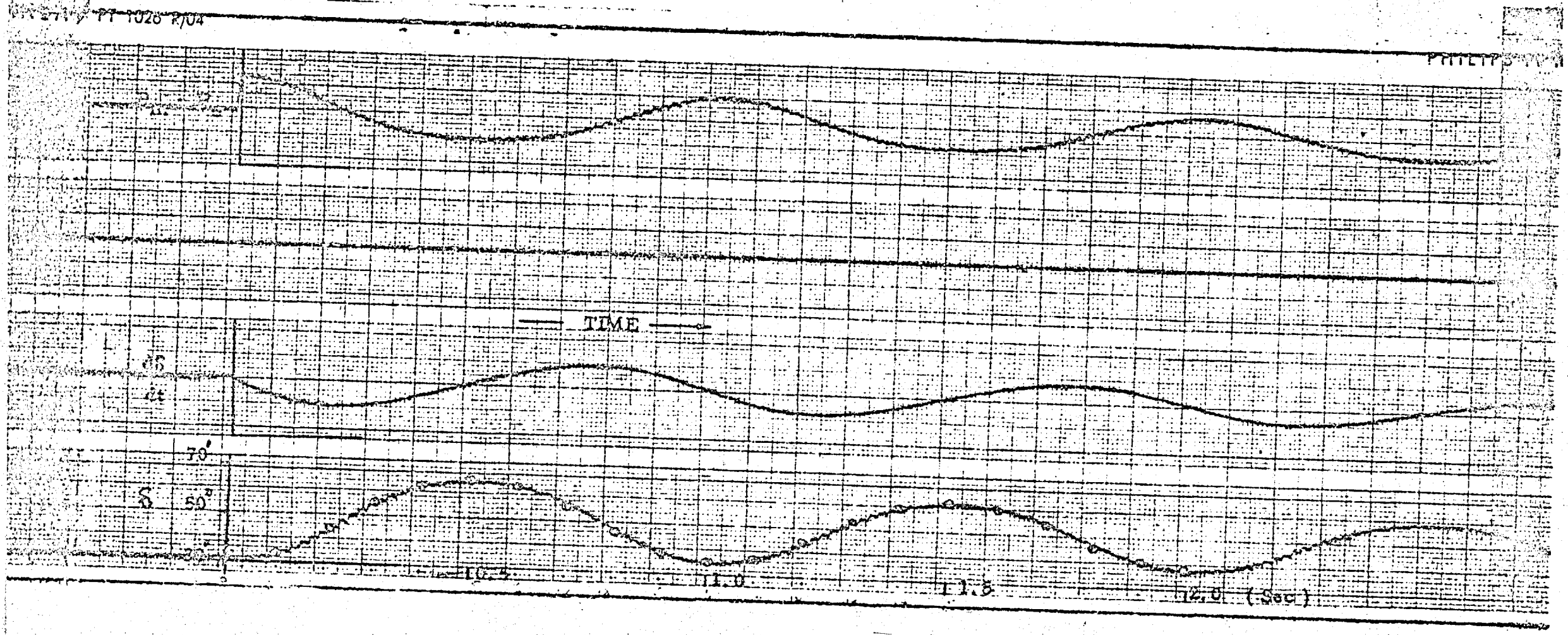

FIG : 2.27 SWING CURVE FOLLOWING LOSS OF A LINE

$H = 3$; $K_d / w = 3$

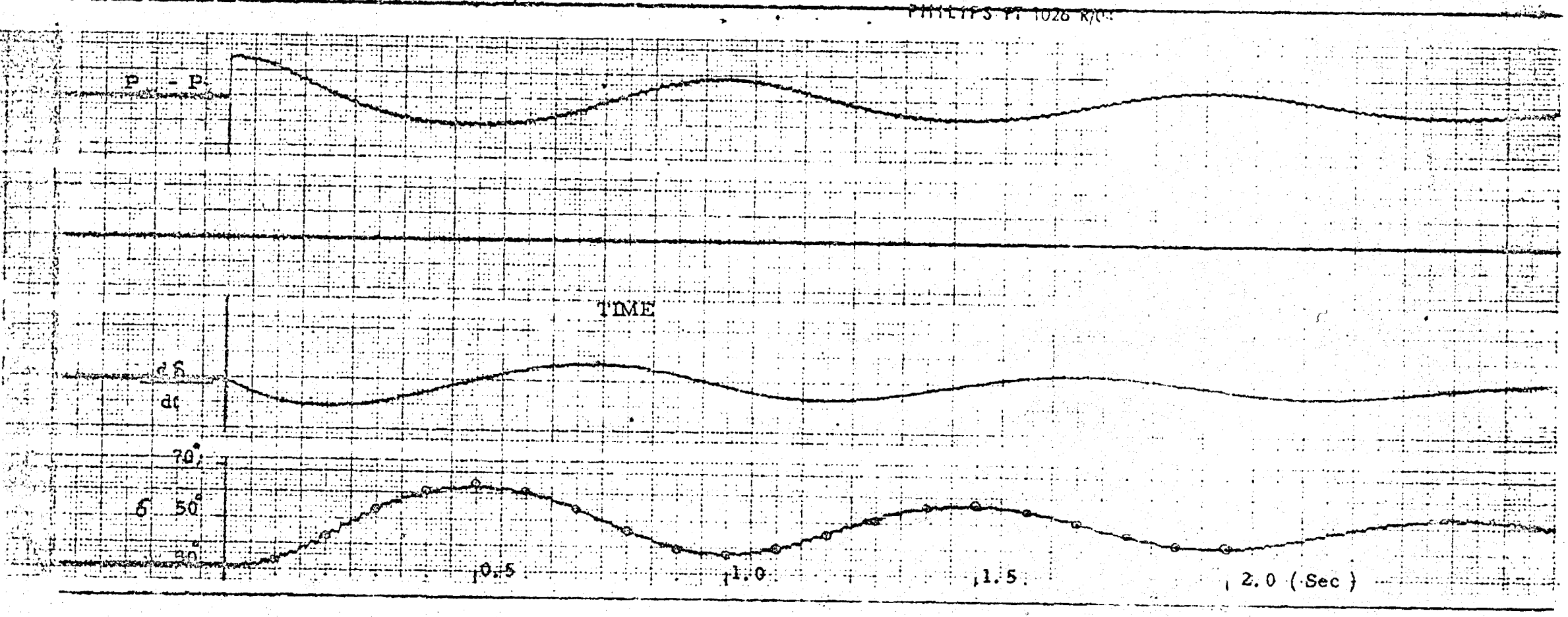

FIG : 2.28 SWING CURVE FOLLOWING LOSS OF A LINE

H = 3 ; K_d / w = 6

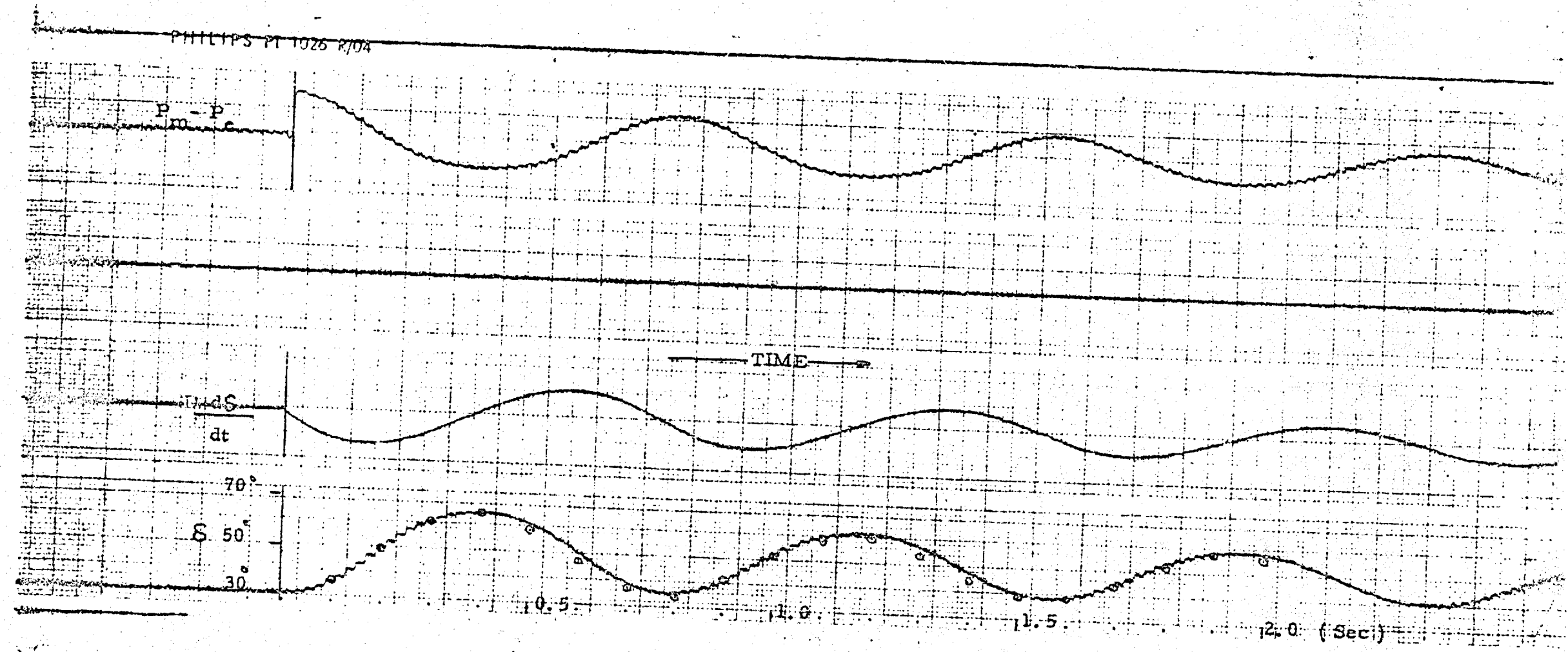

FIG : 2.29 SWING CURVE FOLLOWING LOSS OF A LINE

H = 2 ; $K_d / w = 3$

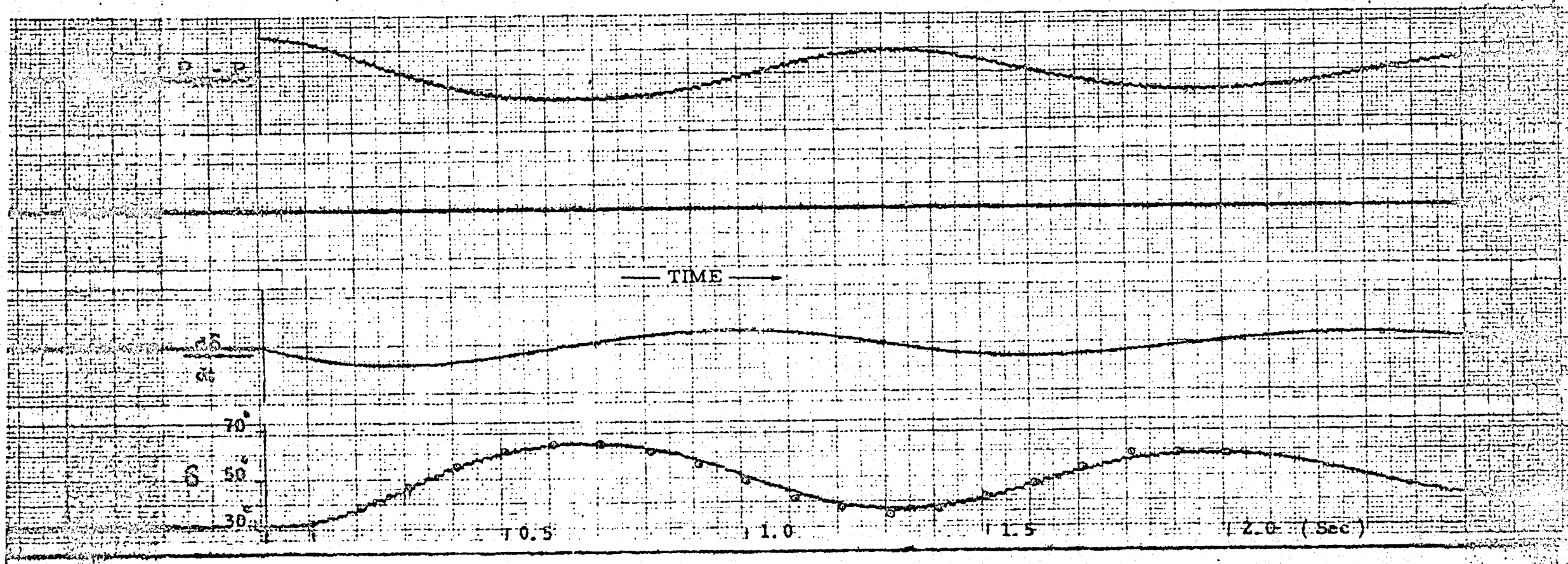

FIG : 2.30 SWING CURVE FOLLOWING LOSS OF A LINE

$H = 5$, $K_d / w = 6$

asymmetry depends on the instant of reclosure. Since the reactance coils have very high X/R ratio the asymmetric part of the current decayed only very slowly.

Normally, aerial transmission lines have a Q-factor in the range of 3 to 10. This would make the decay of the asymmetric component fast and its effect on the rotor swing calculation will be almost negligible. The transmission line network was then changed to one shown in fig. 2.26(c). Swing curves obtained under these conditions are shown in figs. 2.31 through 2.34.

2.3.8. ACCURACY & FLEXIBILITY OF SIMULATION

The results obtained from the simulator were checked against those obtained from a digital computer. The computer program is discussed in the next section (2.3.9

The encircled points on the swing curves are plotted from the computed results. The simulator in most cases shows point by point accuracy. The tests were made several times and good repetitive accuracy was shown. Inertia constants and damping co-efficient can be continuously varied.

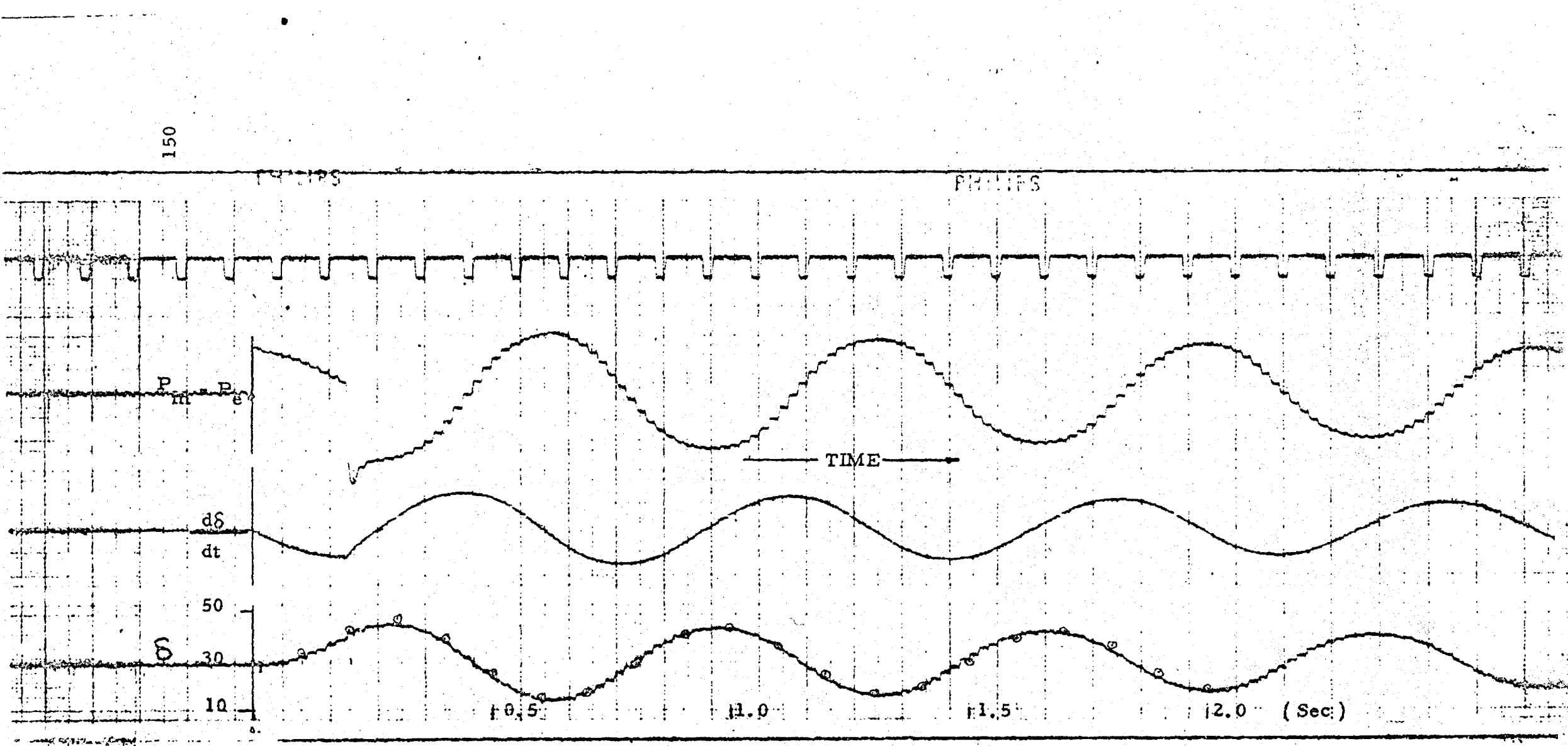

FIG : 2. 31 SWING CURVE FOLLOWING LOSS OF A LINE RECLOSED AFTER 0.2 SEC.

$H = 3$; $K_d / w = 3$

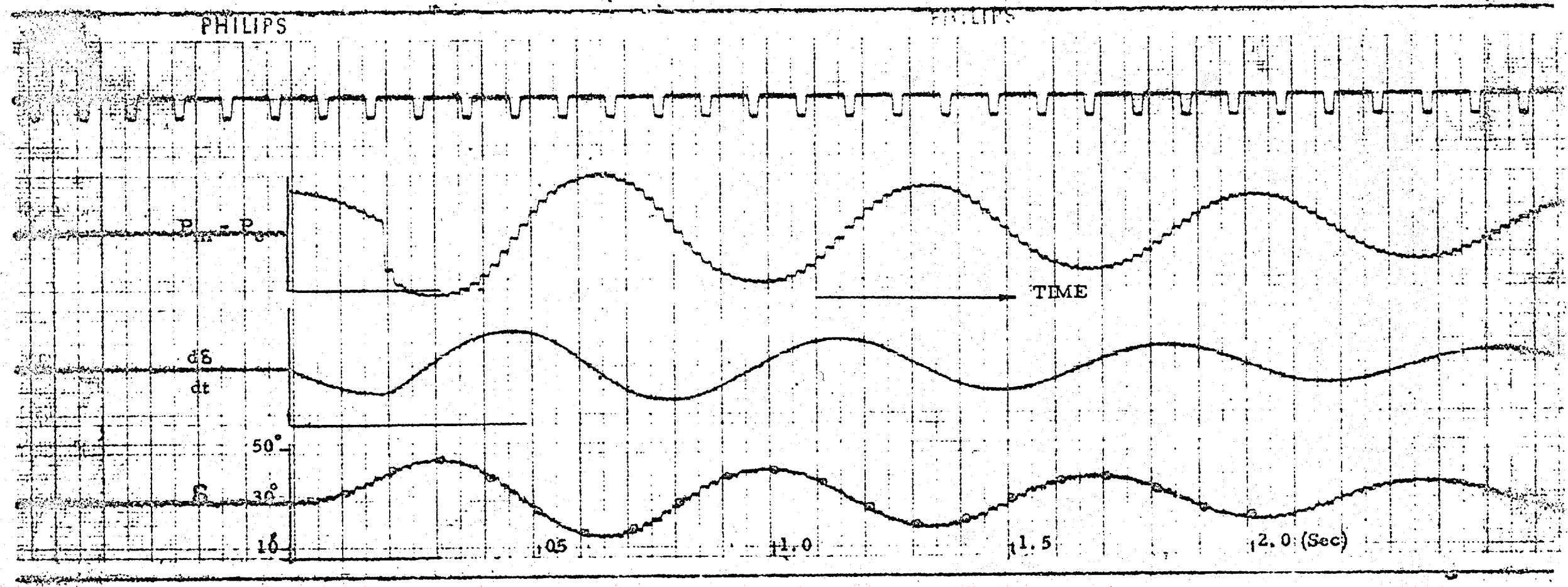

FIG : 2. 32 SWING CURVE FOLLOWING LOSS OF A LINE RECLOSED AFTER 0. 2 SEC

H = 3 ; $K_d / w = 6$

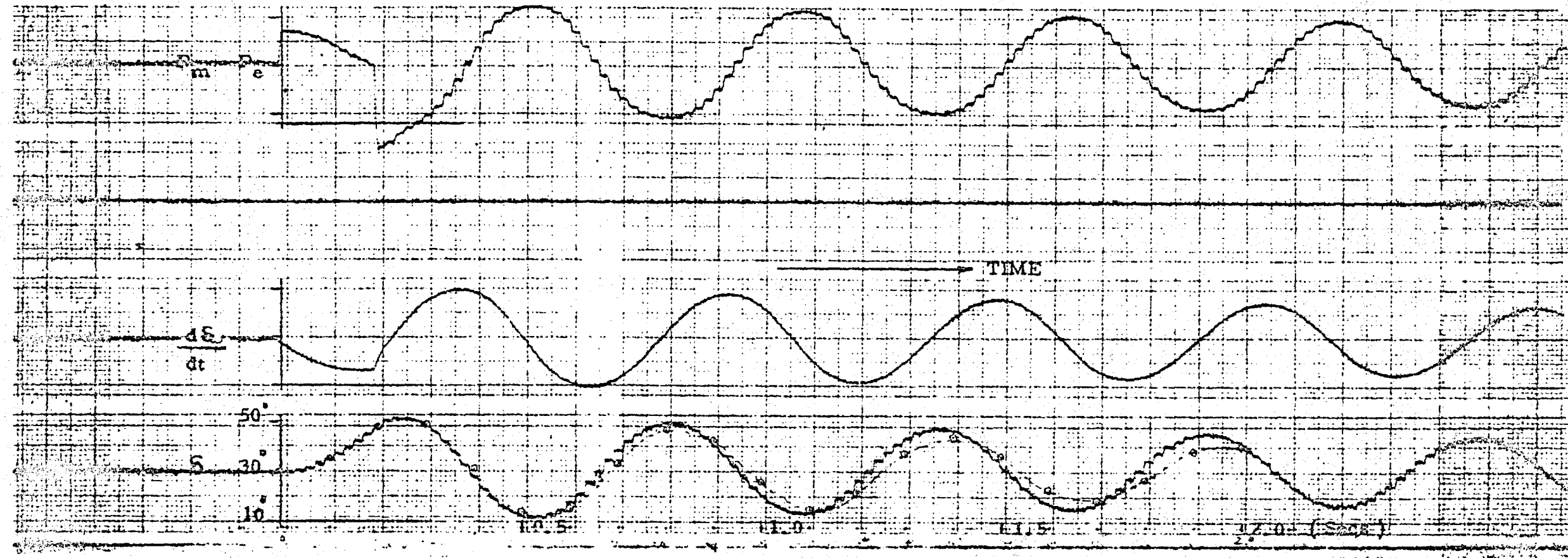

FIG : 2.33 SWING CURVE FOLLOWING LOSS OF A LINE RECLOSED AFTER 0.2 SEC.

H = 2 K w = 3

BLANK PAGE

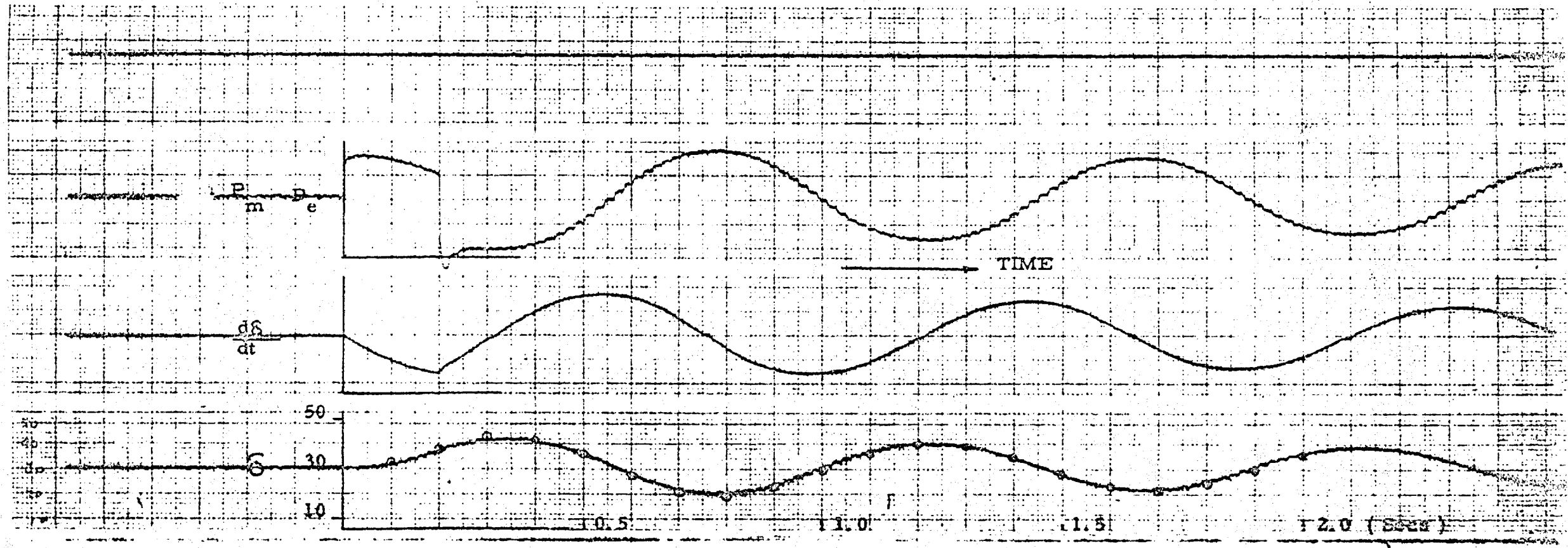

FIG: 2.34 SWING CURVE FOLLOWING LOSS OF A LINE RECLOSED AFTER 0.2 SEC.

H = 5 $K_d / w = 6$

2.34

The simulator solves a set of differential and algebraic equations. The results from it are plots of continuously time varying quantities and are recorded on a "Phillips Ozilloscript". An accuracy criterion in this case is very difficult to define but to give, at a glance, some idea of the accuracy of the plots shown in figs. 2.27 through 2.34 estimates of errors are summed up in Table 2.2. Column 3 of this table shows % error in the rotor angle δ on the 1st and 2nd peak of the outward swing. The base for the percentage calculation is the amplitude of the swing. Column 4 shows the % error in time at which the 1st and the second peak is reached. The figures appear to be high as the errors are estimated from plots where the spread is limited for measurement of angle up to 1^{o} and time up to 10 m.sec. In the swing curve computations the error in any one quantity at any instant of time will be transmitted forward and because of the integration process will tend to increase. This tendency is not shown in most of the plots obtained from the simulator and it can be safely inferred that the errors are considerably less

than the estimated figures shown in Table 2.2. Increasing divergence of the swing curve from the computed curve is seen only for simulated machines with H, constant of 2. This accumulative error is considered to be caused by the electrical power measuring technique. The wattmeter consists of a sampling device and the samples are taken at an interval of 20 m.sec. In between two samples the output of the device is held constant at the value of the last sample taken. (see section 3.5 and fig. 3.16) This interval is considered large for a machine having low rotor inertia. A turbo-generator with an H-constant of 2 is most unlikely to be encountered, the most common values are between 3 and 7 and the simulator can represent these values with good accuracy.

TABLE 2.2

1		2		3		4	
Test No.&	Fig.No.	H	K_d	% error in 1st peak	2nd peak	% error in time 1st peak	2nd peak
(i)	2.27	3	3	<3	<3	<2	<1
(ii)	2.28	3	6	"	"	"	"
(iii)	2.29	2	3	"	"	"	"
(iv)	2.30	5	6	"	"	"	"
(v)	2.31	3	3	<5	<5	<4	<1
(vi)	2.32	3	6	"	"	"	"
(vii)	2.33	2	3	"	"	<5	<2
(viii)	2.34	5	6	"	"	<3	<1

2.3.9. DIGITAL COMPUTER PROGRAM

In the recent past some digital analogue simulation languages have been developed. One of them named 'MIMIC' is available at Imperial College and was used to program the different mathematical models of the turbo-generator discussed in this thesis. The language provides a simple but effective and very flexible method for programming the solution of a system of ordinary differential equations. The programming language could be used on an IBM 7090/7094 computer with a FORTRAN IV IBSYS monitor. Because of less available storage on 7094 it was found necessary to change the INPUT-OUTPUT control system when the computer installation at the college was changed to 7094. With a FORTRAN IV IBSYS monitor several options for input-output control system are provided. With FIOCS the program could be used on 7090 but for 7094 ALTIØ had to be used. This control drops nearly 1 K core locations used as buffers in FIOCS.

'MIMIC' language enables the user to program the digital computer as an analogue computer. Whereas in a normal FORTRAN IV program the instructions are executed in

the same order as they are written (unless a jump instruction is used to transfer the control to any other instruction), the instructions in the MIMIC can be written in any order and the SORT routine puts the variables to be integrated in a sequence which is convenient for a centralised integration sub-routine. Some instructions can be controlled with 'Logical Control Variables'.

MIMIC language consists of 9 - subroutines written in FORTRAN IV, the heart of which is an integration routine. This routine is based on Fourth Order Runge-Kutta (Ref. 8.1) method of numerical integration. The programming language provides the facility for having a fixed step interval of integration or variable step interval. The time interval for the print out is taken as the step interval for the integration initially and then integration is repeated in two steps with half the print-interval as the integration step. The two results are compared and if the difference is more than 1×10^{-6} the integration is repeated with $\frac{1}{4}$ th of the print interval as the integration step. This process of successively reducing the integration step interval is

continued until the accuracy figure mentioned above is achieved or the minimum interval specified in the program is reached.

In the integration sub-routine with fixed step interval, two instructions have been left in wrong sequence and because of this, the instructions for computing the 4th Runge-Kutta Co-efficient is never reached. This introduces a considerable error in the results. The use of the fixed interval integration is, therefore, discouraged.

The MIMIC processor performs the following steps in generating executable statements and computing,

(i) The alphameric program is assembled into a common array of single function statements. The integrate functions are counted, and variables to be integrated are placed in sequence for the convenience of a centralised integration routine.

(ii) This array is sorted.

(iii) An executable machine language sub-routine is generated from this array by using a convenient set of MAP functions.

(iv) Solutions are computed with the integration subroutine under control of the processor. The generated program is controlled primarily by the integration subroutine.

2.3.8. SUMMARY

A simplified mathematical model of the synchronous machine of section 2.1.4. consisting of a constant voltage behind direct axis transient reactance has been simulated with economy, flexibility and accuracy.

The use of network-analyser and the analogue computer has been made possible by the coupling units. Each coupling unit consists of a Magslip and an I-Pot conventionally used for generator representation on a network-analyser. The magslip is driven by servo-mechanism on command from the analogue computer. The magslip rotor follows the synchronous generator rotorswing. A graduated dial is mounted on the shaft of the magslip and a visual and physical feel of the behaviour of the system is achieved. The magslip drive mechanism is a velodyne system. The system is easy to design and high accuracy of follow-up can be achieved. The system is capable of working on a real time basis.

CHAPTER 3

SPECIAL PURPOSE EQUIPMENT

This chapter is devoted to the design and development of the special purpose equipment for use in the simulator. The equipment falls into four categories.

1. The servo-amplifiers and associated power supplies and constant current supplies for the servo-motors.

2. The electronic metering equipment for angle, power, voltage and current components and special purpose operational amplifiers.

3. Fault Sequence Relay.

4. Network-analyser reactance unit.

3.1. SERVO-AMPLIFIERS

Commercial servo-amplifiers had some defects such as non-linearity and unacceptable drift. These are discussed first and modification is proposed which provides improved linearity and lower drift.

3.1.1. COMMERCIALLY AVAILABLE SERVO-AMPLIFIER

Servomex Servo-Amplifiers type SA 61 were available in the Laboratory suitable for driving standard split field D.C. servo-motors.

The amplifier consists of two stages of cathode coupled "long tailed pairs".

The amplifier is provided with two controls marked 'BALANCE' & 'SET +95V'. (Fig. 3.1.) The 'BALANCE' control can be used to take up differences between the two input valves and 'SET +95V' is for fixing the quiescent point. The current in the tail of the first stage is so adjusted as to give +95V at the cathode junction of the next stage. When the two input terminals are earthed it is possible to get 40 mA -40mA in the two halves of the split field by adjusting the above mentioned two controls.

For small input the gain of the amplifier is 2000mA/volt i.e. if a signal of 1mV is applied at one input other being earthed the field current changes from a balanced condition of 40/40 mA to 39/41 mA. Maximum unbalance 0/80 mA is obtained for signal input of between 65 mV - 80 mV.

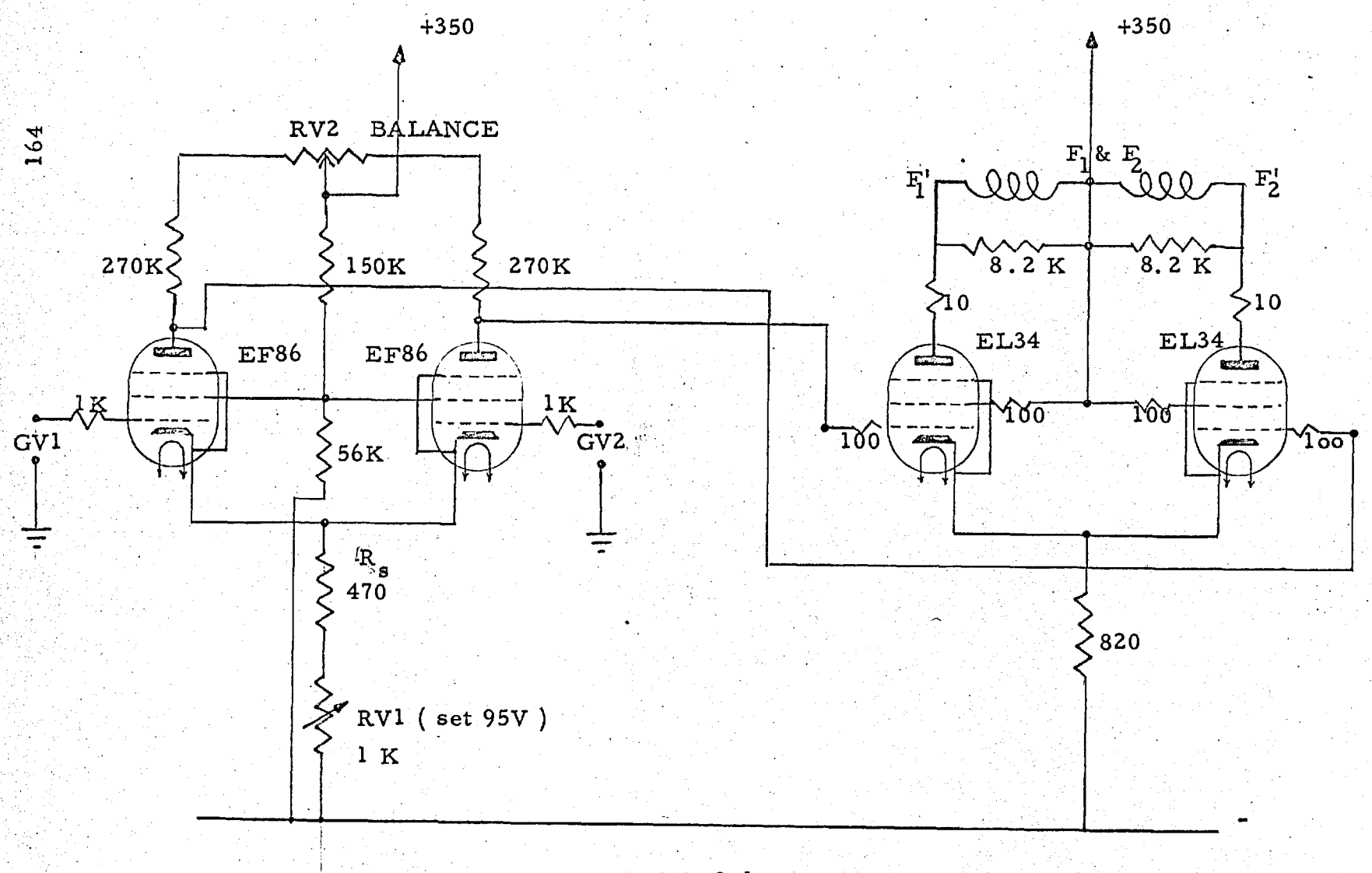

FIG: 3.1

SERVOMEX SERVO-AMPLIFIER SA 61

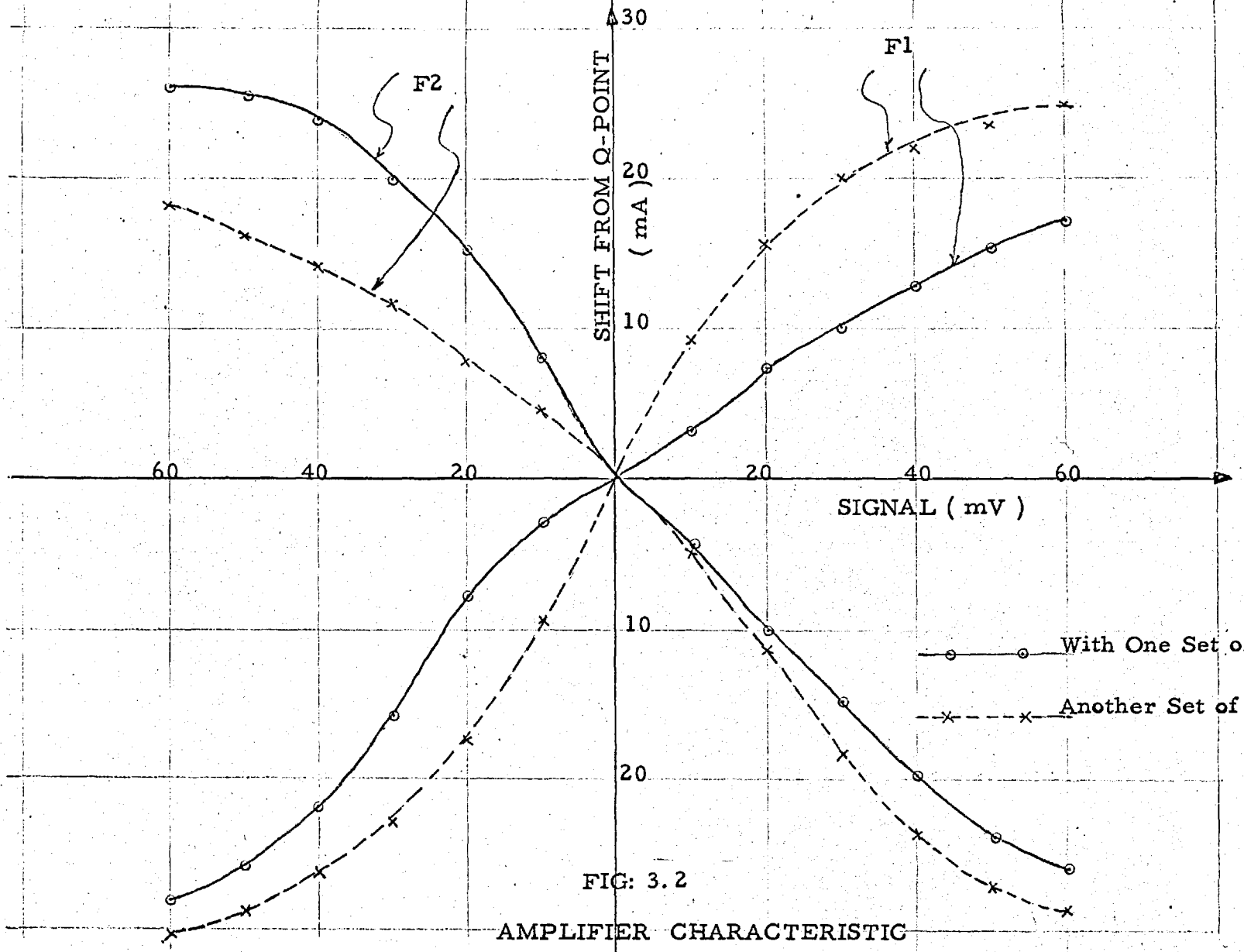

FIG: 3.2

AMPLIFIER CHARACTERISTIC

(D.C.)

The gain is subject to variation of about 2:1 due to changes in valve characteristics.

Fig. 3.2. shows characteristics of the amplifier.

Apart from the non-linearities and being very sensitive to the valve characteristics, the amplifier design is very poor in handling the drift problems, especially with no provision for gain control.

3.1.2. PERFORMANCE OF A SINGLE STAGE CATHODE COUPLED LONG TAILED PAIR

Copious analytical treatment on the analysis of the D.C. Differential Amplifiers is found in the literature (ref. 61-68)

In order to explain the benefits of certain modifications, the performance of a single stage cathode coupled long tailed pair should be specified as three separate gain figures (Appendix 1)

1. Differential Mode Gain
2. Common Mode Gain
3. Inversion Gain

A ratio termed as 'Rejection Ratio' by A.M. Andrew (ref. 64) is used as a figure of merit for the differential

amplifier.

Ideally for any common mode input the differential mode input should be zero but because of the unbalance in the parameter R, r_p & μ some differential output appears. As shown in the appendix by making the resistance in the tail very large, we can swamp the differences in the valve characteristics and tolerances on the other components. The performance of the amplifier for a single ended input is also considerably improved.

3.1.3. MODIFICATIONS OF SA61 AMPLIFIER

For the reasons described in section 1.2 a constant current source providing an infinite R_c was used to replace the tail consisting of resistors RV1 + R_s (fig.3.3.)

Control for setting the quiescent point now appears in the cathode resistor of the constant current valve.

The improvements in the performance of the amplifier are evidently increased linearity over extended range of input voltage (fig. 3.4.) The amplifier in this form showed lower drift.

For the gain adjustment negative differential / mode feed back arrangement is also provided.

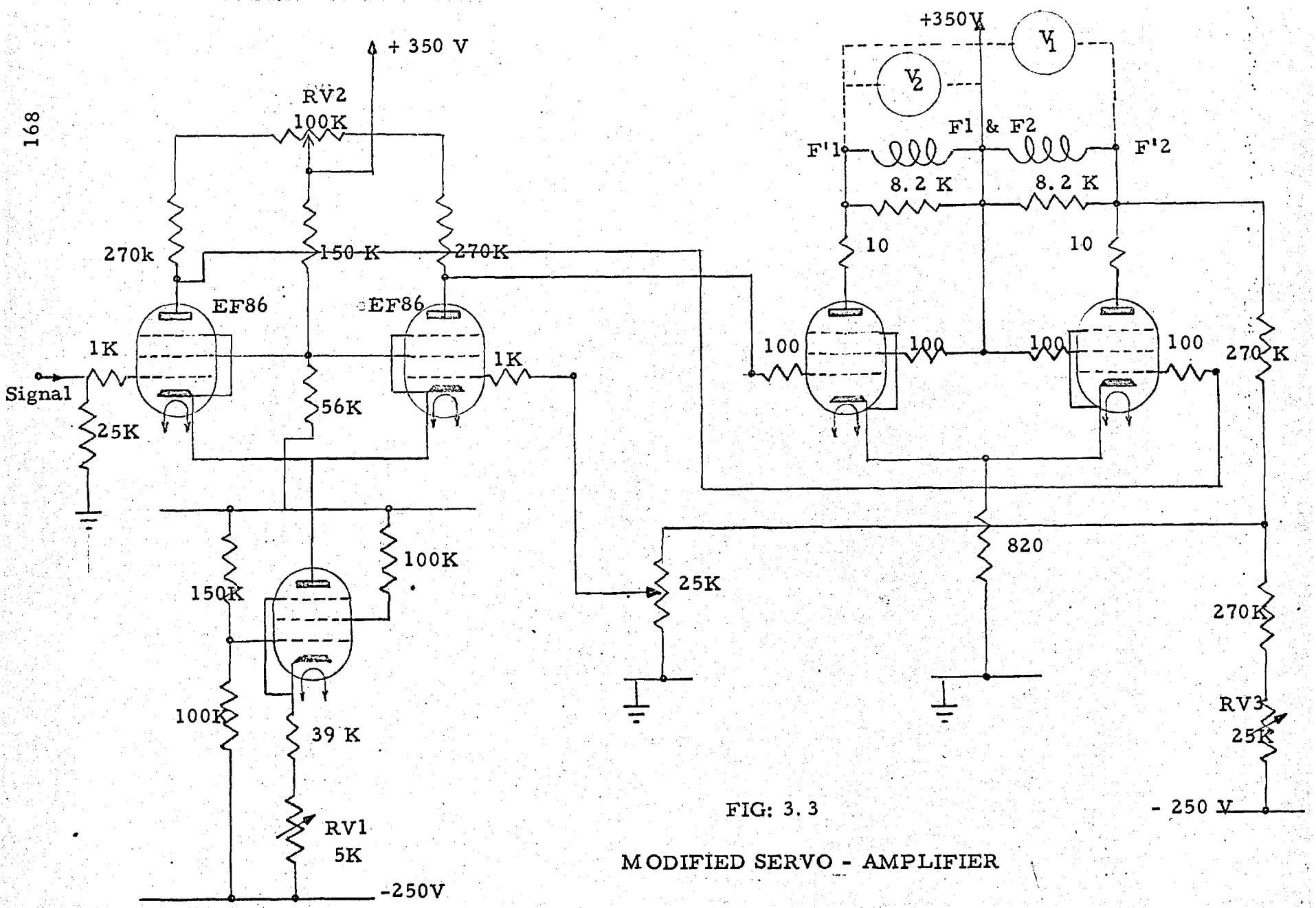

FIG: 3.3

MODIFIED SERVO - AMPLIFIER

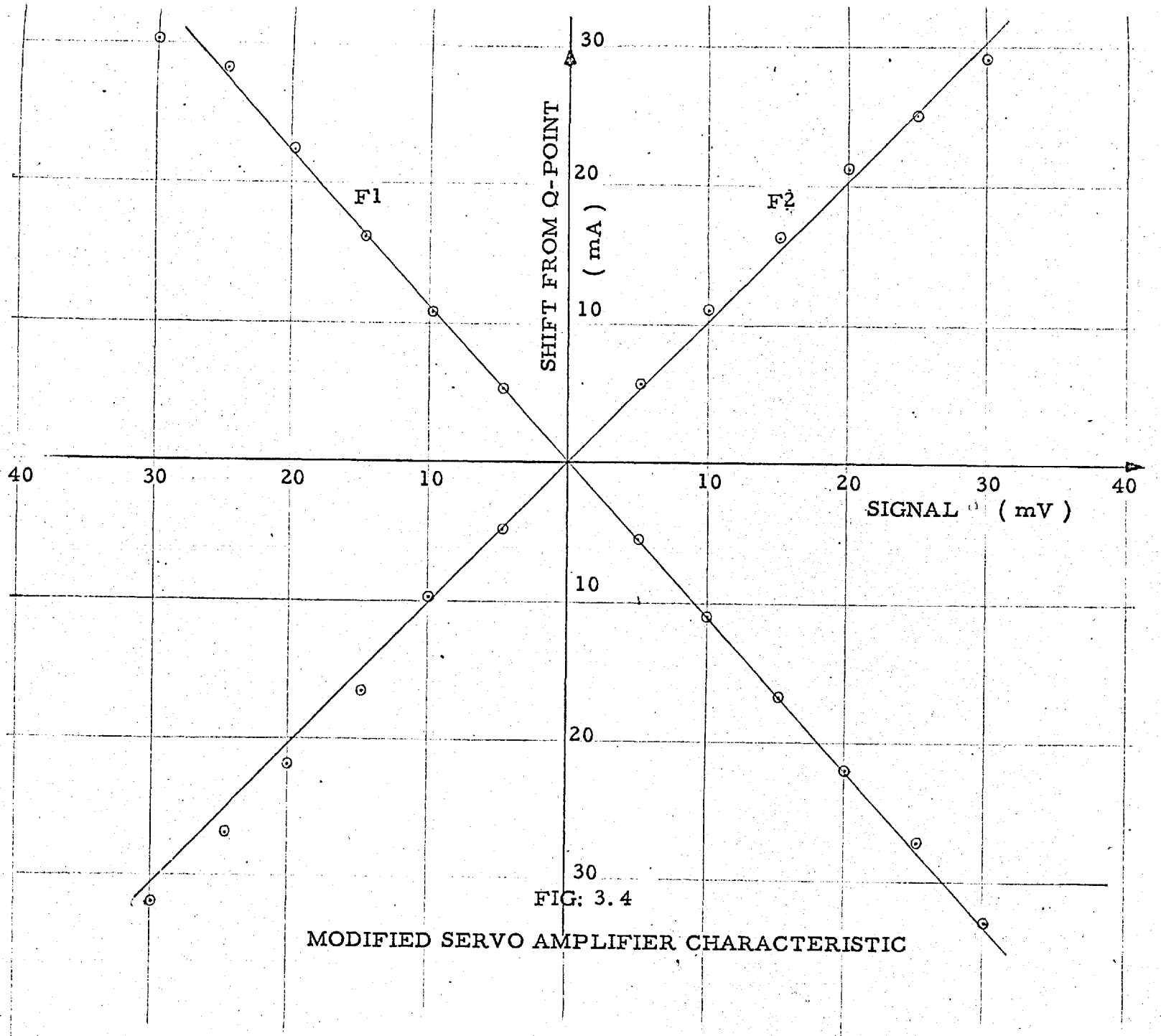

FIG: 3.4

MODIFIED SERVO AMPLIFIER CHARACTERISTIC

Five servo amplifiers in a standard post office sliding rack provide a capability for driving five servo-motors. An arrangement to select any one of these amplifiers and setting the Q-point and the balancing of the amplifier is provided on the front panel. These two operations are performed by setting the potentiometers RV1 and RV2. A centre-zero voltmeter V1 in fig.3.3. indicates balance and the volt drop across one half of the field winding gives a measure of Q-pt current. Voltmeter connections are also shown in fig. 3.3.

3.2. STABILISED POWER SUPPLIES FOR SERVO AMPLIFIERS

The servo amplifiers in their modified form need +350 volts and -250V supply rails.

The drift in the supply rails is seen by the amplifier as a common mode input. The amplifier provides a high rejection of the common mode inputs and therefore high stabilization of the power supplies is not essential, although repeated initial adjustments can be avoided by arranging a fair degree of stabilization.

Decision for the form of stabilizer was very largely determined by the availability of components in the laboratory.

3.2.1. +350V -750 mA

Fig. 3.5. shows the rectifier and stabiliser combination.

The rectifier section consists of four 5U4 double-diodes each capable of supplying 450 mA current, in a reservoir capacitor of 32 /uF. In a full-wave rectifier configuration two of these are connected in parallel.

A CLC-Π-section, most familiar with full wave large current output rectifiers, is used as filter. Output of the rectifier filter combination is 600 volts with a ripple of 1 volt peak to peak at full load.

A series type of regulator in its simplest form was chosen for twin reason of convenience of design and capability to meet large variations of load. We may or may not use all the amplifiers at the same time.

Tubes T_2 to T_9 share the total output current and are connected in series with the load. Each one of these is capable of dissipating 25W and can easily carry 100 mA. The effective resistance of these tubes is controlled by the output of a D.C. Amplifier. A fraction of the load voltage is applied against a Voltage Regulator tube VR-91

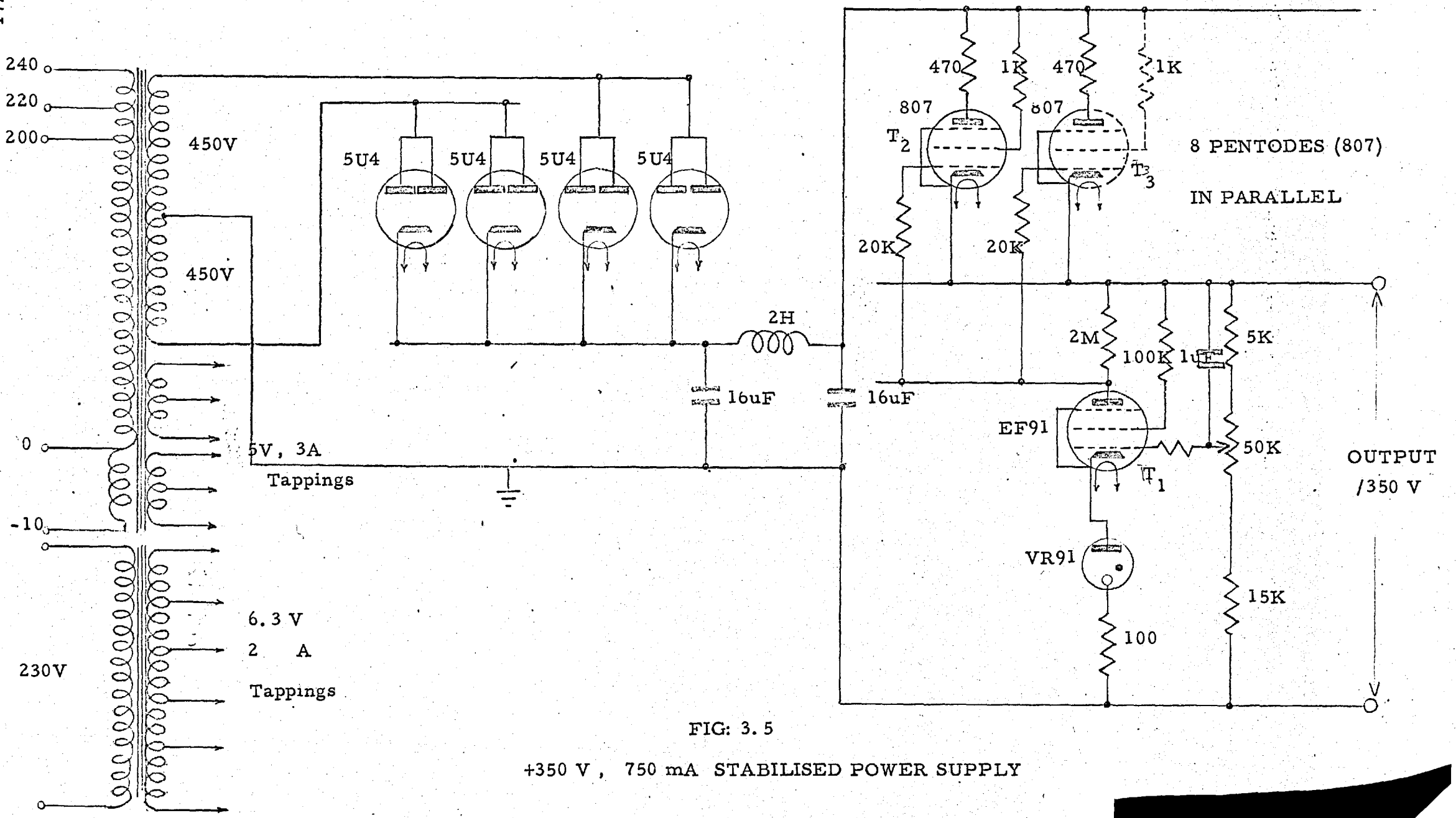

FIG: 3.5

+350 V , 750 mA STABILISED POWER SUPPLY

and any difference is amplified and applied to the control grids of the series tubes altering their resistance.

An increase in the output voltage makes the grid of T_1 more positive the plate current of T_1 increases which makes the grid of T_2 more negative, increasing the series resistance and reducing the output voltage towards its original level.

Voltage regulation achieved was better that 0.5% over full range.

3.2.2. 250V 60mA POWER SUPPLY

This power supply is built up on lines very similar to those described in section 2.1 and is shown in fig.3.6.

Double diode EZ81 provides the full wave rectification.

Lower output current made it possible to use one reservoir capacitor as filter.

A fraction of the output voltage is again compared against a Voltage Regulator tube 85 A 2, and the difference amplified controls the resistance of EL8I tube in series with the load. EL8I is an output pentode and is capable of supplying full load.

The amplifier in this case is a two stage cathode

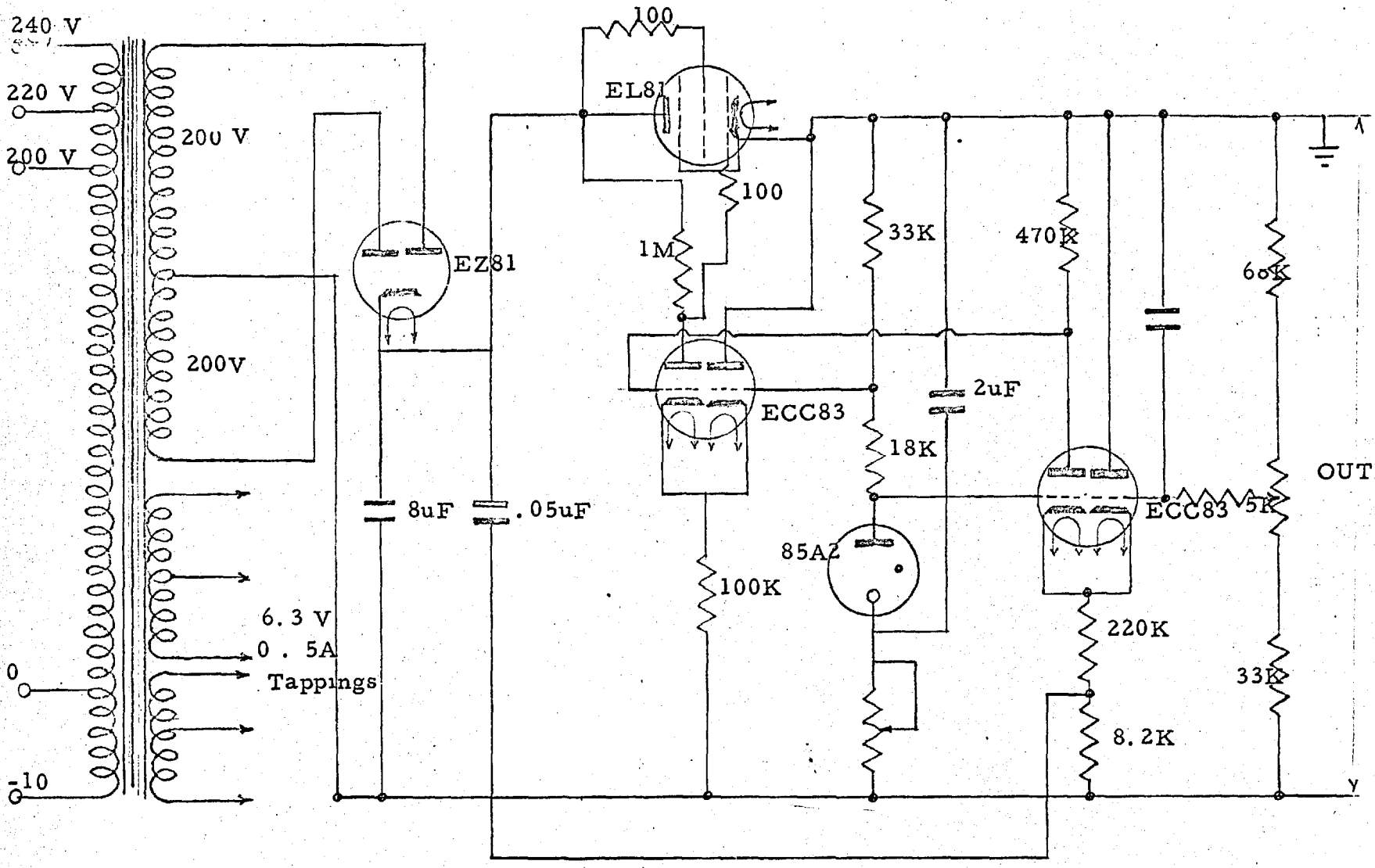

FIG: 3.6

-250 V, 60 mA , STABILISED POWER SUPPLY

coupled long tail pair, each stage using a double tri-ode.

The two power supplies are in the two bottom racks and connected by plug and socket system to amplifiers rack.

3.3. CONSTANT CURRENT SUPPLIES FOR ARMATURES OF SERVOMOTORS

Both the velodyne driving the magslip and position control setting the e.m.f. of the machine-simulator are essentially torque controlled servos (section 2.3.2. & 4.1.1.)

The motor field is split in two halves and supplied from a push-pull D.C. Amplifier (or Servo Amplifier Section 3.1.) With balanced conditions the resultant field excitation is zero and the torque developed by the servo-motor is zero. With an error signal producing an unbalance, and therefore a resultant field excitation, the motor initially develops a torque proportional to the excitation but this falls off as the motor speeds up.

$$\text{Armature Current } I_a = \frac{V-E_b}{R_a}$$

where V is the voltage applied

accross the armature

E_b is the back E.M.F.

& R_a is armature resistance.

$E_b = K_1 \phi w$

where K_1 is constant

ϕ is flux.

and w is the speed

T_g is the gross torque developed by the motor and is given by the following eq=n

$$T_g \, w = E_b \, I_a$$

$$T_g = K_1 \phi w \, I_a = \frac{V - K_1 \phi \, w}{R_a}$$

A great simplification in the design of the servo-system is obtained if the gross-torque developed is proportional to the resultant field excitation. This can only be achieved by providing a constant current through the armature of the servo-motors.

A simple arrangement would be to connect a large resistance in series with the armature. This is not only power wasting but needs a high voltage D.C. source.

In developing the constant current supplies, described

below, use has been made of the reverse biased base-collector junction of the transistor in the emitter-follower configuration.

3.1. 1.5 AMPS CONSTANT CURRENT SUPPLY

The Eversheds and Vignoles servo-motor type FBA/A1/BD used for the velodyne requires 1.5 Amps of current in the armature.

Two BDY 11 Transistors (see fig.3.7) T_1 and T_2 share the total load current and the third T_3 provides the base drive current for T_1 and T_2. The emitters of the transistors T_1 & T_2 will follow that of transistor T_3.

If we connect a constant voltage source to the base of transistor T_3, such as by Zener diode, as shown in fig. 3.7 (a) the load current will be approximately given by Vz/R_3.

The sharing of the load current can be improved by adding a series resistance with each emitter as shown in fig. 3.7 (b). A bleed resistor R_4 is also added to improve the current gain of transistor T_3.

To further improve the output impedance of this

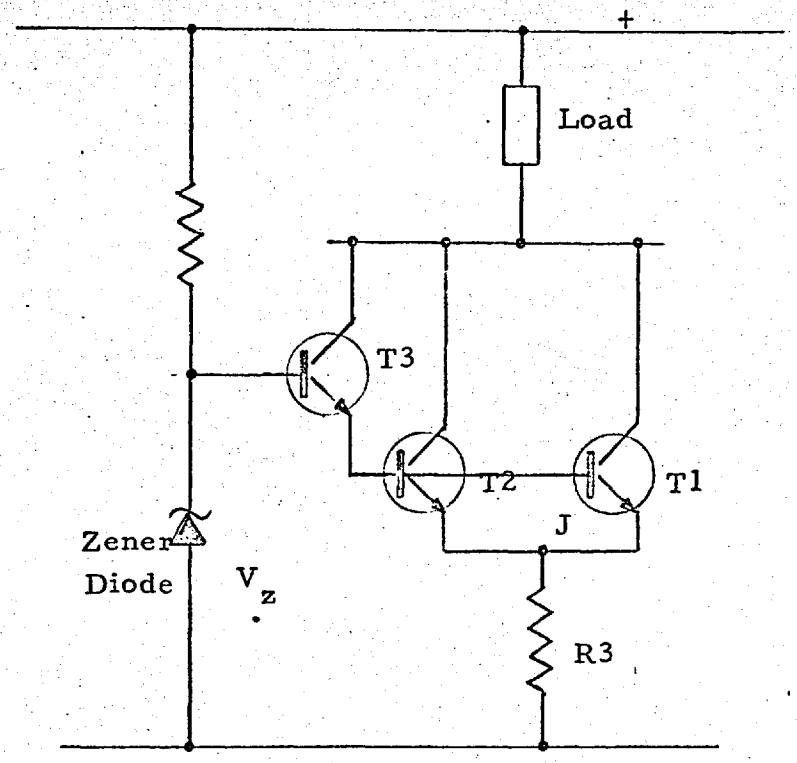

(a)

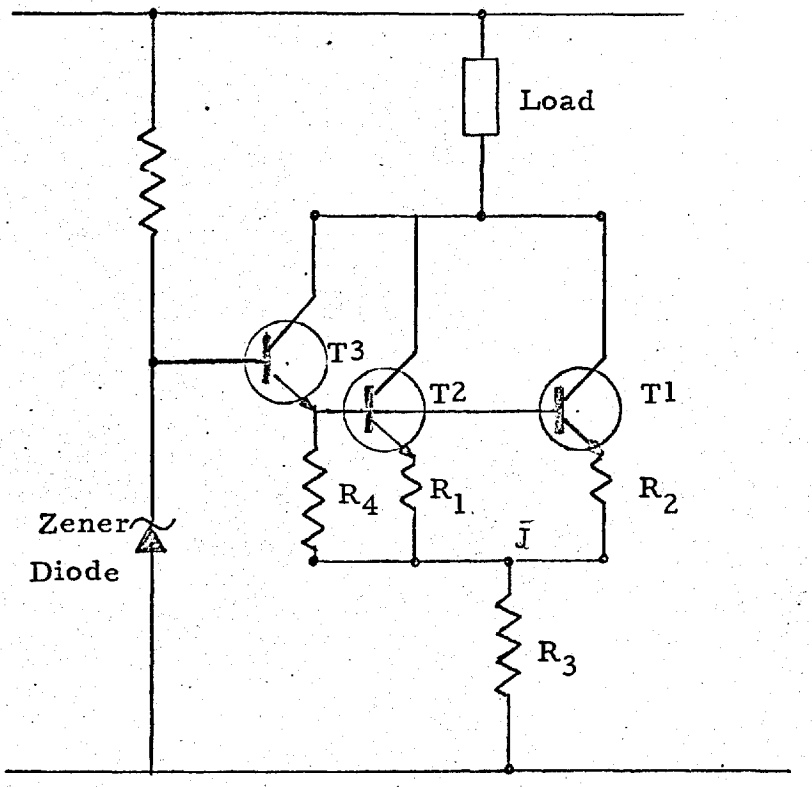

(b)

FIG: 3.7

DEVELOPMENT OF CONSTANT CURRENT SUPPLY

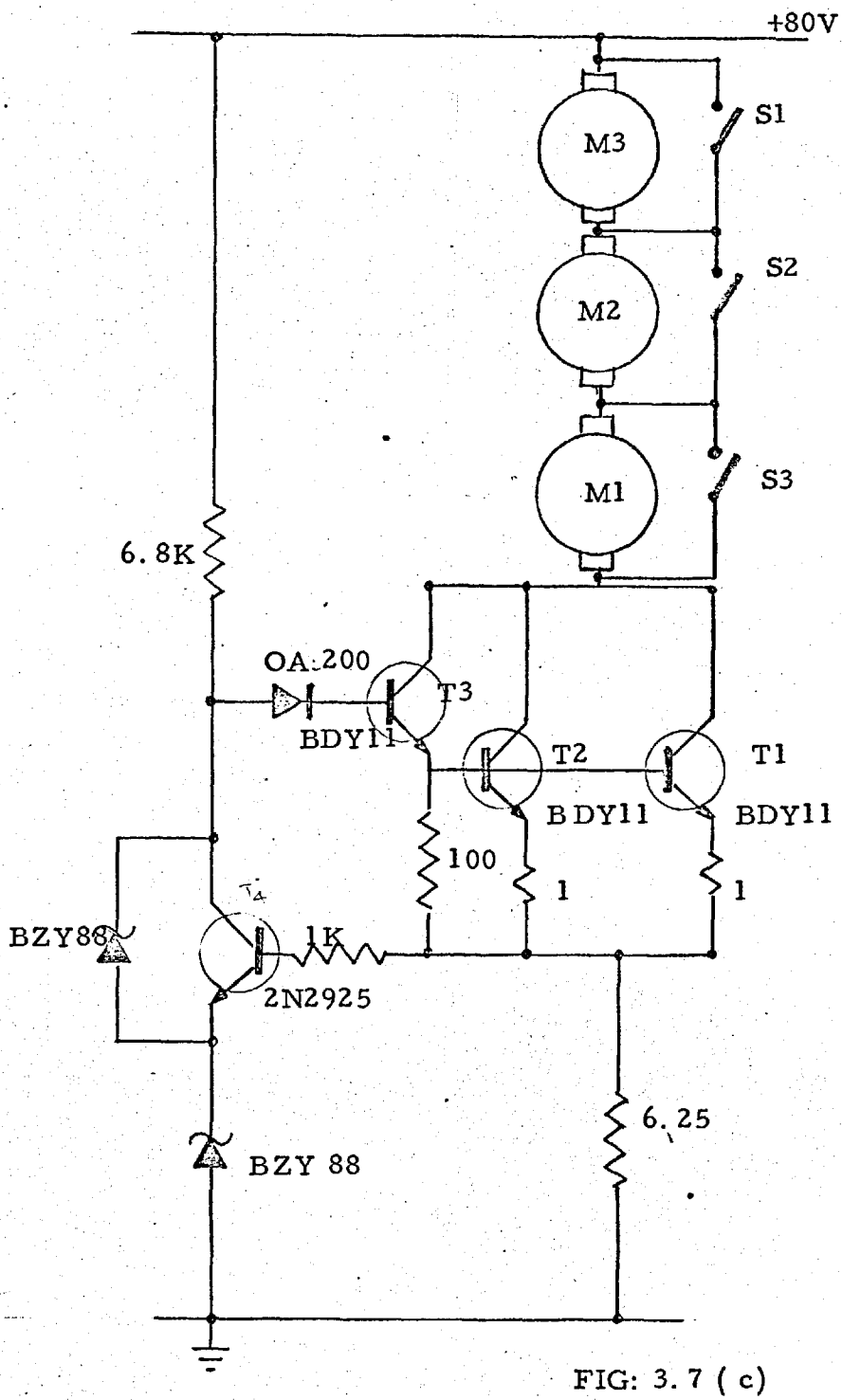

FIG: 3.7 (c)

1.5 Amps., CONSTANT CURRENT SUPPLY

device the voltage at the junction J of the resistances R_1 R_2 & R_3 is compared against voltage across a zener diode and the difference amplified is applied at the base of transistor T_3. This is shown in fig. 3.7 (c).

A diode from the collector T_4 to the base of T_3 ensures that the amplifier is always working in the active region.

In case the load gets disconnected accidentally transistor T_4 will be cut off bringing the collector to the positive rail voltage. This would result in reverse voltage breakdown of the transistor T_4 which is capable of withstanding 25V. It will also result in high dissipation of base-emitter diode of T_3. A zener-diode connected across T_4 safeguarding against such a damage.

The output impedance of the device is 16 K and was measured by injecting a 6.3 volts A.C. in the load by connecting in series with the load a filament transformer winding and finding the variation of current resulting from it.

Three armatures can be connected in series.

Switches in parallel with the armature provide the facility of taking an armature out of the circuit.

3.3.2. 0.48 AMPS CONSTANT CURRENT SUPPLY

The Ever-shed and vignoles FAD/G4/BD used for I-pot position control requires 0.48 Amps of current in the armature.

A power supply developed on the same principles as described in section 3.1 is shown in fig. 3.8

The device has an output impedance of 18KΩ.

3.3.3. HEAT SINKS

The BDY 11 transistors in the constant current power supplies (section 3.3.1. & 3.3.2.) have to be mounted on suitable heat sinks in order that they can dissipate about 60 watts without excessive rise in the junction temperature. Commercially available heat sinks were either two small or too big. The bigger one's are generally made for mounting thyristors. Therefore heat sinks had to be designed in the Laboratory.

A rough guide is given by the transistor manufacturers. A 7" x 7" x 1/16" aluminium sheet offers a thermal

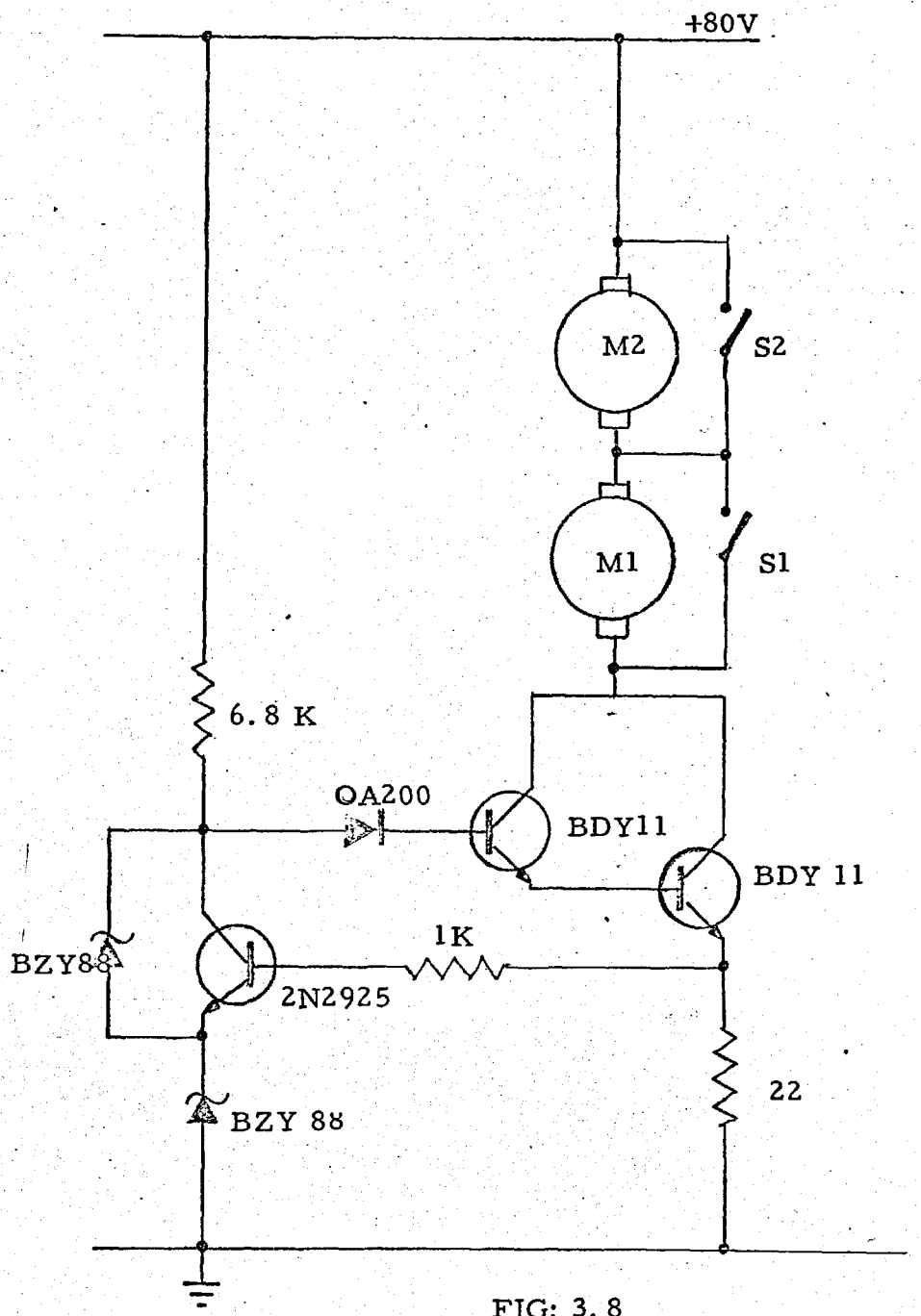

FIG: 3.8

0.48 A, CONSTANT CURRENT SUPPLY

resistance of 2.2°C/watt with the transistor mounted in the centre.

Three times the sheet thickness and three times the radiating surface was provided by bolting together three sheets. The arrangement is shown in fig. 3.9. A film of silicone grease in between the sheets was used to provide better conduction. The thermal resistance can be expected to be reduced 9 times.

The contact between the transistor can and the surface of the heat sink is 0.2°C/watt with silicone grease film in between.

The thermal resistance of the transistor can is 1.5°C/watt.

Taking the ambient temperature to be 25°C the maximum junction temperature can be $25^{\circ}C+(\frac{2.2}{9}+ 0.2+1.5)$ $60 = 142^{\circ}C$.

The transistor is capable of working at a junction temperature of 175°C. A fan is also used for increased ventilation.

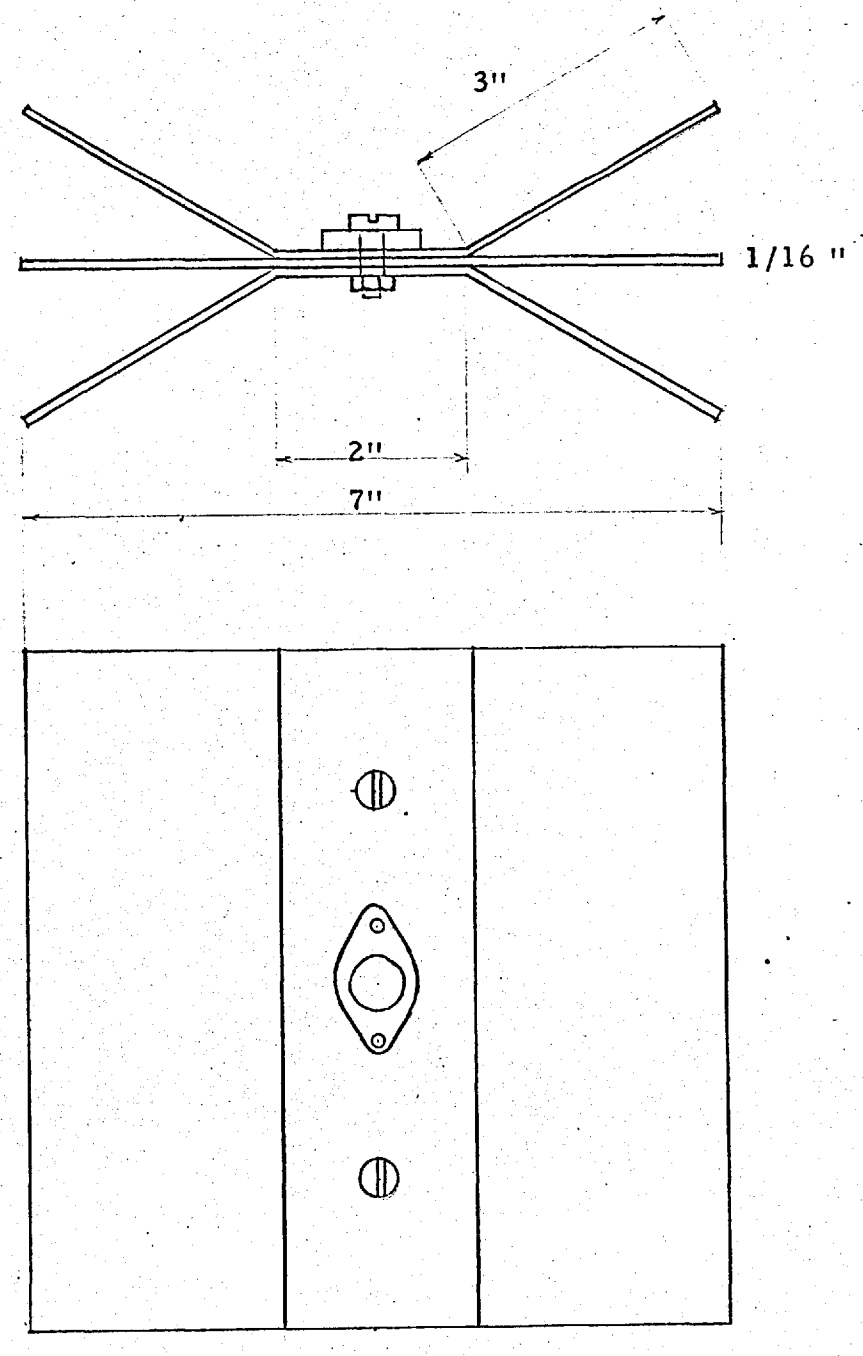

FIG: 3.9

HEAT SINKS

ELECTRONIC METERING EQUIPMENT

The following sections (3.4 through 3.8) describe transistorised metering and measuring devices for rotor angle, electrical power, voltage and current measurement. The devices have some common features which are described below and the details follow.

1. The network analyser works on a current base of 2.5mA and to avoid any burden all circuits have a buffer stage at all input points.

2. For avoiding phase shift, all amplifying circuits are direct coupled and adequate feed-back is provided to keep the drift to a minimum.

3. The output of all metering devices is a d.c. voltage proportional to the quantity being measured. This allows an appropriate link between the network analyser and the analogue computer. The recording of the different quantities is also facilitated when ordinary pen recorders are to be used.

4. All measurements are made without any time delay and usual R-C filters are almost completely avoided. Techniques have been developed to make measurements every cycle of the AC voltage. The details may vary, but in general, a measured quantity is stored and held constant till new measurement is made during the next cycle, at which instant the previous store is destroyed.

3.4 LOAD ANGLE MEASUREMENT :

3.4.1 GENERAL

A satisfactory method of displaying and recording the dynamic behaviour of the machine rotors is an important requirement of the power system simulator.

Rotor angle measurement is also required to record the swing of the micromachine or the actual machine rotor for checking the accuracy of the simulator.

As described in section 6.3.3 the simulator can be used for on line security assessment. The rotor angle can form one of the suitable signals to set up the initial conditions of power flow on the system simulator prior to the application of the faults.

Rotor angle may also form a suitable signal for voltage regulation to increase the stability limit.

3.4.2 REQUIREMENTS FOR A LOAD ANGLE METER :

The following are the important requirements for the device.

(i) The output of the device should be a D. C. voltage and linearly proportional to the angle.

A system for recording the rotor swing in an article by Dr. Adkins (Ref. 10) uses an oscilloscope, the normal time base of which is triggered by the reference voltage and a pulse at the zero cross over of another voltage in phase with the quadrature

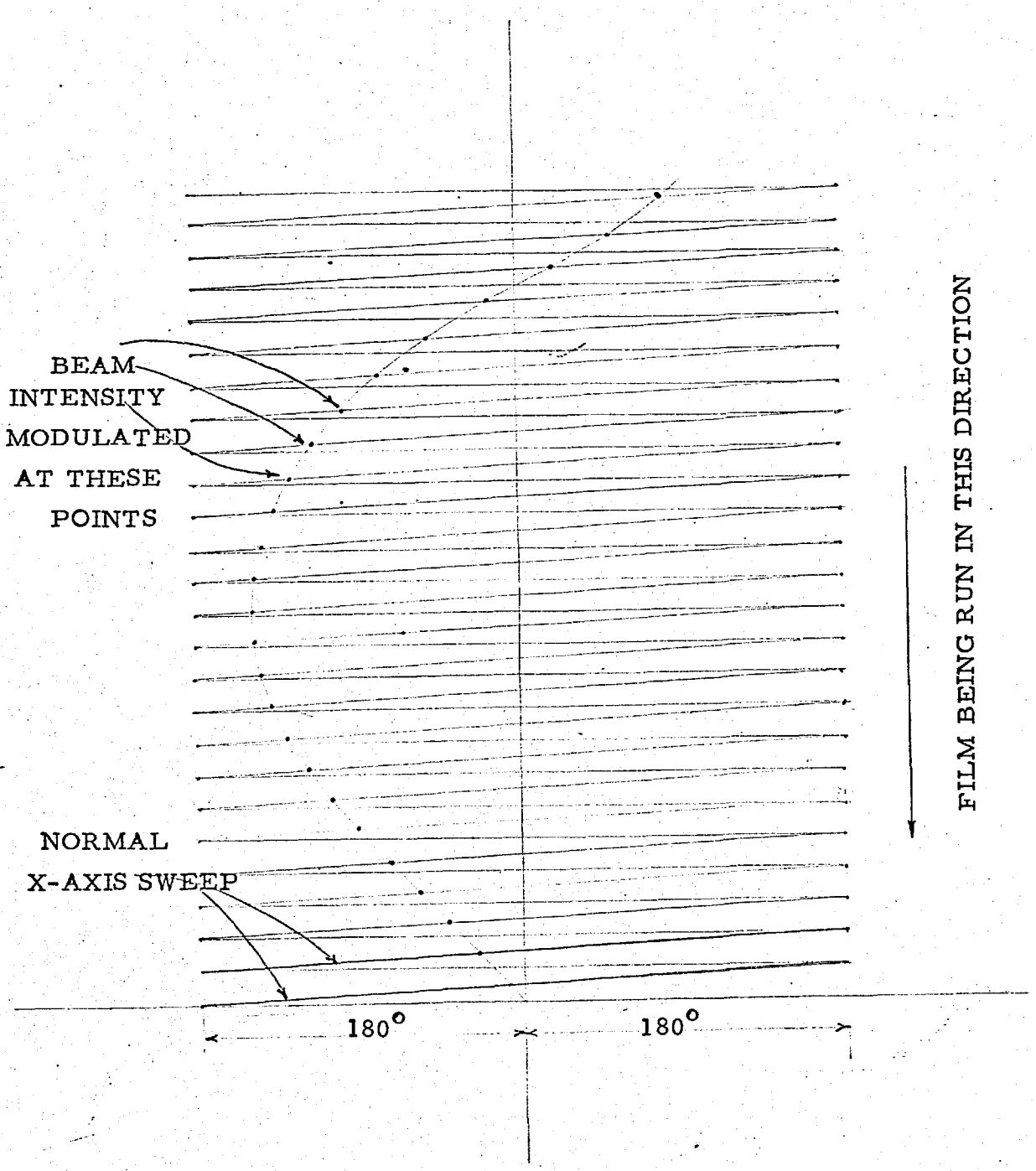
BEAM
INTENSITY
MODULATED
AT THESE
POINTS
NORMAL
X-AXIS SWEEP
180°
180°
FILM BEING RUN IN THIS DIRECTION

FIG

FIG : 3.9 (a)

axis of the machine modulates the intensity of the oscilloscope beam. A film continuously running in the Y-direction gives the bright spots as shown in fig. 3.9 a. A smooth curve through these dots can then be drawn.

Conversion of the rotor angle to the proportional D. C. voltage is preferable to this system because pen recorders or display scopes are easier to use than the continuously running film. Also conversion to the D. C. voltage enables one to set the initial conditions of power automatically by means of servo-mechanisms and use this in a voltage regulator.

(ii) A range of $\pm$ 180° with an appropriate change in the sign of the voltage. The device can then be interchangeably used with the motor as well as the generator simulator.

The wide range is also required because the machine may swing upto very nearly 180° before losing the synchronism. With the aid of the voltage regulator it is possible to extend the stable region of the machine upto 120°.

It has also been found that a three phase short circuit at the terminals of the generator may produce braking torque of such a magnitude that the generator may swing backwards into the motoring region. In this case, the change in the sign of the output of angle measuring device as the machine passes from generating to the motoring region is advantageous.

alternator. As the machine rotor now advances or retards according to the different loading conditions the phase of the tacho EMF will also shift by the same amount with respect to the bus bar voltage.

The rotor angle measurement is , therefore, the phase difference between two voltage vectors.

A pulse train is obtained in which the pulse width is proportional to ($180^{\circ} - \theta^{\circ}$) when θ is a lagging angle and is ($180^{\circ} + \theta^{\circ}$) when θ° is a leading angle. The pulses have the front at the positive going zero cross over of the signal and the tail at the negative going zero cross over of the reference wave. The pulses are integrated to give a D. C. voltage proportional to the pulse width i. e. ($180^{\circ} \pm \theta^{\circ}$) . From the output of the integrator, a voltage proportional to 180° is subtracted. Thus the final output of the device is proportional to the angle θ° but the sign is opposite according as θ is angle of lead or lag.

The integrator is a ramp generator in which a capacitor is charged from a constant current source. The ramp generator can be operated in three modes, sweep, hold and reset modes. The objective of no time delay is achieved by using two integrators and the pulses are alternately routed to the two circuits. The routing of the pulses and the mode control of the ramp generators is achieved by using logical functions.

The development of these logical functions is

explaind in fig. 3.10 (a) and 3.10 (b) for lagging and leading cases respectively. The two AC sine waves are converted to square wave forms in schmitt trigger circuits. The square wave form in the reference channel is inverted.

The frequency of the square waveform is then divided by two in two bistables circuits. The output of the bistables is labelled as logical variables A and B. Complementary signals $\overline{A}$ and $\overline{B}$ are also available from the bistable circuits.

The logical functions for controlling the ramp generators are derived from these logical variables A, $\overline{A}$, B, $\overline{B}$ in four AND gates.

The pulse of width ($180^{\circ} \pm \theta$) obtained during one cycle of the REFERENCE and SIGNAL waves is integrated in one ramp generator. The output of this integrator is held till the pulse obtained during the next cycle of the two waves has been integrated in the other ramp generator circuit. At this instant the first ramp generator is reset and the second circuit goes into the hold mode. Thus at any instant one of the ramp is in the hold state. The outputs of the integrators are connected to a buffer stage through a diode gating arrangement. The buffer output voltage is proportional to ($180^{\circ} \pm \theta^{\circ}$) .

In the final stage the buffer output is offset by a voltage proportional to 180° and thus the final output is the voltage

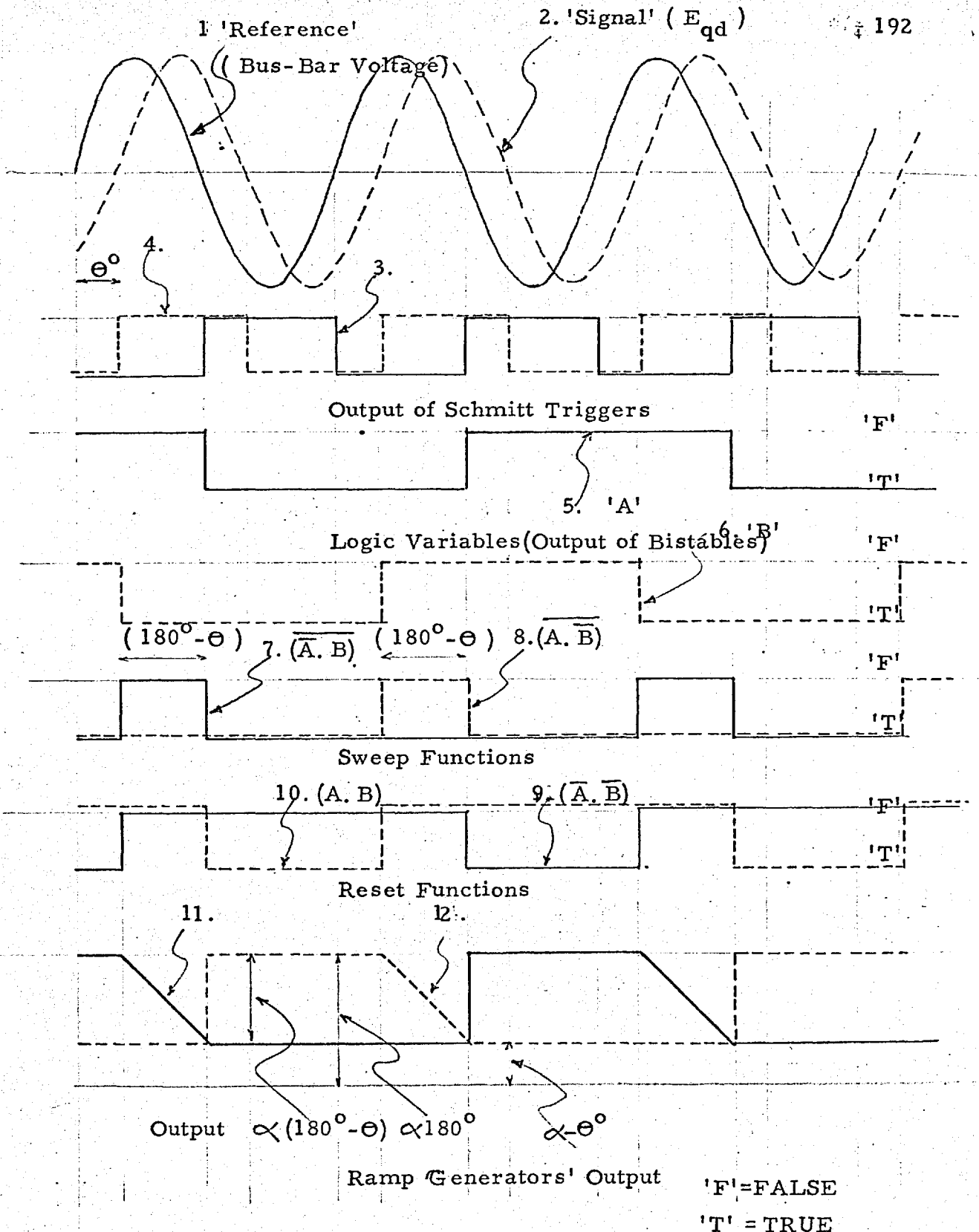

FIG: 3. 10(a) PRINCIPLE OF ROTOR ANGLE MEASUREMENT

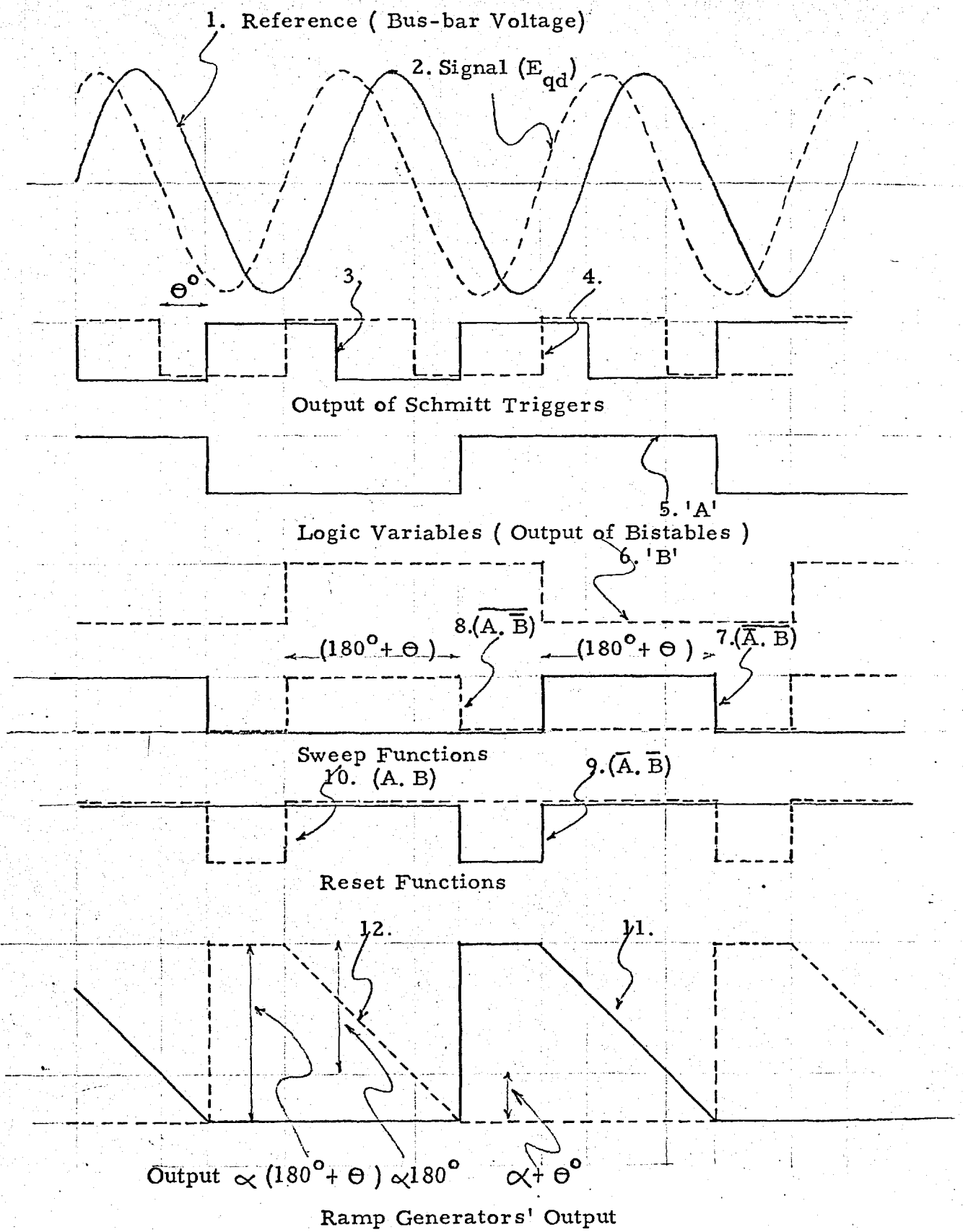

FIG: 3.10 (b)

PRINCIPLE OF ROTOR ANGLE MEASUREMENT

proportional to $\pm \Theta^{o}$.

Fig. 3.11 shows a block diagram. The function of each block has been explaind above. The first stage is a buffer having an input impedance of 12 M ohms and therefore the device draws only a negligible current from N. A.

Details of the circuits in each block is shown separatly in fig. 3.12.

Calibration curve is shcwn in fig. 3.13.

Fig. 3.14 shows the difference between a continuously measuring device and the device discussed above, whose output remains constant over discreet intervals of time.

3.5. ELECTRONIC WATTMETERS :

3. 5. 1 GENERAL :

An electronic wattmeter is required to deliver a DC voltage proportional to the average electrical power output from the simulated machine unit.

Other important requirements for the electronic watt-meter are as follows:-

1. Over the working range of the voltage and the current the output should be linear within 1%.

2. Time delay in producing the output signal should be as small as possible.

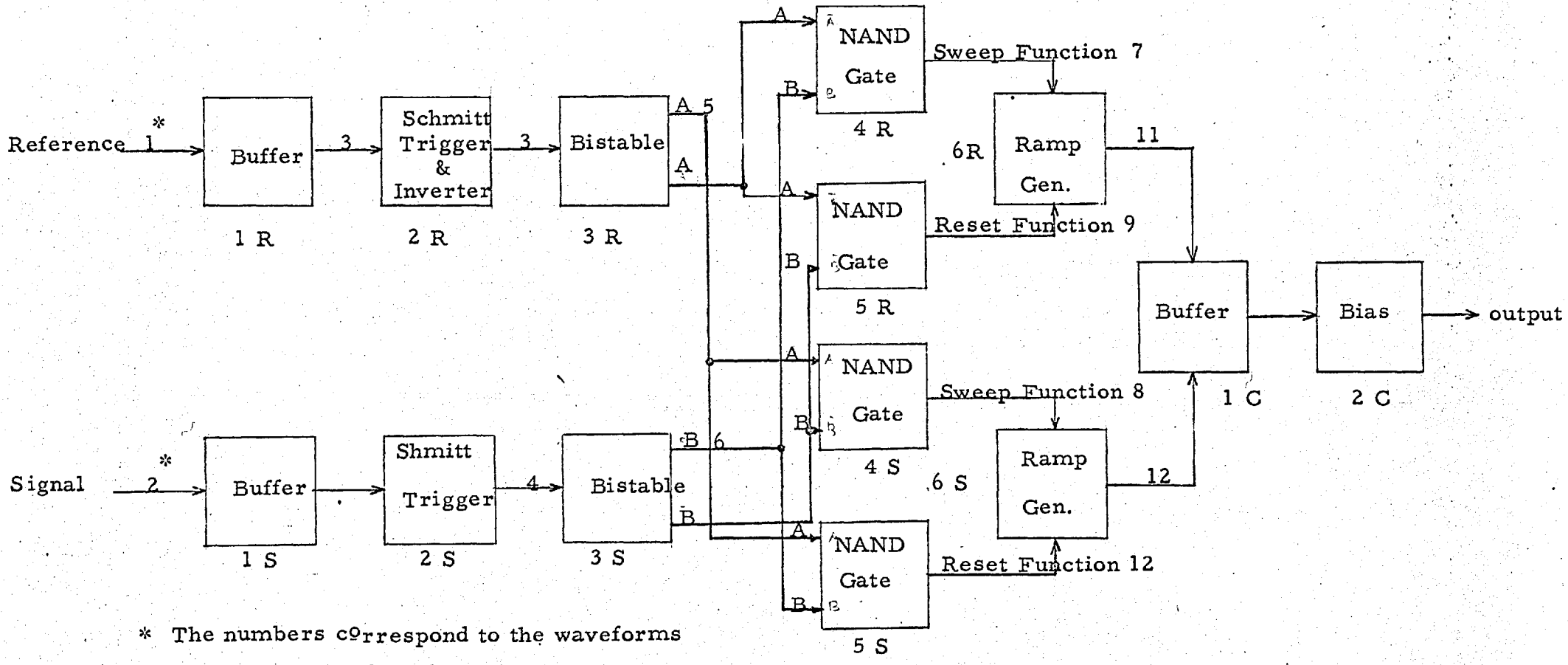

* The numbers correspond to the waveforms shown in fig. 3.10

FIG; 3.11 BLOCK SCHEMATIC FOR ANGLE MEASUREMENT DEVICE

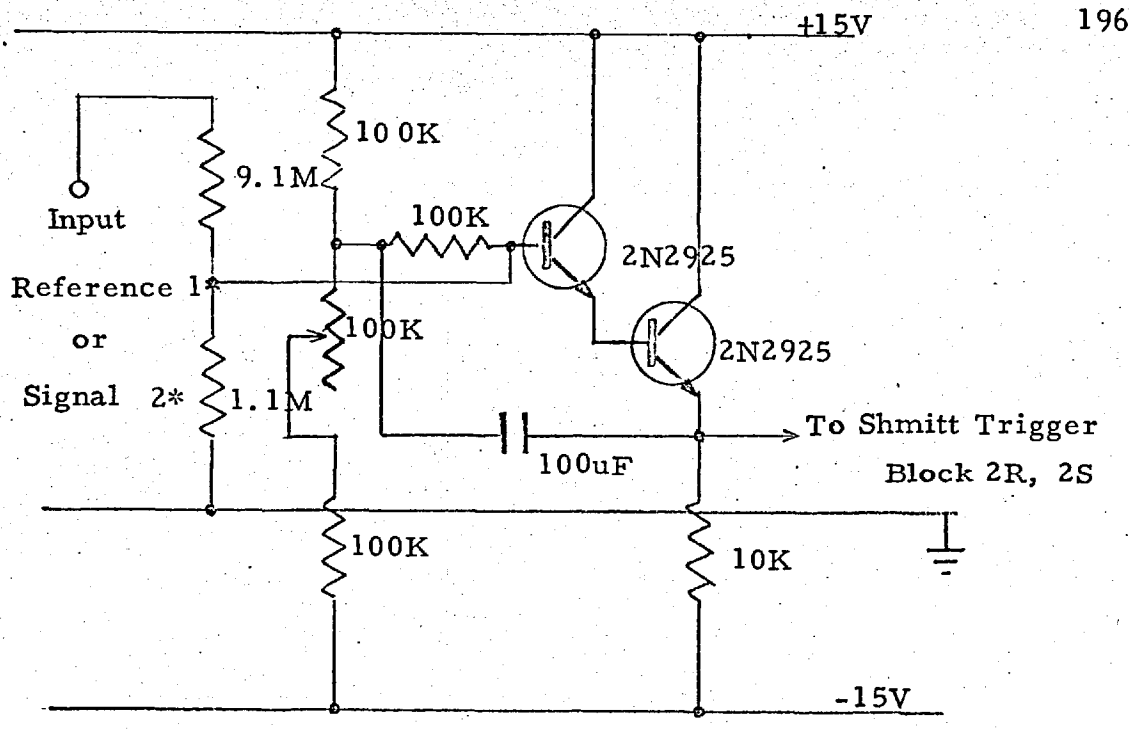

FIG: 3.12 BUFFER (BLOCK 1R & 1S)

* The numbers at the inputs and outputs correspond to the waveforms shown in fig. 3.10

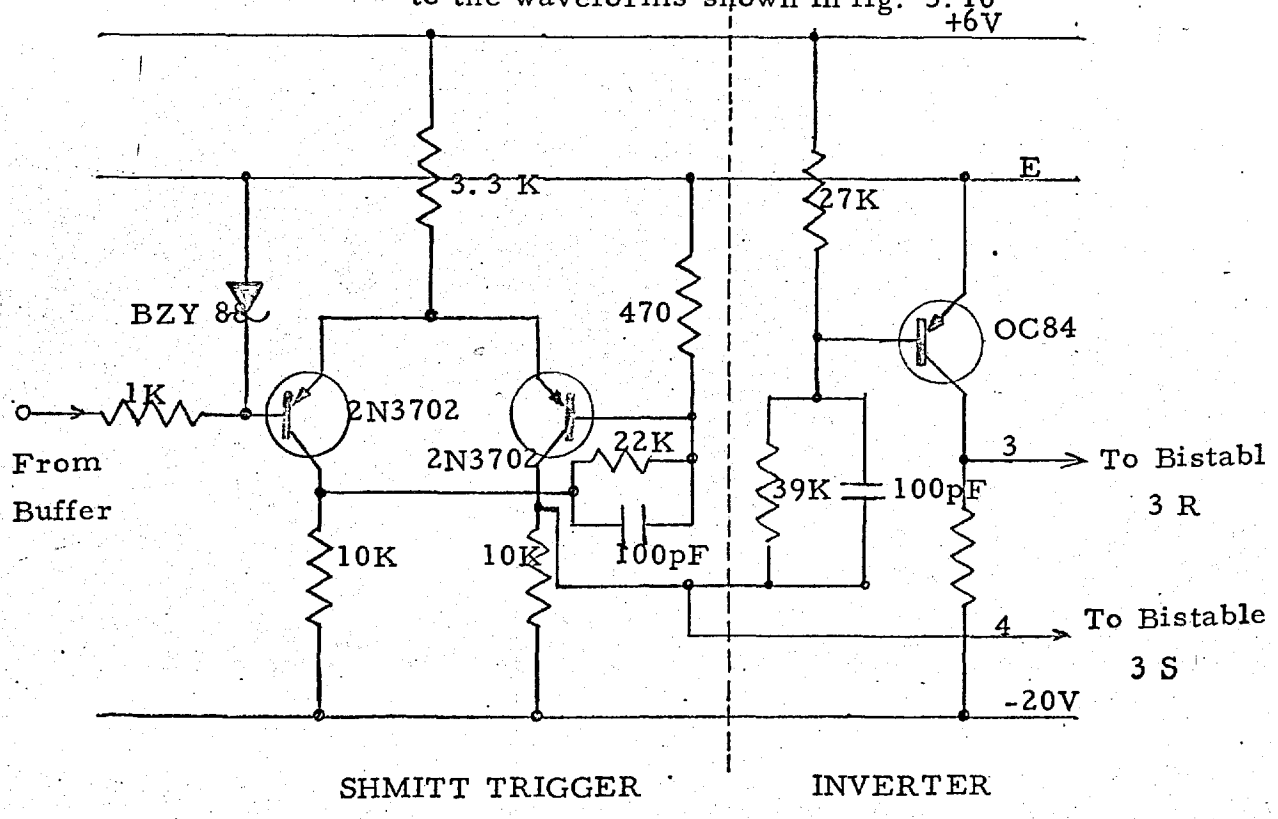

FIG:3.12 BLOCK 2R & BLOCK 2S (Without Inverter)

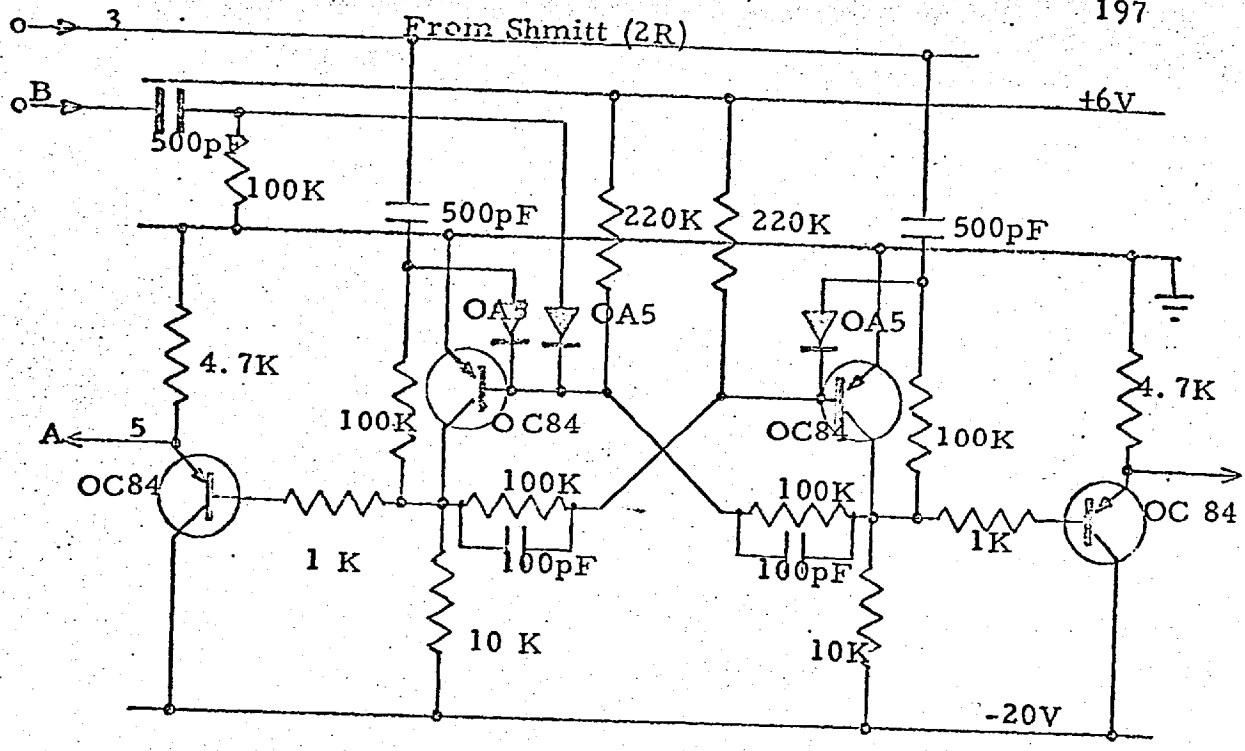

FIG: 3.12 BISTABLE (BLOCK 3R)

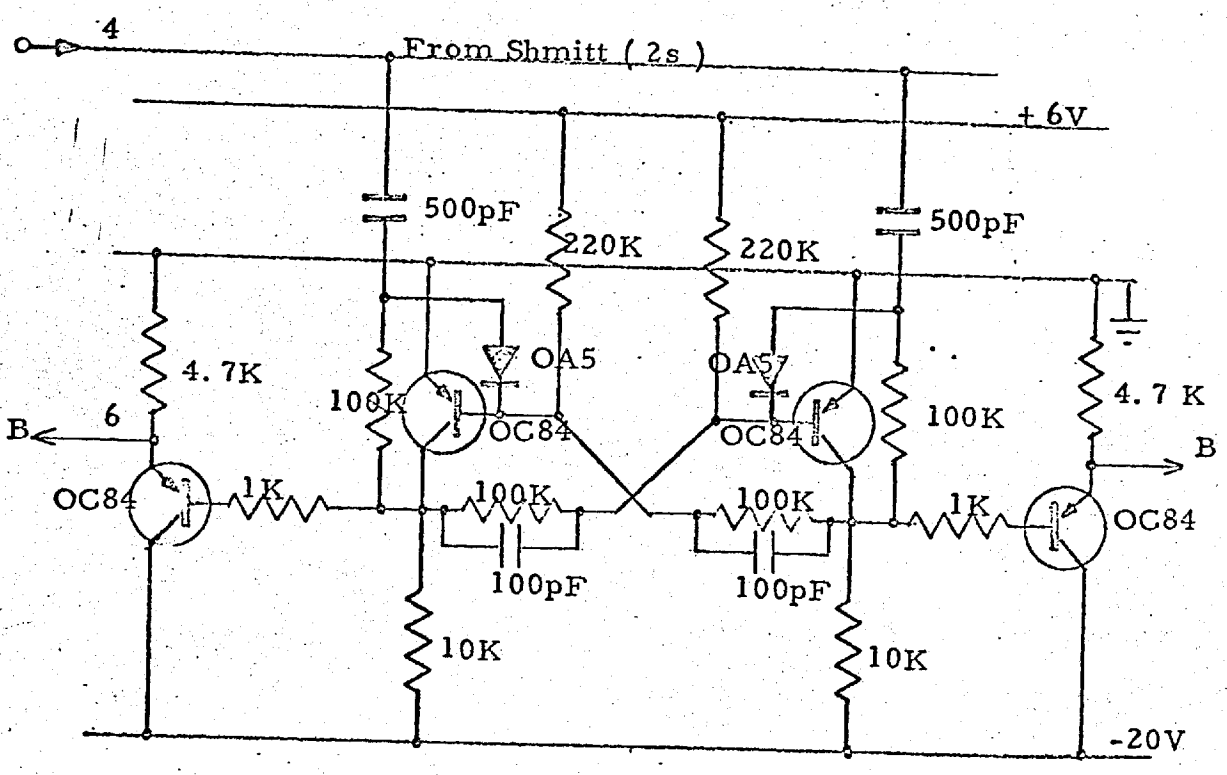

FIG: 3.12 BISTABLE (BLOCK 3S)

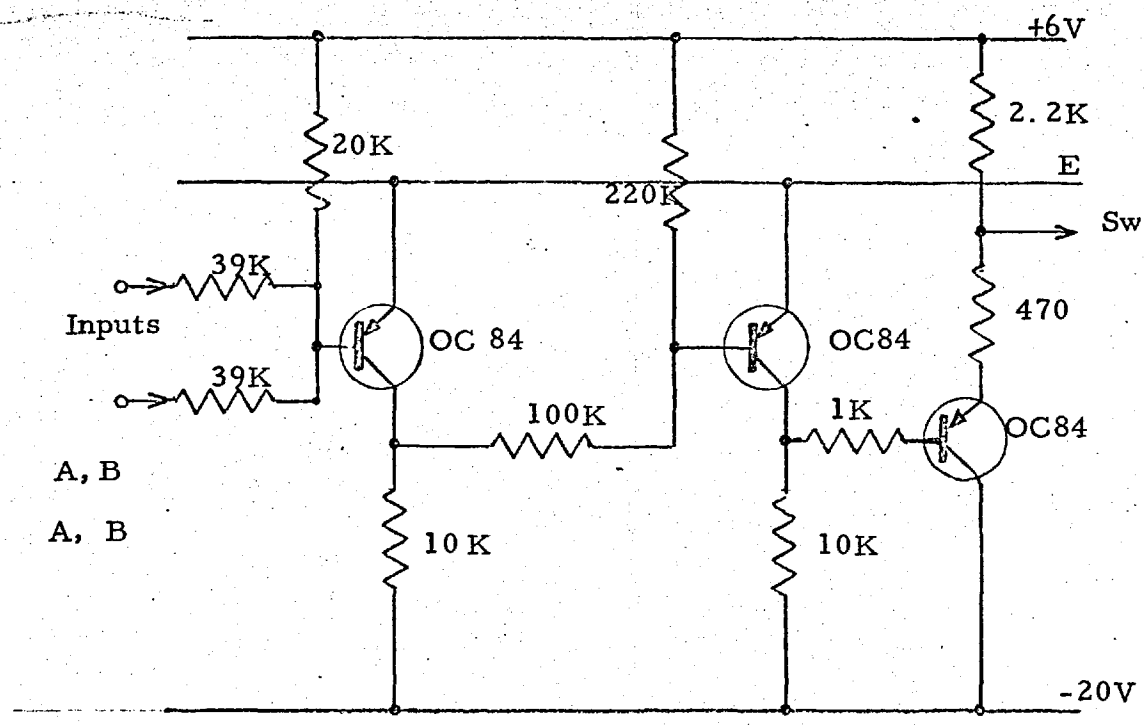

FIG:3.12 'NAND' GATE INVERTER BUFFER

BLOCK 4R or 4S

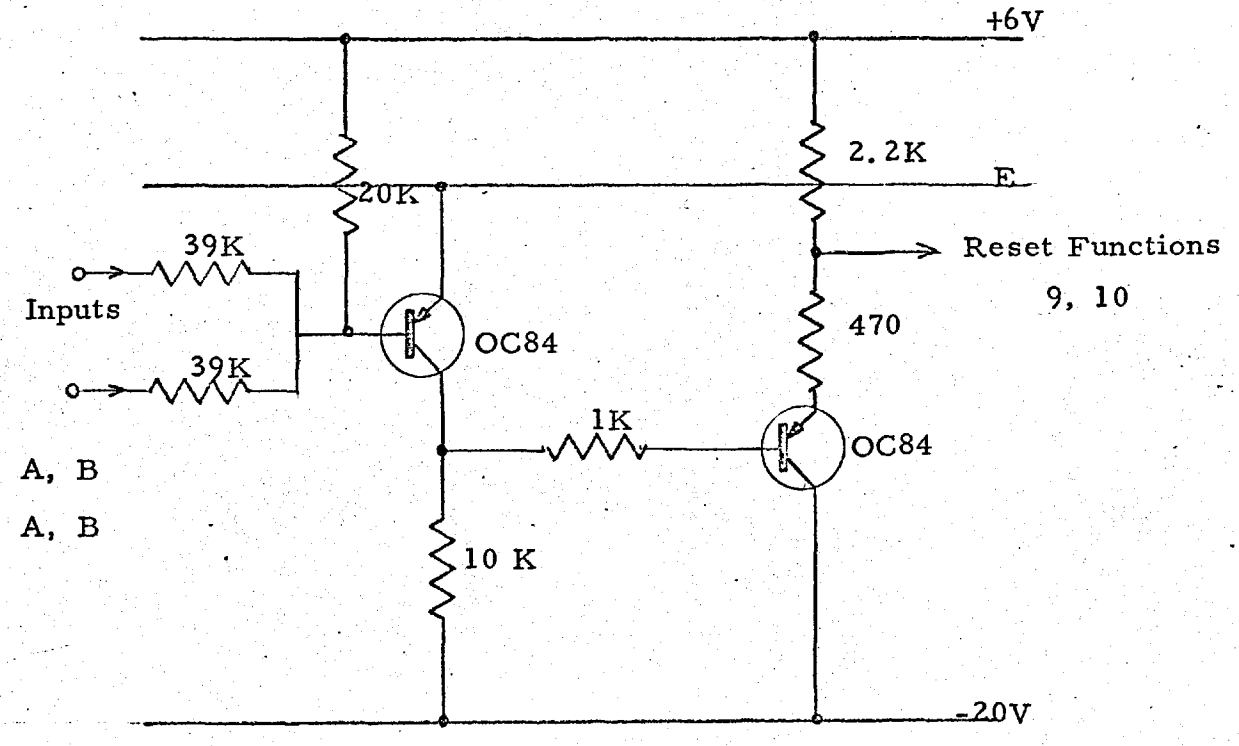

FIG: 3.12 'NAND' GATE BUFFER

BLOCK 5R or 5S

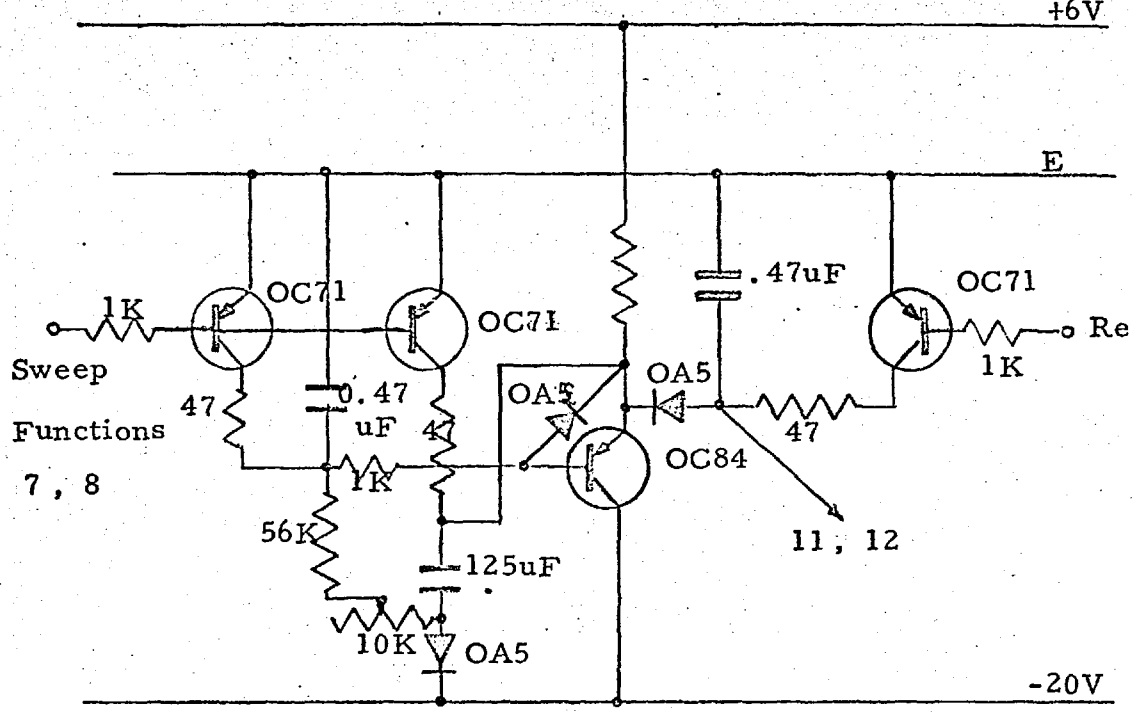

FIG: 3.12 RAMP GENERATOR (BLOCK 6R or 6S)

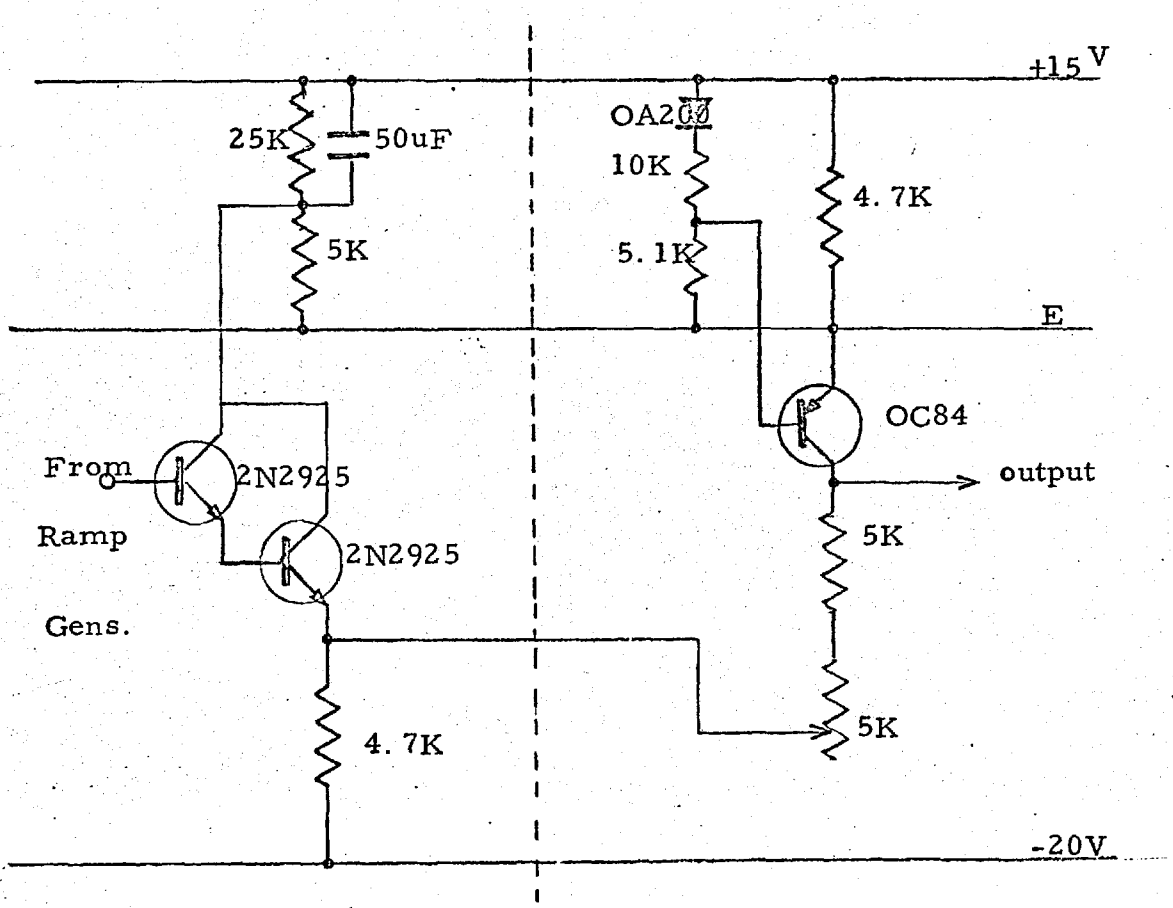

FIG: 3.12 BUFFER (BLOCK 1C) BIAS (BLOCK 2C)

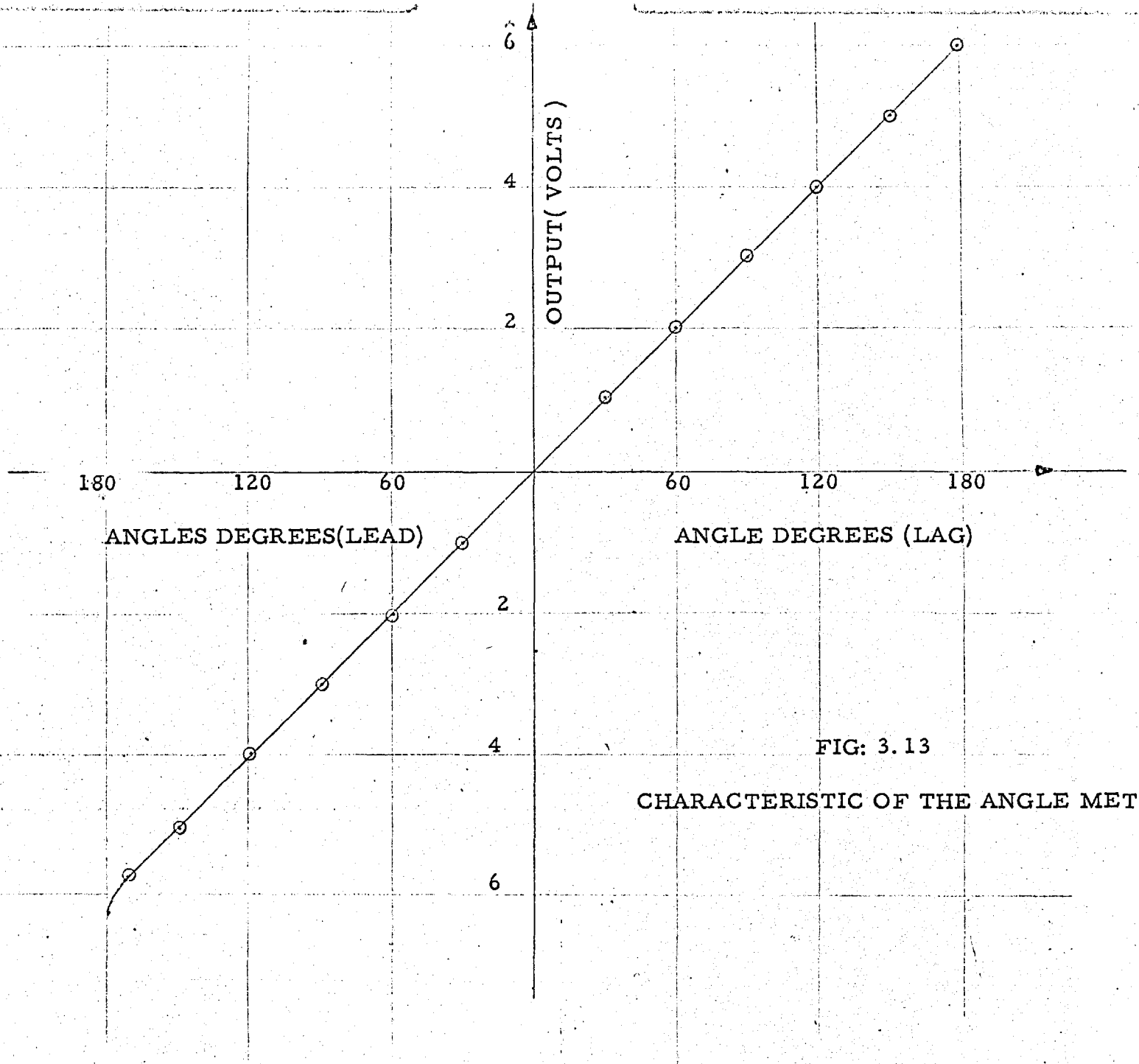

FIG: 3.13

CHARACTERISTIC OF THE ANGLE METER

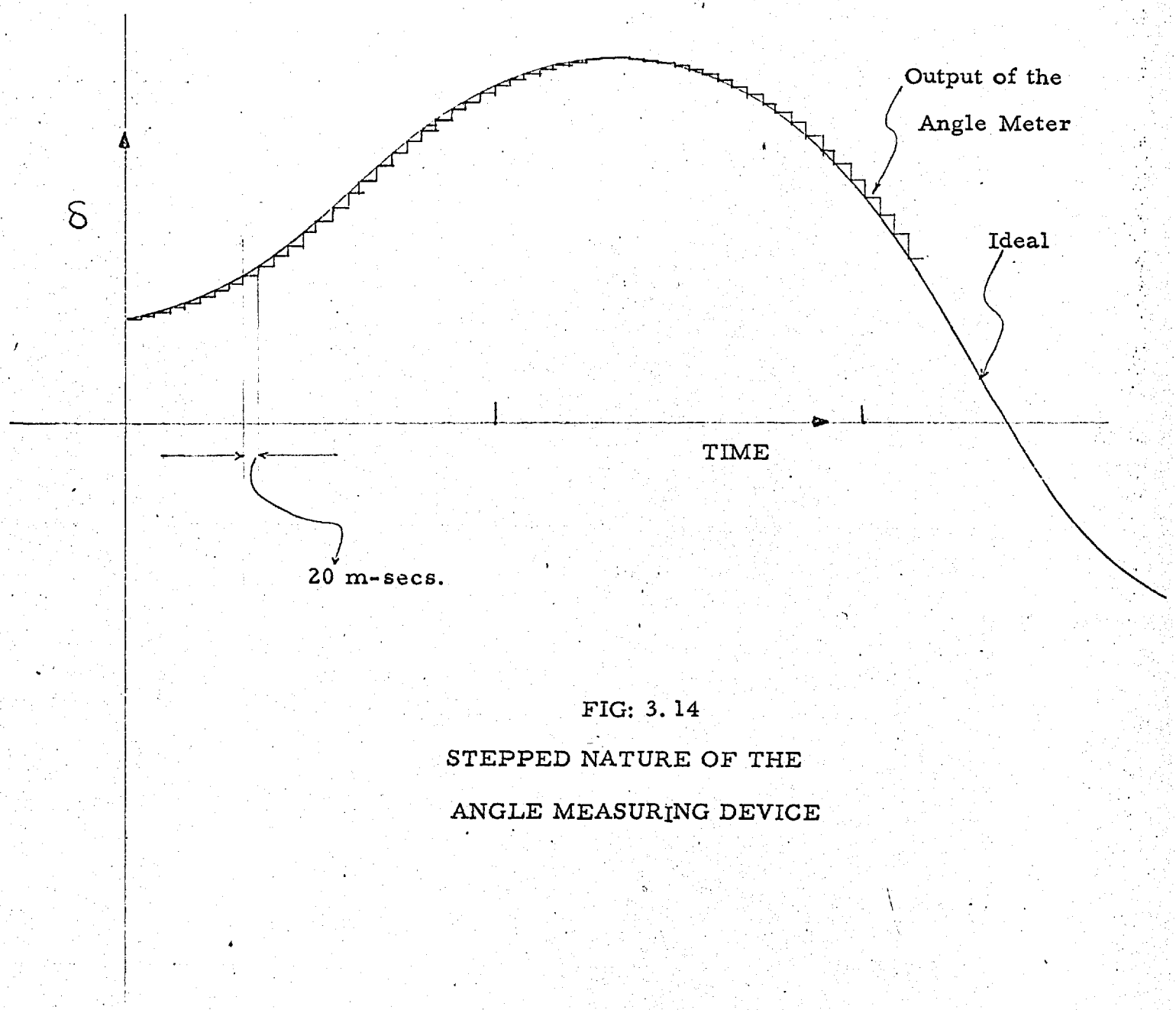

FIG: 3. 14

STEPPED NATURE OF THE

ANGLE MEASURING DEVICE

3. Drifts must be non-existent and the long term stability is essential to avoid frequent adjustments.

4. As for all other equipment used in conjunction with this simulator, one important requirement is no burden on the network analyser.

The enthusiasm for automatically solving the generator swing equations using network analyser having dynamic generator units grew in early 1950's. Various papers described some method of measurement of electrical power. All of them are unsuitable for a simulator working in real time.

Van Ness (Ref. 41) used the wave chopping principle to get the quadrature axis component of the generator current and a servo multiplier for getting the product of E_{qd} and I_q i. e. the voltage behind the Q-axis synch. reactance and the current in phase with it. Filters were used to extract the DC component of the chopped current wave.

Kaneff (Ref. 37) developed a special three element dynamometer type wattmeter. The device is quite complicated and its stability rather poor. One second of the true time is 50 seconds on this simulator.

Adamson, Barnes and Nellist (Ref. 34) used a wattmeter which is servo driven and is built round a single dynamometer movement. The instrument is deflected by amplified voltage and current signals derived from the network analyser but is restored

to a null position by the servo-mechanism. The power is given by the deflection of a potentiometer wiper mounted on the servo system output shaft. This device is again very slow in operation. In the same paper another wattmeter is described where the current wave is chopped in a phase sensitive rectifier system very much similar to one described by Van-Ness.

Short (Ref. 1) also suggested an arrangement similar to the one described above and alternatively Electronic multipliers but the smoothing circuit renders them unsuitable for a simulator working in real time..

In what follows two methods have been described for the measurement of power. One measures only I Cos ϕ and the other one V I Cos ϕ but the need for using smoothing circuits has been eliminated by using "SAMPLE & HOLD " technique.

3.5.2 I Cos ϕ METER : (WATTMETER 1)

In certain cases the generator can be represented by a constant voltage behind direct axis transient reactance (x'_d). In these cases the power is proportional to the component of current in phase with the voltage i. e. I Cos ϕ (where ϕ is the phase angle between the voltage and the current) and power can then be scaled for voltages.

3.5.2.1 PRINCIPLE OF OPERATION :

Fig 3.15 shows the basic principle of operation .

Every time the voltage wave passes through the peak, the current wave has the value I Cos ϕ which is stored and held constant till about 50 μ-secs before the next peak at which instant the previous store is discharged and the new value is recorded.

Fig. 3.16 shows how this device will measure the electrical power output during a transient disturbance.

3.5.2.2 CIRCUIT DETAILS :

A block schematic of this device is shown in fig. 3.17.

Block-wise circuit details are shown in fig. 3.18.

It is easier to detect zero-cross overs than the peaks of the voltage wave so the voltage wave has to be advanced or retarded by 90°. In a prototype this phase shift was provided by two passive networks separated by buffer stages. (see section 3.7.3.2). Although later on a magslip, having two windings separated in phase by 90° on the rotor, was prefered for other reasons and this phase shift network was no more required.

The voltage wave is buffered through a boot strapped Darlington pair emitter fdlower. The buffer has input impedance of 12 M ohms. The output is so biased that the schmitt trigger fires about 50 μ-sec before the zero cross over. The square wave differ-

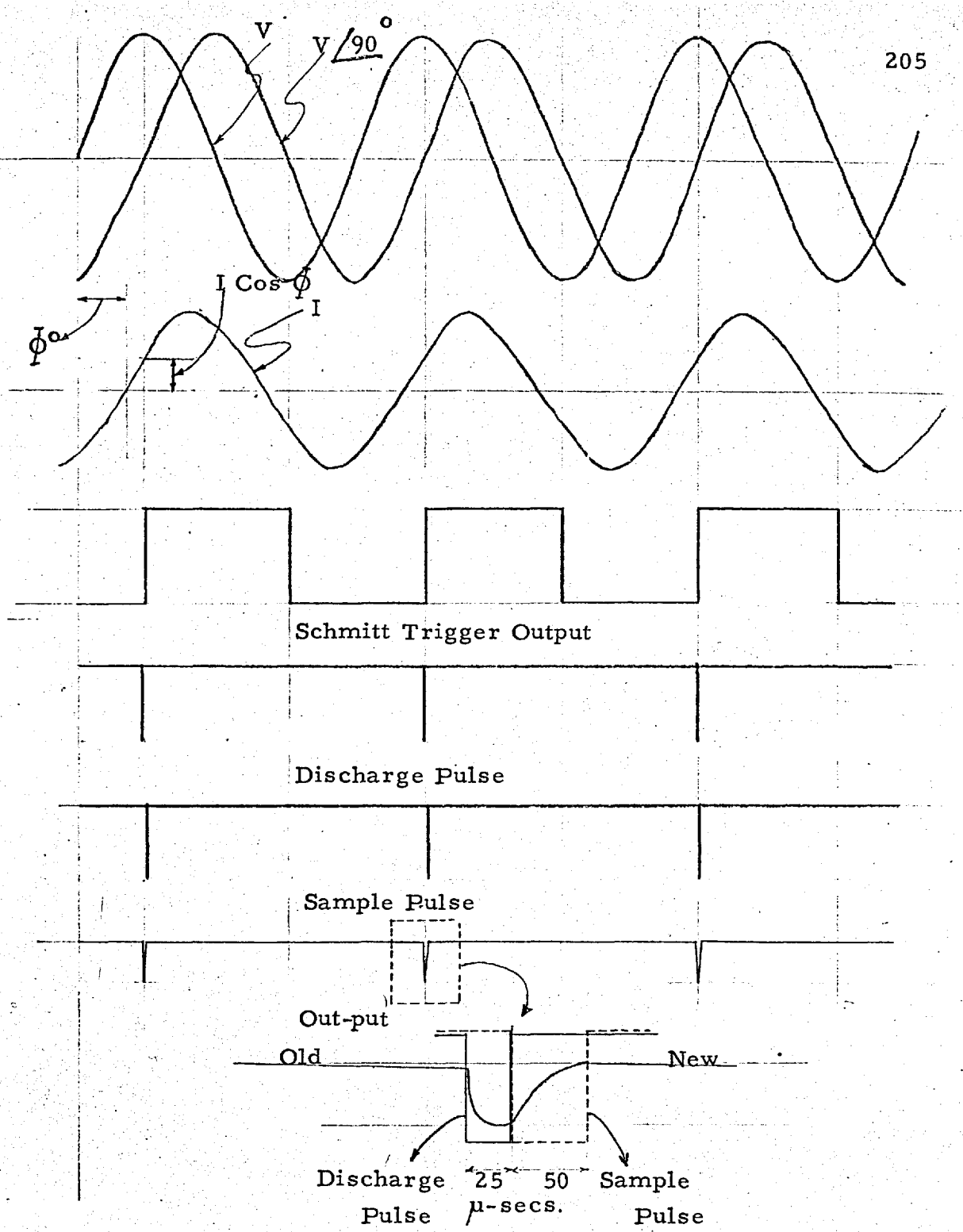

FIG: 3.15

PRINCIPLE OF POWER MEASUREMENT(WATT-METER 1)

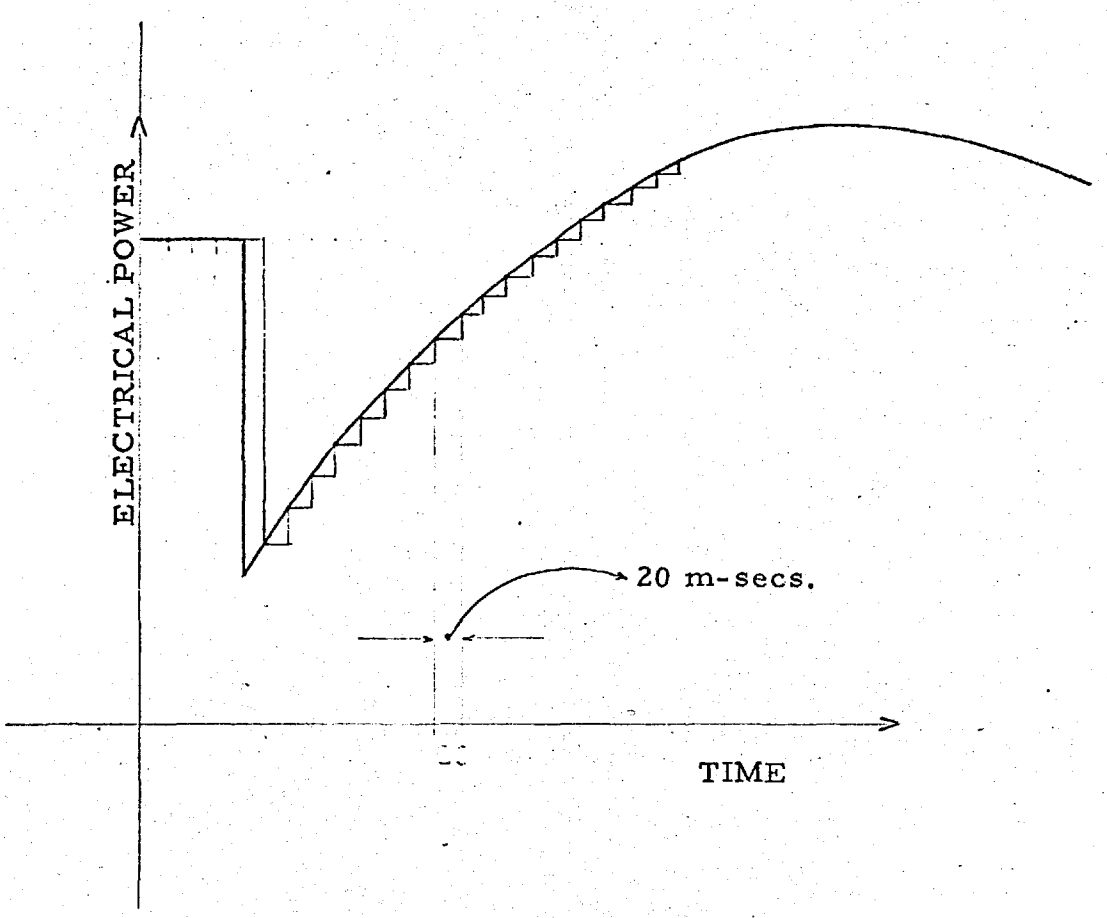

FIG: 3.16

MEASUREMENT OF ELECTRICAL POWER

DURING A TRANSIENT DISTURBANCE

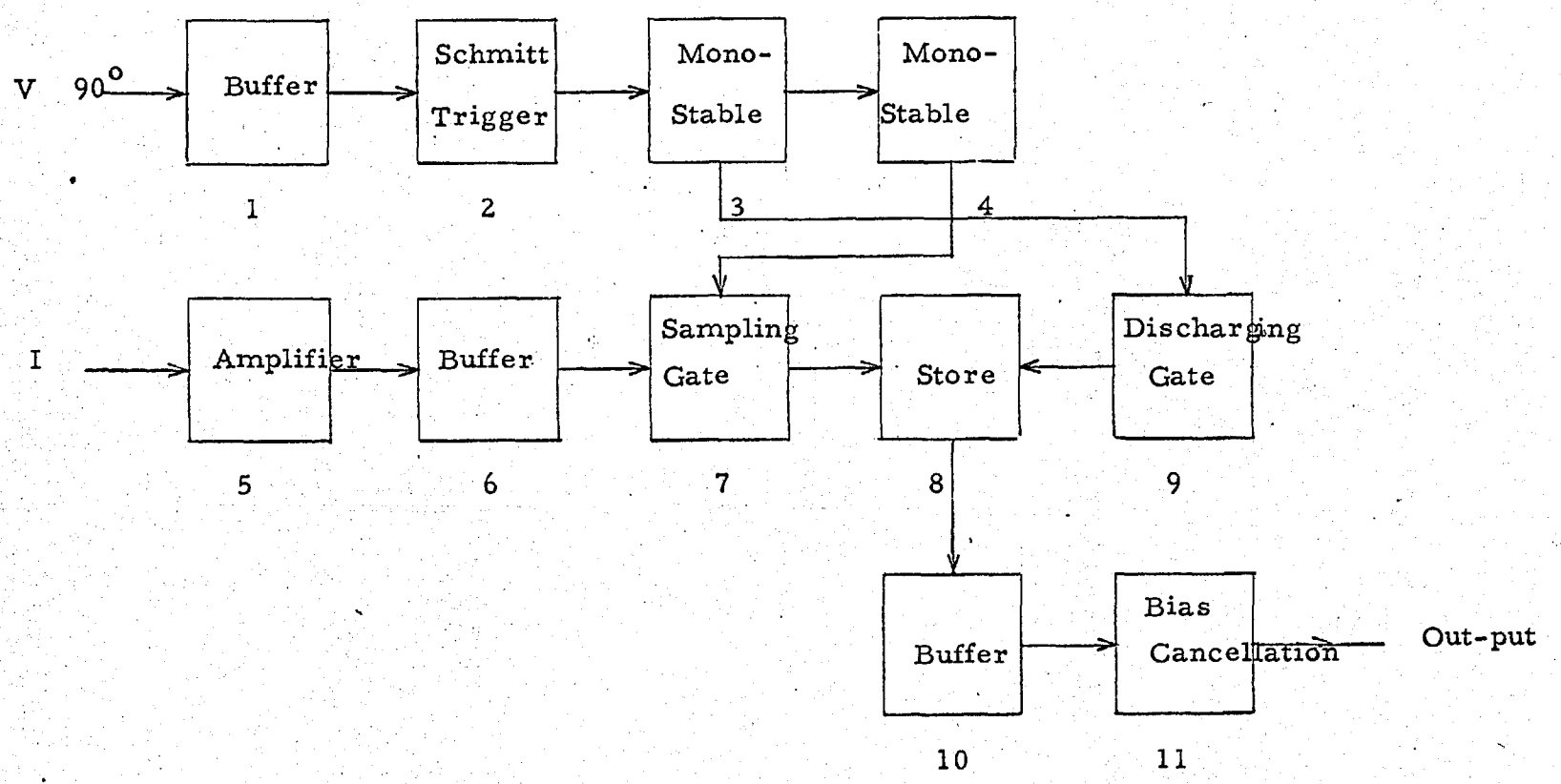

FIG: 3.17 BLOCK SCHEMATIC OF WATT-METER -1

entiated triggers a monostable with approximately 25 μ-sec delay. This in turn fires another mono-stable circuit having a delay of 50 μ-sec. The output of both mono-stable circuits is buffered and is biased to work at approximately + 1 V and -12 V levels.

A 50 ohms resistor in the path of the current gives a volt drop proportional to the current. This is amplified. The amplifier is DC coupled and has been stabilised by both current and voltage feed backs. The sampling and discharging gates are single pole and therfore sufficient DC bias has to be provided so that all points on the current wave are in the negative region.

Both the sampling and discharging gates are operated from the mono-stable output pulses. The current wave sample is stored on a capacitor which feeds into a very high input impedance buffer stage. The bias is cancelled in the final stage. To eliminate very sharp pulses, an RC circuit with a time constant of $\frac{1}{2}$ m-sec has been used.

Two calibration curves fig. 3.19 and fig. 3.20 give an idea of the accuracy of the device over the working range. The error is in unacceptable limitswhen the current is maximum and the power factor is zero, which occurs at load angles of $180.^{o}$

When the resistance of the lines is considered the error is of very much reduced magnitude as shown in fig. 3.20.

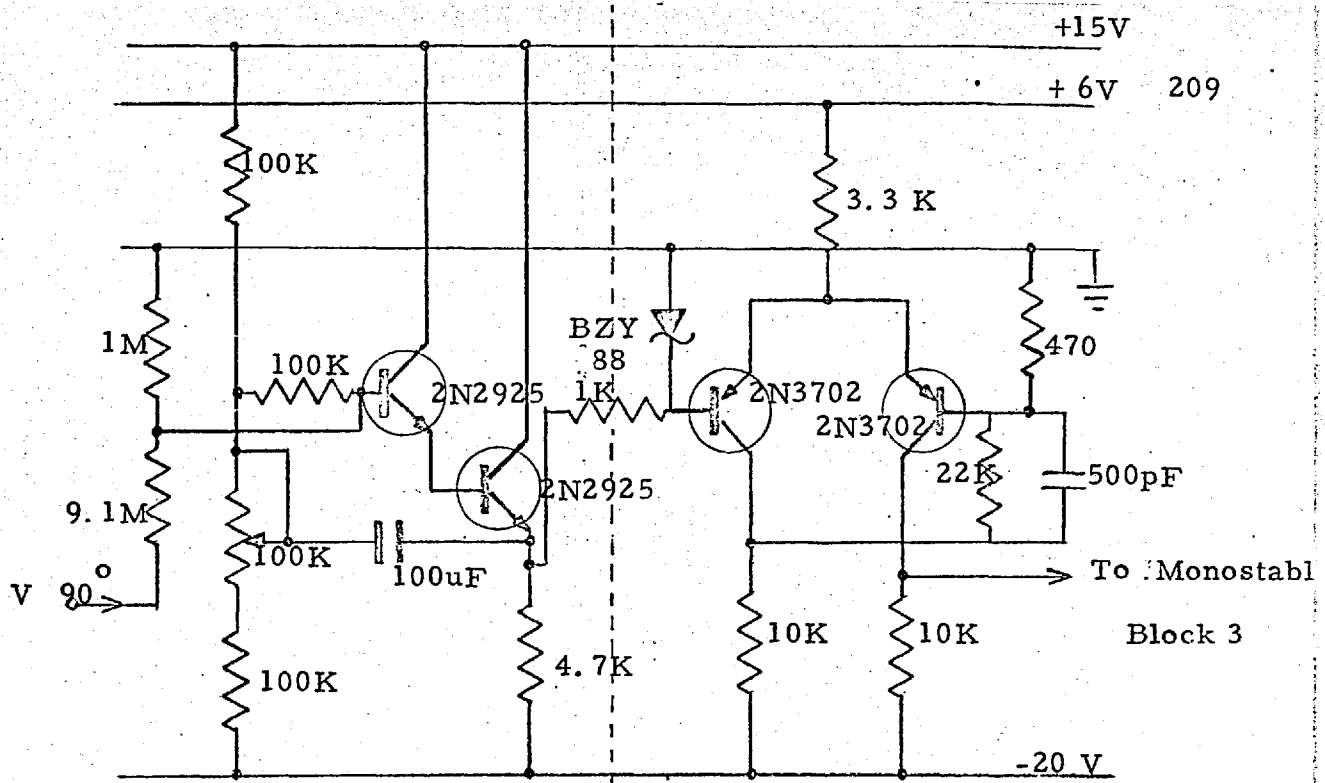

FIG: 3.18 BUFFER(BLOCK 1) SCHMITT TRIGGER(BLOCK 2)

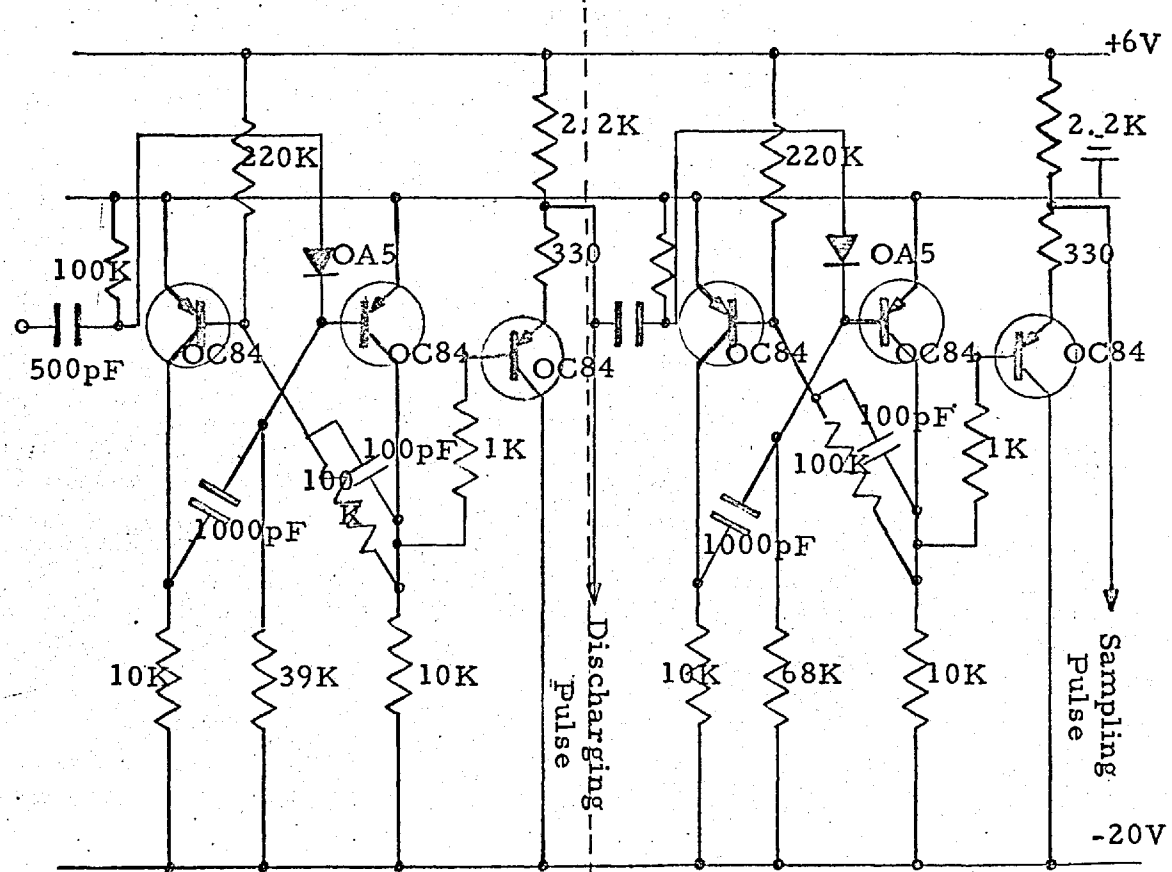

FIG: 3.18 MONO-STABLE (BLOCK 3) MONO-STABLE (BLOCK 4)

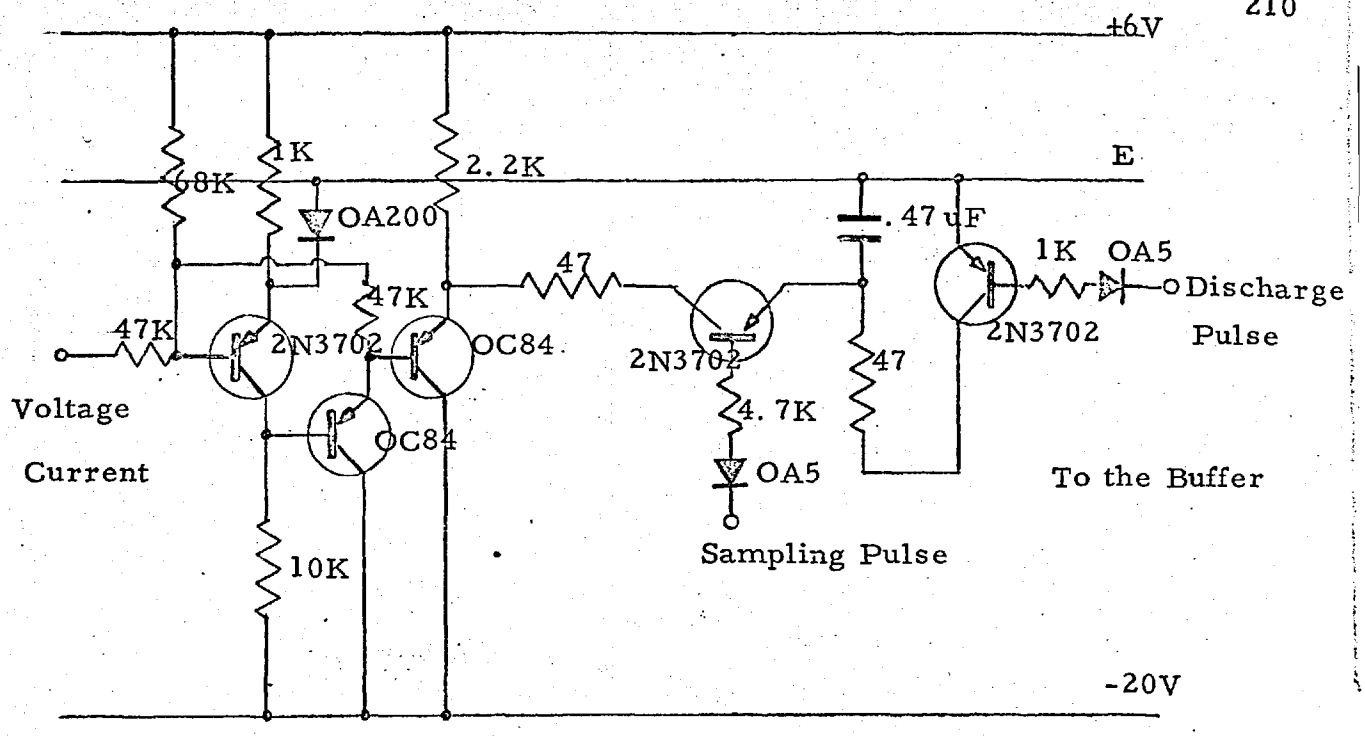

5 & 6 AMPLIFIER & BUFFER | 7 SAMPLING GATE | 8 STORE | 9 DISCHARGING GATE

FIG; 3.18

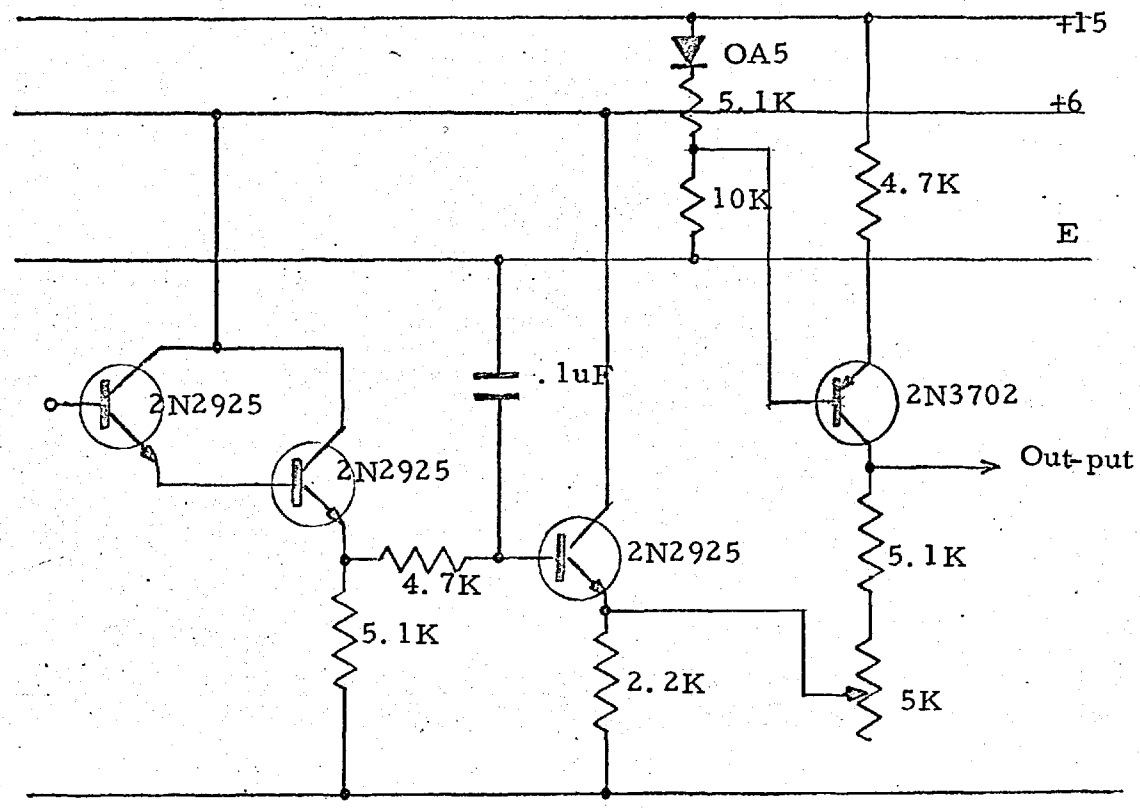

FIG: 3.18 BUFFER (BLOCK 10) BIAS OFF-SET (BLOCK 11)

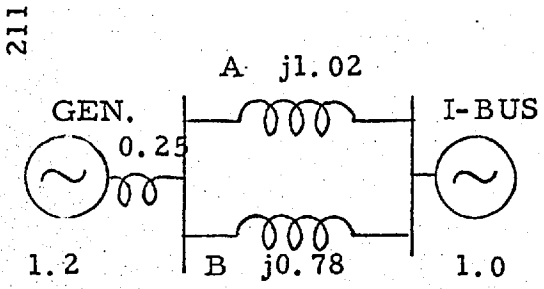

(All Values in p.u.)

FIG: 3.19 ANGLE - POWER CURVE

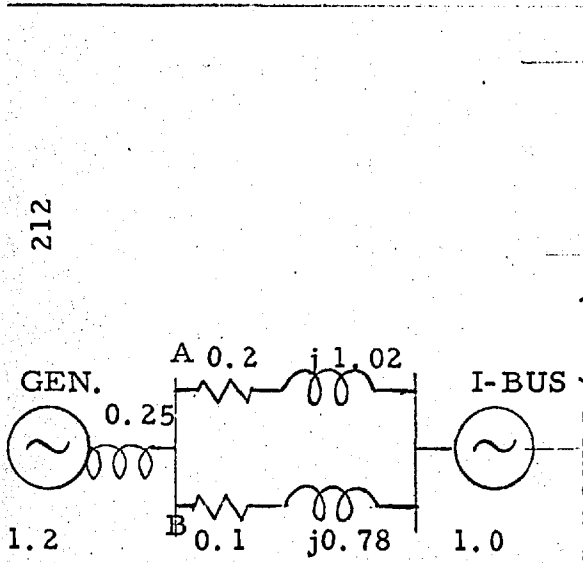

(All Values in p.u.)

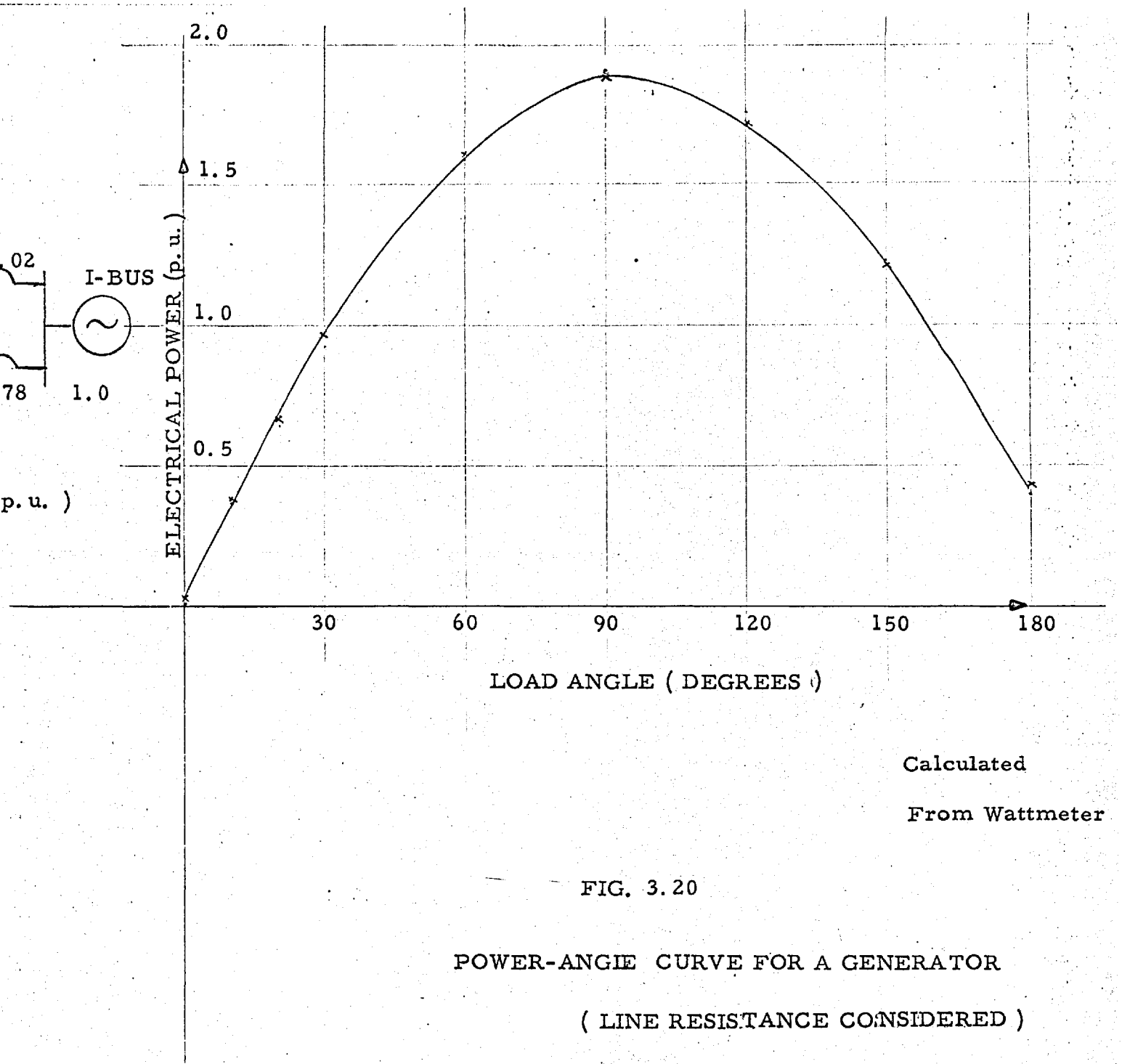

FIG. 3.20

POWER-ANGIE CURVE FOR A GENERATOR

(LINE RESISTANCE CONSIDERED)

3.5.3 WATTMETER 2 :

The wattmeter of section 3.5.2is suitable for working with a very simple generator simulator, consisting of constant voltage behind direct axis transient reactance. For a more general case, a variable voltage behind Q-axis synchronous reactance is used. (see section 2.1.5). In this case a multiplier is used for power measurement.

3.5.3.1 PRINCIPLE OF OPERATION :

In the scheme proposed below the product of the voltage (corresponding to the voltage behind the Q-axis transient reactance) and a voltage proportional to the current is obtained from a quarter square multiplier. The product contains a term which alternates at twice the network analyser frequency. For if,

$$V_v = V_v \text{ Sin } wt$$

$$V_i = V_i \text{ Sin } (wt - \phi) \quad \text{where } \phi \text{ is the angle of lag.}$$

then $$V_v . V_i = V_v . V_i . \text{ Sin } wt \text{ Sin } (wt - \phi)$$

$$= \tfrac{1}{2} . V_v . V_i . \text{ Cos } \phi - \text{Cos } (2wt - \phi)$$

Filtering has been avoided by the process of integration coupled with " Sample and Hold " device, as explained below,

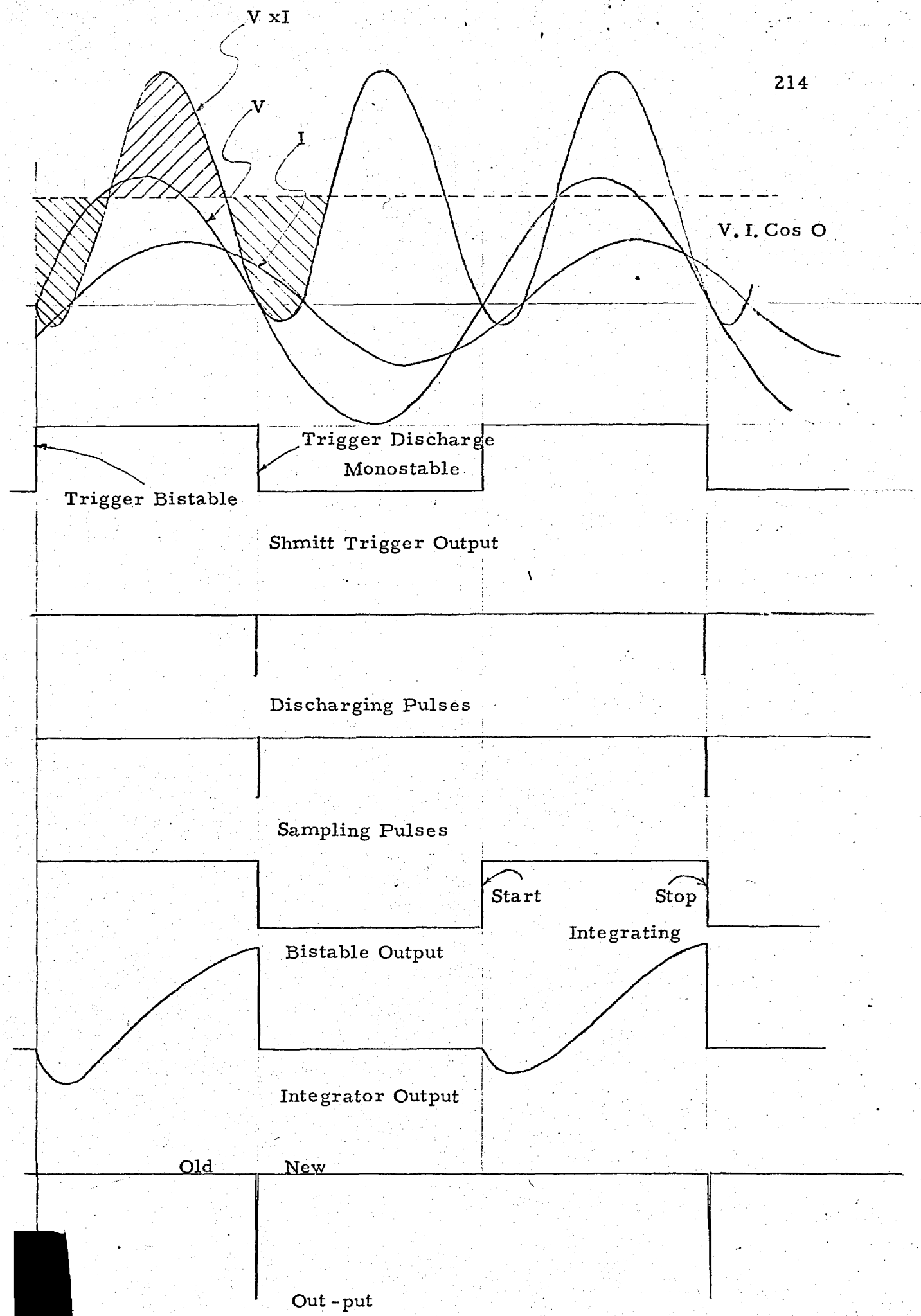

FIG: 3.21 PRINCIPLE OF POWER MEASUREMENT

(WATTMETER 2)

The multiplier output is integrated over the positive half of the voltage wave; the value is stored and held constant, while the integrator is reset during the negative half of the voltage wave. The integrator output is proportional to the average electrical power $\frac{1}{2} \cdot V_v \cdot V_i \cdot \cos \phi$ because the term $\frac{1}{2} V_v V_i \cos (2wt - \phi)$ integrates to zero. Fig 3.21 shows eloquently the basic principles described above.

3.5.3.2 CIRCUIT DETAILS :

Fig 3.22 shows a block diagram for the circuit of Wattmeter 2 and the detailed circuit is shown in fig. 3.23.

The voltage wave is buffered to lessen the burden on the network analyser. Schmitt trigger is used to detect the zero cross overs. The positive going zero cross over triggers a bistable circuit which sets the integrator in the integration mode. Schmitt is arranged to change its state about 50 μ-sec before the negative going zero cross over and at this instant a monostable is triggered. The pulsed output from this monostable is used to discharge the sample taken in the previous cycle. This monostable in turn triggers another monostable which gates another sample to the storing capaciter. This monostable provides a trigger to the bistable which turns the integrator into the reset mode.

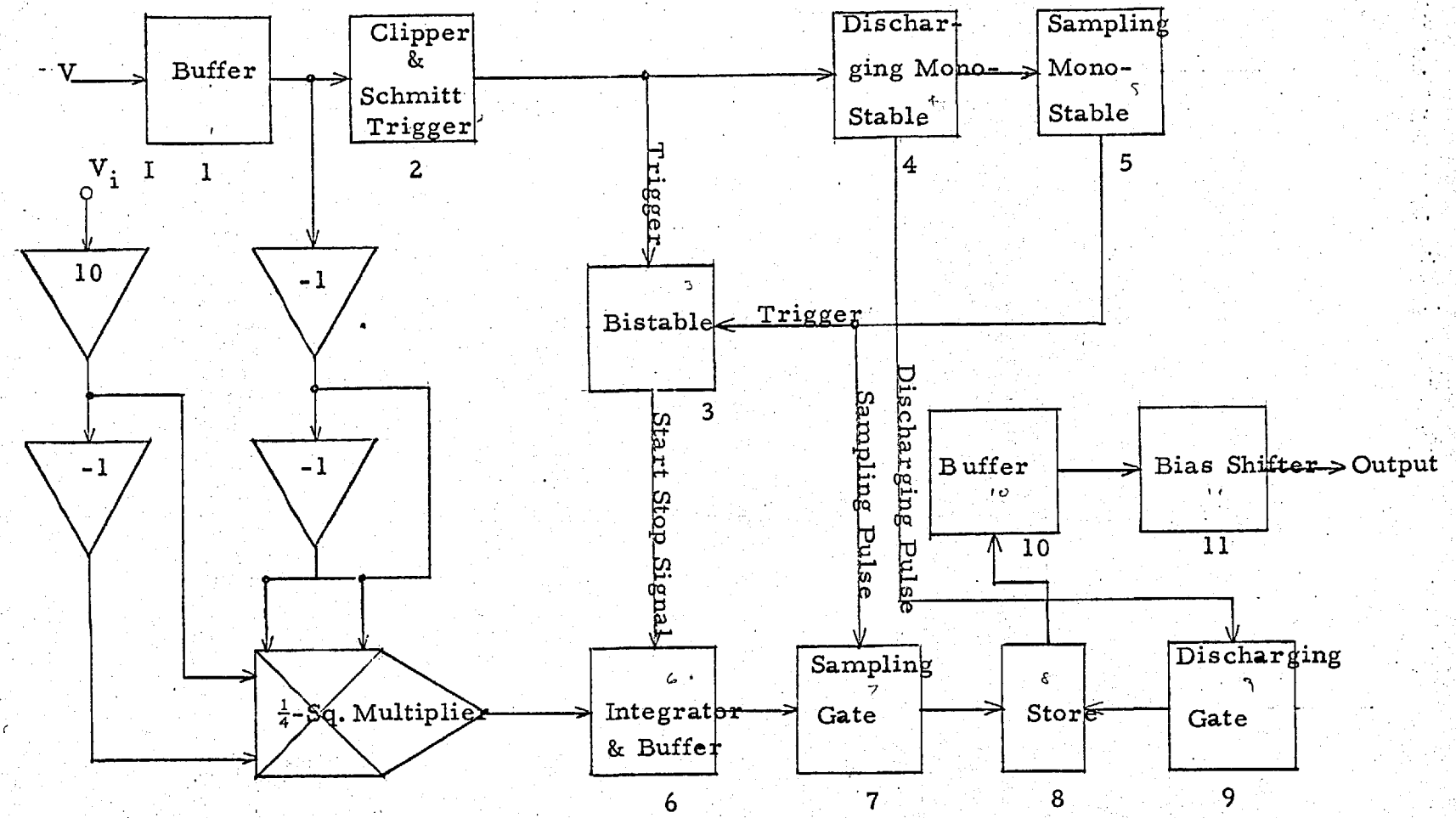

FIG: 3.22 BLOCK SCHEMATIC OF WATTMETER 2

FIG: 3.23

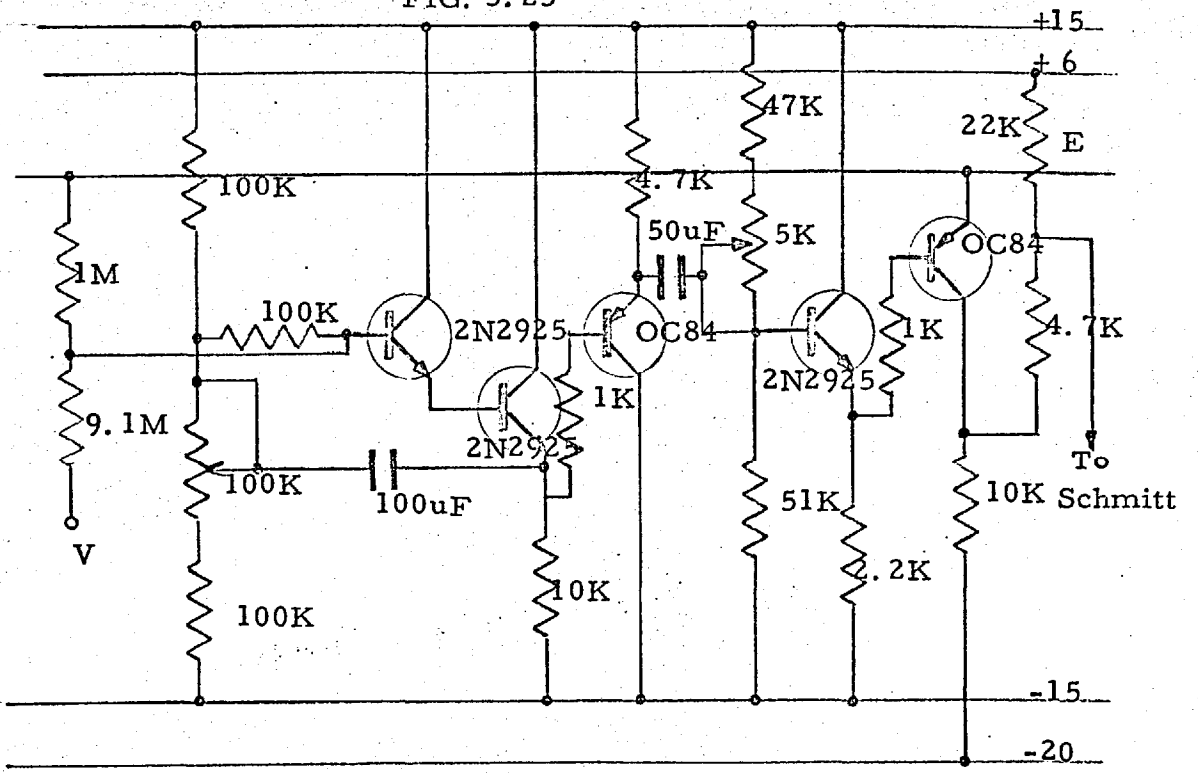

BUFFER (Block1) &

CLIPPER(Block 2)

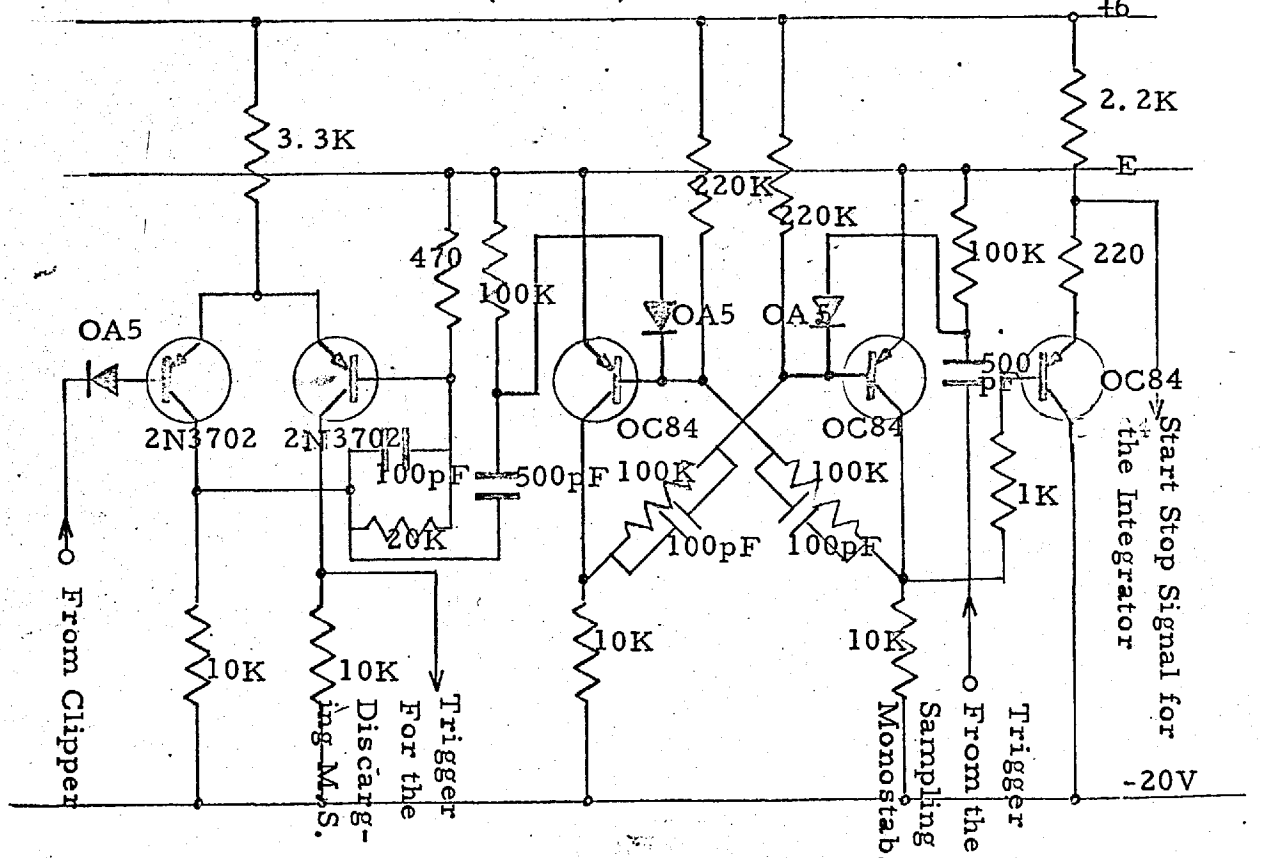

SCHMITT TRIGGER(Block 2)

BISTABLE (Block 3)

FIG. 3.23

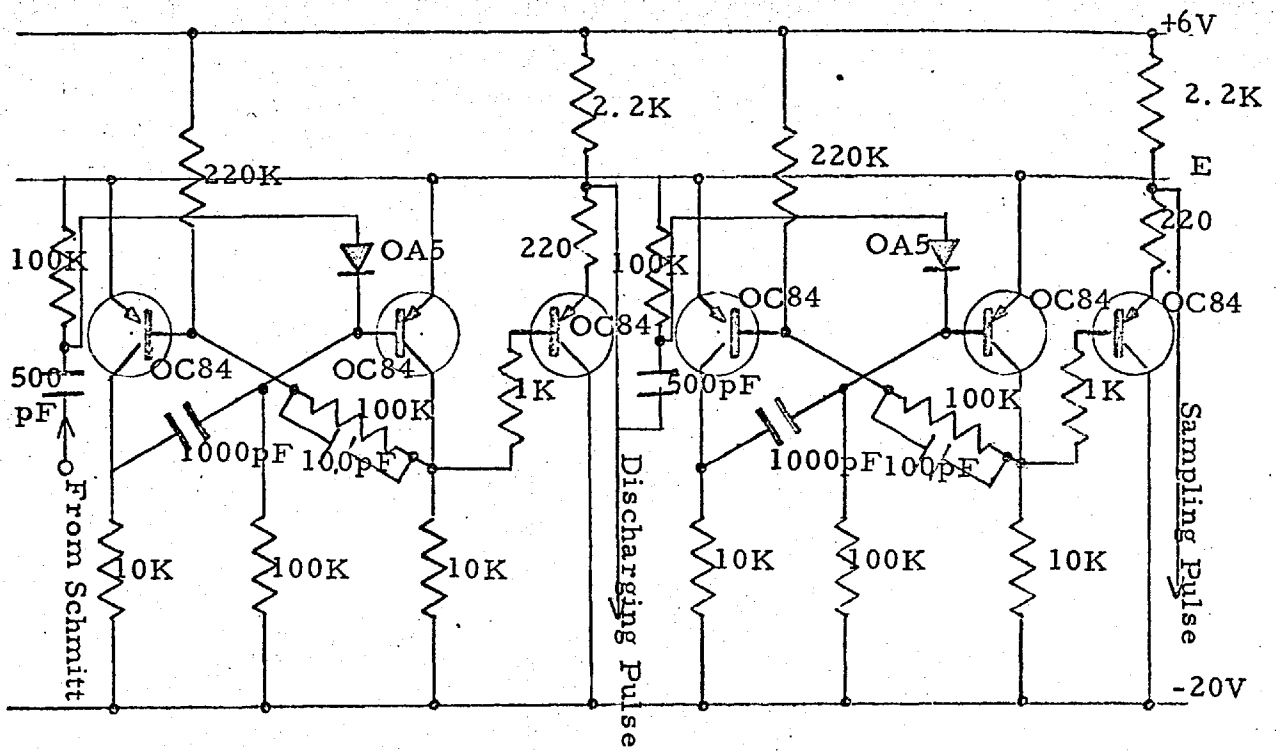

DISCHARGING MONOSTABLE (Block 4)

SAMPLING MONOSTABLE (Block 5)

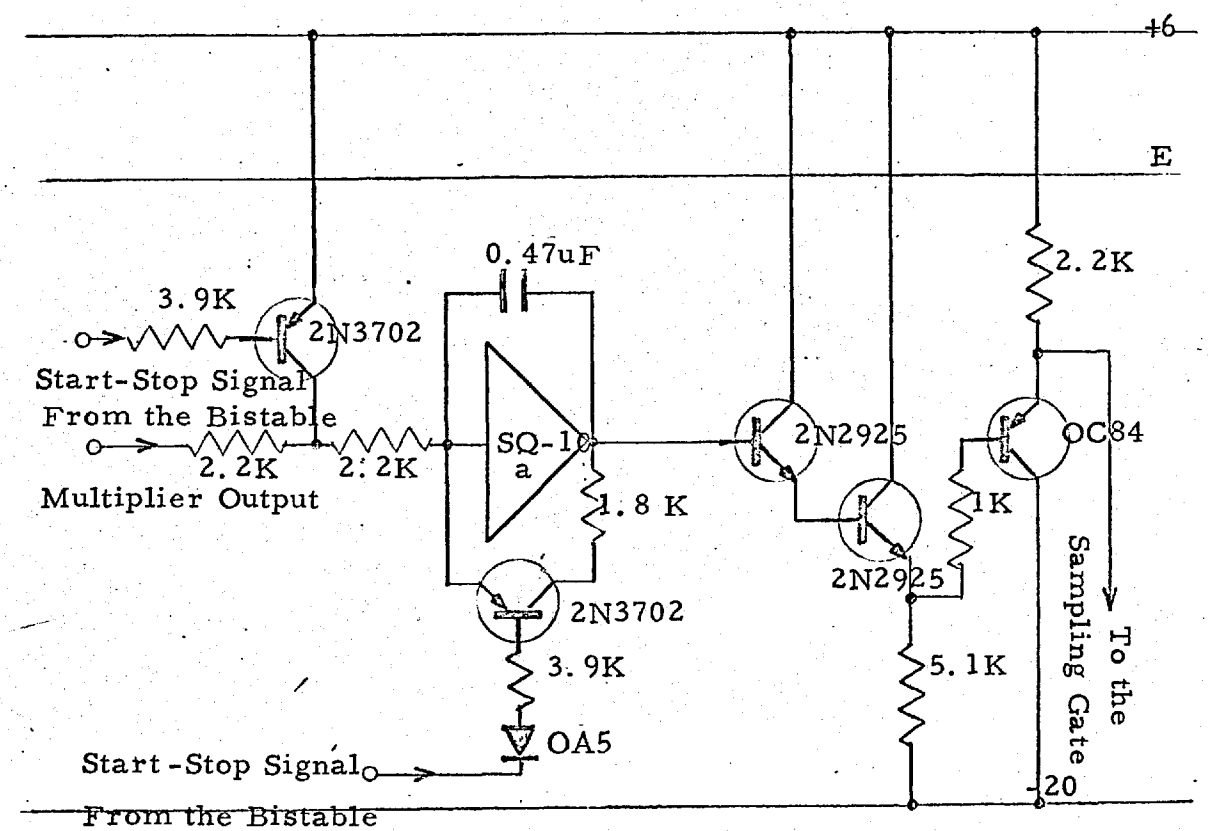

INTEGRATOR (Block 6)

BUFFER(Block 6)

FIG: 3.23

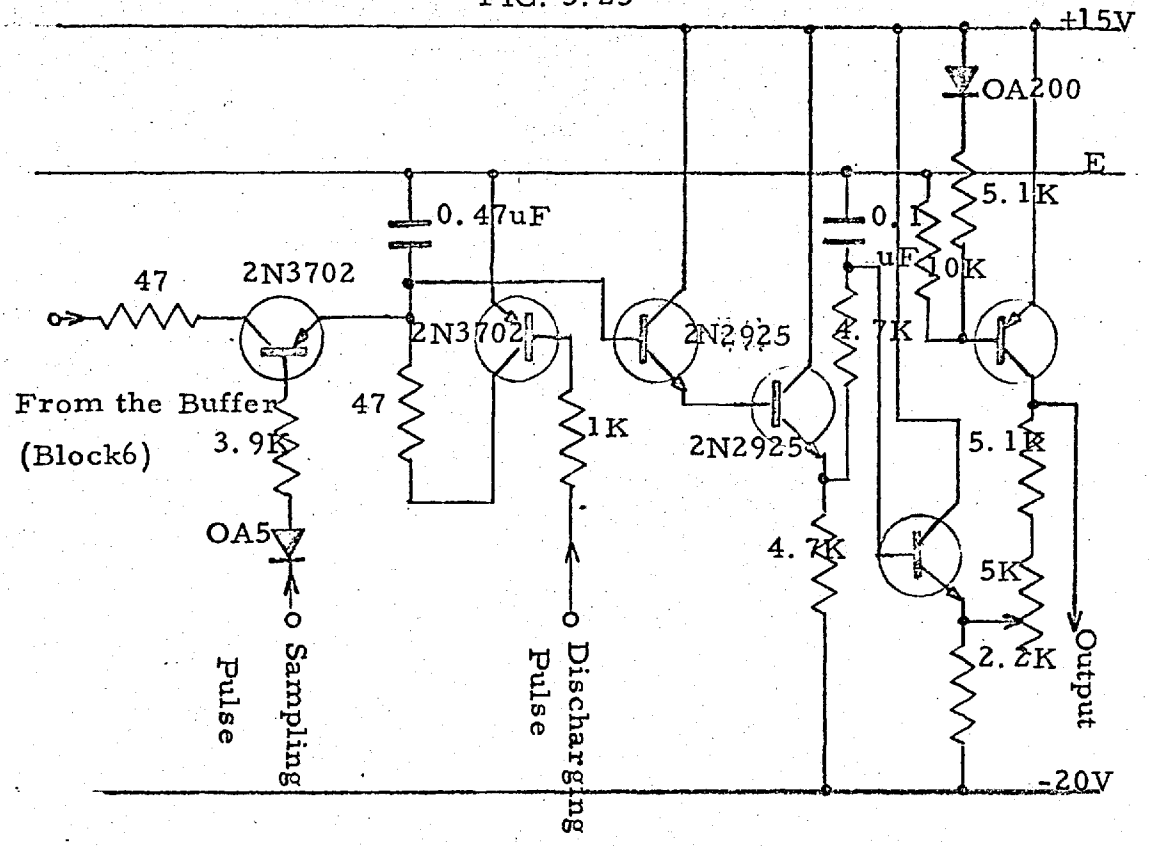

SAMPLING GATE (Block 7) | STORE (Block 8) | DISCHARGING GATE (Block 9) | BUFFER & BIAS SHIFTER (Block 10 &11)

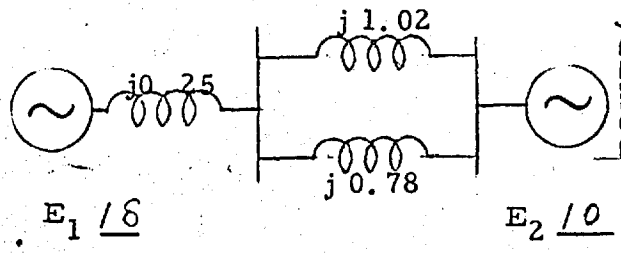

A. E_1 = 1.0 p.u. E_2 = 1.0 p.u.

B. E_1 = 1.2 p.u. E_2 = 1.0 p.u.

POWER (p.u.)

1.5
1.0
0.5
0.5
1.0
1.5

B
A

90 60 30 30 60 90 120 150 180

LOAD ANGLE

× From Wattmeter

• Calculated

FIG; 3.24 POWER - ANGLE CHARACTERISTIC

between the calculated and the observed values of the electrical power is greatest at very low power factors as observed in the case of wattmeter 1.

3.6 CURRENT COMPONENT RESOLVER :

In a scheme for the generator unit simulation the effect of the transient saliency can also be included. (section 4.1)

It requires the component of current in phase with the direct axis. The magnitude is given by I Sin ϕ where ϕ is the angle between the current vector and the Q-axis.

The device is very similar to the Wattmeter 1 (I Cos ϕ) discussed in section 3.5.2. The only difference is that the current wave is sampled at the zero cross over of the voltage and not the peak of the voltage as shown in fig. 3.25.

3.7 VOLTAGE MEASUREMENT :

3.7.1 GENERAL:

Voltage measurement in the simulated machine unit is needed at two points.

(i) At the terminal of the machine unit.

(ii) At the point behind the reactance representing the generator unit.

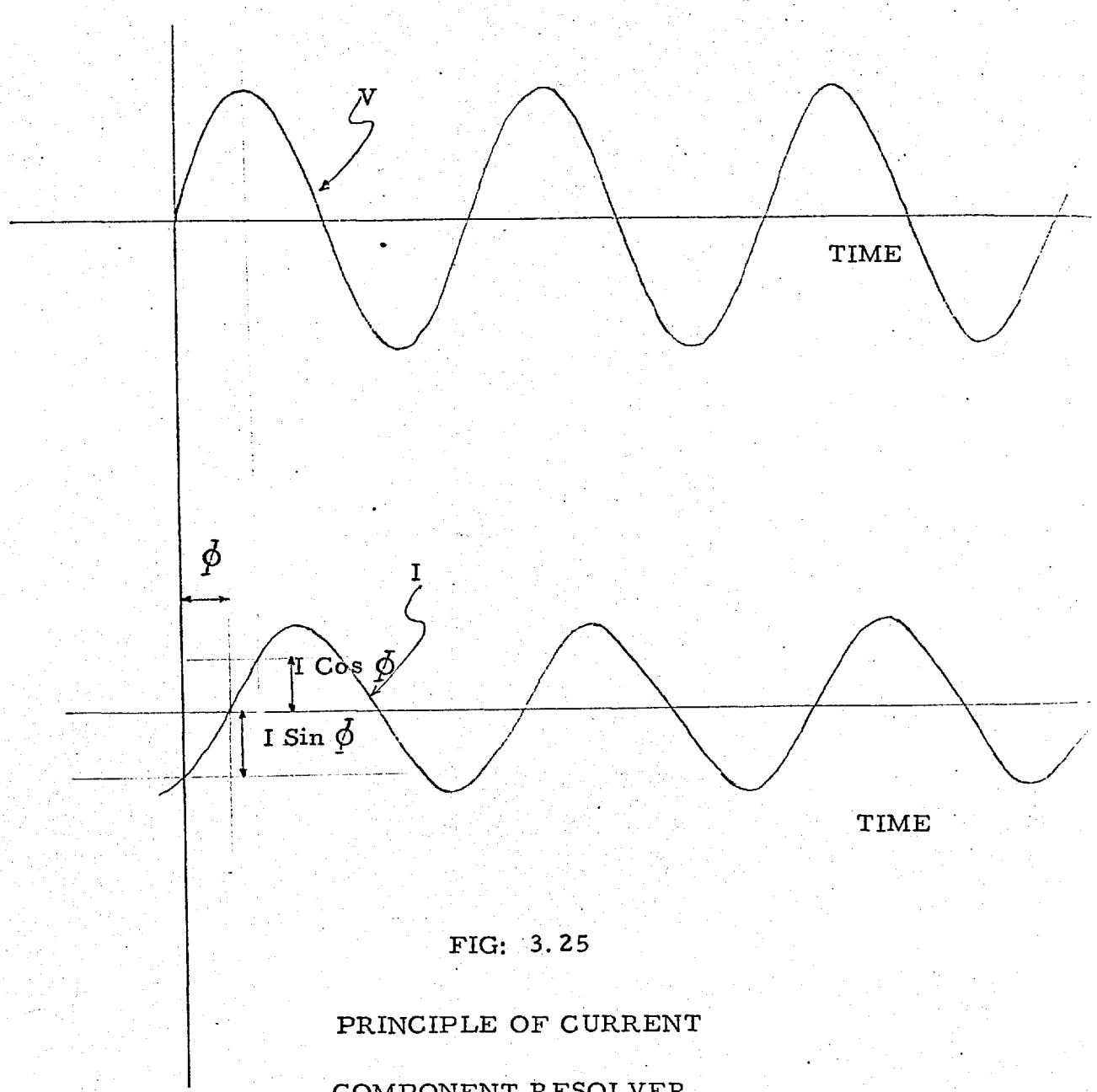

FIG: 3.25

PRINCIPLE OF CURRENT

COMPONENT RESOLVER

Since the equations of the voltage regulator are solved on the anlogue computer and a DC servo is used to change the voltage magnitude behind the machine reactance , the voltage measuring device should have DC voltage proportional to the AC voltage.

Other important requirements are

(i) Linearity over the working range.

(ii) No time delay.

(iii) Minimum burden on the N. A.

Although the details of the simulated machine unit which includes the transient saliency and the effect of variable flux linkages has been discussed in chapter 4, a brief mention as to why voltage measurement is required is given below.

$E_{qd'}$ the voltage behind the Q-axis synchronous reactance (x_q), is computed on the analogue computer to satisfy the machine equations 2. 1. 20, 2. 1. 21, 2. 1. 22 and 4. 2. 3. The computed value is then set on the I-Pot by a servo-mechanism. The voltage off the wiper of the I-pot is required as the feed back signal for the servo-mechanism.

The terminal voltage of the machine is required for AVR simulation, in which case it is compared with a fixed reference and the error is used to compute the output voltage of the exciter. Transfer functions of the amplifier, limiter, stabiliser and exciter are patched up on the analogue computer. The output is the voltage at

the field terminals, which is combined with the machine equations, listed above, to compute E_{qd}.

3.7.2 PRINCIPLE OF OPERATION :

Rectification and filtering will not be appropriate in view of the requirements discussed above. The filtering circuits can only be avoided by working with the ' Sample ' and "Hold " device, similar to that discussed in section 3.5 for power measurements. The sample in this case is taken of the peak of the voltage wave and is held constant untill about 50 μ-sec before the next peak.

The working principle is illustrated in fig. 3.26 and the block schematic is shown in fig. 3.27.

3.7.3 CIRCUIT DETAILS :

3.7.3.1 VOLTAGE BEHIND THE MACHINE REACTANCE :

Since zero cross overs are easier to detect than the peaks, a voltage wave having a phase difference of 90° from the voltage wave being sampled is needed.

The magslip rotor has two windings at 90° to each other. One winding through the I-Pot is used as a voltage source for machine representation, and the other can be used for detecting the sampling instant. The block schematic and the circuit diagram in figs. 3.27 and 3.29 are very much the same as in figs. 3.17 & 18

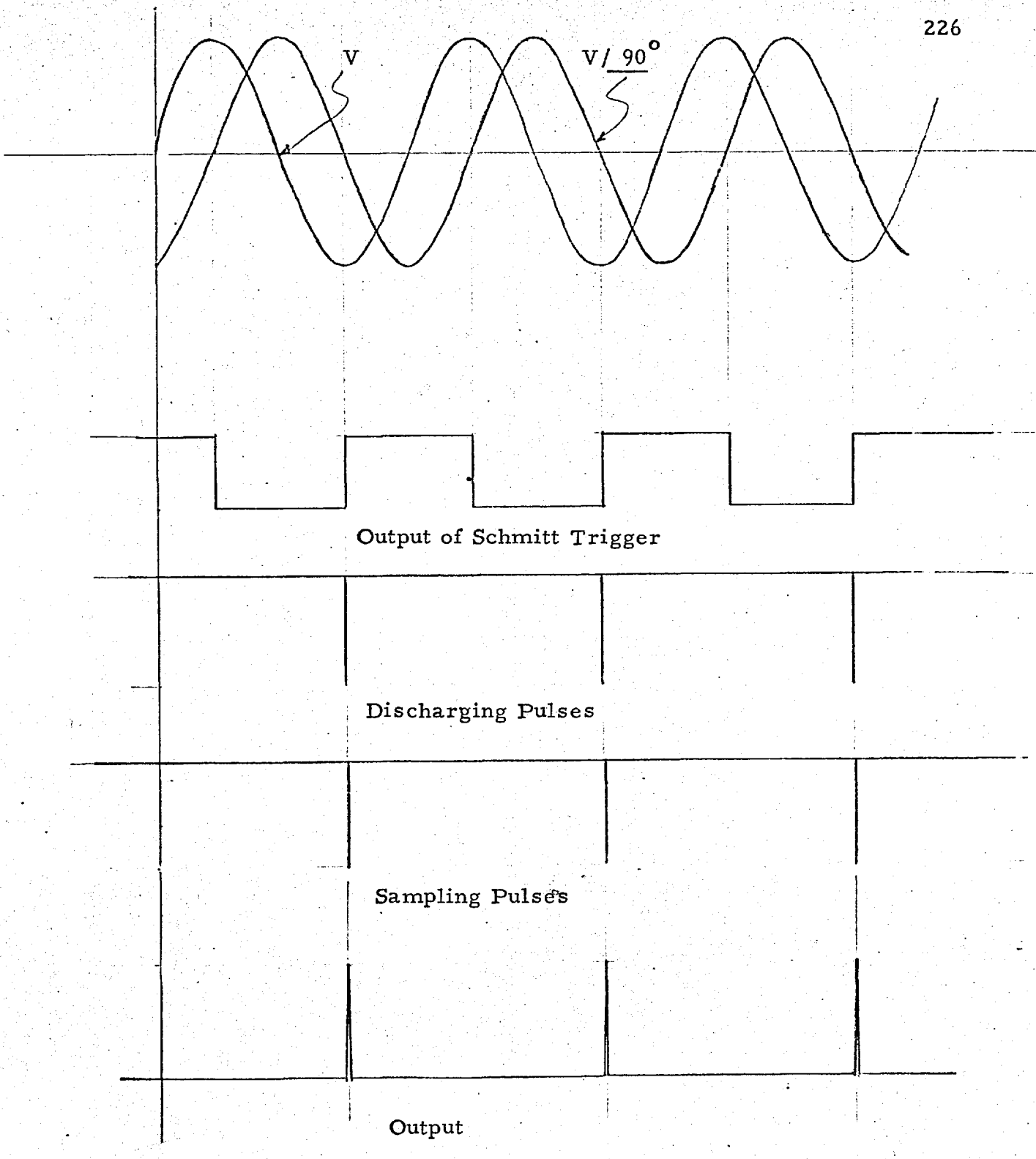

FIG: 3.26 PRINCIPLE OF VOLTAGE MEASUREMENT

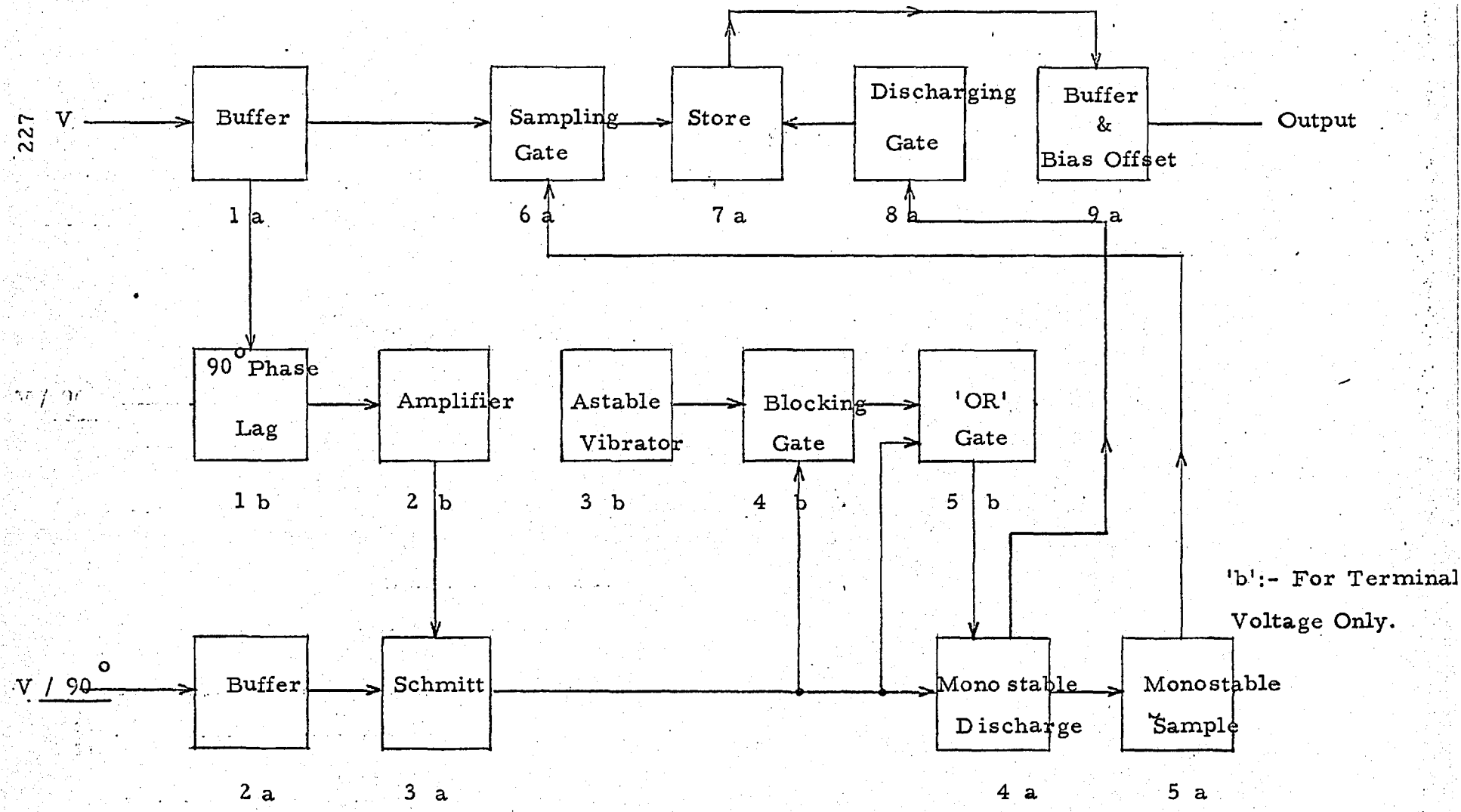

FIG : 3.27 BLOCK SCHEMATIC OF VOLTMETER

for Wattmeter 1.

3.7.3.2 MACHINE TERMINAL VOLTAGE :

In this case the terminal voltage is shifted in phase by 90°. A pure integrator, or the differentiator circuit, ideally provides a phase shift of 90° independent of the frequency of the input. An integrator is to be preferred to a differentiator as the harmonics in the voltage wave can get amplified and the noise may be introduced by the differentiator.

A three stage common emitter transistor amplifier with an open loop gain of 3000 was tried as an integrator with a capacitive feed back. This could provide a phase shift of 78° only. Another disadvantage was that during the periods of rapid changes the voltage wave becomes asymmetric and the DC offset stays for a long time.

A passive lag circuit seemed most promising. The circuit and its phase characteristic and the Nyquist Diagram is shown in fig. 3.28. Two of these circuits were cascaded to obtain a phase shift of 90°. It is clear from the phase characteristic that over a region of frequency, the phase shift is not appreciably changed. The maximum phase shift can be arranged to occur at the normal N.A. frequency.

Other advantages of this configuration are that the attenuation of the signal is minimum compared to any other

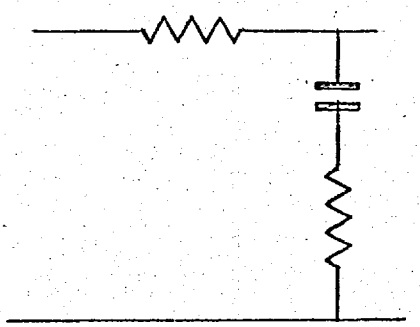

(a) LAG NETWORK

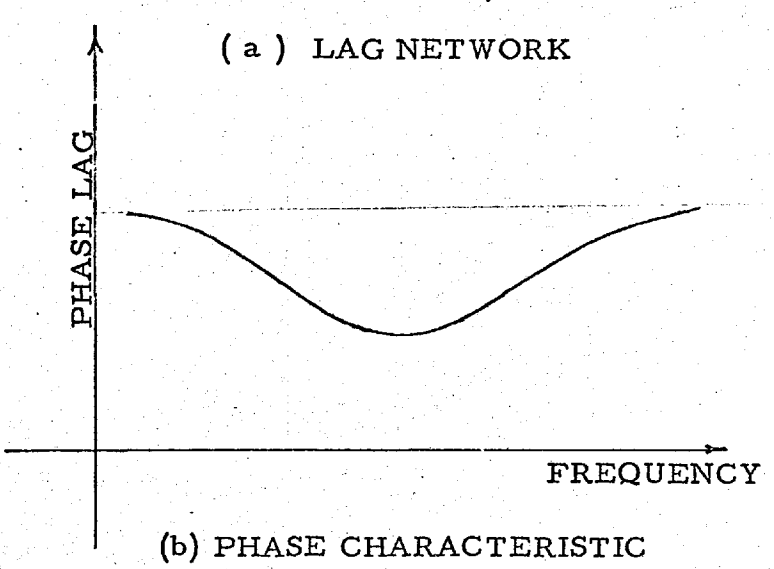

(b) PHASE CHARACTERISTIC

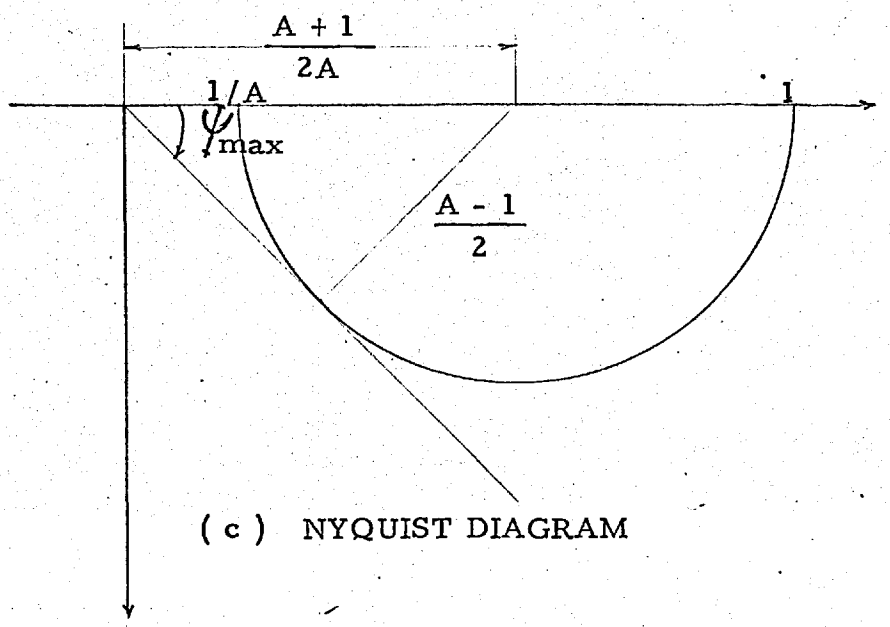

(c) NYQUIST DIAGRAM

FIG : 3.28

combination of the R and C's and that the DC offset on step changes dies fastest.

Transfer function is given by

$$f(p) = \frac{1 + p\,CR}{1 + p\,C(r+R)} =$$

$$= \frac{1 + p\,T}{1 + p\,A\,T} \quad \text{where } T = CR \text{ and } A = \left(\frac{r+R}{R}\right)$$

Frequency response

$$f(jw) = \frac{1 + j\,w\,T}{1 + j\,w\,A\,T}$$

From the Nyquist plot $\angle f(jw)$ is maximum when

$$\sin \psi_{max} = \frac{A-1}{A+1}$$

$f(jw)$ for this value of A and w is $= 1/\sqrt{A}$

Two circuits each providing a phase shift of 45° are cascaded. The value of A and T are worked out for 45^{0} phase shift to occur at 50 c/s.

The change in the phase shift due to 1 c/s change in frequency is only 0.1°. D.C. offset dies off in $1\frac{1}{2}$ cycle after a step disturbance.

In case the short circuit occurs at the terminal of the machine, the discharging and sampling pulses will cease to exist and therefore the last sample taken will stay for a long time. This situation is avoided by the following artifice.

An astable circuit provides an alternative source of square wave form. This is fed into an OR gate through a blocking circuit. The circuit blocks these pulses when the schmitt is working normally and allows it to go to the OR gate when the schmitt fails. The other input to the OR gate is the schmitt trigger pulses. The trigger from the discharge mono-stable is derived from this OR gate. By this means, the sample gets discharged with-in two cycles of the appearance of the short at the terminal of the machine unit.

The block diagram in fig, 3.27 shows the additional circuits required for machine terminal voltage measurement and are labelled with the suffix 'b'. The block wise detailed circuits are shown in fig. 3.29. A calibration curve for the device is given in fig. 3.30.

3.8 SQ-10 a OPERATIONAL AMPLIFIER :

The price of the chopper stabilised computing amplifier being prohibitively high it was thought prudent to look into the possibility of using low cost operational amplifiers for some applications particularly for inversion and amplification in conjunction with quarter square multipliers.

FIG : 3.29 VOLTMETER CIRCUIT DETAILS

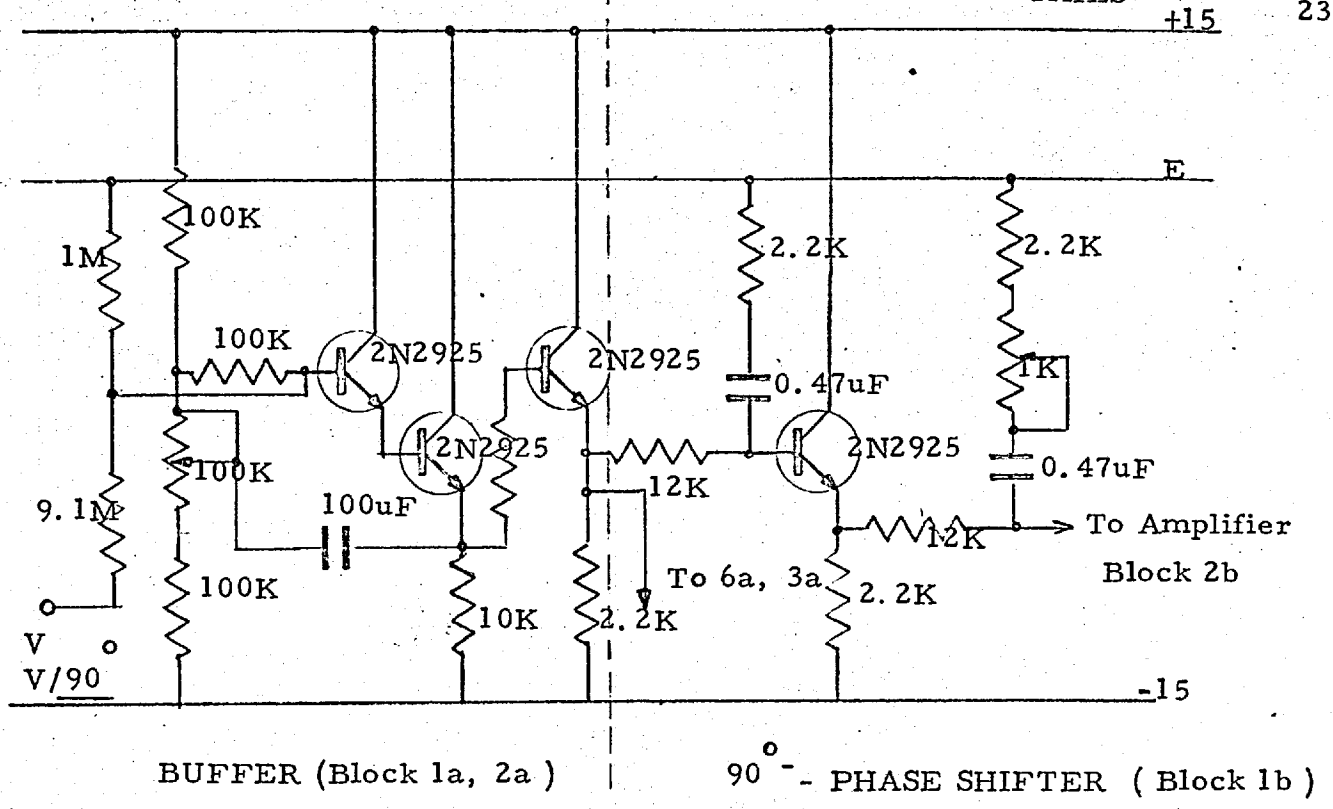

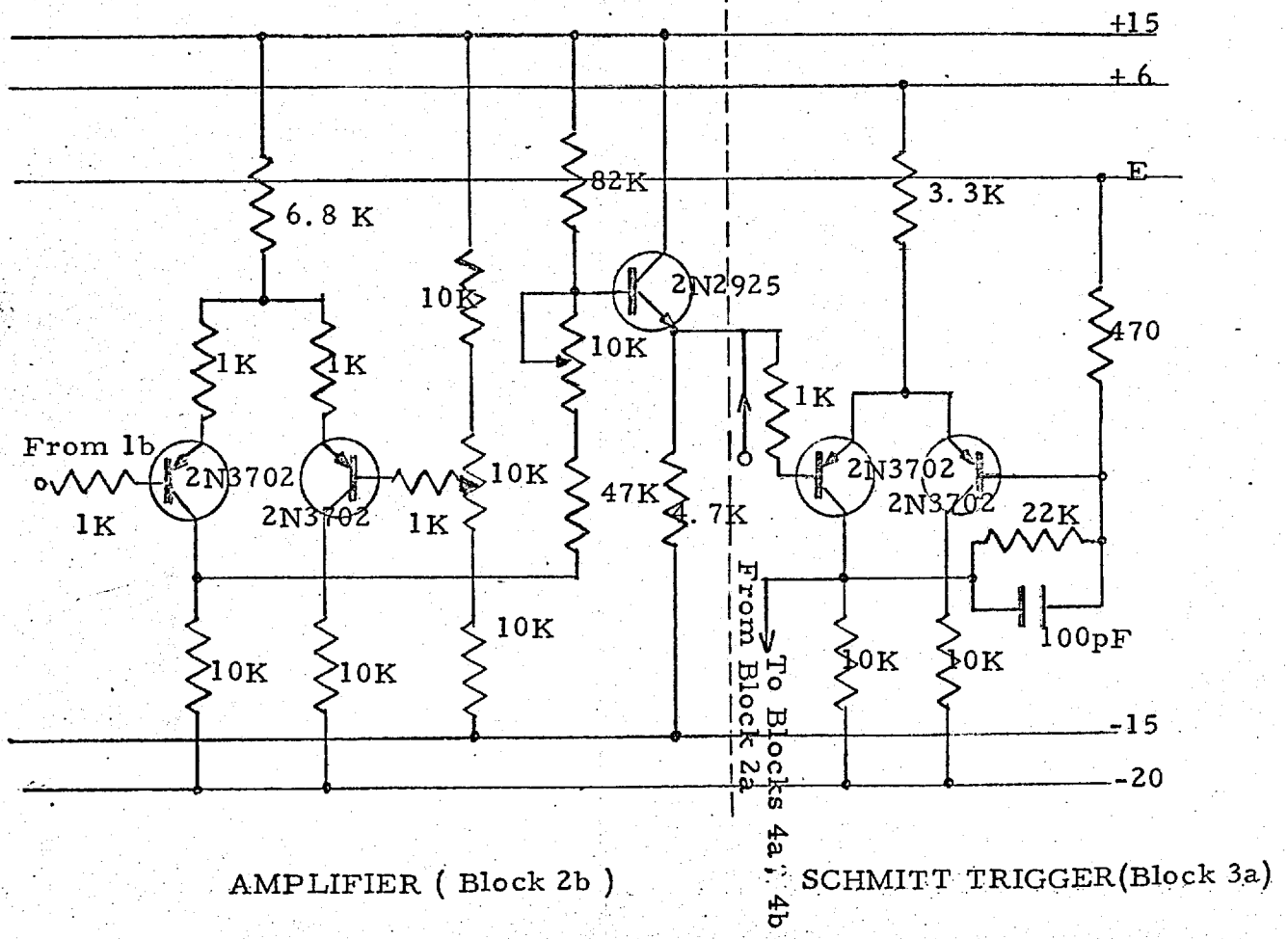

FIG : 3.29

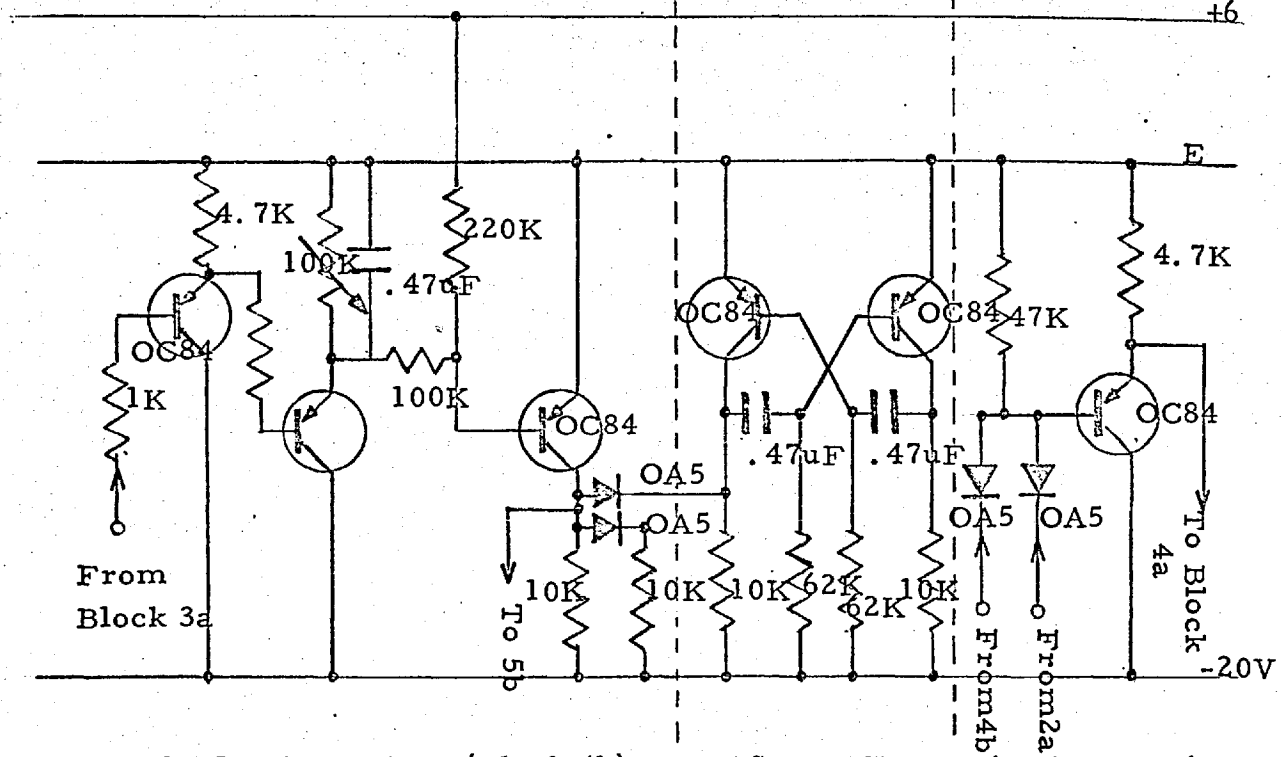

BLOCKING GATE (Block 4b) ASTABLE MULTIVIBRATOR (Block 3b) 'OR' GATE (Block 5

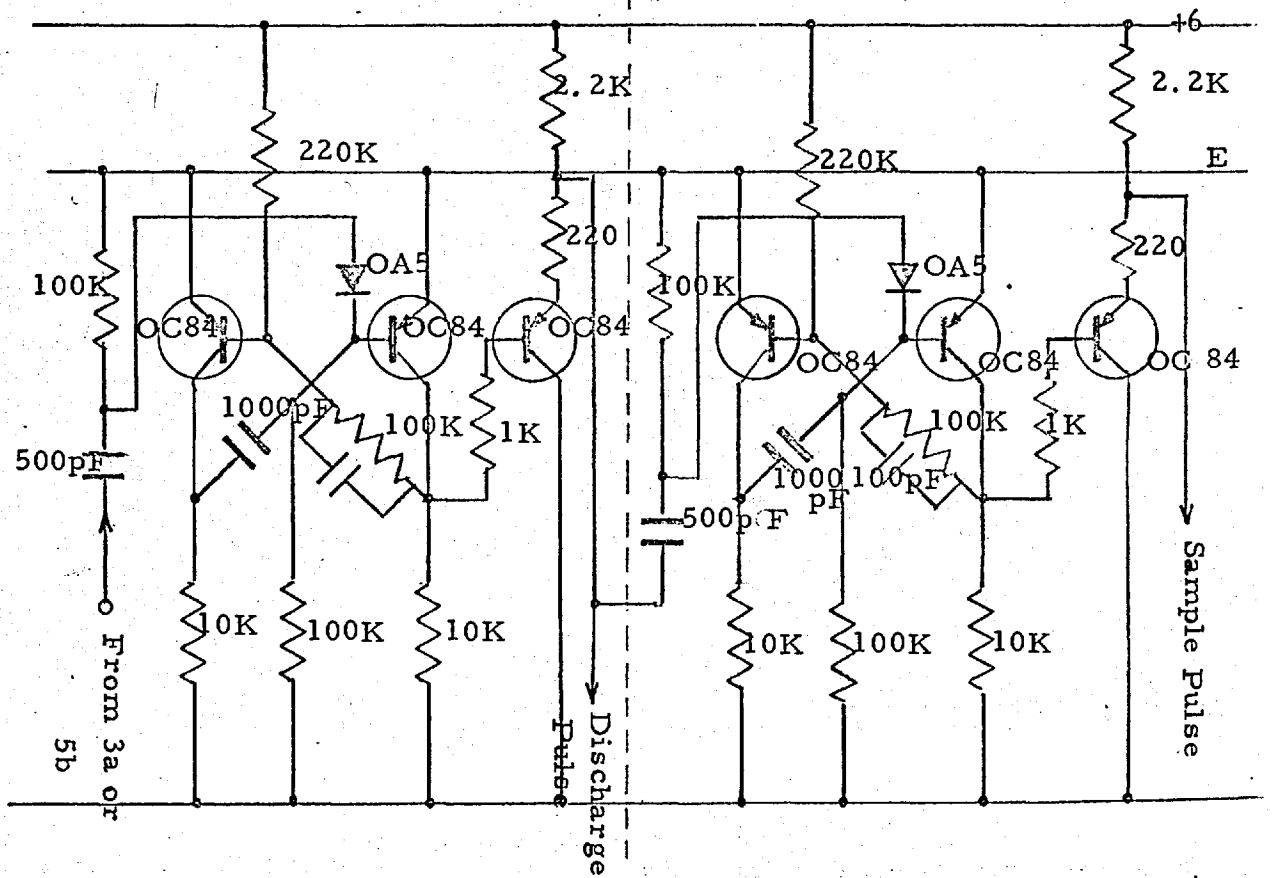

DISCHARGING MONOSTABLE (Block 4a) S AMPLING MONOSTABLE (Block 5a)

FIG: 3.29

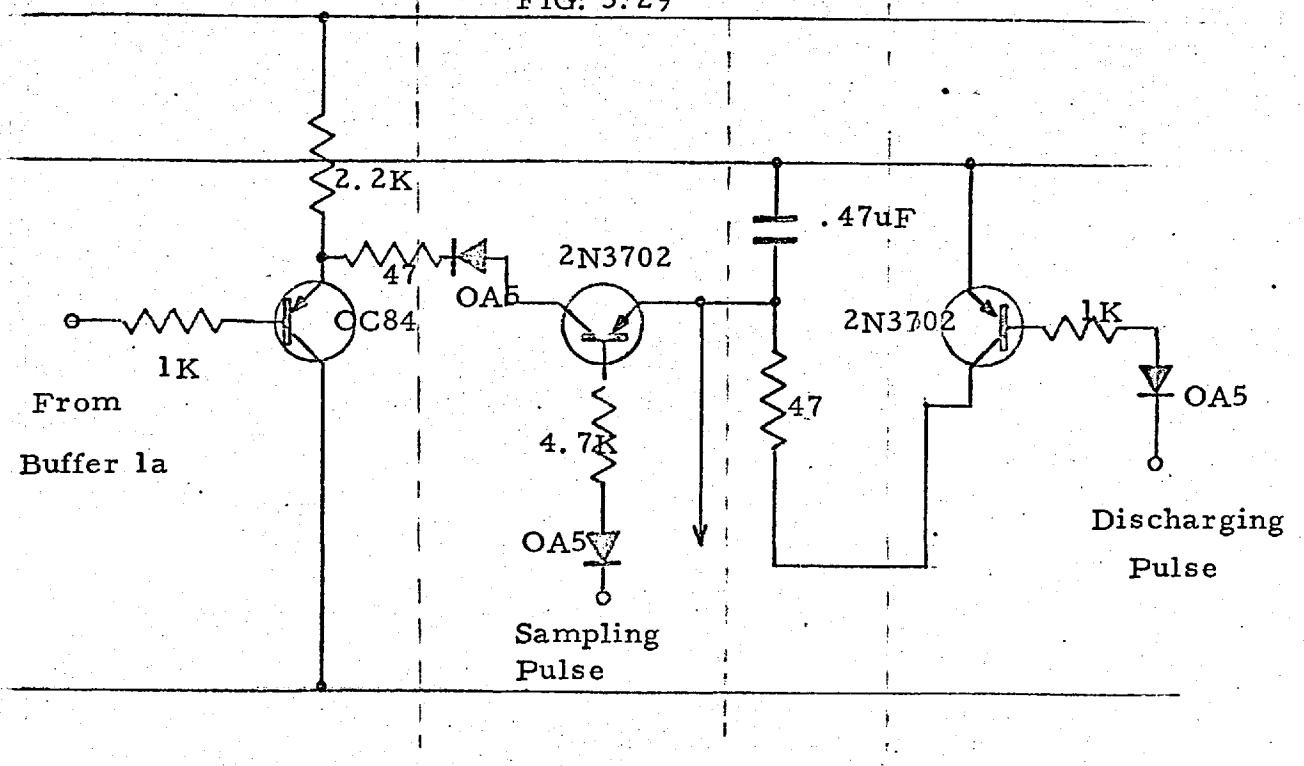

SAMPLING GATE STORE DISCHARGING GATE

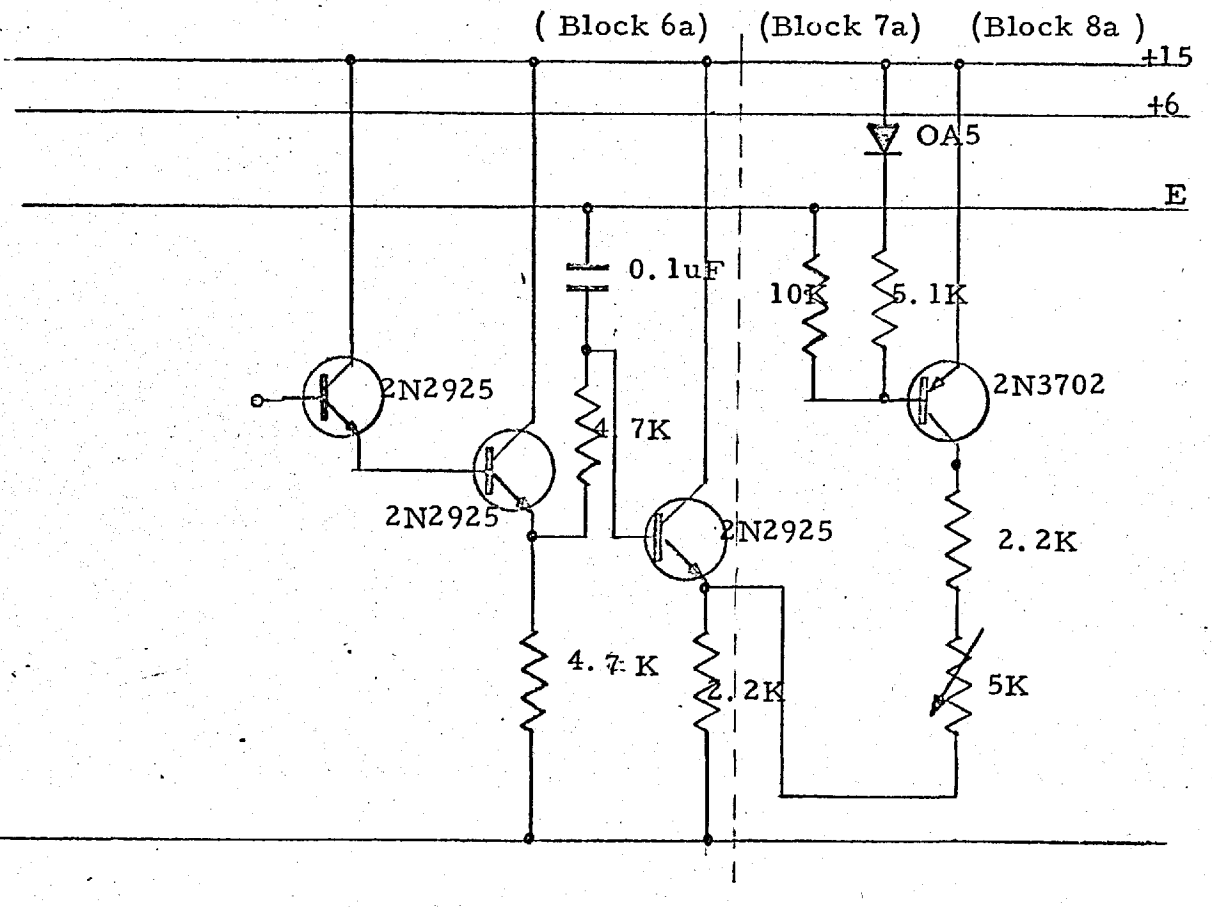

BUFFER & BIAS SHIFTER (Block 9a)

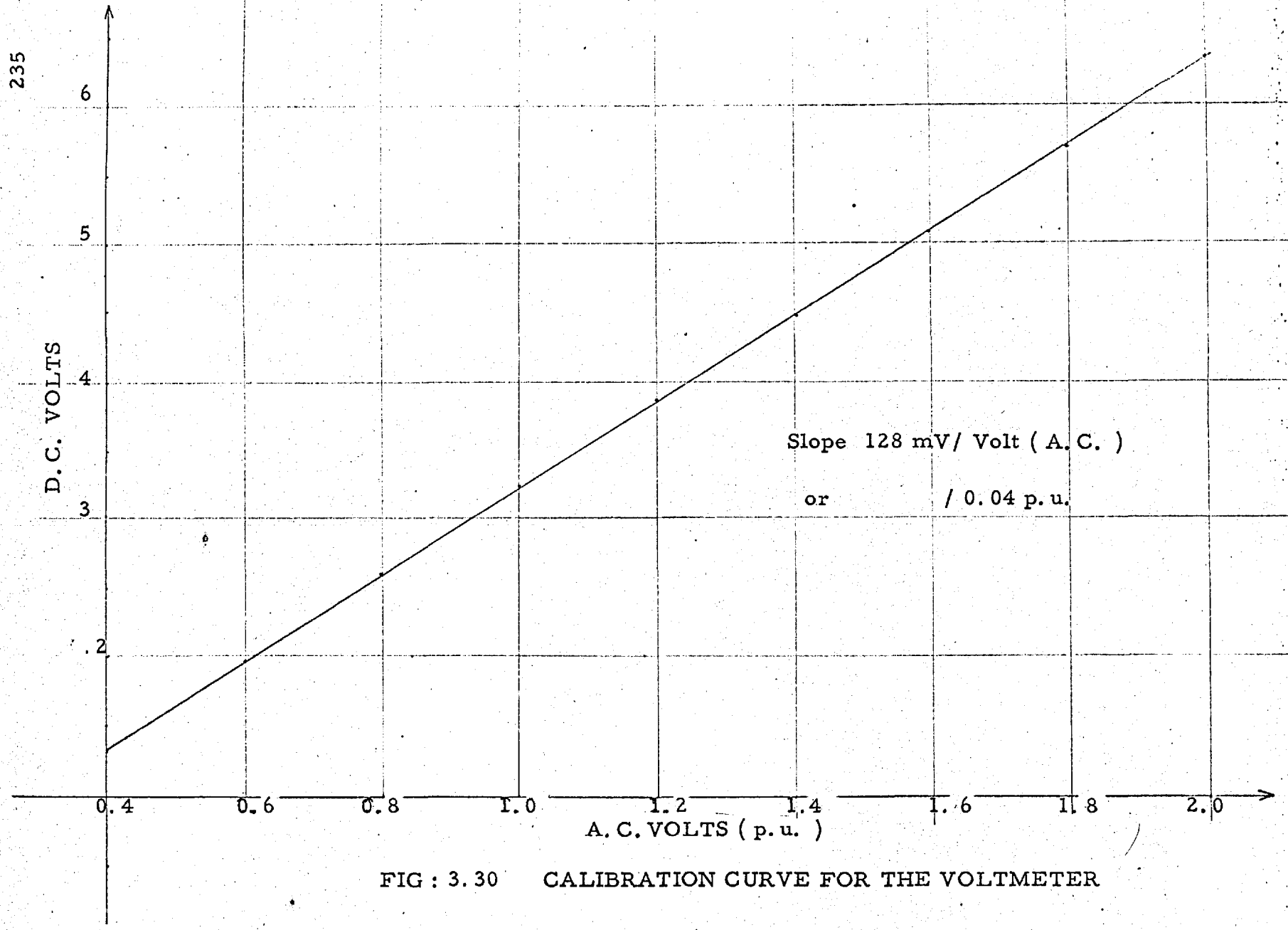

FIG : 3.30 CALIBRATION CURVE FOR THE VOLTMETER

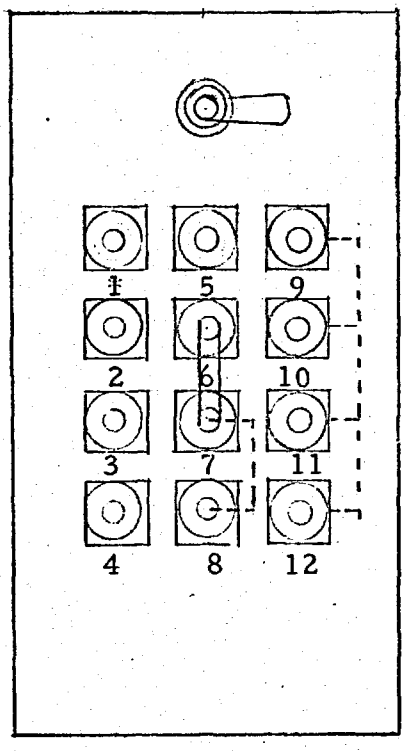

(a) PATCH PANEL

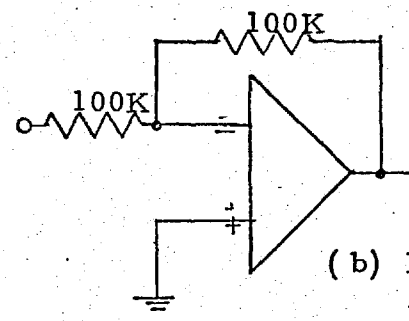

(b) INVERSION UNITY GAIN

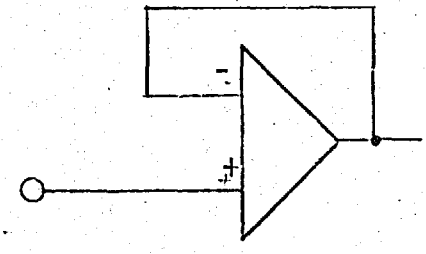

(c) NON-INVERTING IMPEDANCE TRANSFORMATION

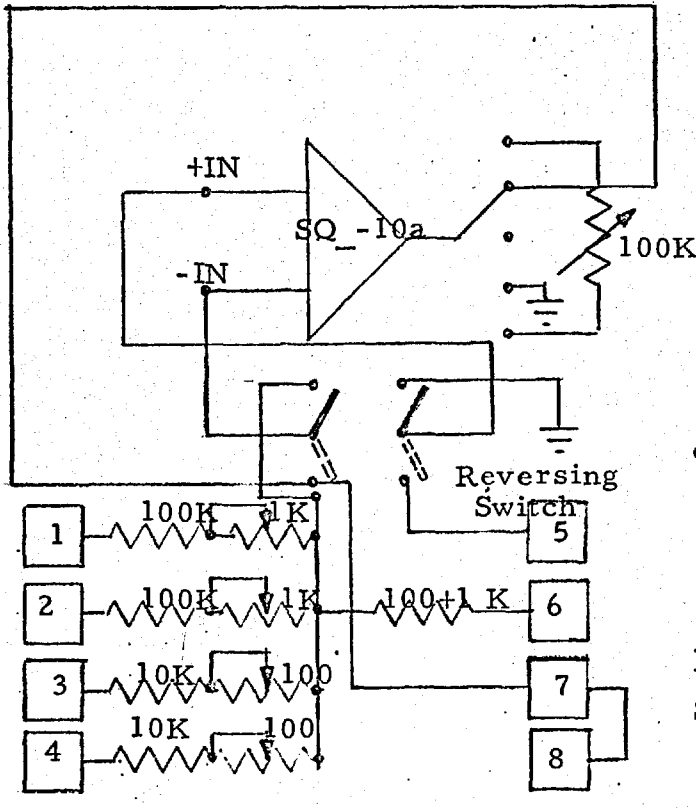

(d) INTERNAL CONNECTIONS

COLOUR CODE

1 & 2	Blue
3 & 4	Red
5	Green
6, 7 & 8	Yellow
9, 10, 11, 12	White

FIG : 3.31

PATCHING ARRANGEMENT FOR SQ-10 a OPERATIONAL AMPLIFIERS

Nexus Research Laboratories were making and marketing a range of all silicon solid state operational amplifiers in compact encapsulated modules. Although these units donot have exceptionally high stability, they give reliable operation primarily in closed loops. Provided with external negative feed back the amplifiers can be used for most analogue configurations for such applications as D.C. amplification, sign inversion, summing, active filtering, A.C. amplification and isolation.

Some of the important performance figures are given below.

Open loop D.C. Gain	100,000
Output	± 10 V ; 5 mA
Input Impedance	0.3 M Ohms (Differential Mode)
	30.0 M Ohms (Common Mode)
Output Impedance	0.05 to 5.0 Ohms(for different gains)
Voltage Stability	5 µV / oC
Frequency Response	2 MHz (Small signal unity gain)

Twelve amplifier modules were bought and were

provided with input and the feed back resistors, so that these can be used as unity gain inverters, D. C. amplification and summers. To get an accuracy of 0. 1 % high stability resistors of 1% tolerance were trimmed with low value resistive potentiometers. The arrangement on the patch panel is shown in fig. 3. 31 (a).

A change over switch is provided and the amplifier can be used for impedance conversion in non-inverting common mode configuration.

PROTECTION: The input circuitry is protected against damages due to accidental connection of the input terminal across the supply. The output circuitry is also protected against short circuits to the ground.

3.9 FAULT RELAY :

A scheme shown in the form of blocks in fig. 3. 32 is used to initiate disturbances and fault clearances in a sequential manner.

Rotor swings are recorded following two types of disturbances.

(i) Loss of line with or without a reclosure subsequently.

(ii) Short circuit is applied on one line. The line is disconnected at both ends after a fixed interval of time.

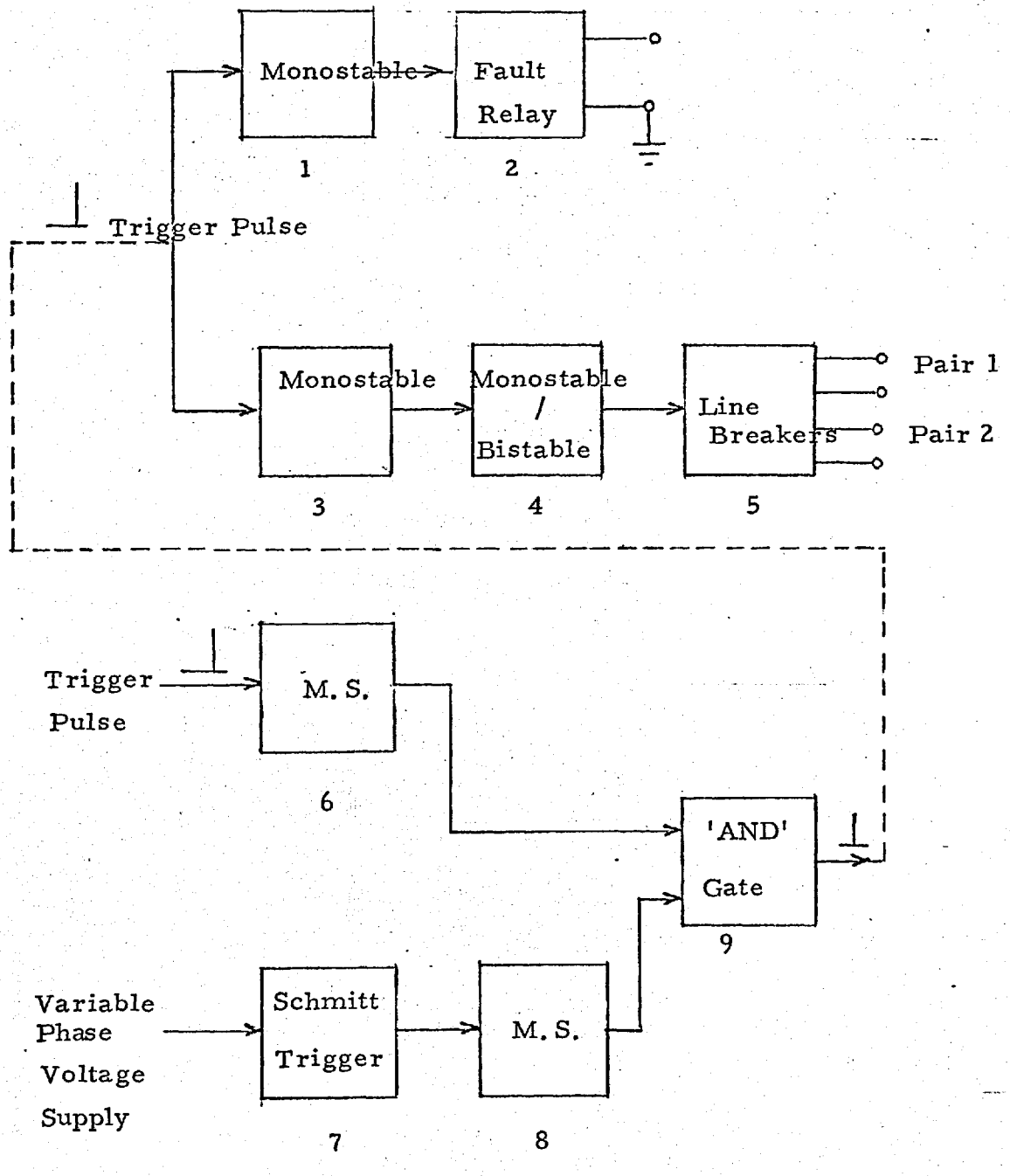

FIG : 3. 32 FAULT RELAY

The line may be recolsed after another preset interval.

(i) In the first case, a trigger pulse is supplied from a spring loaded toggle switch to monostable in block 3. After a preset interval it provides a trigger pulse to block 4. A switch is provided to select either a monostable or a bistable circuit in block 4. Block 4 drives the reed relay having two pairs of contacts. Both contacts operate simul_taneously.

If a bistable circuit is selected in block 4, the relay contacts open as soon as the trigger pulse is received from the block 3. The contacts remain open until another trigger pulse is externally supplied to reset the bistable in block 4.

Alternatively in block 4 a monostable circuit can be selected. In this case the contacts open removing the line but reclosed after a preset interval.

(ii) In the second case the point at which the short is to be applied is connected to one contact of the relay in block 2. The other contact is joined to earth. This relay is driven by a monostable in block 1 and the duration of the short circuit is pre-set on the monostable.

The trigger pulse now fires the monostables in blocks 1 and 3 simultaneously. The delay between the application of short circuit and opening of the contacts of the relay in block 5 can be set

on monostable 3. The duration of the short circuit can be set on monostable 1. and should be higher than the setting on monostable 3. The line breakers can be operated as reclosing type if block 4 is selected as monostable. The time interval between the opening of the contacts and reclosure can then be set in block 4.

Short circuiting produces asymmetry in the current wave. This is often neglected in simple stability calculations. Also in an actual system the effects of the asymmetry on the rotor swing is independent of the instant of the application of short circuit. In an equivalent single phase representation the instant of short circuit produces appreciable difference in the rotor swing. This is true only in cases where the simulator is working in real time. When the problem is solved on the simulator with slower time base the asymmetric component will die fast enough not to affect the rotor swing significantly.

Fig. 3.33 shows the current waves before and after the fault. If the short circuit is applied at the instant of the cross over point 'a' no asymmetry will be produced. This instant can be determined analytically in a simple case of a single machine feeding into an infinite bus-bar, but in a general case the instant has to be determined by measuring the actual phase difference between the two waves. A variable phase voltage source has now to be added to the fault sequential relay. This source is set such that its zero

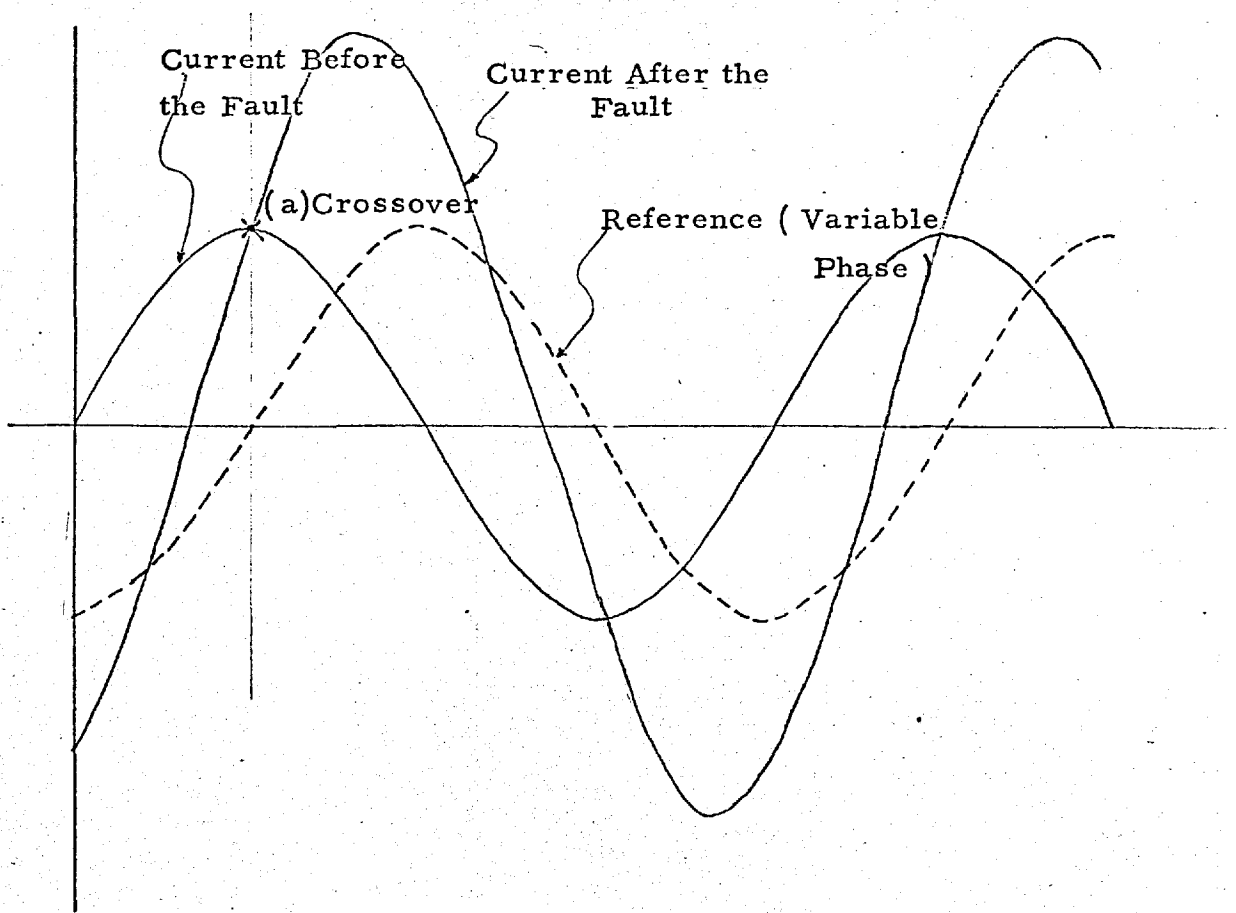

FIG : 3.33

SELECTING INSTANT OF SHORT CIRCUIT TO AVOID ASYMMETRY IN THE CURRENT WAVE.

cross over coincides with the cross over point 'a'.

The start of the operations is then made by triggering a monostable in block 6. A pulse is also obtained at the zero cross over of the variable phase voltage source in block 8. An ' AND ' gate provides a trigger pulse to the monostables in blocks 1 & 3 when pulses from 6 & 8 are both present. The other operational sequences are as described above.

3.10 NETWORK ANALYSER IMPEDANCE UNIT :

A conjugate network analyser working at 50 c/s, made by NASH & THOMPSON is installed in the Power System Laboratory and it was initially planned to use it for transmission lines, loads and generator impedances. The inductive and the capacitive elements of the actual network are transposed in their representation on the network analyser. This enables the lines to be represented by capacitors instead of inductors which for suitable base quantities are less bulky and more economic than the equivalent inductors.

Unfortunately, the machine units introduce harmonics in the voltage wave form. As the transfer impedance of the network between two nodes become smaller with the rise in frequency , severe distortion of the current wave form . is caused.

Wave analysis showed:

0.7 % of 3rd; 1.1 % of 5th and 0.5 % of 7th harmonic in the voltage waveform.

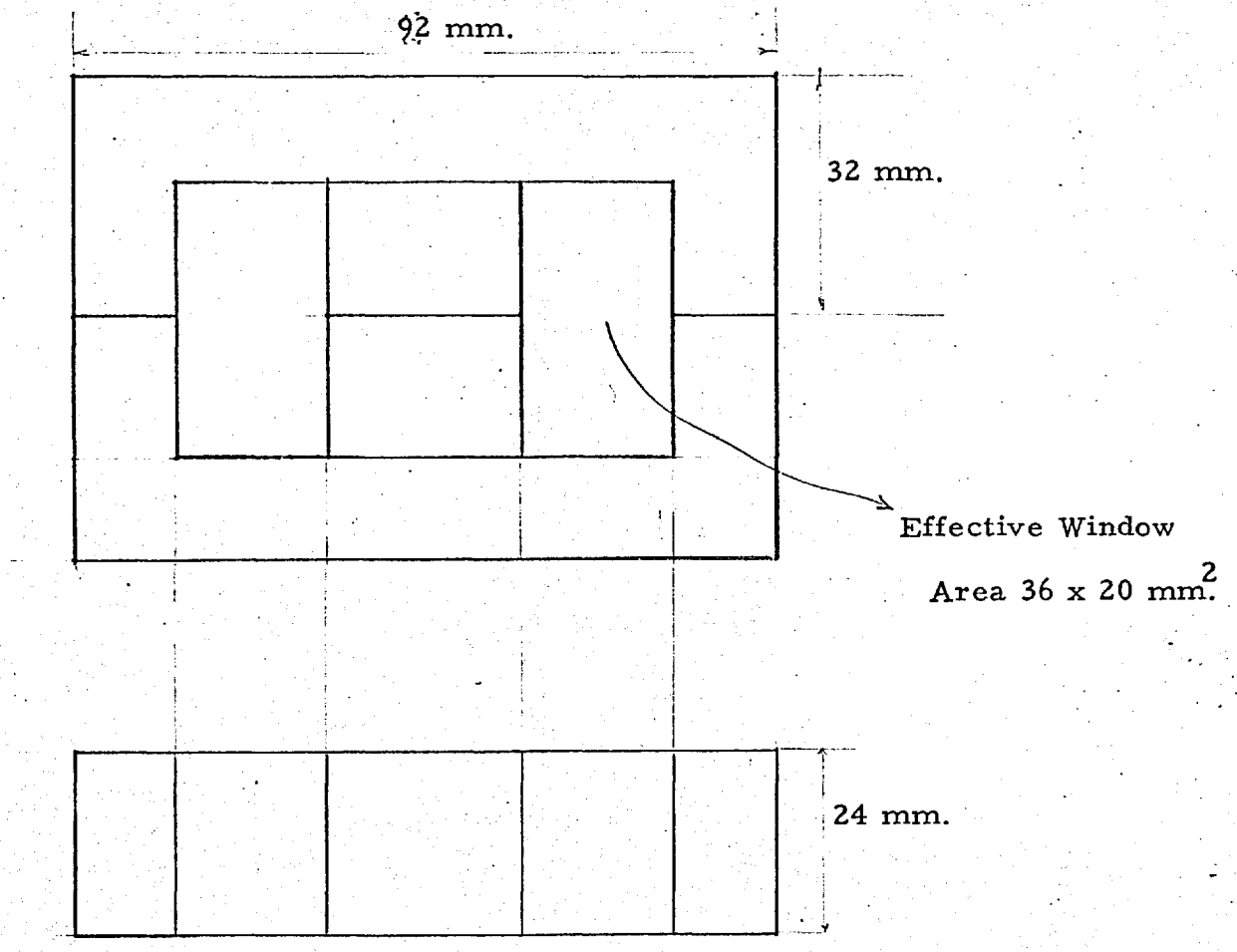

FIG : 3. 34 FERROX CUBE TYPE FX1653 (MULLARD)

The harmonic components of the current wave form will, of course, be different for different generator angles and transfer impedances, but to give an idea of distortion in the current waveform two machine units with 30° angle difference and transfer impedance of $0.738/82.5^{\circ}$ connected across them showed 1% of 3rd, 0.95% of 5th and 0.45 % of the 7th harmonic.

High harmonic contents of this order in the current wave form are highly undesirable for the power measurement. It was, therefore, decided to make inductors for direct representation of the transmission lines etc.

The largest commercially available ferrite core was chosen for the inductor. The choice was mainly determined by ready availibility than for any other technical advantage, although a low loss core is good for making high Q-inductors.

The dimensions of the core type FX1653 are shown in fig. 3.34.

The manufacturer's Data sheet provides the approximate guide for choosing the number of turns. The figure is 14 turns per milihenry. Inductance of 16 H is needed to get 5 KΩi. e, $\frac{1}{2}$ p. u. impedance at 50 c/s. The number of turns required are

$$\sqrt{14^2 \cdot 1000 \cdot 16} = 1770$$

Core saturation starts at 24 ampere-turns.

To increase the linearity, an air-gap of the thickness of the sellotape was provided between the butting faces to cut down the effective permeability by half. The number of turns were appropriately increased to $\sqrt{2}$. 1770 = 2500.

The available window area was good enough to accommodate 2500 turns of SWG 24 wire, but because of the bad winding machine available, the packing factor was very poor and enammeled copper wire of size SWG 26 had to be used.

One prototype winding showed that for $\frac{1}{2}$ p. u. reactance only 2100 turns are necessary. The unit was tapped at intervals of 0. 1 p. u. impedance and the number of turns at each tap are shown in the table below.

Reactance (p. u.)	No. of Turns
0. 1	980
0. 2	1400
0. 3	1630
0. 4	1880
0. 5	2100

Another reactance unit tapped at 0. 25 p. u. and 0. 5 p. u. is connected in series with the unit described above through the selector switches. 1% high stability resistors are also provided with each unit. The arrangement is shown in fig. 3. 35.

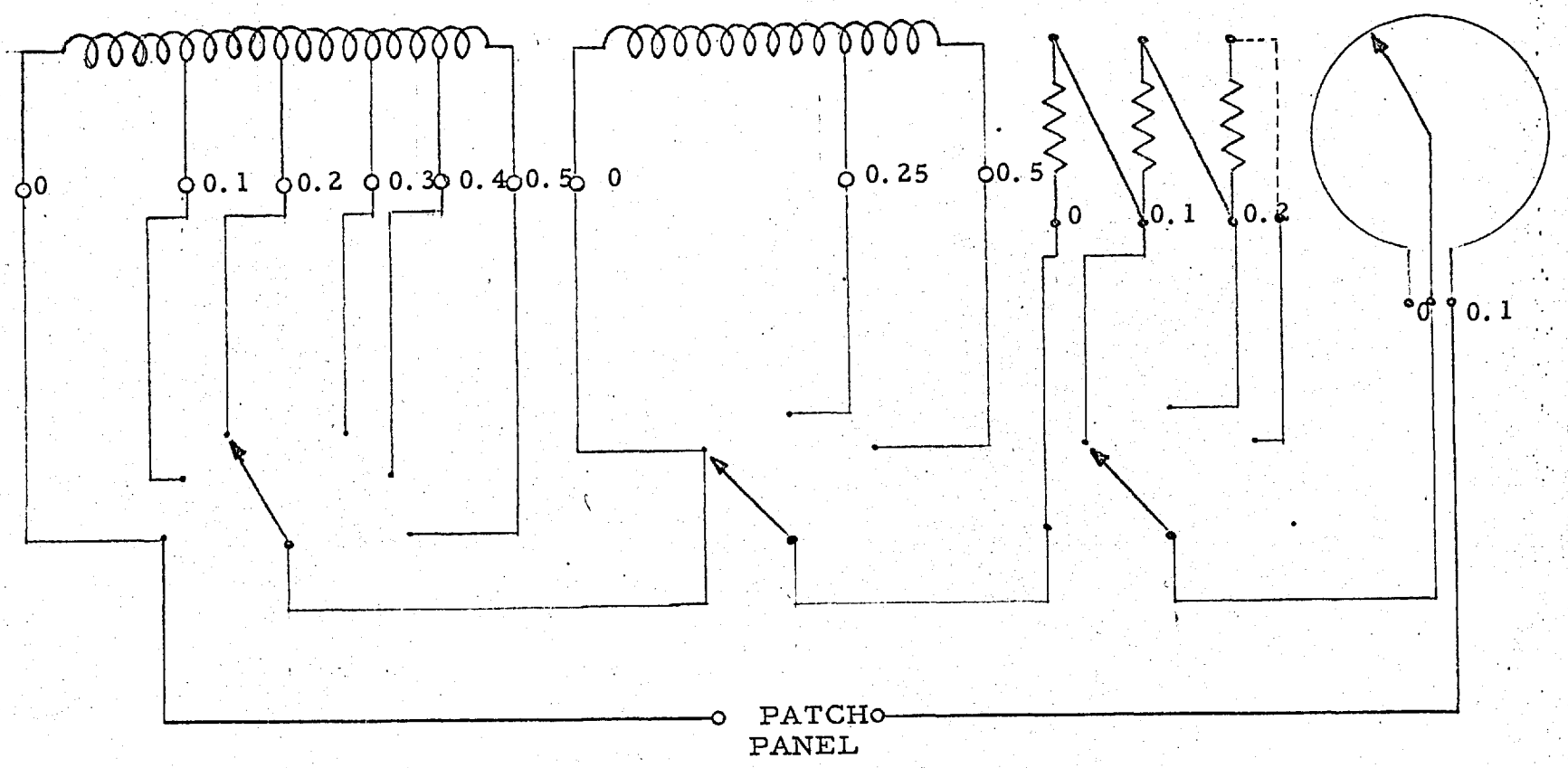

FIG : 3.35 ARRANGEMENT OF SELECTOR SWITCHES FOR NETWORK ANALYSER IMPEDANCE UNIT.

The ends were brought out on a patch panel to give the facility for connecting the units in any desired network configuration.

Q-Factor: Resistance of $\frac{1}{2}$ p. u. reactance coil is 0. 004 p. u. giving a Q-factor of 125.

Non-linearity : With a steady current of 10 mA i. e. 4 p. u., inductance is dropped by 4 %.

CHAPTER 4

MORE ACCURATE SIMULATION

The fundamentals of the theory of synchronous machines and the very elementary form of the machine simulator based on the assumption of constant flux linkages has been discussed in chapter2. The strategy of simplifying the fundamental equations, making them suitable for application to a network analyser in the form of a voltage behind a constant reactance has also been demonstrated in chapter 2. This chapter is devoted to the application of the same technique in developing more accurate simulators where factors such as transient saliency, flux decay, voltage regulator and governor action will be included. Damping is included only as a constant damping coefficient and saturation is neglected. The results from the simulator have been checked against the digital computer output. Digital-Analogue Simulation language " MIMIC " (section 2. 3. 7) has been used for simplicity and ease in programming.

The validity of the assumptions involved in developing these simulators is a highly controversial subject and some criticism and discussion of these assumptions is included in the next chapter.

4. 1 INCLUDING TRANSIENT SALIENCY :-

The derivation of equations and the vector diagram for a machine under the conditions of transient disturbance is discussed in section 2. 1. 3 and 2. 1. 5. It is from these general equations that the machine representation as constant voltage behind transient reactance was derived by assuming $x'_d = x_q$ i. e. the direct axis transient reactance equal to the quadrature axis synchronous reactance. As discussed in section 2. 1. 5 , the more general case of $x'_d \neq x_q$ can be simulated by a variable voltage behind x_q, the quadrature axis synchronous reactance. This representation has the twin advantage that the machine reactance is a single unit and the phase of the voltage behind this reactance correctly gives the position of the quadrature axis.

The difference between the results obtained from the constant voltage behind transient reactance and the more general case which takes transient saliency into account is directly dependent on the ratio x'_d / x_q ; the nearer this ratio is to unity the closer will be the results to those obtained from the simple representation of constant voltage behind x'_d . Often the reactance of a long transmission line can swamp the difference in the results obtained from the two different representations. It has been shown that there is almost a negligible difference in the transient stability limit of a generator with a 600 miles long transmission line, if the two different methods are used. (Ref. 69)

If the assumption of constant flux linkages is not accurate enough and it is desired to include in the analysis the effect of the change of flux linkages due to the decrement during the period of short circuit and voltage regulator action, then the transient saliency must also be taken into account; this is true for salient and non-salient pole machines. Although under steady conditions and over the working range of load angles the error in the terminal voltage and power is less than 15% whether the saliency is included or not, but under transient conditions the terminal voltage changes with the load angle (saliency neglected) at twice the rate compared to the case when the saliency is taken into account. (Ref. 70)

The method of including the saliency in the analysis is clear from the equations 2.1.17 and 2.1.18. The simulator, in addition to setting the angles as determined from the mechanical equations, has to set up magnitude of the voltage behind x_q.

E'_q defined as the voltage proportional to the direct axis flux linkages is kept constant and represented on the analogue computer as a D.C. voltage level. A current component resolver (section 3.6) provides a D.C. voltage proportional to the direct axis component of the current. The drop $I_d(x_q - x'_d)$ can be obtained simply by a potentiometer setting since x_q and x'_d are both assumed constant during the period of the swing. If $I_d(x_q - x'_d)$ is added to the constant E'_q, it gives the magnitude of E_{qd}. (see vector diagram of fig. 2.5 and figs. 4.9 & 4.10) The I-pot

servomechanism sets the magnitude of this voltage continuously. This mechanism is described in the following section.

4. 1. 1 I-POT POSITION CONTROL MECHANISM :-

The arrangement is a fairly conventional position control servomechanism except that the potentiometer is inductive instead of resistive and the voltage applied across this is A. C. and not D. C. The command signal is derived from the analogue computer and is a varying D. C. voltage and therefore the voltage taken off the wiper has to be converted into D. C. Rectification and filtering will result in delays in the output signal and slowing down of the response. Therefore, a sampling technique is employed where the peaks of the A. C. voltage wave are sampled and therefore the information is updated every cycle of the A. C. wave. The difference between the command fromthe analogue computer and the output signal is fed through a compensation network to a servoamplifier (section 3. 1.1.) supplying a split field D. C. motor-tacho-generator set, field current proportional to the input signal. The D. C. motor used is Evershed & Vignoles type FAD/ G 4 / BD. The motor armature is supplied from a constant current source described in section 3. 3. 2 .

The speed reduction from the motor to I-pot shaft is 5:1 and a steel reinforced toothed rubber belt more commonly known as, timing belt, is used for convenience of location of the

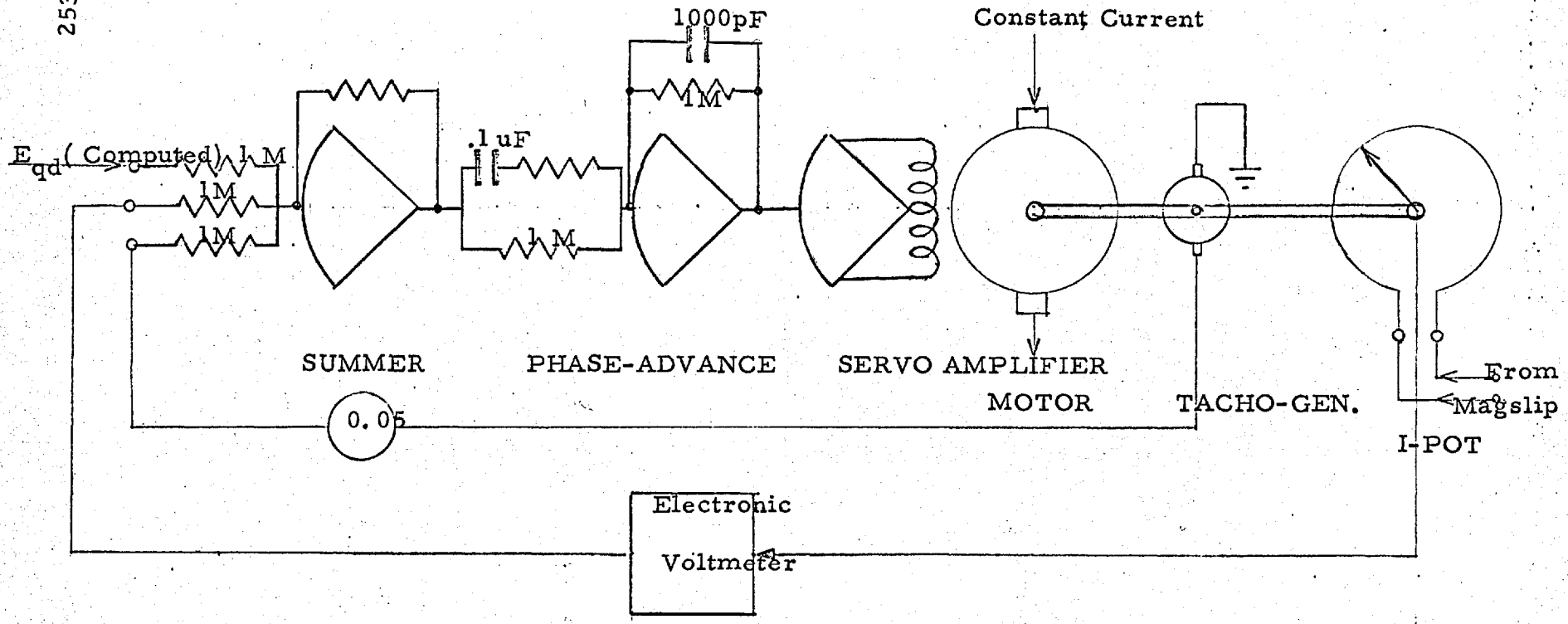

FIG : 4.1 I-POT POSITION CONTROL SERVO MECHANISM

components on the base plate and there is less frictional torque to overcome than with metallic gear wheels.

A few other essential points about the investigations leading to the final design and compensating network are as follows.

The time constants in the forward path are estimated by performing a frequency response test of the system but as a speed control system with a small fraction (1%) of the output speed used as the feed back signal. The frequency response curve is shown in fig. 4.2(a) The estimated transfer function is $\frac{21576}{(p+6)(p+40)}$. Pole-zero diagram on the complex p-plane is shown in fig. 4.2. (b). As a position control the system will have one additional pole at the origin. Two compensating zero's were added one in the forward path and one in the feed back path. In the feed back path the derivative signal is available from the tachogenerator. The gain was just sufficient for the closed loop pole locations to be at the point where the 180° line after bending away from the imaginary axis intersects the negative real axis. The closed loop frequency response curve is shown in fig. 4.4. Fig. 4.5 through 4.7. show the demand and output voltage for a low frequency A.C. signal, ramp and step demand signals. The response time following a step for no overshoot is 80 m-secs.

4.1.2 TIME SCALING:-

Although a response time of 80 m-secs.

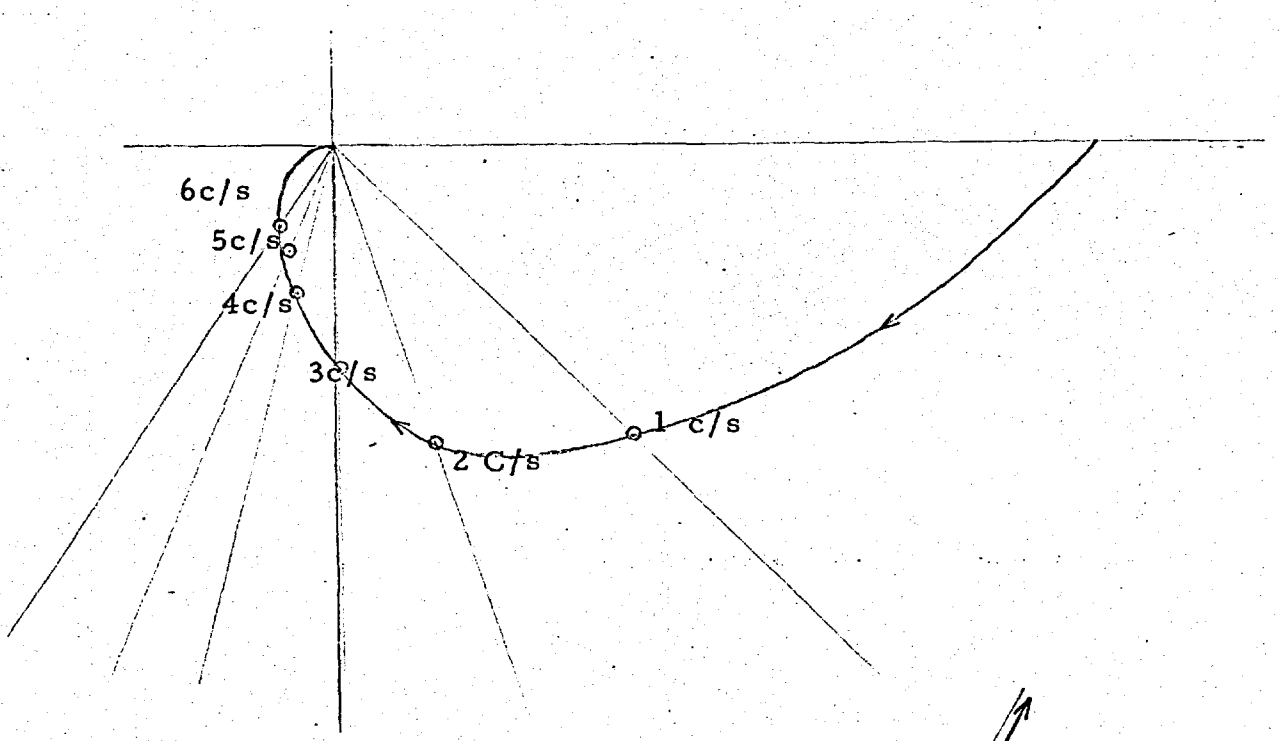

(a)

OPEN LOOP FREQUENCY RESPONSE

(SPEED) OF I-POT SERVO-MECH.

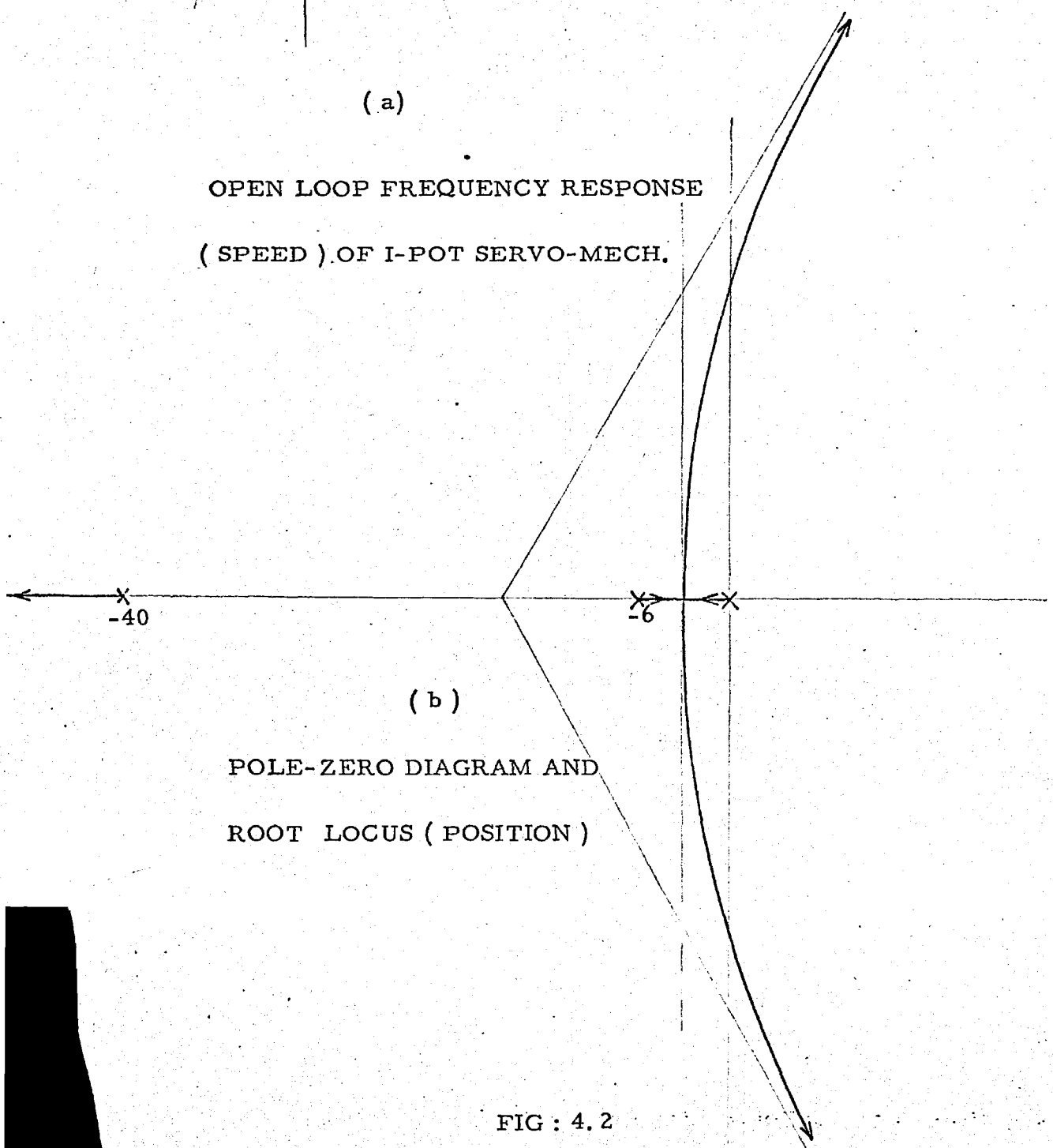

(b)

POLE-ZERO DIAGRAM AND

ROOT LOCUS (POSITION)

FIG : 4.2

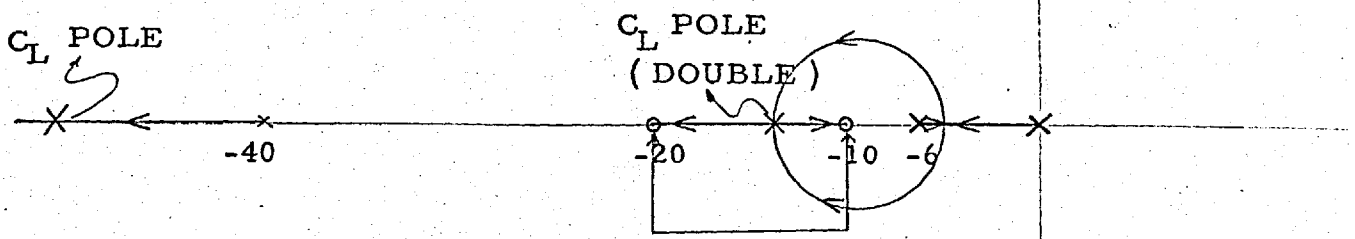

FIG : 4.3 ROOT-LOCUS MODIFIED BY TWO ZEROES

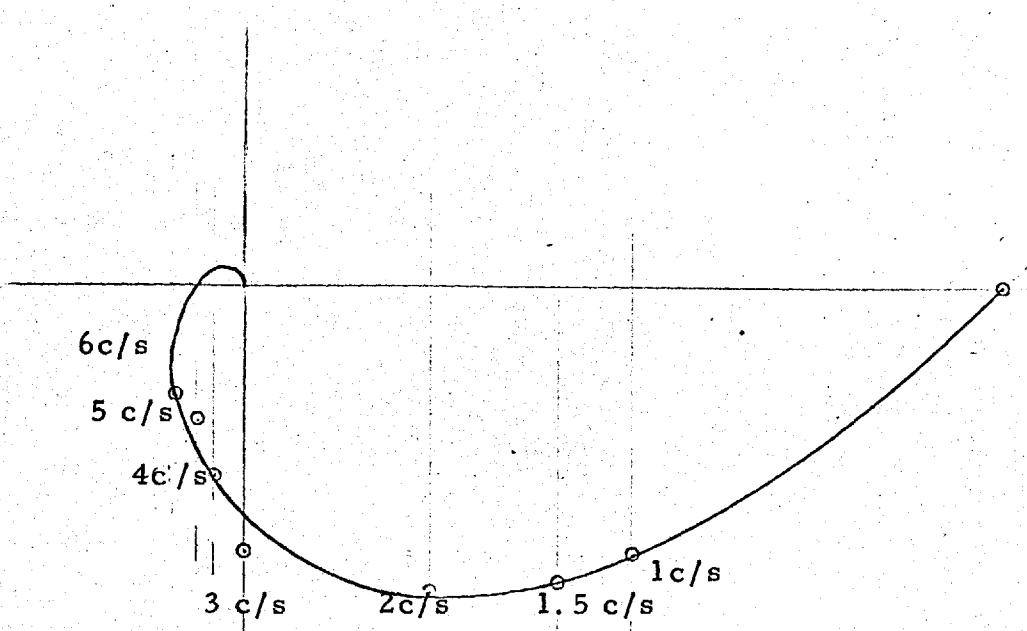

FIG : 4.4 CLOSED LOOP FREQUENCY RESPONSE

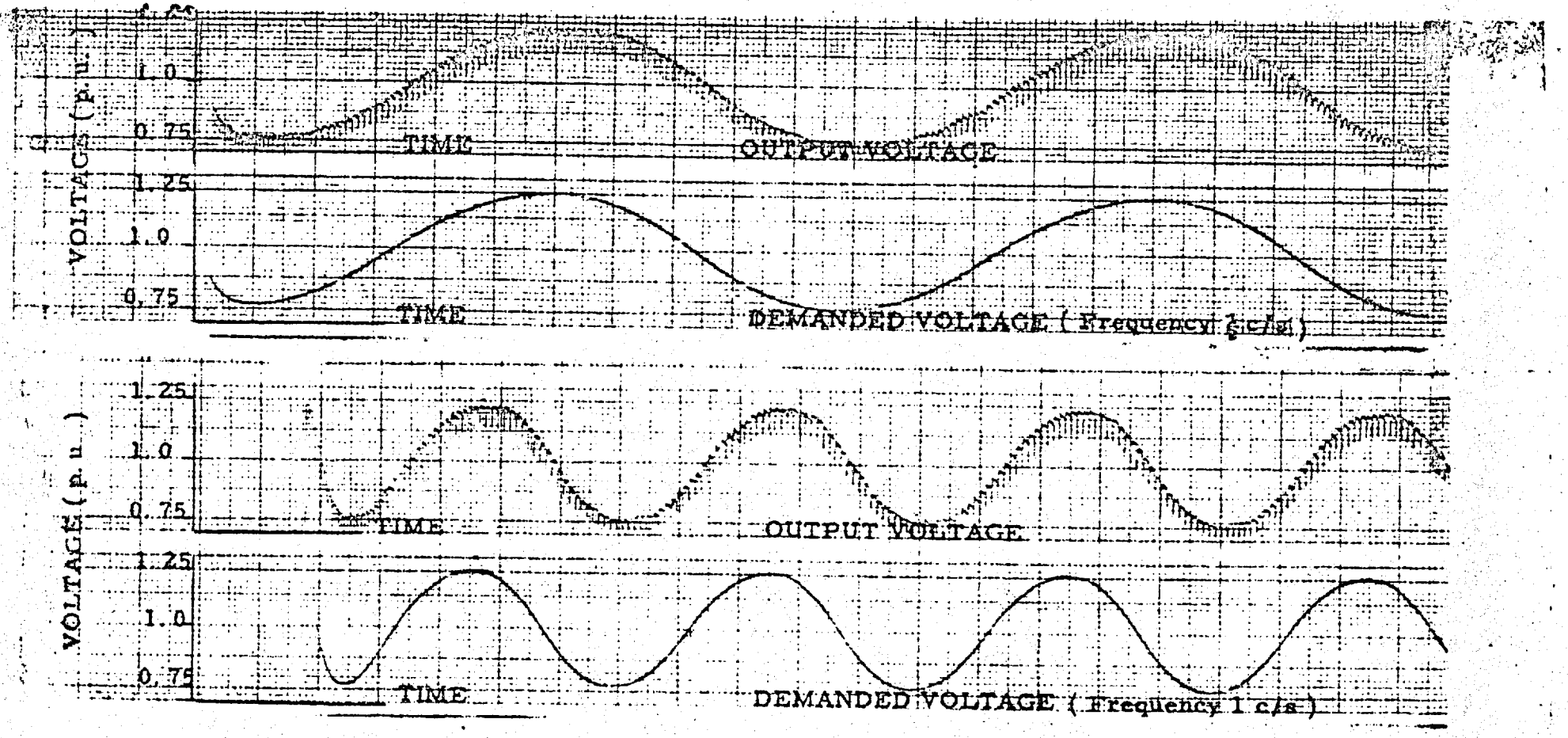

FIG : 4.5

I-POT CONTROL MECHANISM CLOSED LOOP

RESPONSE TO LOW FREQUENCY SIGNALS

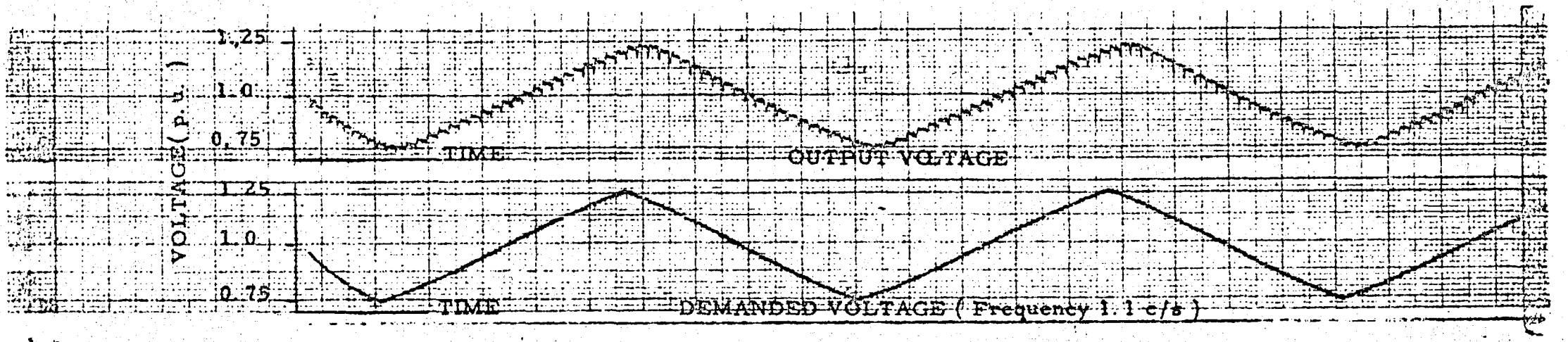

FIG : 4.6

I-POT CONTROL MECHANISM CLOSED LOOP

RESPONSE TO RAMP INPUT SIGNALS

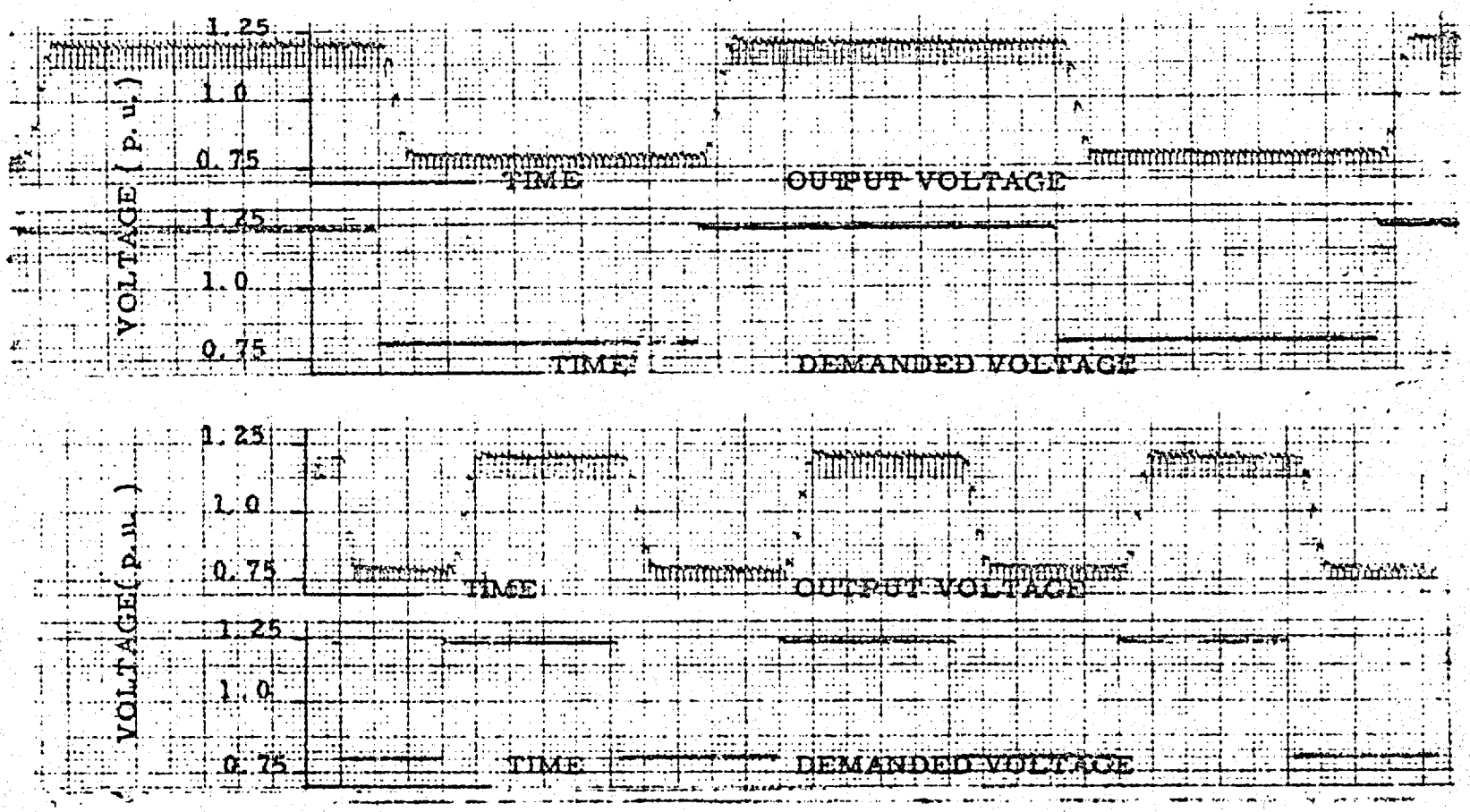

FIG : 4.7 I-POT CONTROL MECHANISM CLOSED LOOP RESPONSE TO STEP INPUTS

without any overshoot following a step input seemed reasonable for solving the machine equations with transient saliency included on a real time basis, the interdependent nature of the equations implied that the solution for E_{qd} needs more time at the instant of a step change in the stator current. The magnitude of E_{qd} is a function of E'_q and I_d, but I_d in turn is a function of E_{qd} (both magnitude and phase), all other voltage sources in the system, the relative phase angles, and the intervening network. Thus the simulating mechanism solves the system equation in an iterative manner. It was found that following disturbances like short circuits or loss of line, E_{qd} took nearly 200 m-secs to reach the final correct value. This introduced considerable error in the calculations for δ (the machine rotor angle). This difficulty forced the system to be run at slower than the real time. For convenience a factor of 10 was used.

In the swing equation the coefficients for $\frac{d^2\delta}{dt^2}$ and $\frac{d\delta}{dt}$ have to be changed. For working out the settings for the potentiometers, the method is substantially the same as in section 2.3.4.

If $t_s = s.\ t$, where t_s is the simulator time then equation 2.1.23 can be modified to describe the simulater swing as

$$\left(\frac{2H}{w}\right)\frac{d^2\delta}{d(st)^2} + \left(\frac{K_d}{w}\right)\frac{d\delta}{d(st)} = f_m - f_e$$

$$\frac{2H}{s^2 w}\cdot\frac{d^2\delta}{dt^2} + \frac{K_d}{s\,w}\cdot\frac{d\delta}{dt} = f_m - f_e \qquad \ldots\ldots 4.1.1$$

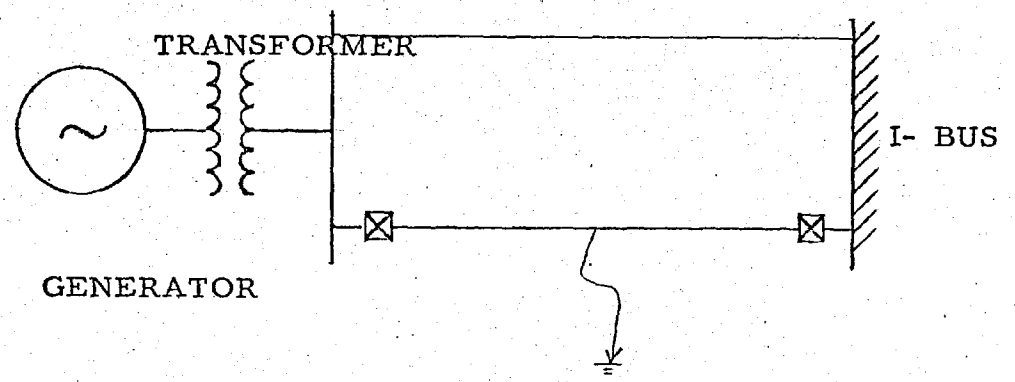

(a)

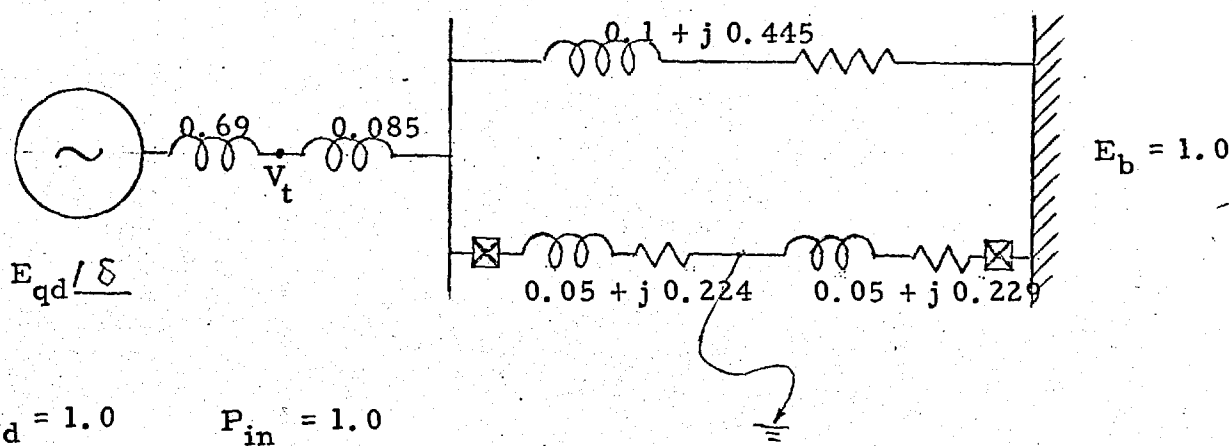

$x_d = 1.0$ $P_{in} = 1.0$

$x_q = 0.69$ $V_t = 1.11$

$x_d' = 0.23$ $H = 3.0$

$T_{do}' = 5.0$ sec. $K_d/w = 3.0$

(b)

FIG : 4.8

(a) LINE DIAGRAM FOR PROBLEM 4.1.3

(b) LINE DATA FOR PROBLEM 4.1.3

So the coefficient pot settings for inertia and damping simulation are made as if the machine has an inertia constant of (H/s^2) and damping coefficient of (K_d/s).

4.1.3. TEST PROBLEM :-

The problem selected for setting up on the simulator is shown in fig. 4.8. A generator is supplying 1 p.u. power through two parallel transmission lines. The terminal voltage of the generator is 1.11 p.u.

A short circuit in the middle of the transmission line is followed by simultaneous opening of the circuit breakers at the two ends of the transmission line. A relay doing these operations in sequence is described in section 3.9.

A complete set up of the simulator is given in a schematic form in fig. 4.9. The set up for computing E_{qd} is in fig. 4.10.

The plot of the rotor angle with time is shown in fig 4.11. The results from the digital computer are plotted as encircled points.

Comparison with the digital computation shows that accurate simulation has been achieved. Delays in the computation and setting up of the magnitude of E_{qd} , because of the nature of the machine equations explained in section 4.1.2 , is seen in the plots

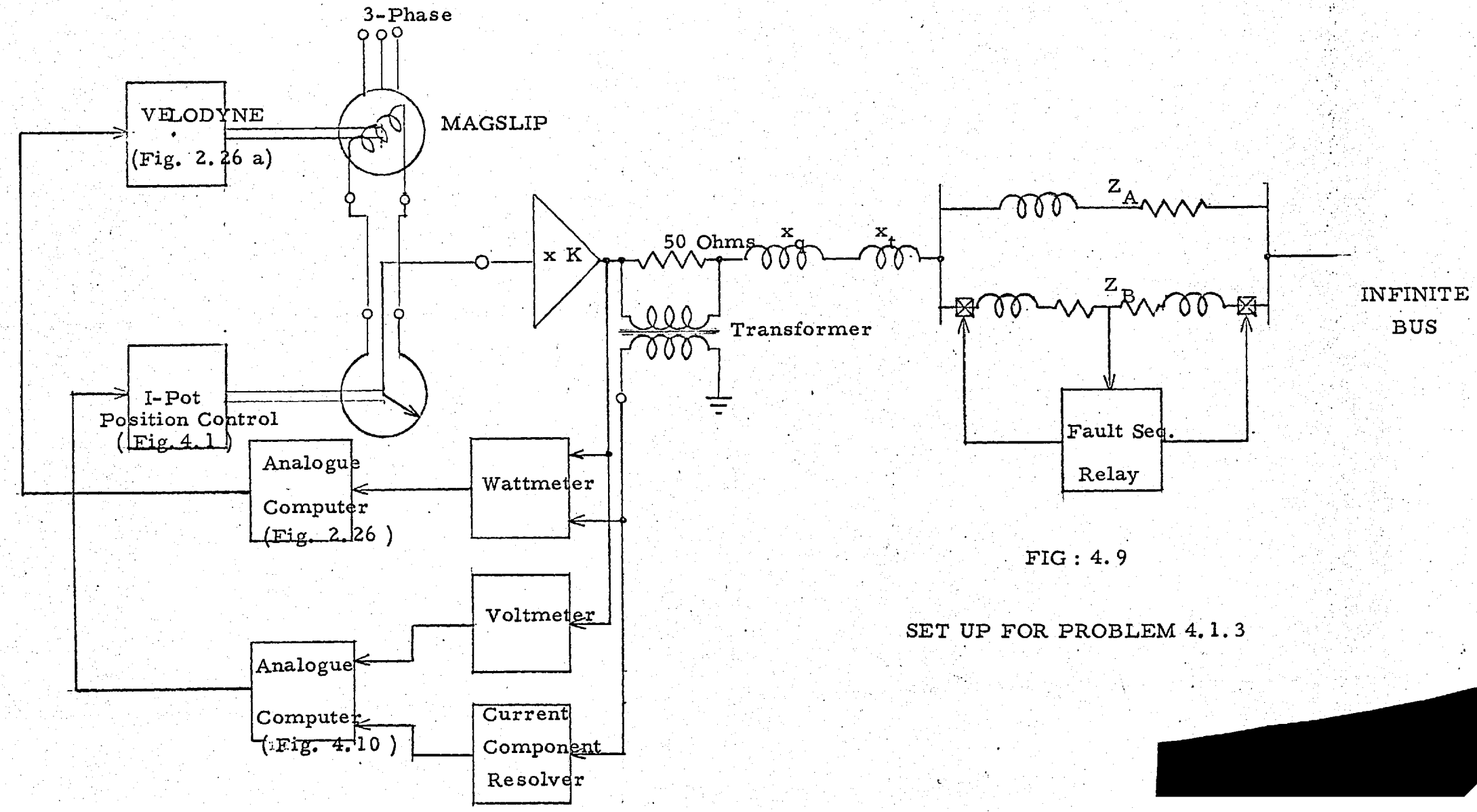

FIG : 4.9

SET UP FOR PROBLEM 4.1.3

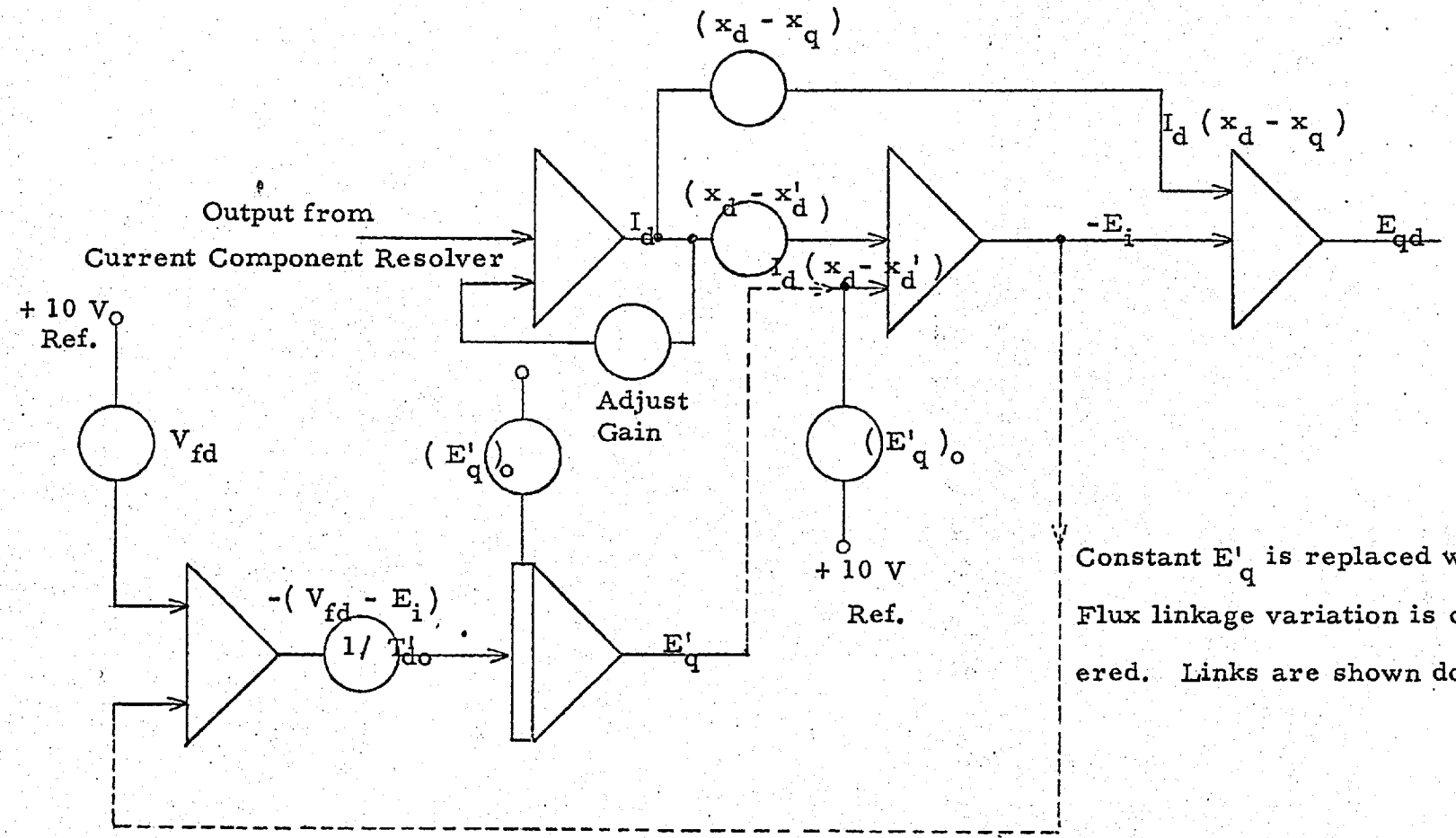

FIG : 4.10 SET UP FOR COMPUTING E_{qd}

PHILIPS PT 1026 R/04

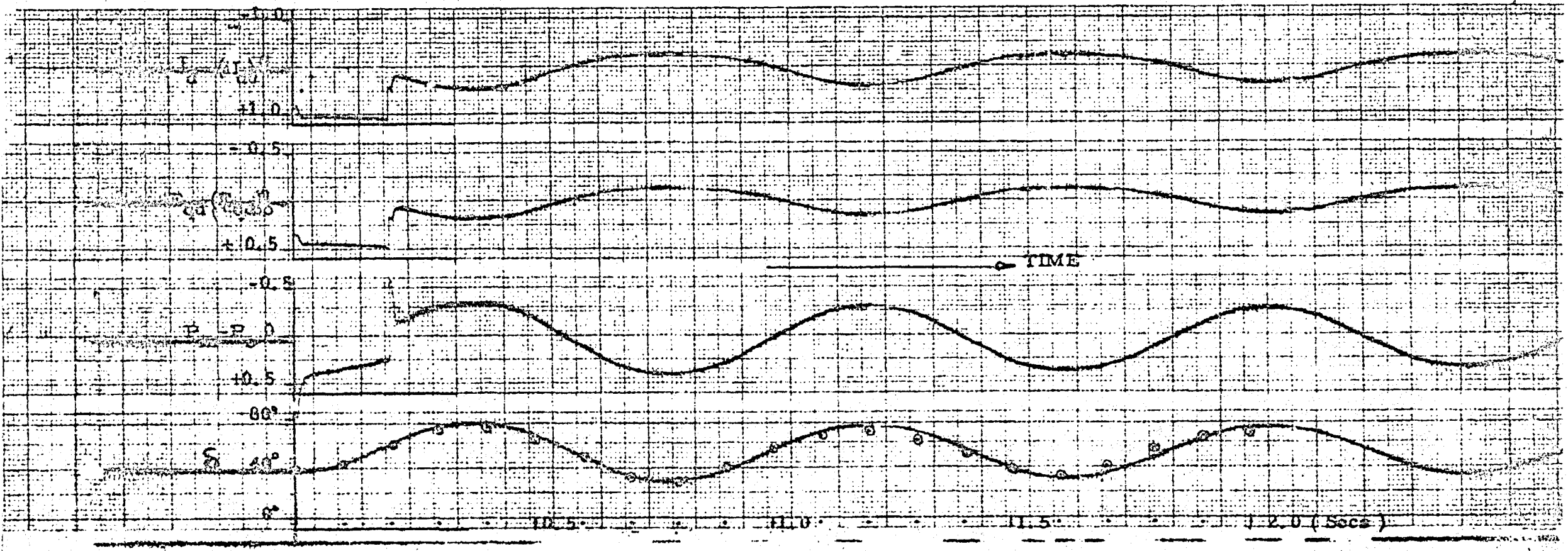

FIG : 4.11 SWING CURVE FOR TEST PROBLEM 4.1.3.

of I_d , E_{qd} , and P_a . At the instants of the application and removal of the faults sharp spikes are seen in the accelerating power curve. Correct conditions are established in 200 m-secs of real time which is only 20 m-secs. on the simulator. Thus the error in the computation for rotor angle δ is not serious.

4. 2 INCLUDING THE EFFECTS OF VARIABLE FLUX LINKAGES:

If the transformer induced voltages are neglected, a simple relation between E'_q , the voltage proportional to the flux linkages, and open circuit no load voltage E_I can be derived very easily. (Ref. 54, 55)

The voltage applied to the field circuit is related to the current and flux linkages as,

$$v_{fd} = r_f i_f + \frac{d\psi_f}{dt} \qquad \ldots\ldots\ 4.2.1$$

This equation may be put into terms of the stator circuit by multiplying it throughout by $\left(\frac{wM_{fd}}{\sqrt{2}\ r_f} \right)$ and making certain substitutions.

$$\frac{wM_{fd}}{\sqrt{2}\ r_f}\ v_{fd} = \frac{wM_{fd}}{\sqrt{2}\ r_f}\ r_f\ i_f + \frac{wM_{fd}}{\sqrt{2}\ r_f} \cdot \frac{d\psi_f}{dt}$$

$$= \frac{wM_{fd}}{\sqrt{2}}\ i_f + \frac{L_{ff}}{r_f}\ \frac{wM_{fd}}{\sqrt{2}\ L_{ff}} \cdot \frac{d\psi_f}{dt}$$

$$\ldots\ldots\ 4.2.2.$$

$$\frac{wM_{fd}}{\sqrt{2}} \cdot i_f = E_i \qquad \text{(section 2.1.1)}$$

$$\frac{wM_{fd}}{\sqrt{2}\ L_{ff}} \cdot \psi_f = E'_q \qquad \text{(section 2.1.3)}$$

and therefore,

$$\frac{wM_{fd}}{\sqrt{2}\ L_{ff}} \cdot \frac{d\,\psi_f}{dt} = \frac{d\,E'_q}{dt}$$

$$\frac{L_{ff}}{r_f} = T'_{do} \quad \text{(open circuit direct axis transient time constant)}$$

$$\frac{wM_{fd}}{\sqrt{2}\ r_f} \cdot v_{fd} = V_{fd} \quad \text{(field circuit voltage refferd to the stator side)}$$

Making these substitutions in equation 4.2.2

$$V_{fd} = E_i + T'_{do} \frac{dE'_q}{dt}$$

or

$$\frac{dE'_q}{dt} = \frac{V_{fd} - E_i}{T'_{do}} \qquad \ldots\ldots \qquad 4.2.3.$$

Equation 4.2.3 includes both the flux decay due to armature demagnetising reaction and also the rise in the flux under the action of the voltage regulators. In the former case V_{fd} is constant but in the later case V_{fd} is a known function of time.

4. 2. 1 A NOTE ON PER-UNIT (p. u.) SYSTEM:-

The equations for the synchronous machine are almost always written in the p. u. system. In simple cases of stability calculations so far discussed only the stator quantities were needed. The base values for these quantities are almost always taken as the RMS rated phase voltage and current. When the rotor circuits are also considered there are various possibilities for selecting the base quantities for the rotor circuits in relation to the stator quantities. All these possibilities are discussed in the two papers by Rankin. (Ref. 71) Generally, however, there is need only for two p. u. bases to provide convenient methods of representation. (Ref. 55)

The first method is known as the vector diagram or non-reciprocal method and is very convenient for the vector diagram representation. Since in developing the basic equations of the synchronous machine for the simulator (chapter 2) the damper windings have been neglected and transformer induced voltages have been neglected, it is possible to draw vector diagrams under transient conditions. The method for selecting rotor base quantities has accordingly been chosen in which the unit field current is that which produces rated voltage at normal speed on the air gap line and the unit field voltage may be defined as that which circulates unit current through the field winding under steady conditions. This

method cannot be conveniently adopted for cases where the rotor circuits other than the main field winding are considered.

The second method is known as the equivalent circuit method or the reciprocal method. The base for the rotor current is such that the mutual reactances between the rotor and the stator circuits are equal and reciprocal, if looked from either side.

In a case where only the main field winding is considered on the rotor the base quantities selected by the two methods are related through constant factors and are given by Crary. (Ref. 55)

4.2.2 TEST PROBLEM:-

The effects of variable flux linkages were added to the problem in section 4.1.3 . This change requires only a few additional computing elements on the analogue computer. The set up for this is shown in fig. 4.10.

The rotor swing plot was again compared with the solution of the simulated equations from the digital computer and showed good agreement.

4.3 AUTOMATIC VOLTAGE REGULATORS :-

It has long been recognised that the automatic voltage regulator affects considerably the stability of the synchronous machine. The improvement in the steady state stability limit .

PHILIPS PI 1026 R/04

has been investigated both theoretically and experimentally and many papers have reported on this subject. (Ref. 18, 72, 73) To a limited extent the A.V.R. effect on the machine performance following transient disturbances. is also found in the literature. The subject remains higly controversial and methods are not known with any degree of certainty for adjusting the gains and time constant in the various channels of the voltage regulator circuit which will give optimum performance both as a first swing stability limit and subsequent damping of the oscillations. Some recent digital computer studies of large systems have shown that certain machine groups start pulling out of step when the swing curves are extended to several oscillations. It was, therefore, decided to include some simple form of automatic voltage regulator in the machine simulation.

Although some investigations have been carried out using signals additional to the terminal voltage error applied to the voltage regulator loop and have shown that these signals offer appreciable improvement in the stability limit, this type of voltage regulator is still not found in frequent use. The analogue computer provides a great flexiblity in the representation of the excitation regulation commensurate with the available data.

4. 3. 1 PROPORTIONAL VOLTAGE REGULATOR :-

A simple proportional regulator is shown in the form of block diagram (fig. 4.13) and is probably the minimum

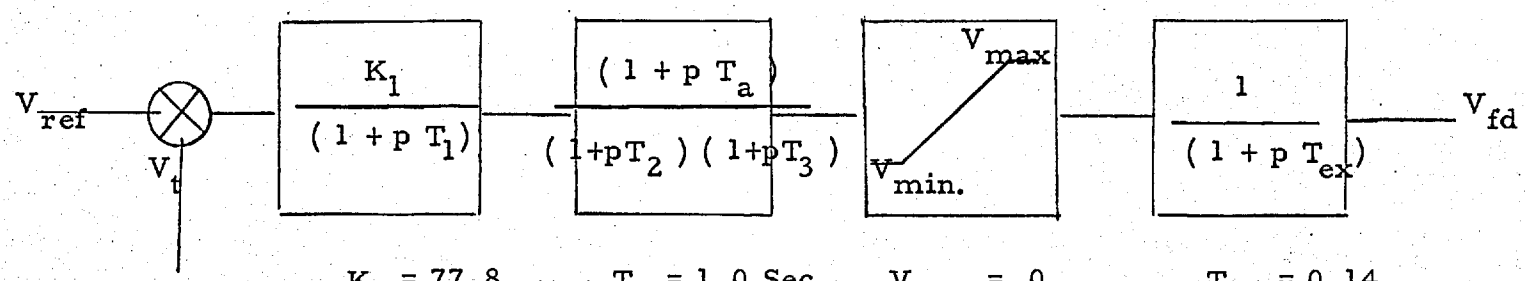

$K_1 = 77.8$ $T_a = 1.0$ Sec $V_{min} = 0$ $T_{ex} = 0.14$

$T_1 = 7.0$Sec $T_2 = 0.001$ Sec $V_{max} = 5.06$

$T_3 = 0.002$ Sec

FIG : 4.13 SIMPLE PROPORTIONAL VOLTAGE REGULATOR

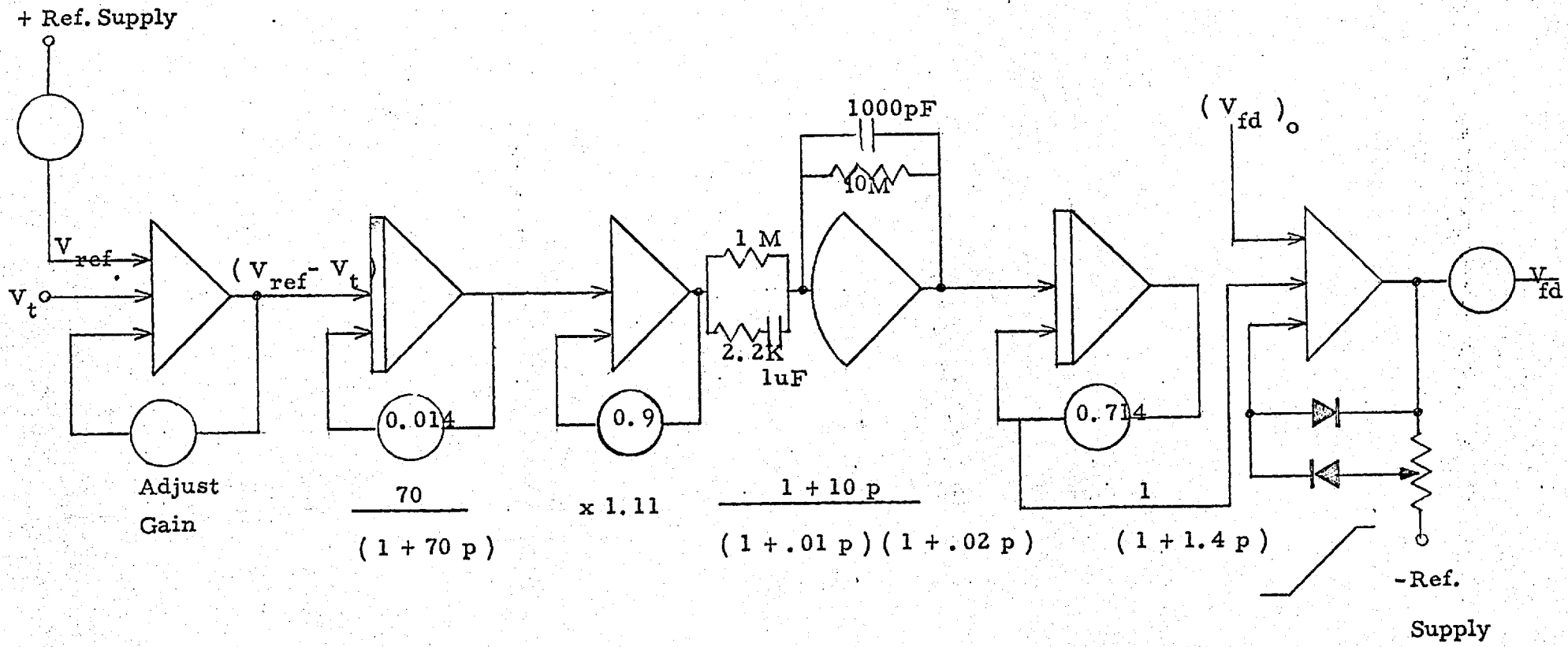

FIG : 4.14 PATCHING SCHEME ON COMPUTER

FOR SIMPLE PROPORTIONAL REGULATOR

necessary for an adequate representation of the proportional regulator. The function of each block is expressed in the form of a transfer function in terms of Laplace's operator. The first block represents the gain of the regulator loop lumped together and a time constant. The second block is a derivative stabilizer. The output of this block is then limited. This limiter represents the saturation of the exciter and the non-reversal of the field voltage, when an A. C. exciter and rectifier is used. The exciter itself is represented by a single time constant. The output of this block is the voltage applied to the field terminals. The gain of the loop is arbitrarily lumped into one block for the convenience of the preparation of the data. The typical figures for the proportional regulator are also given in fig. 4.13 and are for a Westinghouse brushless excitation system having a speed of response of 2 p.u. (Ref. 28)

4.3.2 TEST PROBLEM :-

The problem of section 4.2.2 is now expanded to include the automatic voltage regulator. The patching set up is shown in fig. 4.14. V_{fd} computed, now, replaces the constant V_{fd} shown in fig. 4.10. for problem 4.2.2.

The plot of the rotor swing is shown in fig. 4.15 and shows good agreement with the results obtained from the digital computer. The points obtained from the digital computer output are shown encircled.

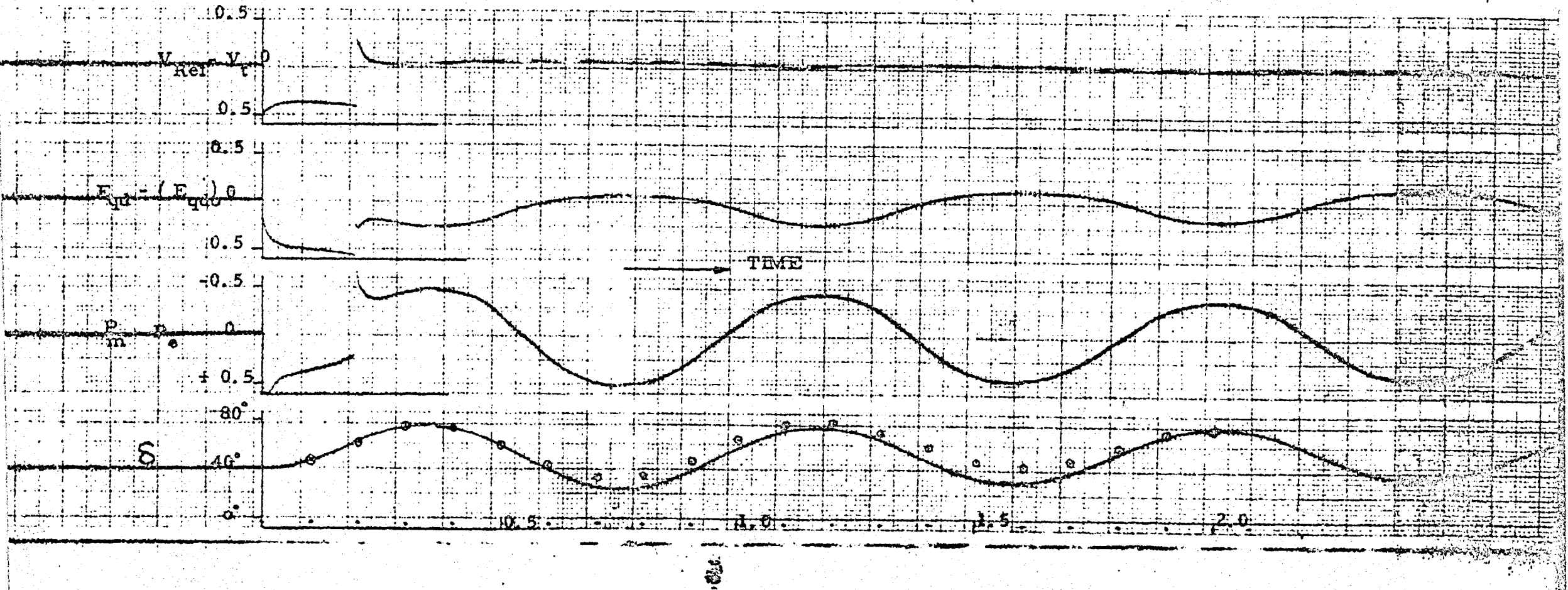

FIG : 4.15 SWING CURVE FOR PROBLEM 4.3.2

4. 4 GOVERNORS :-

Conventional speed governors are almost universally used with both water and steam turbines. Governors are commonly slow to respond and therefore, make little contribution to improving the transient stability limit of the system. They play an effective part in the control of the frequency, sharing of the loads and inter-area transfers of power.

In some recent studies it has been shown that the conventional speed governors have very little potential for affecting the stability. Inclusion of an acceleration term may have an appreciable contribution to make, though it is still unexplored. Other forms of controlling the input energy, such as controlling the steam pressure on the conventional turbo-generator, are also being considered. With very large sets which will have a computerised control, discontinuous controls are also being considered.

In some recent schemes of machine controllers, where automatic control for the whole grid is being provided by a large digital computer, there are inputs to the governing system in addition to the speed signal. These inputs are , generally, the difference between the programmed power and the output of the generator and the deviation from the target frequency. The fly-ball governor and the speeder motor setting control the power input to the turbine through a set of governing valves. The additional signals

are also being applied to the same speeder motor and they regulate the turbine through the common hydraulic system. Representation of these additional signals could be useful for observing their effect on the system stability. At present the machine controllers cease operation under rapid changes.

The deviation of the machine speed away from the synchronous speed is available as a D.C. signal from the tacho-generator coupled to the magslip drive. The governor equations are solved on the analogue computer and the output from the computer is the steam turbine output.

The analogue computer provides a great facility for simulating the governor control mechanism to any degree of accuracy required. Details of such a simulation is given by Dineley. (Ref. 74) Simulation to such fine details has to be balanced against the availability of data and the economics of providing the additional computing elements. A preliminary study could be carried out to determine what is essentially a simple equivalent of the detailed governing system.

4. 4. 1 A SIMPLE SPEED GOVERNOR :-

A conventional speed governing system can be described in the form of a functional block diagram as in fig. 4.16.

This simplified representation is based on the

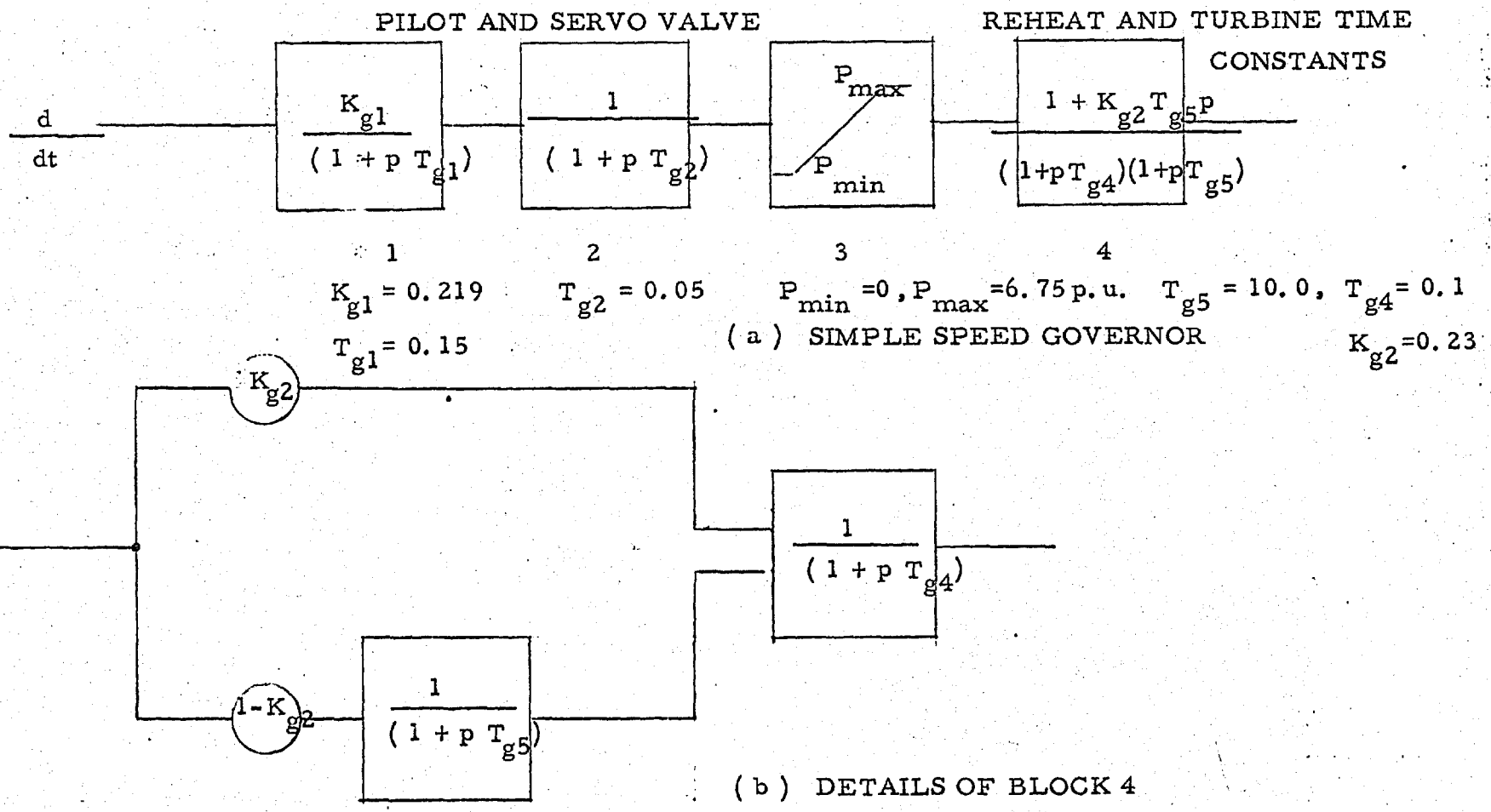

(a) SIMPLE SPEED GOVERNOR

(b) DETAILS OF BLOCK 4

FIG : 4.16

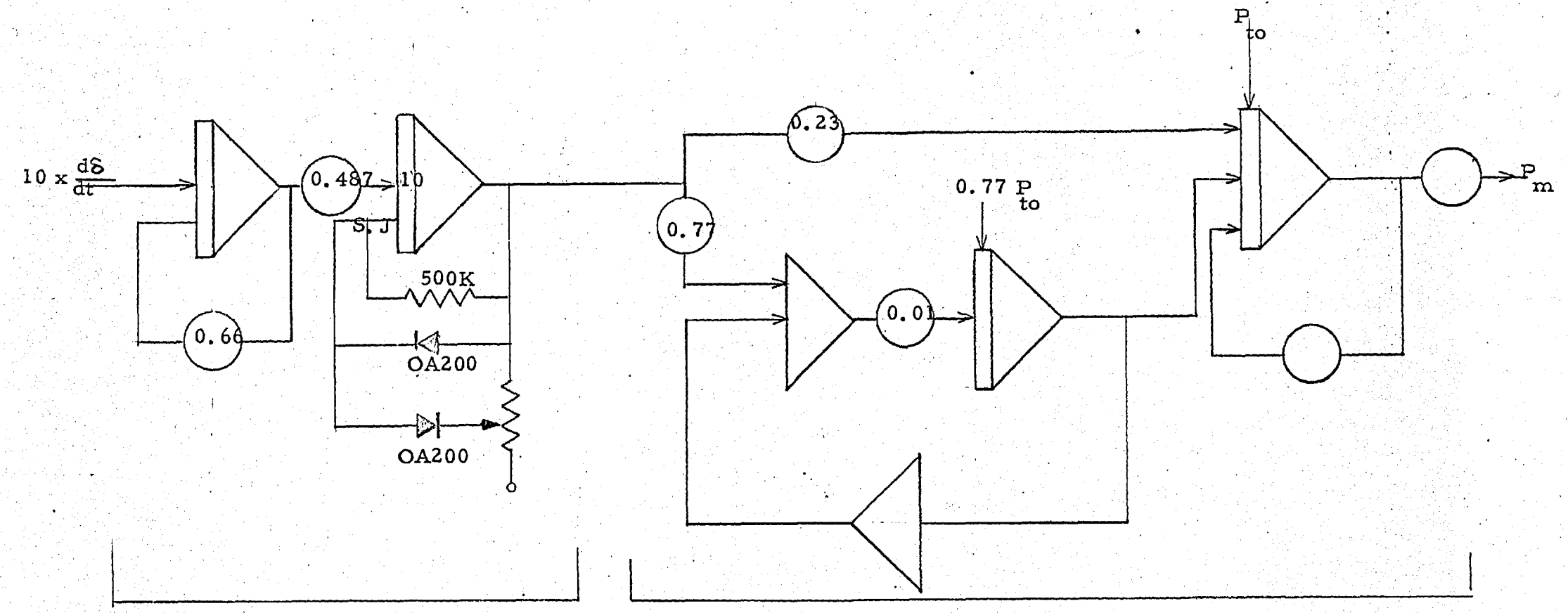

$$10 \times \frac{0.219}{(1 + 1.5\,p)(1 + 0.5\,p)}$$

$$\frac{1 + 0.23 \times 100\,p}{(1 + 1.0\,p)(1 + 100\,p)}$$

FIG : 4.17 ANALOGUE COMPUTER PATCHING SCHEME FOR GOVERNOR

following assumptions:-

1. The governor sleeve movement is proportional to the turbine speed and so is the valve movement.

2. The boiler provides a source of steam at constant temperature and pressure and the steam power at the input to the turbine is proportional to the valve position.

3. The efficiency of the turbine remains constant over the small range of speed deviation.

The input to the first block is speed deviation. The gain is again lumped in the first block. The two time constants are generally the pilot valve and the servo valve. The steam input is then limited. The next block, the transfer function of which looks like a lag lead network, is the simplified form of the turbine and reheat system time constants. The turbine itself is represented by a single time constant. Now the portion of the steam power is converted into mechanical power at the high pressure end and then the steam goes through a reheater which has a very large time constant. This being furthur delayed by the turbine time constant. This situation can also be described by a block diagram shown in fig. 4. 16 (b) in which a portion of the steam power k_{g2} is delayed by the turbine time constant alone and the remaining i. e. $(1 - k_{g2})$ goes through two time constants.

Typical figures for the gains and time constants are given in the block diagram (Ref. 28) . (fig. 4. 16)

following assumptions:-

1. The governor sleeve movement is proportional to the turbine speed and so is the valve movement.

2. The boiler provides a source of steam at constant temperature and pressure and the steam power at the input to the turbine is proportional to the valve position.

3. The efficiency of the turbine remains constant over the small range of speed deviation.

The input to the first block is speed deviation. The gain is again lumped in the first block. The two time constants are generally the pilot valve and the servo valve. The steam input is then limited. The next block, the transfer function of which looks like a lag lead network, is the simplified form of the turbine and reheat system time constants. The turbine itself is represented by a single time constant. Now the portion of the steam power is converted into mechanical power at the high pressure end and then the steam goes through a reheater which has a very large time constant. This being furthur delayed by the turbine time constant. This situation can also be described by a block diagram shown in fig. 4.16 (b) in which a portion of the steam power k_{g2} is delayed by the turbine time constant alone and the remaining i.e. $(1 - k_{g2})$ goes through two time constants.

Typical figures for the gains and time constants are given in the block diagram (Ref. 28) (fig. 4.16)

4. 4. 2 TEST PROBLEM :-

The speed governor shown in fig. 4. 16 is added to the problem discussed in section 4. 3. 1 . Patching diagram is shown in fig. 4. 17 . The output of the governor block now replaces the previous constant input level.

The swing curve obtained from the simulator is shown in fig. 4. 18 . The digital computer output is plotted with encircled points.

4. 5 EFFECTS ON GENERATOR STABILITY STUDIES WITH MORE ACCURATE SIMULATION :-

Fig. 4. 19 shows the swing curves obtained with different degree of detail in representing the turbine and the generator.

Only a few general comments can be made about the effects of including various factors in machine equations and control devices. These relate to the amplitude of the first swing and the damping.

Machine representation with constant voltage behind direct axis transient reactance gives the most pessimistic results. and the degree of pessimism will differ largely with the severity of the fault and the network configuration.

Including the transient saliency reduces the amplitude of the first swing and the transient swing frequency.

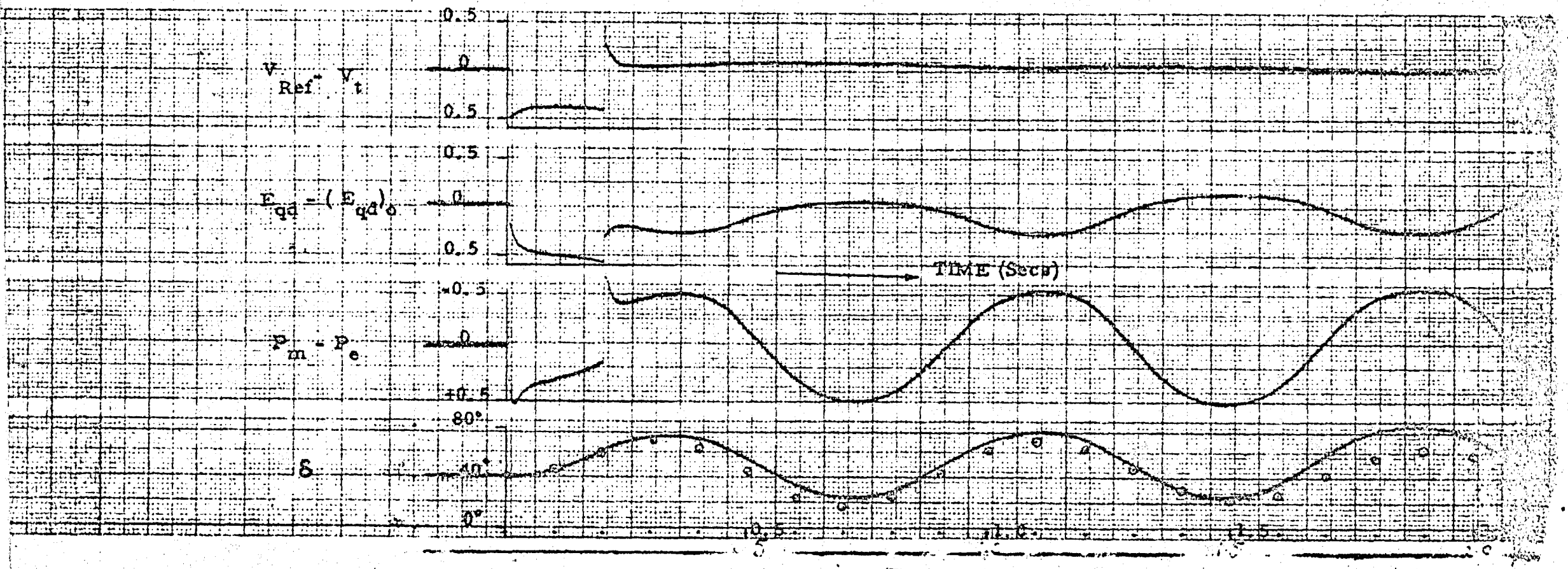

FIG : 4.18 SWING CURVE FOR PROBLEM 4.4.2

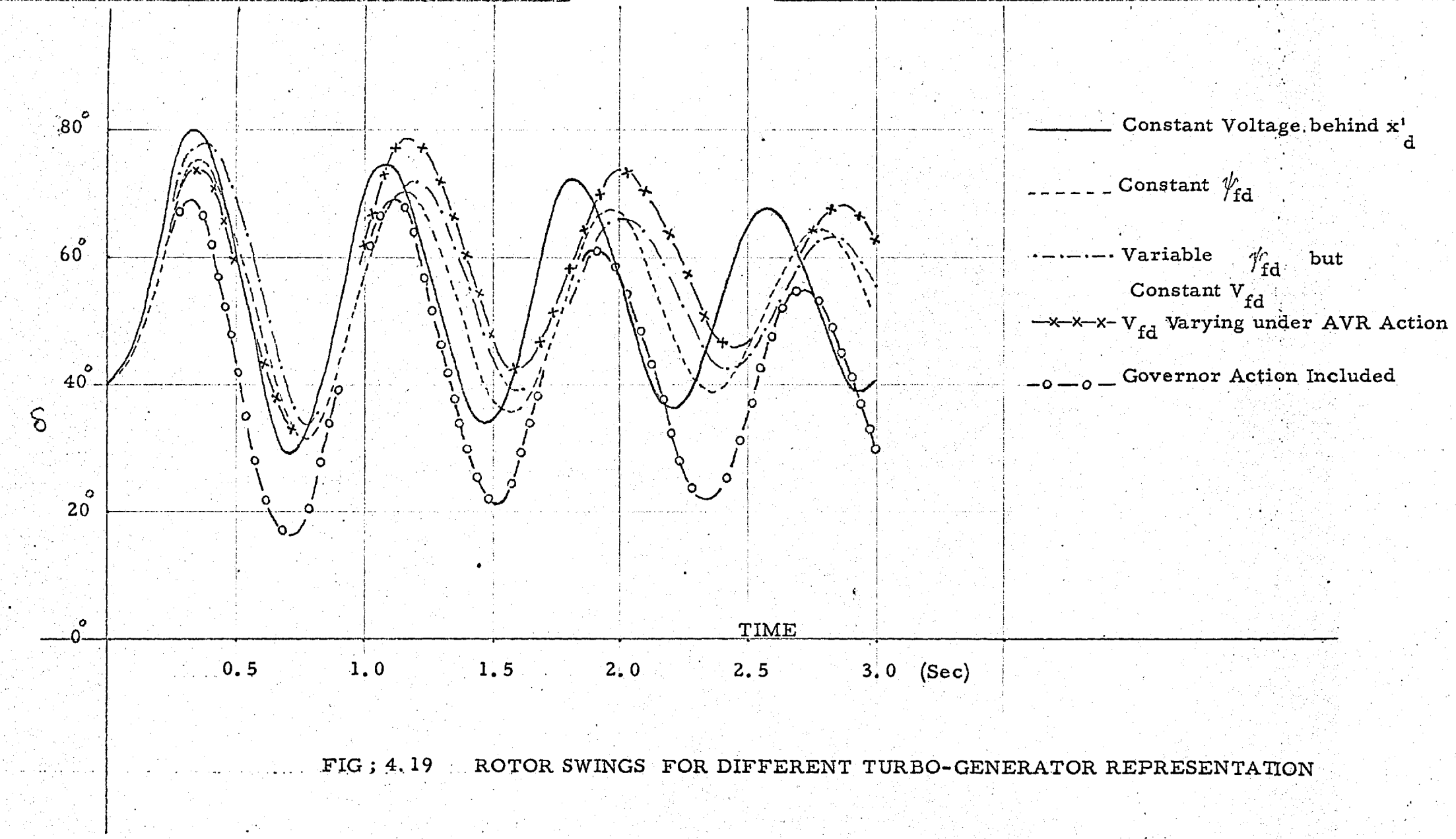

FIG ; 4.19 ROTOR SWINGS FOR DIFFERENT TURBO-GENERATOR REPRESENTATION

Inclusion of the flux decay due to the armature demagnetising reaction increases the amplitude of the first swing and reduces the swing frequency.

An automatic voltage regulator does contribute to the reduction of the first swing amplitude but may or may not contribute to the subsequent damping of the oscillations.

Governor action has a marked effect on reducing the first swing amplitude towards an improvement but subsequently is reducing the damping of the oscillations.

Wherever the assumption of the infinite bus-bar is valid, the assumption of the constant voltage behind the direct axis transient reactance might be a very good guide as to whether the machine will remain stable or not. The conditions of the infinite bus-bar though seem extreme are not impossible to find in actual practice. The pessimistic results obtained from this study would mean that the capability of the generator is not being fully utilized. The fast acting terminal voltage control can help to limit the first swing but may hamper the damping of the oscillations. The same is true of the governor action.

In an extensive system with several generators of comparable size the disturbance may travel to other machines and then the relative phases of the rotor swings may appreciably effect the system performance. The control devices like AVR and governor which cause considerable change in the swing frequency should then

be represented in the system simulation.

There is a continuous trend towards greater concentration of generating capacity and the likelihood of the disturbances simultaneously affecting large quantities of the plant., has increased. Preservation of sufficient attenuation of the disturbance throughout the network will become an increasingly important design consideration.

From the present study, which infact has been carried out with the sole purpose of finding out the extent of the details which can be included in this type of simulation technique and the accuracy, sufficient confidence in the operation of the simulator has been achieved. Various refinements in the turbo-generator representation have produced the corresponding effect on the swing curve faithfully. More elaborate excitation schemes or governing schemes can be legitimately investigated on this simulator.

It is difficult to define the accuracy criterion for the simulator (section 2.3.6), neverthless, an idea can be framed from table 4.1. The table shows the %error in the rotor angle at the first and the third peaks and in time at which these peaks are reached, compared with the digital computer results.

TABLE 4.1

Test No. & Fig. No.		Machine Representation	% Error in δ		% Error in Time	
			1st Peak	3rd Peak	1st Peak	3rd Peak
1)	4.11	Transient Saliency included	Less than 3%	Less than 5%	Less than 4%	Less than 5%
2)	4.12	Flux Decay included	" "	" "	" 1%	" 1%
3)	4.15	A.V.R. action included	" 1%	" 3%	" "	" "
4)	4.18	Governor action included	" 5%	" 10%	" "	" 5%

4. 6. FAULT NEAR TO THE SYNCHRONOUS MACHINE :-

For studies where the interest is to see the effects of varying several different parameters in the AVR and governor, a fault location should be so chosen as to cause bigger rotor swings.

Network conditions for the test problem of section 4. 1. 3 were considered and the rotor swings were recorded following a short circuit on one line but at the sending end of it. Initial output power is 0. 8 p. u. and terminal voltage of 1. 03 p. u.

In fig. 4. 20 rotor swing records are shown for constant direct axis field flux linkages, constant voltage across the field but variable flux linkages and voltage regulator action included. Fig. 4. 21 shows the effect on the rotor swing when the principal time constant T_1 is changed. These plots also confirm some of the observations in the previous section. The simple proportional regulator does not seem to reduce the first swing amplitude when the principal time constant is reduced below that of the field time constant because then the field time constant continues to be more predominant. Making AVR very fast may infact cause negative damping of the rotor oscillations as is shown in fig. 4. 21 with T_1 = 2. 0 seconds and the forward path gain constant at 77. 8. This could be explained in simple terms as follows.

When the machine is swinging in the direction of increasing load angles the terminal voltage tends to drop due to the

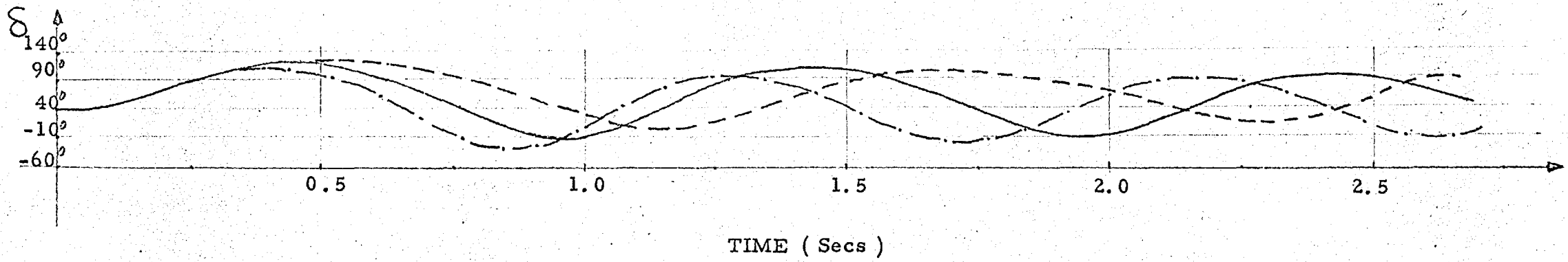

FIG : 4.20 SWING CURVE FOR PROBLEM IN SECTION 4.6

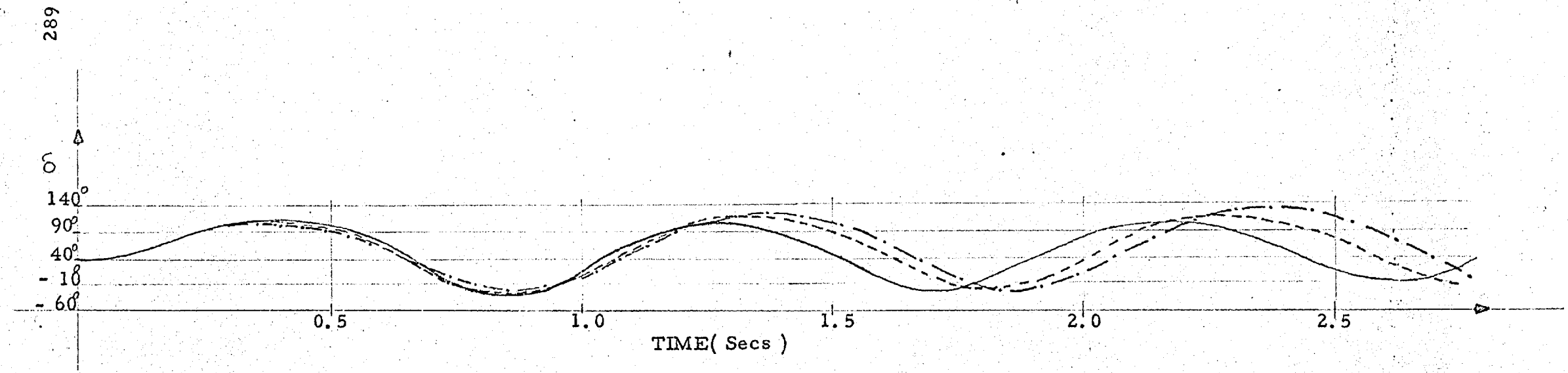

——————— T_1 = 7.0 Sec. & 5.0 Sec

– – – – – – T_1 = 3.0 Sec

—.—.—.— T_1 = 2.0 Sec (T_1 = 7.0)

FIG : 4.21 SWING CURVES FOR PROBLEM IN SECTION 4.6, SHOWING THE EFFECT OF REDUCING PRINCIPLE TIME CONSTANT IN AVR LOOP

increased armature reaction and the increased drop in the leakage impedance. However, because of the effect of the very large time constant of the field circuit the effect of the armature reaction is delayed, as a result the terminal voltage of the machine at any load angle will be higher than the corresponding conditions during the steady state operation. During the recovery swing similarly the terminal voltage will be lower than the corresponding steady-state conditions. This produces damping action because the incremental acceleration torque during the outward swing and the incremental decceleration torque during the recovery swing both decrease. If the terminal voltage is rigidly controlled this mechanism is lost. With T_1 of 2.0 secs. and K_1 of 77.8 it is found that the terminal voltage shot higher than the reference on the start of the recovery swing causing slower speed when the machine passes through the equilibrium angle conditions.

Governor action (parameters shown in fig. 4.16) was added along with the voltage regulator with its principal time constant T_1 =5.0 secs. As shown in fig. 4.22, the machine looses stability as the swing amplitudes are increasing. Reducing the reheat time constant to 5 sec. does not improve the situation. It can be appreciated that if the time delay between the governor sleeve movement and the turbine power output is of the order of 2 secs. the governor will have positive damping for rotor swing oscillations when the frequency is slower than 0.1 cycle/sec.

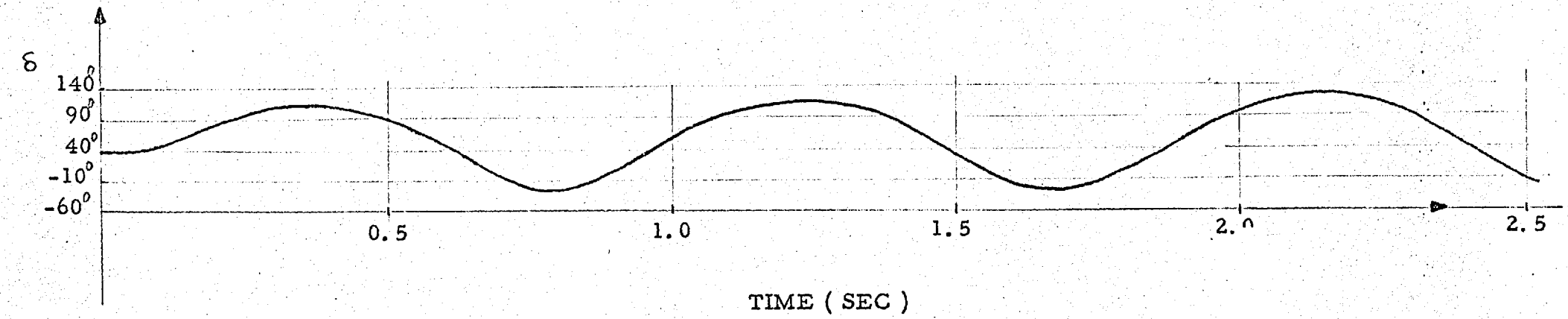

FIG: 4.22 NEGATIVE DAMPING DUE TO THE GOVERNOR

CHAPTER: 5

CRITICISM OF SYNCHRONOUS MACHINE ANALYSIS AND FULL SCALE TESTS.

5.1. NEED FOR FULL SCALE TESTS:

The stability of generators on a large interconnected system is an important consideration both in design and operation. The study of the problem of stability can best be done by tests on an operational system. The testing of large equipment in a modern power system presents considerable difficulty particularly when abnormal conditions are being considered.

The theory of the synchronous machine has been completely developed by R. H. Park and several special cases since have been treated at length. The purely theoretical methods present the difficulty of vast and complex calculations and to help with the calculations, digital computers, network analysers and electromechanical or electronic simulators have been used. These aids and their relative merits have been discussed in chapter 1.

Small scale laboratory models to simulate the large synchronous generators, micro-machines, have rightly acquired importance for the study of the power system stability problems. They help even to formulate the mathematical models. Tests on these machines can be performed more fully and repeated as often as needed and the parameters can of course be determined more precisely. The micro-machine equipment at the present stage of

its development gives a larger loss torque on short circuits. This has been mentioned in chapter 1 as well. A micro-machine set available at Imperial College Power System Laboratory uses an auxilliary equipment (TIME CONSTANT REGULATOR) which reduces the field circuit resistance of the micro-machine and makes the value of the field time constant equal to a large sized machine. (Ref. 9) Although micro-machines are very largely over-dimensioned, the available space for the copper on the rotor is still limited and therefore the resistance of the field winding has to be compensated by the feed back arrangement. The time constant regulator which at present consists of a d. c. exciter, the field of which is supplied from a d. c. amplifier, is poor to respond to very fast changes and is being replaced by a wholly electronic scheme.

The ultimate comparison of the reliability of different methods of studying the problem of stability can only be made if the tests on the operational system are performed and recorded in detail. The tests on the system can also provide a wealth of information to the design and operations engineers, as this is the only way to find out if the system gives satisfactory performance in operation.

Tests on the grid system have been performed in this country. (Ref. 77, 78) Both papers in their conclusions make the statements that the existing analytical techniques and simulation methods (constant voltage behind direct axis transient reactance) predict the generator rotor first swing with good accuracy and

give pessimistic indication of the system recovery. These papers do not present the results of the simulation study and there is insufficient system data given for any comparison to be made with the swing curves that could be obtained using other methods of analysis.

Another paper (Ref. 17) which includes system data in comprehensive detail for the generator, the voltage regulator and the governor became a more adequate guide for checking the the computer method for a later paper. (Ref. 31) Digital computer methods have recently been developed in Power System Laboratory at Imperial College, (Ref. 79) and the Goldington test results have been used as the guide.

A study of the work done by Shackshaft,[17] Humpage and Saha[31] and Harley[79] shows that exact representation even of a single generator with its control gear cannot be constructed which holds true under all conditions. Two reasons are generally attributed to this; one is the lack of available data such as non-linearities and second is the increasing complexity of computations. The results of these papers suggest that analogue computation and digital computer programmes that allow for saliency, damping and control system can duplicate the swing curves obtained from the actual tests by slightly correcting the actual parameters in terms of the equivalent simplified models, but it is still doubtful whether they can be used with certainty to predict the swing curves. There is a need for more tests on the real system to check the validity of different computation-

al techniques and the simplification on a broader basis.

5.2. COMPARISON WITH GOLDINGTON TEST:-

The synchronous machine simulation, which includes the effects of saliency, variable flux linkages, A.V.R. and governor action, developed in the last chapter is based on the assumption that the effect of the damper windings can be simply represented by a damping torque proportional to the slip and that the voltage induced due to the rate of flux on either axis is negligible. These assumptions have been used by Crary (Ref. 55) in the development of synchronous machine transient stability theory and have been found attractive to those developing digital computer programmes for multi-machine stability studies. Some of the most recent papers describing development of the computer programmes are by Day & Parton, (Ref. 30) and Olive. (Ref. 27) These programming techniques have not been verified with the actual tests and some people have expressed doubts about the validity of these assumptions. Digital computer programmes for the same reason, have been developed for better and more accurate theoretical models for the synchronous generators.

The Goldington generating set was subjected to short circuit faults and the results as well as data are exhaustively given in Ref. 17. Unfortunately, taking saliency into account, the values of x_d and x_q were too high for a representation to be set up on the

power system simulator described in this thesis. The limitation is the available voltage swing from the magslip - I-pot combination. Amplification of the voltage seems the obvious answer. The vacuum tubes usually manufactured for use in radio circuits are incapable of providing such a high voltage swing. The only alternative is to use a transformer with fixed turns ratio. Such a transformer has to be specially designed so that it does not give variable phase shift at different loads. Another alternative is to use an amplifier in which positive and negative halves of the A. C. wave are amplified in two sections. This limitation of the simulator is, however, not very serious because the Goldington machine is perhaps the smallest in rating being used in large sized system. The Goldington generator is a 30 MW set and the unsaturated value of the synchronous reactance is 2 p. u. A 60 MW set at Marchwood has synchronous reactance of 1. 52 p. u. Turbo-generator sets of higher capacity would fall well within the capability of the simulator.

Nevertheless the system equations as represented on the simulator were used to compute the swing curve for the Goldington machine.

Fig. 5. 1 shows that for the stability criterion used in the past, i. e. stability on the first swing and ultimate stability under the new operating conditions, the approximate methods were quite satisfactory. It is recognised that if these criteria are satisfied a machine without the voltage regulator and governor will be stable and will not lose synchronism.

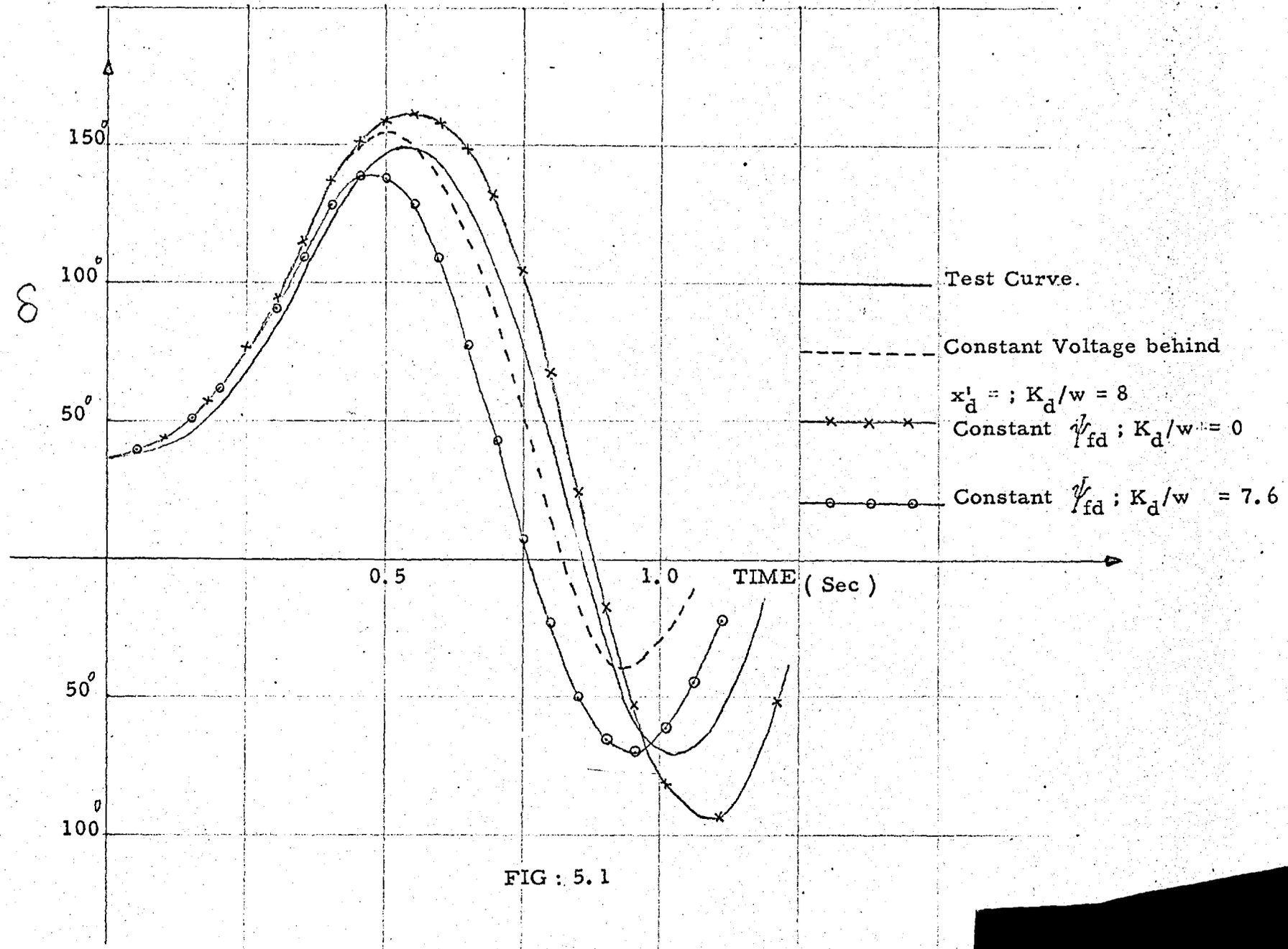
150°
100°
50°
δ
0.5
1.0
TIME (Sec)
50°
100°
Test Curve.
Constant Voltage behind
x'd = ; Kd/w = 8
Constant ψfd ; Kd/w = 0
Constant ψfd ; Kd/w = 7.6

FIG : 5.1

In fig. 5.2 the swing curve for the Goldington machine has been plotted taking all the different factors into account on the lines similar to those discussed in chapter 4. The damping coefficient has been calculated based on Crary's formula,

$$K_d = E^2 \left(\frac{x'_d - x''_d}{(x_e + x'_d)^2} \right) T''_{do} \sin^2 \delta + \left(\frac{x'_q - x''_q}{(x_e + x'_q)^2} \right) T''_{qo} \cos^2 \delta$$

Fig. 5.3 shows the field circuit quantities and fig. 5.4 the machine terminal voltage. Fig. 5.5. shows a plot of slip and mechanical output torque of the turbine.

The following points are observed form these plots :-

1. The first outward swing of the rotor follows the test curve accurately untill the point where the fault ' (short circuit) is removed.

2. The damping of the subsequent oscillations is very low.

3. The terminal voltage of the machine is too high at the point of the removal of short circuit.

4. Field quantities are also faithfully reproduced until the short is removed.

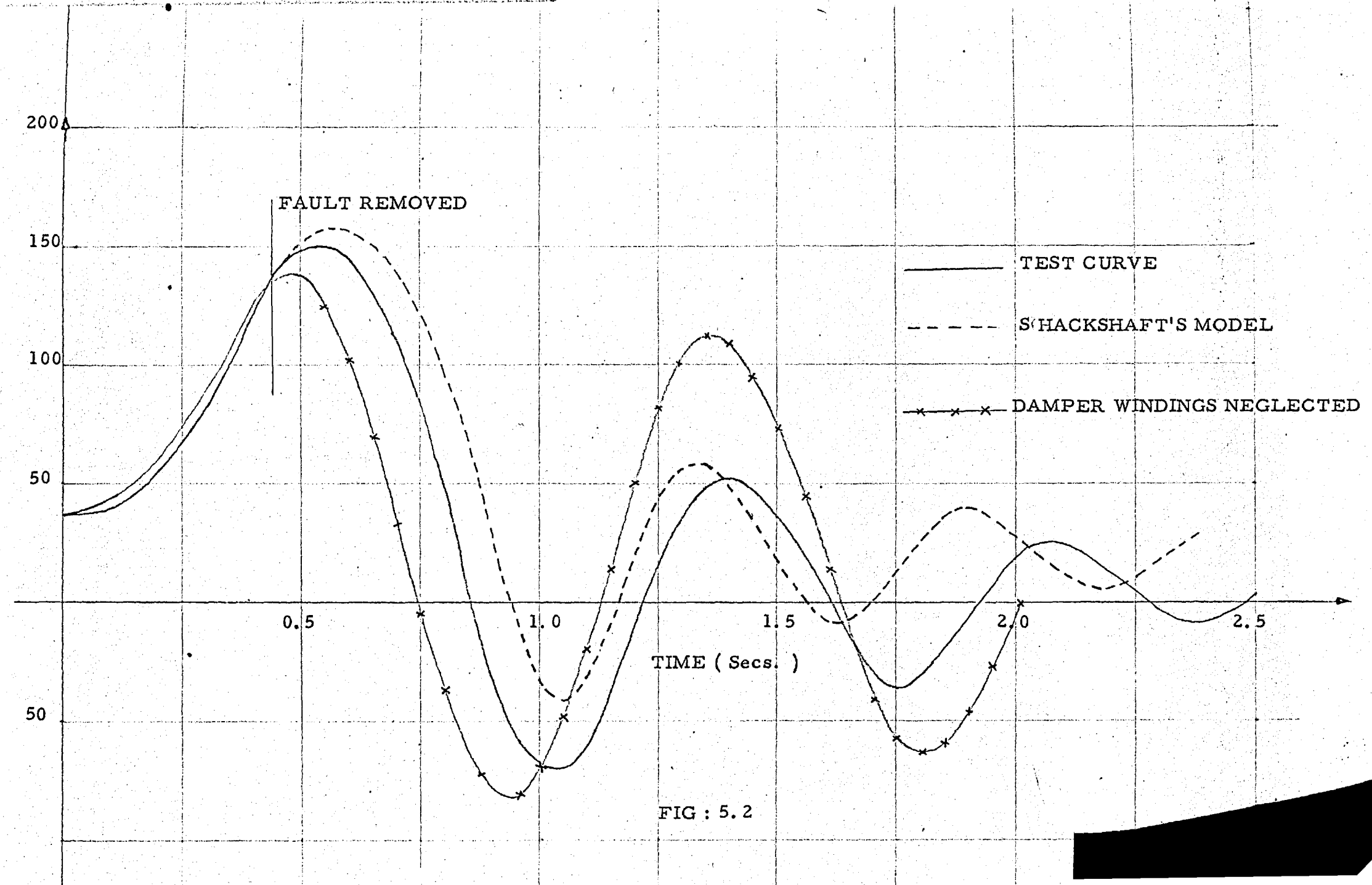
200
150
100
50
50
FAULT REMOVED
0.5
1.0
1.5
2.0
2.5
TIME (Secs.)
TEST CURVE
SHACKSHAFT'S MODEL
DAMPER WINDINGS NEGLECTED

FIG : 5.2

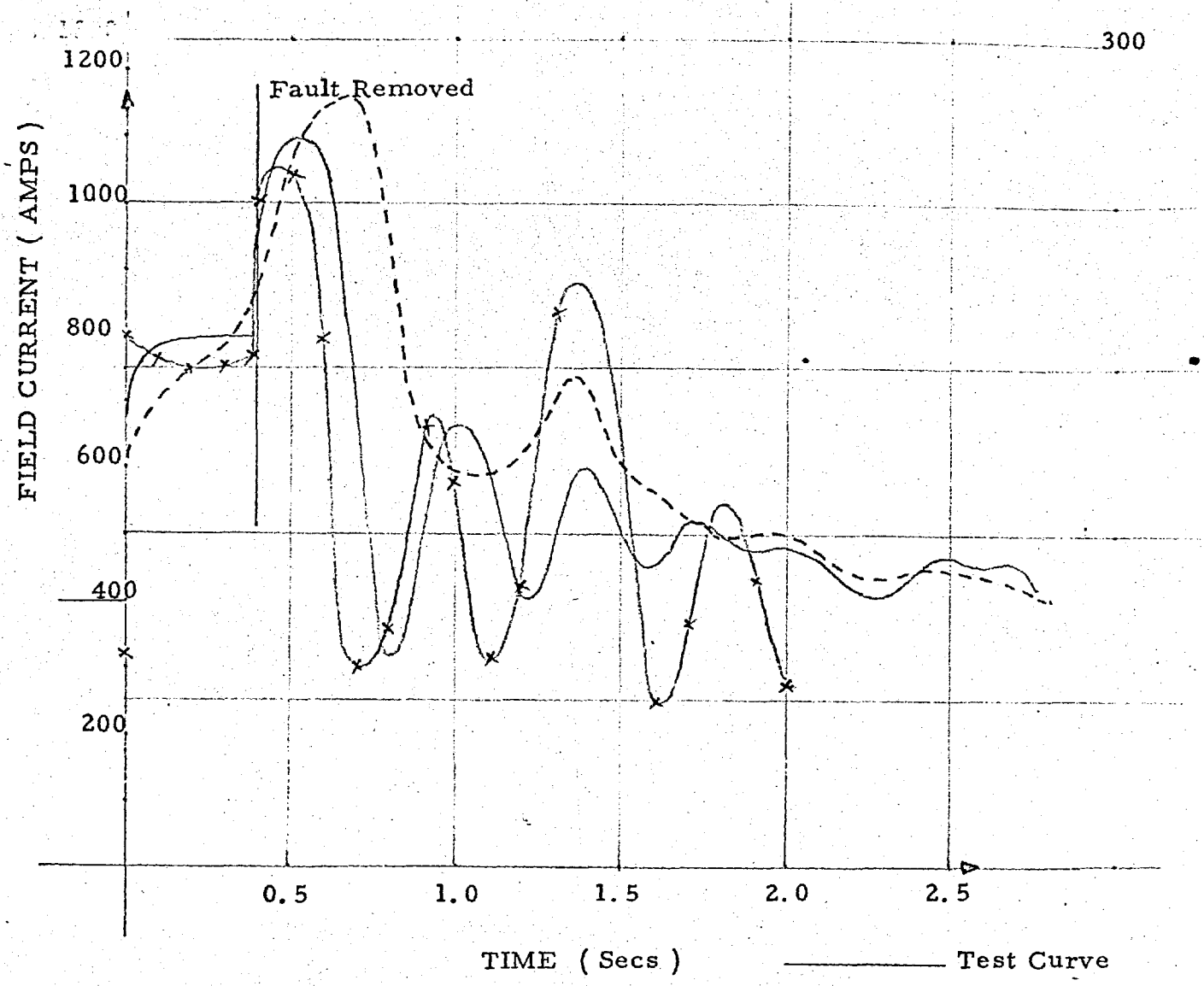
Fault Removed
FIELD CURRENT (AMPS)
1200
1000
800
600
400
200
0.5
1.0
1.5
2.0
2.5
TIME (Secs)
Test Curve

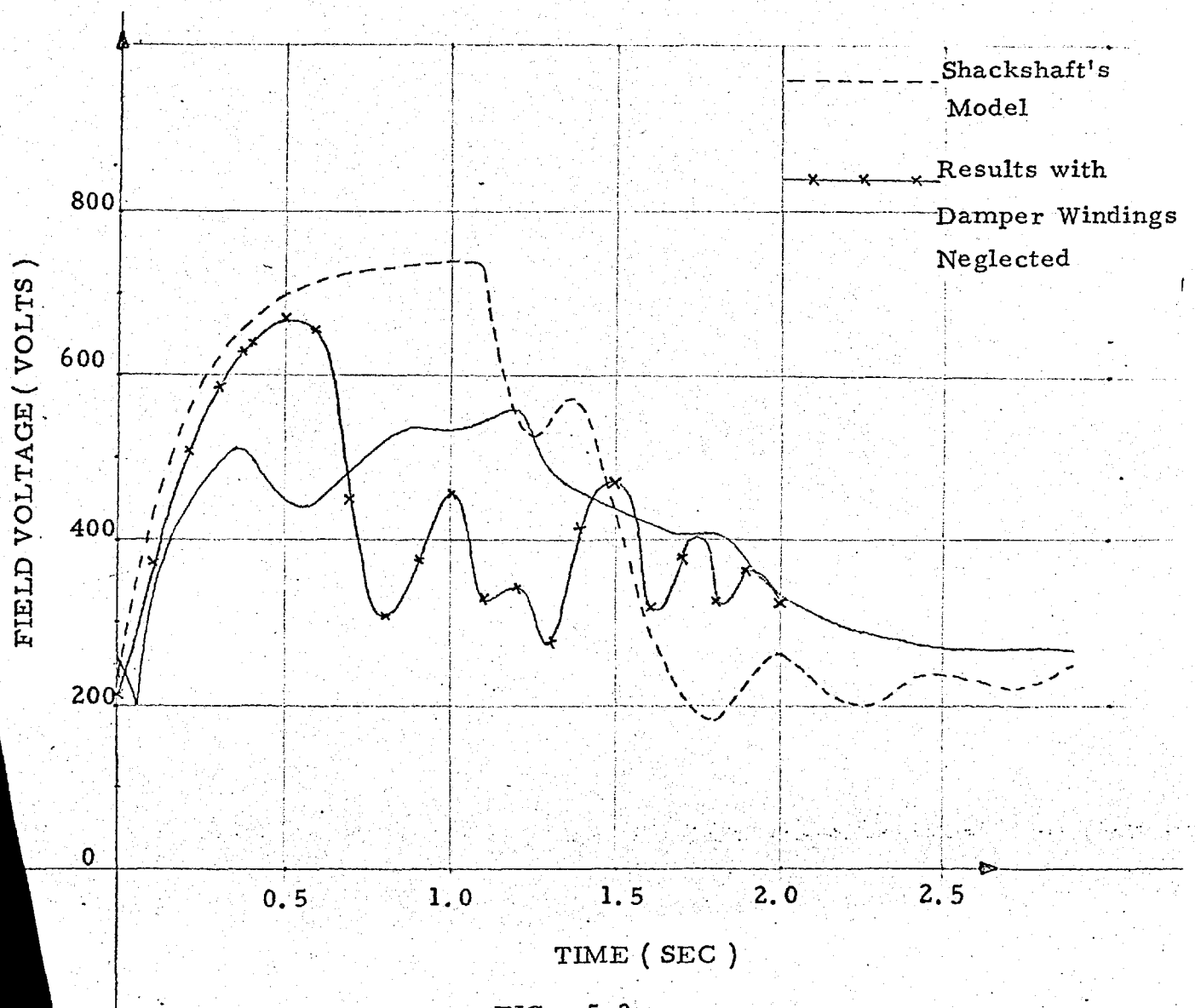
Shackshaft's Model
Results with Damper Windings Neglected
FIELD VOLTAGE (VOLTS)
800
600
400
200
0
0.5
1.0
1.5
2.0
2.5
TIME (SEC)

FIG : 5.3

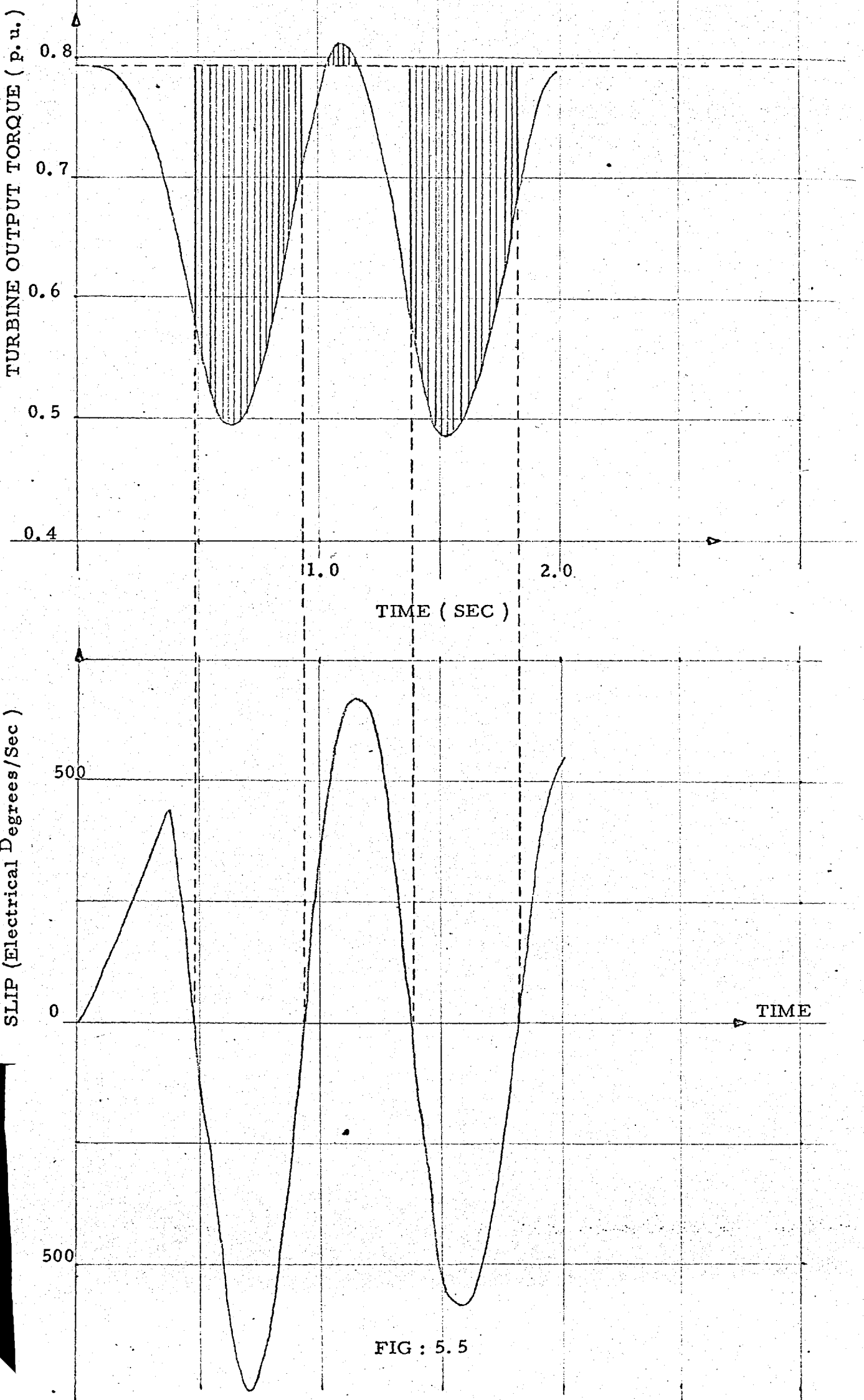
TURBINE OUTPUT TORQUE (p.u.)
0.8
0.7
0.6
0.5
0.4
1.0
2.0
TIME (SEC)
SLIP (Electrical Degrees/Sec)
500
0
TIME
500

FIG : 5.5

5. The governor produces negative damping.

The energy fed in to the rotor in the direction opposite to that of the sign of the slip is shown as a shaded area in the turbine output torque.

An explanation of these discrepancies is sought in the following sections.

5.3. SYNCHRONOUS MACHINE THEORY WITH DAMPER WINDINGS:-

To understand fully the behaviour of the machine during short circuits or other faults and the inadequacy of the generator simulation it is essential to look at the general operational equations of the machine including at least one damper coil each on direct and quadrature axis. The assymetrical components of current are still neglected and it is assumed that the rate of the alternating quantities is very much slower than the A.C. cycle. Both these assumptions enable one to use the relationships between the transformed axes components of the phase voltages and currents and therefore it is possible to draw a vector diagram in a general transient case. The equations are written in the p.u. system which makes the mutual inductances between any two windings on either axis equal if looked at from either side.

The sign conventions are the same as in section 2.1.2. and differ from Adkin's conventions only in the signs for i_d and i_q both of which are considered negative for the generator.

The general operational equations are written in the way explained in section 2.1. , but now contain two more equations because of the inclusion of damper coils. The equations are written in the matrix form.

v_f	$r_f+(L_{md}+l_f)p$	$L_{md}p$	-	$-L_{md}p$	-	i_f
$v_{kd}=0$ e_1	$L_{md}p$	$r_{kd}+(L_{md}+l_{kd})p$	z_1 -	$-L_{md}p$	z_2 -	i_{kd} i_1
$v_{kq}=0$ =	-	-	$r_{kq}+(L_{mq}+l_{kq})p$	-	$-L_{mq}p$	i_{kq}
v_d e_2	$L_{md}p$	$L_{md}p$	$-L_{mq}\omega$ z_3	$-[r_a+(L_{md}+l_a)p]$	$(L_{mq}+l_a)\omega$ z_4	i_d i_2
v_q	$L_{md}\omega$	$L_{md}\omega$	$L_{mq}p$	$(L_{mq}+l_a)\omega$	$-[r_a+(L_{mq}+l_a)p]$	i_q

..... 5. 3. 1

Matrix partitioning techniques are used to eliminate the quantities i_f , v_{kd} , v_{kq} , and i_{kd}, i_{kq}. The partioning is shown above and the matrix can now be written as:

$$\begin{bmatrix} e_1 \\ e_2 \end{bmatrix} = \begin{bmatrix} z_1 & z_2 \\ z_3 & z_4 \end{bmatrix} \times \begin{bmatrix} i_1 \\ i_2 \end{bmatrix} \qquad 5.3.2.$$

or $e_1 = z_1 i_1 + z_2 i_2$ (a)

and $e_2 = z_3 i_1 + z_4 i_2$ (b) 5.3.3

From 5.3.3. (a)

$$z_1 i_1 = e_1 - z_2 i_2$$

or $$i_1 = z_1^{-1} (e_1 - z_2 i_2)$$

substituting in 5.3.3. (b)

$$e_2 = z_3 (z_1^{-1} e_1 - z_1^{-1} z_2 i_2) + z_4 i_2$$

or

$$e_2 - z_3 z_1^{-1} e_1 = (z_4 - z_3 z_1^{-1} z_2) i_2$$

or

$$e_2' = z_4' i_2 \quad \ldots\ldots 5.3.4$$

This equation can be written as follows :

$$\begin{vmatrix} v_d - p \frac{G(p)}{w} v_f \\ v_q - \frac{G(p)}{w} v_f \end{vmatrix} = \begin{vmatrix} -r - p \frac{x_d(p)}{w} & \frac{x_q(p)}{w} \\ \frac{x_d(p)}{w} & -r - p \frac{x_q(p)}{w} \end{vmatrix} \times \begin{vmatrix} i_d \\ i_q \end{vmatrix} \quad \ldots\ldots 5.3.5.$$

Where $G(p)$, $x_d(p)$ and $x_q(p)$ are defined by Adkins. (Ref. 50)

Adding

$$\begin{bmatrix} - & x_q \\ -x_d & - \end{bmatrix} X \begin{bmatrix} i_d \\ i_q \end{bmatrix}$$

on both sides of eq=ns 5.3.5 and transposing all the terms containing the operator p on to the right hand side.

$$v_d - \left(p \frac{G(p)}{w} v_f - p \frac{x_d(p)}{w} i_d + \omega \frac{x_q(p)}{w} i_q - x_q i_q \right) = -r i_d + x_q i_q$$

$$v_q - \left(\omega \frac{G(p)}{w} v_f - \omega \frac{x_d(p)}{w} i_d - p \frac{x_q(p)}{w} + x_d i_d \right) = -x_d i_d - r i_q$$

.....5.3.6

or

$$\begin{bmatrix} v_d - \xi_d \\ v_q - \xi_q \end{bmatrix} = \begin{bmatrix} -r & x_q \\ -x_d & r \end{bmatrix} \begin{bmatrix} i_d \\ i_q \end{bmatrix}$$

With resistance neglected the above matrix reduces to,

$$\begin{bmatrix} v_d - \xi_d \\ v_q - \xi_q \end{bmatrix} \quad \begin{bmatrix} - & x_q \\ -x_d & - \end{bmatrix} \quad \begin{bmatrix} i_d \\ i_q \end{bmatrix} \quad \ldots\ldots 5.3.7$$

where

$$\xi_d = p \frac{G(p)}{w} v_f - p \frac{x_d(p)}{w} i_d + \nu \frac{x_q(p)}{w} i_q - x_q i_q$$

$$\xi_q = \nu \frac{G(p)}{w} v_f - \nu \frac{x_d(p)}{w} i_d - p \frac{x_q(p)}{w} i_q + x_d i_d$$

$$\ldots\ldots\ldots\ldots\ldots 5.3.8$$

The machine equations written in this form have the merit that the equivalent representation of these on the network analyser is at once visualised and that the physical phenomena during the transient conditions can be more easily explained. The equations in this form have been derived by R. A. Hore. (Ref. 80)

With the assumtions explained in the beginning of this section, it

is possible to draw the vector diagram as shown in fig 5. 6.

For a machine having a single field winding on D-axis, ℓ_d under steady state conditions is zero and ℓ_q is proportional to $x_{md} / r_f \cdot v_f$.

Under transient conditions ℓ_d and ℓ_q are incremented due to the transient rotor currents. These rotor currents arise in the following three ways.

1. Due to the changes in the magnitude of the stator current, in which case rotor M. M. F. is induced to keep the flux linkages constant.

2. They may be caused by changes in the voltage applied to the field.

3. Transient rotor currents may be caused by changes in the speed of the machine relative to the system frequency.

Incremental excitation can be calculated for each of the above conditions, taken one at a time . and the principle of superposition allows adding them together.

5. 4. INCREMENTAL EXCITATION DUE TO INCREASE IN STATOR CURRENT :-

When the stator current increases suddenly, currents are induced in the rotor circuits to keep the flux linking them constant. For calculating the increase in excitation due to this, the amortisseur windings can be neglected

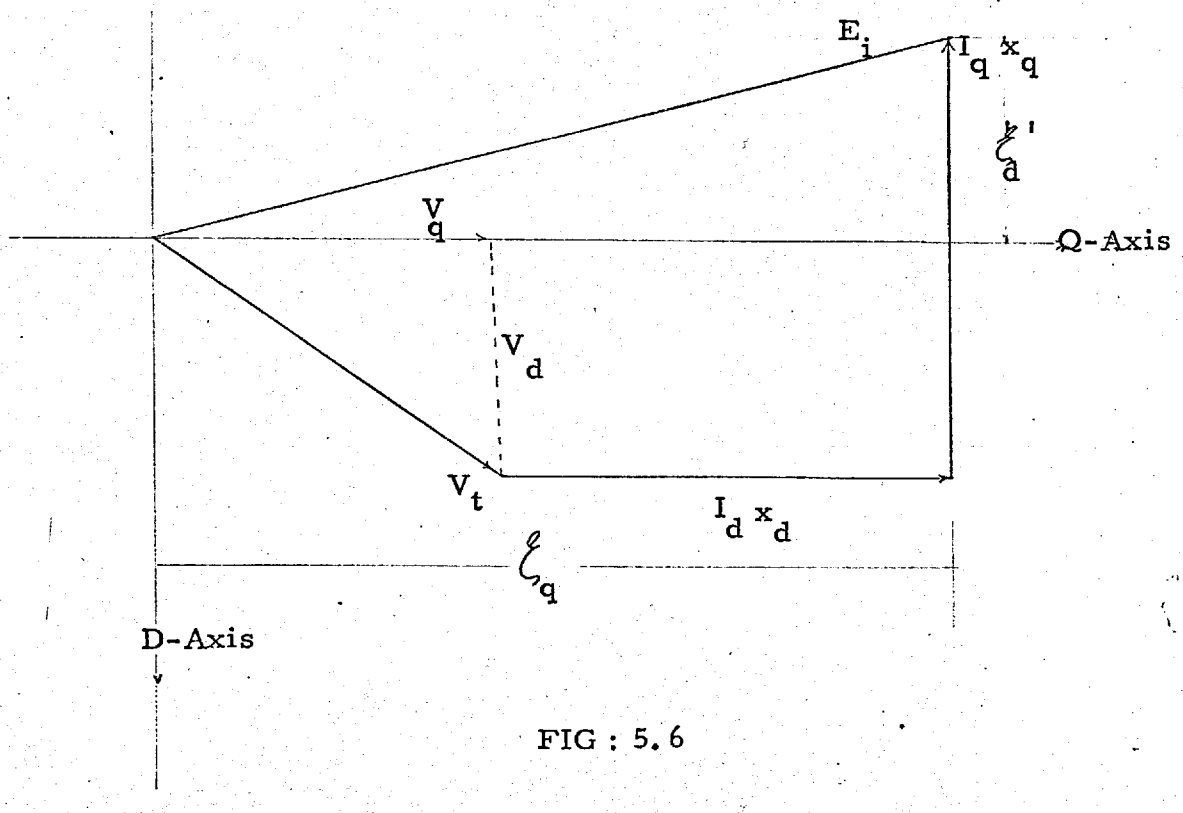

FIG : 5.6

VECTOR DIAGRAM UNDER

GENERAL TRANSIENT CONDITIONS

because the time constants of these windings are small. Under these conditions $x_d(p)$ and $x_q(p)$ can be simplified to,

$$x_d(p) = \frac{(1 + T'_d p)(1 + T''_d p)}{(1 + T'_{do} p)(1 + T''_{do})} x_d$$

$$= \frac{(1 + T'_d p)}{(1 + T'_{do} p)} x_d$$

$$= \frac{x_d + x'_d T'_{do} p}{(1 + T'_{do} p)}$$

$$x_q(p) = \frac{(1 + T''_q p)}{(1 + T''_{qo} p)} x_q = x_q \qquad \ldots\ldots 5.4.1$$

Now if i'_d and i'_q are the increments in the axes currents then from eqn 5.3.8.

$$\zeta_d(p) = -p\frac{x_d(p)}{w}(i_d + i'_d.1) + \omega\frac{x_q(p)}{w}(i_q + i'_q.1)$$

$$- x_q(i_q + i'_q.1)$$

where .1 is unit step.

If $\omega = w$ then

$$\zeta_d(p) = -p\frac{x_d(p)}{w}(i_d + i'_d.1)$$

or

$$= - p \cdot \frac{x_d + x'_d \, T'_{do} \, p}{w (1 + T'_{do} \, p)} \cdot \frac{i'_d}{p}$$

Therefore

$$\mathcal{E}_d (t) = \left(\frac{x_d - x'_d}{w \, T'_{do}} \right) \cdot e^{-t/T'_{do}} \cdot i'_d \qquad \ldots\ldots 5.4.2.$$

and

$$\mathcal{E}_q (p) = - \frac{\vartheta}{w} \, x_d (p) \cdot (i_d + i'_d \cdot 1) + x_d (i_d + i'_d \cdot 1) - p \, \frac{x_q (p)}{w} (i_q + i'_q \cdot 1)$$

$$= - \frac{\vartheta}{w} \left(\frac{x_d + x'_d \cdot T'_{do} \cdot p}{1 + T'_{do} \cdot p} \right) (i_d + i'_d \cdot 1) + x_d (i_d + i'_d) - p \, \frac{x_q (p)}{w} (i_q + i'_q \cdot 1)$$

$$= - \frac{\vartheta}{w} \left[x_d - \frac{(x_d - x'_d) \, T'_{do}}{1 + T'_{do} \cdot p} \, p \right] (i_d + \frac{i'_d}{p}) + p \, \frac{x_q}{w} (i_q + \frac{i'_q}{p})$$

$$= \frac{\vartheta}{w} \, \frac{(x_d - x'_d) \, T'_{do}}{(1 + T'_{do} \, p)} \cdot i'_d - \frac{x_q}{w} \cdot i'$$

and therefore

$$\mathcal{E}_q (t) = + (x_d - x'_d) \, e^{-t/T'_{do}} \cdot i'_d \qquad \ldots\ldots 5.4.3$$

5. 5. INCREMENTAL EXCITATION DUE TO INCREASE IN THE FIELD VOLTAGE:-

The effect of the damper winding can again be neglected because the sub-transient time constants are very small and the terms due to these will decay very fast. The function G (p) can then be taken as,

$$G(p) = \frac{(1 + T_{kd}\, p)}{(1 + T'_{do}\, p)(1 + T''_{do}\, p)} \cdot \frac{x_{md}}{r_f}$$

$$= \frac{1}{(1 + T'_{do}\, p)} \cdot \frac{x_{md}}{r_f}$$

Now if v'_f is the increase in the voltage applied to the field winding,

$$\mathcal{E}_d(p) = p \frac{x_{md}}{w\, r_f (1 + T'_{do}\, p)} \cdot (v_f + v'_f \cdot 1)$$

$$\mathcal{E}_d(t) = \frac{x_{md}}{w\, r_f} \cdot \frac{1}{T'_{do}} \cdot v'_f \cdot e^{-t/T'_{do}}$$

..... 5. 5. 1

and

$$\mathcal{E}_q(p) = \frac{\gamma}{w} \cdot \frac{x_{md}}{r_f} \cdot \frac{1}{(1 + T'_{do}\, p)} \cdot (v_f + v'_f)$$

$$\mathcal{E}_q(t) = \frac{x_{md}}{r_f} \cdot v_f + \frac{x_{md}}{r_f}(1 - e^{-t/T'_{do}})$$

..... 5. 5. 2

5 . 6. INCREMENTAL EXCITATION UNDER SLIP CONDITIONS:

The value of the incremental excitation under slip conditions can be worked out if it is assumed that the slip of the rotor remains constant or at least that the rate of change of slip is low enough as to enable the rotor conditions to keep pace with the changes in slip. With this assumption synchronising torque of the amortisseur becomes very small. Another factor which is neglected in the derivation which follows now is the negative damping of the stator circuit. Because x/r ratio of the stator is large and the rate of change of slip is small during the power swings, the negative damping of the stator is small.

In the eq=ns 5. 3. 8 p is replaced by jsw and by (1- s) w to obtain the values for $\mathcal{E}_d$ and $\mathcal{E}_q$ in complex numbers.

$$\mathcal{E}_d(jsw) = -jsw \frac{x_d(p)}{w} i_d + (1 - s) w \frac{x_q(p)}{w} \cdot i_q - x_q i_q$$

$$= - jsx_d(p) i_d + (1 - s) x_q(p) i_q - x_q \cdot i_q$$

and $$\mathcal{E}_q(jsw) = -(1 - s) x_d(p) i_d + x_d \cdot i_d - jsx_q(p) i_q$$

In real form the expression can be obtained by transferring imaginary terms to the axis 90^{o} in advance when they are preceeded by the operator +j .

$$\mathcal{E}_d\,(jsw) = s\,x_q\,(p)\,i_q + (1-s)\,x_q(p)\,i_q - x_q\,i_q$$

$$= -\left[x_q - x_q\,(p)\right]\,i_q \qquad \ldots\ 5.\ 6.\ 1$$

$$\mathcal{E}_q\,(jsw) = -\,s\,x_d(p)\,i_d - (1-s)\,x_d\,(p)\,i_d + x_d\,i_d$$

$$= \left[x_d - x_d\,(p)\right]\,i_d \qquad \ldots.\ 5.\ 6.\ 2.$$

From the equations 5. 3. 5 and neglecting terms containing r, $p\,i_d$, $p\,i_q$ and putting $v_f = 0$

$$v_d = x_q\,(p)\,i_q$$

$$v_q = -\,x_d\,(p)\,i_d$$

therefore,

$$i_q = \frac{v_d}{x_q\,(p)} = \frac{\sqrt{2}\ V_t\ \mathrm{Sin}\delta}{x_q\,(p)}$$

and

$$i_d = -\,\frac{v_q}{x_d\,(p)} = -\,\frac{\sqrt{2}\ V_t\ \mathrm{Cos}\delta}{x_d\,(p)}$$

Substituting the above values for i_d and i_q in 5. 6. 1 and 5. 6. 2

$$\mathcal{E}_d(jsw) = -\left[\frac{x_q - x_q(p)}{x_q(p)}\right] \cdot \sqrt{2} \cdot V_t \cdot \sin\delta$$

$$\mathcal{E}_q(jsw) = -\left[\frac{x_d - x_d(p)}{x_d(p)}\right] \sqrt{2} \cdot V_t \cdot \cos\delta$$

Transforming $\frac{x_d - x_d(p)}{x_d(p)}$ following the method of Park, (Ref. 52)

$$\frac{x_d - x_d(p)}{x_d(p)} = \frac{x_d - x''_d}{x''_d} \sum_{1}^{n} a_{dn} e^{-\alpha_{dn} t}$$

Now putting $\cos\delta = \cos$ swt and using Duhamel's integral,

$$f(p) \cdot F(t) = F(0) \cdot \phi(t) + \int_0^t \phi(t-u) F'(u) \cdot du.$$

where

$$f(p) = \frac{x_d - x_d(p)}{x_d(p)}$$

$$F(t) = \cos \text{ swt}$$

and $\phi(t) = f(p) \cdot 1$

it has been proved by Hore (Ref. 80) that,

$$\mathcal{E}_q(t) = \mathcal{L}^{-1}\sqrt{2} \cdot V_t \cdot \cos\delta \left[\frac{x_d - x_d(p)}{x_d(p)}\right]$$

$$= \sqrt{2} \cdot V_t \cdot s\omega \cdot T''_{do} \sin\delta \cdot \left(\frac{x_d - x''_d}{x_d}\right)$$

..... 5. 6. 3

and similarly,

$$\mathcal{E}_d(t) = -\sqrt{2} \cdot V_t \cdot s\,w \cdot \cos\delta \left(\frac{x_q - x''_q}{x_q}\right) \cdot T''_{qo}$$

..... 5. 6. 4.

5. 7 NEGLECTED TERMS :-

The machine representation suitable for use in conjunction with a network analyser is possible only when $\mathcal{E}_d = 0$ i. e. if there is no interpolar excitation.

$\mathcal{E}_d$ for a normal single field winding machine is negligibly small for conditions of increase in stator current and changes in the voltage applied to the field under the action of the automatic voltage regulator. $\mathcal{E}_q$ in both these conditions is represented in the machine simulation discussed in chapter 4.

$\mathcal{E}_d$ and $\mathcal{E}_q$ arising from the slip conditions are the most difficult conditions to represent in the present simulation technique. The expressions are fairly complex and then the

simulator has no facility to represent ξ_d. The effects of these increments in excitation have been included by a constant damping coefficient as a first order correction. This coefficient is calculated from equation 5. 2. 1 due to Crary. In the opinion of the author the ommission of the satisfactory representation of these effects. · is the single major source of error in the synchronous machine simulation. The rapid braking of the rotor and higher terminal voltage, at the instant of fault clearance, compared to the test values are both caused by the inadequate representation of the damper windings. From equations 5. 6. 3 and 5. 6. 4. ξ_d and ξ_q are both negative and from the vector diagram of Fig. 5. 6 it is evident that the terminal voltage and power transfer will be lower than that calculated, when these are neglected.

Crary's formula for the damping coefficient is based on the analysis first given by Park (Ref. 52) for a machine oscillating with a small amplitude about a steady load angle and is also explained in Adkin's book. (Ref. 50) The expression for the damping coefficient is a function of axes impedances in the operational form and the trignometric functions of the load angle and is given by

$$K_d = \frac{V^2}{m}\left[\text{Real}\left\{\frac{1}{j x_d(jm)}\,\text{Sin}^2\delta + \frac{1}{j x_q(jm)}\cdot \text{Cos}^2\delta\right\}^q\right] \quad \ldots\ldots 5.7.1.$$

where $(m/2\pi)$ is the oscillation frequency.

Crary suggested neglecting the effects of the damper windings in the main stability calculations and supplementing them by means of the damping torque coefficient given above. The expressionsfor $1/x_d(p)$ and $1/x_q(p)$ are derived for an ideal machine in which the damper windings are represented by one coil on each axis. These expressions are given below.

$$\frac{1}{x_d(p)} = \frac{1}{x_d} + \left(\frac{1}{x'_d} - \frac{1}{x_d}\right)\frac{p\,T'_d}{1 + p\,T'_d} + \left(\frac{1}{x''_d} - \frac{1}{x'_d}\right)\frac{p\,T''_d}{1 + p\,T''_d} \quad \ldots 5.7.2$$

$$\frac{1}{x_q(p)} = \frac{1}{x_q} + \left(\frac{1}{x''_q} - \frac{1}{x_q}\right)\frac{p\,T''_q}{1 + p\,T''_q} \quad \ldots . 5.7.3$$

Only the last terms of the expressions given above are substituted in eq=n 5.7.1 to get,

$$K_d = V^2\left[\text{Real}\left\{\left(1/x''_d - 1/x'_d\right)\frac{T''_d}{1 + jwT''_d}\cdot \text{Sin}^2\delta + \left(1/x''_q - 1/x'_q\right)\frac{T''_q}{1 + jw\,T''_q}\,\text{Cos}^2\delta\right\}\right]$$

If now, for the low frequency in consideration, $w\,T''_d$ and wT''_q are negligible compared to 1 the formula for K_d becomes,

$$K_d = V^2 \left[\left(1/x''_d - 1/x'_d \right) T''_d \sin^2\delta + \left(1/x''_q - 1/x_q \right) T''_q \cos^2\delta \right]$$

$$= V^2 \left[\frac{x'_d - x''_d}{x''_d \cdot x'_d} T''_d \sin^2\delta + \frac{x_q - x''_q}{x''_q x_q} T''_q \cos^2\delta \right]$$

$$= V^2 \left[\frac{x'_d - x''_d}{x'^2_d} T''_{do} \sin^2\delta + \frac{x_q - x''_q}{x_q x''_q} T''_{qo} \cos^2\delta \right] \quad \ldots\ldots 5.7.3$$

If there is an external reactance between the fixed voltage supply and the machine, it should be added to the machine reactance. Treating this coefficient as a constant is true only for a linear model applicable to small oscillation conditions and is only a crude simplification for a general transient condition.

Damper windings are only represented accurately (as accurate as Park's equations) on Shackshaft's model, where the two axes equations are completely programmed on the analogue computer. This technique is not suitable for an economic extension to a multimachine system. The unsaturated transient and sub-transient reactances and time constants used in this model were obtained from the short circuit test and all other parameters were calculated from these tests. The amortisseur resistance obtained from the sub-transient time constant was reduced by a factor of four. This constant amortisseur resistance in Shackshaft's opinion was still unsatisfactory because the resistance of the damper current paths

depends on the depth of penetration which in fact is frequency dependent. Some parameters of the voltage regulator circuits were also adjusted so as to get the results of the step increase in reference voltage on the model closest to the test results.

The inadequacy of the Park's theory, which assumes no saturation in the magnetic material and the damping current paths consisting of finite number of discreet circuits, for the calculation of the damping action was pointed out by Bharali and Adkins. (Ref.13) For steam turbo-alternator using solid iron rotor the eddy currents are distributed and need an infinite number of coils for accurate representation. The saturation in some locations may be very high and cause a considerable change in the values of reactances. Suggestions were made to modify the expressions for operational impedances as derived for an ideal machine to take in to account the distributed nature of the rotor currents. The saturation of the rotor magnetic paths cannot exactly be accounted for and the solution for the impedances of the damper windings are obtained assuming constant permeability which could be taken as complex to take hysterisis into account or a rectangular approximation to the B - H curve to allow for saturation. Bharali derived an expression for damping coefficient based on Crary's method but modified to take the frequency dependent nature of the damper impedances. Strictly speaking this coefficient can still only be used for problems

of small oscillations. The inaccuracies in calculations for general transient conditions arise on the following two accounts.

1. The damping coefficient cannot be treated as constant.

2. Neglecting damper windings in the main stability calculations and then working out damping power by using a constant coefficient gives incorrect machine terminal and network conditions. The damping power infact flcws from the terminals of the machine in to the positive sequence network. The damping under slip conditions can be correctly handled only by calculating the incremental excitation as explained in section 5.6.

Humpage and Saha (Ref. 31) used the techniques explained by Bharali and Adkins by varying parameters representing the solid rotor damping current paths in the main stability calculations. Equations for the system are the same as for Shackshaft's model. This technique of varying the machine parameters can be used only on digtal computers. The swing curve obtained by Humpage and Saha for the Goldington 30 MW generator is very close to the test results. In their model voltage regulator parameters and the governor parameters are different from those used by Shackshaft and therfore the benefits of these laborious techniques of varying the parameters in the swing curve calculation are not very evident.

The simulating techniques discussed in chapter 4

they
suffer from the limitation that it cannot represent the interpolar excitation ξ_d. Also the formulae for the calculation of ξ_d and ξ_q during the slip conditions are very complicated. A function generator giving the asynchronous torque corresponding to slip values may be used. This seems the only way out. The asynchronous torque characteristics should be experimentally obtained for each generator. This characteristic is non-linear and it is found that for low values of slip the damping torque coefficient could be as high as 100 or 250 compared to that calculated from Crary's formula which lies between 3 and 25 depending upon the tie line reactance. The pessimistic recovery conditions in the swing curve for the Goldington machine (fig: 5. 2) calculated with a constant damping coefficient is also explained from the assynchronous torque characteristic.

This proposal will find some criticism on the account that the asynchronous torque found on the basis of constant slip is different from the general transient condition when the rotor does not slip past the pair of poles and the flux in the rotor does not reverse. The difference is made because of the skin effect of the rotor currents under constant slip conditions.

5. 8 OTHER NEGLECTED TERMS:-

(a)ASYMMETRIC CURRENTS:-

In the discussion of section 5. 4 through 5. 6 the incremental excitation terms due to

the transformer induced emf's were found small in magnitude as these terms contain wT'_{do} and $w\,T'_{qo}$ in the denominators and decay exponentially. These terms give rise to asymmetric components in the armature current and these components cause braking of the rotor. In the case of faults which are not close to the machine terminals these components decay so fast as to cause negligible error in the transient swing curve calculaions. In the case of faults directly on the terminals of the machine these components persist long enough to cause an appreciable slowing down of the initial rotor acceleration. If the machine is initially lightly loaded but is supplying a large amount of reactive power the braking torque may be higher than the accelerating torque and the machine may swing backwards before δ starts to increase.

The asymmetric components of the armature currents induce in the rotor currents of fundamental frequency which give rise to the braking torque. This torque can be approximately included by the method of Kimbark (Ref. 54) using an equivalent induction motor circuit. The braking power is given by

$$P_b = i^2_{d.c.} (r_2 - r_1)$$

where r_2 is the negative sequence resistance

and r_1 is the positive sequence resistance.

$i_{d.c.}$ is the instantaneous value of the direct current in one phase when the switching angles are such as to give this phase the maximum asymmetry. The asymmetrical component decays

exponentially with the armature time constant $x_a / w r_a$.

The Goldington machine swing curve calculations with 0.8 p.u. power and 0.6 p.u. reactive power were repeated with the braking torque included but showed no difference from the one calculated without including the braking torque, but using a a constant damping coefficient. If the machine has an initial load of 0.2 pu but the reactive power level is kept the same the machine showed a back swing initially. The back swing can be appreciable if the machine has a lower inertia constant.

The simulator does not include the braking torque and it can only be included with considerable expense.

(b) SATURATION :-

The synchronous machine theory discussed in chapters 2 and 4 and the simulator developed from that, neglect saturation. When saturation is considered even the validity of Park's theory becomes doubtful and the concept of constant reactance becomes invalid. If one is concer ned with the fundamental components of the voltages and currents only, a value of reactance does exist which gives the correct relationship between the total excitation on the rotor and the terminal voltage and armature currents under consideration. Methods have been devised to include approximately the effect of saturation within

the realm of Park's theory. These methods are suitable only for use on digital computers and at considerable expense for a pure analogue computer study. It is generally assumed that all the leakage fluxes are independent of the state of iron and that they donot contribute to the iron saturation. It is also assumed that the saturation is independent of the apportioning of the excitation between the main field winding and the damper windings. The saturation is, therefore, mainly determined from the mutual flux. The magnetising reactances x_{md} and x_{mq} are multiplied by a single factor k which is a ratio of unsaturated reluctance to the saturated reluctance of the flux path. This factor is determined conveniently from the open circuit characteristics of the generator. (Ref. 17)

Humpage and Saha (Ref 31) used an 8th order polynomial as the best fit to the O. C. C. for determining this factor and varied the reactances at each step of the stability calculations.

The assumption of leakage fluxes being independent of the state of iron is a weak one because some components of the leakage flux like slot leakages, tooth top and differential leakage have iron paths. Only the end winding leakage has no iron path. The subject of saturation requires furthur investigations, though for a first order correction a single factor for magnetising reactance on the two axes is adequate for most studies. For some faults like

three phase short circuit the main air gap flux in fact falls and, therefore, correcting the reactances for saturation is not so important.

In a synchronous machine simulator to be used in conjunction with the network analyser, it is necessary to use a constant reactance for the machine. In this case the values of reactances have to be shaded according to the problem at hand.

CHAPTER 6

CONCLUSIONS

This chapter opens with a summary of the novel and important features of the simulator described in this thesis, which in the author's opinion represent worth-while improvements over those described in the literature and discussed in section 1.5.5.

Central to the design of the simulator is a direct impedance analyser drawing its power directly from the laboratory A.C. mains. The magslip and I-pot combination conventionally used for representing a generator on the network analyser has been retained. The base values of voltage and current on the analyser are so chosen to make the magslip and I-pot leakage impedance very small compared to the per unit impedance. The amount of special purpose equipment is kept to a minimum since by operating the network analyser at mains frequency, the need for highly stabilised oscillators and power amplifiers is eliminated. Also, because of the low value of the chosen base current, buffer amplifiers are not needed, and the core size of each reactance unit of the analyser is small and has a low cost.

Distortion in the current wave-form is lower than in conjugate analysers and the phase relationship will have

the same sense as in the actual power system. The load increase on the generators will be met by advancing the rotors, as in the actual system, whereas in the conjugate impedance analyser rotors have to be retarded to do this. Coupled with the real time simulation of the machine dynamics, the frequency dependent nature of the loads and the damping caused by the transmission network are correctly represented.

For solving the transient stability problem the machine equations are simplified to allow the machine to be represented by a voltage source variable in phase and magnitude behind a constant reactance. Analogue computing elements are used to compute the rotor speed deviation from the steady synchronous speed and the magnitude of the source voltage, and these quantities are followed by the magslip and I-pot respectively by means of servo-mechanisms to which they are coupled.

The analyser quantities, voltage, current components, power and phase angles are converted to proportional D. C. voltages. The instrumentation is wholly electronic and can respond to transient changes in 20 m-secs. The accuracy is better than 1 %. Being D. C., the outputs from these circuits are suitable for direct use with the analogue computer and pen recorders. Furthur-more the information can be fed to a process control digital computer through an analogue to digital convertor.

The D. C. servomechanisms coupled to the magslip and I-pot combination have very high follow up accuracy and very fast speed of response and have an extra merit that the phase modulation is continuous. This system is also able to represent a permanent change in frequency. The synchronous machine simulator consisting of constant voltage behind direct axis transient reactance described in chapter 2 of this thesis can work in real time with the overall accuracy of the rotor swing better than 3 %.

An I-pot position control servo-mechanism has the merit of being simple compared to the electronic modulators. Again, most of the modulation techniques introduce distortion, and circuits have to be carefully designed and in some cases frequency selective filters have to be used. With the I-pot servomechanism technique no distortion is introduced. Unfortunately the response time is slow and cannot follow step changes in voltage fast enough to give good accuracy of the rotor swing computation, when working in real time. However, when the simulator time is scaled down the synchronous machine simulator, with transient saliency, changing flux linkages with the field circuit under AVR action and governor action included, can solve the transient equations with an accuracy which in most cases is better than 3 % .

The simulator gives the physical feel of the dynamics of the power system and a visual display of the rotor swing is obtained with graduated dials mounted on the magslip and the

I-pot shafts. Thus the major objectives listed in section 1.4 have been achieved.

The following sections contain a summary of discussions and findings arising out of this thesis (6.1), suggestions for improvements and further work (6.2.) and other uses of the simulator (6.3).

6. 1 SUMMARY OF DISCUSSIONS AND CONCLUSIONS:

Because of the ease and cleanliness with which the electrical energy can be transported and converted into a serviceable form where-ever needed, the consumption of energy in the electrical form has increased many fold in the recent past. Recent discoveries, inventions and engineering applications have made electricity continually of greater use to mankind. It is also due to their economic soundness that we have seen enormous growth of power systems.

With this growth, problems of secure and economic operation have also increased. A quote from a recent I. E. E. Colloquium on system control can well serve to emphasise the need for more economic operation of the system; " A 98. 5 % optimum running of the C. E. G. B. system means £ 6 million annually wasted. "

Need for a nationally co-ordinated load scheduling programme and better and faster plant controllers is giving rise to new control philosophies. Automation up to various degrees is already being used at all levels of operation. This is in the form of

pro cessing such information as security checks and future load prediction which is impossible without computational aides; automatic frequency control to relieve the operator of frequent valve and governor settings, and in the case of large modern generators where the safety and efficiency of the plant requires numerous points to be continuously monitored and a very strict schedule of starting and shutting down to keep the thermal stresses with in the safe limits. The next decade should see a fully integrated scheme of control using process control computers.

To make the new investments on control equipment more economic, need also arises to determine the operational limits and constraints more accurately. With more integrated control of turbine, generator and auxilliaries, the increase or decrease of the load may be achieved more rapidly. This would cause revision of the allocations of spinning reserves. Operators may only need to guide the control action of the computers.

A laboratory trial of a new control scheme may give useful information to designers and experience to the system operators. A system model or a simulator is needed for this purpose, where all parts of the system are adequately represented.

Of course, the more realistic modelling technique available is one using micro-synchronous machines, lumped constants for transmission lines, and specially designed induction motors. The machine as well as the auxilliaries are very expensive and in a

multi-machine system, because of the power level involved, tests under fault conditions are quite hazardous.

Once the behaviour of any system has been expressed in the form of mathematical equations, computational aides can be employed to simulate the system. A network analyser is very useful in giving a physical feel of the network behaviour and offers economy and flexibility of simulation. The behviour of the auxiliaries is, in most cases, described in the form of transfer functional blocks. An analogue computer is admirably suited to simulate these blocks.

A coupling unit between the network analyser and analogue computer is a combination of the servo driven Magslip and I-pot and provides a source of voltage which can be varied in phase and magnitude independently. The D. C. servo-mechanisms can be driven directly by the signals from the analogue computer and the network quantities have to be converted into proportional D. C. quantities.

The parallel nature of the analogue computational elements allows the simulator to work on the real time base. On the contrary, a digital computer has a serial nature and expensive interface equipment is required to feed the analyser quantities to the computer. Again, the digital computer output has to be converted into the analogue form to drive the servo.

The synchronous machine is the most important for

any power system study and, of course, for generation this is almost the only type of the machine used. Studies have, therefore, been concentrated on simulating synchronous machines and the associated regulating and governing systems.

Park's equations for the synchronous machine are complete and describe the machine performance in all modes of operation. Park's mathematical model requires vast and complex calculations. The equations are written in the form of a set of reference axes which are the rotor direct and quadrature axes. For a multi-machine system, a common reference for all the machines is required. The network equations are also transformed to the axes form. To obtain such quantities as phase voltages and currents inverse transformation has to be applied.

With some simplifications, Park's model has been converted in to the form of a voltage, variable in phase and magnitude behind a constant reactance. This mathematical model is then directly applicable to a network analyser. The phase of the voltage behind the reactance also defines the rotor position with respect to the system reference. A graduated dial has been mounted on the shaft of the magslip and gives a visual indication of the rotor swing during the disturbances.

The network analyser works at the mains frequency and is of the direct impedance type. High Q-inductors have been designed

which can be used for machine reactance and transformer leakage reactance.

As a starting point, a single machine connected through two reactive tie lines to an infinite system was considered. Loss of one line with or without subsequent reclosure was considered as a transient disturbance on the system. A Simulator using a constant voltage behind constant reactance (x'_d) as the model, uses a simple and minimum of analogue elements. The power output in this case is proportional to the component of current in phase with the voltage. A simple watt-meter was developed which can measure this component and can respond to a step change in 20 m-secs.

The analogue computer gives a signal proportional to the deviation in the rotor speed following a disturbance. A velodyne system with high follow up accuracy and speed of response and capable of simulating all practical values of the inertia constant has been developed to drive the magslip. This basic form of the simulator can work in the real time.

Neglecting the effects of the damper windings in the main stability calculations, the simulator was extended to include effects of transient saliency, varying field flux linkages and actions of automatic voltage regulators and governor. To correct for neglecting the damper windings, a damping coefficient is used, i.e the differential torques on the shaft are reduced by an amount proportional to the deviation from the steady synchronous speed

of the rotor. The synchronous machine simulator now consists of a voltage behind quadrature axis synchronous reactance. The voltage behind this reactance is computed from the direct axis flux linkages and the direct axis component of the armature current. Solution of the equations connecting these quantities is only achieved through a process which is iterative but convergent. The voltage magnitude is varied with an I-pot in a position control servo-loop. The inherent delay in the servomechanism coupled with the iterative nature of the equations produced large errors in the swing curve when there were step changes in the armature current. The simulator time was then scaled down to achieve good accuracy.

Simple AVR and governor loops were considered and the analogue computer provides a great flexibility in simulating more complex control loops.

Various refinements in the simulator were added at various stages and the accuracy of the simulator was checked by solving the equations on IBM 7090/7094 digital computer. The simulator showed in most cases the error to be below 3 %.

The mathematical model on which the simulator is based has also been used by many recent digital computer programmers for the solution of the power system stability problems. Wide differences are seen in the opinions expressed by

different workers about the validity of the mathematical model. Test data on the 30 MW Goldington Generator was used to compute the swing curves following a short circuit on the H. T. side of the transformer. A large discrepancy was found in the machine recovery characteristics, though a good agreement was achieved during the first swing. With the help of synchronous machine analysis, complete with the damper windings, it is seen that the biggest single cause of this large discrepancy in the recovery characteristics is the poor representation of the effect of the damper currents in the solid rotor of the generator.

The damping torque is a non-linear function of the slip and the only simple way to correctly include this is to use a function generator simulating the torque slip characteristic, which is experimentally determined. There is, however, a need for many more full scale tests to ascertain the degree of correction achieved in the recovery characteristics.

6.2 SUGGESTIONS FOR IMPROVEMENTS AND FURTHUR WORK

In the following sections, inadequacies of the mathematical model for simulating the damping characteristics have been discussed and some suggestions made for improvements.

To enable the simulator to work on the real time base, replacement of the I-pot servo-mechanism by an electronic amplitude modulator is suggested.

Suggestions for the extension of the simulator and

representation of the loads have been made.

6. 2. 1 DAMPING CHARACTERISTICS :-

The inadequacy of including the effect of damping circuits on the rotor has been discussed in terms of a steady state vector diagram (see chapter 5) and incremental excitation during the disturbances. For a conventional machine having a single field winding on the rotor, the incremental excitation in the interpolar axis is usually small for increases in armature currents and field voltage. Under slip conditions, the currents in the damper winding or in the solid rotor are important in changing the flux conditions in both the axes. The simulator in its present form is not capable of representing changes in the excitation in the Q-axis . The expression for incremental excitation under slip conditions rise very complex. Because the sub-transient parameters are dependent on the physical dimensions of the rotor and also the pattern and depth of penetration of flux, even these complex expressions cannot be used to determine the damping accurately.

The only simple way to approximate the damping characteristics seemsto be,to determine the torque-slip characteristic experimentally, and to use the function generator to simulate this.

Investigation to calculate this characteristic approximately from the machine data available from the conventional test will then be a desirable step. Suitability of this method can

can only be judged from a number of full scale tests and comparison with the simulator results.

6. 2. 2 SUBSTITUTION OF ELECTRONIC AMPLITUDE MODULATOR FOR I-POT SERVO :-

The settings in the voltage magnitude in the simulator are made by an I-pot position control servomechanism. The response time for the mechanism with critical damping is 80 m-secs. The system is suitable for following up changes in the voltage required to simulate the effects of the flux decay, or flux build up due to AVR action, but introduces considerable error in the swing curve computation following step changes in armature currents caused by short circuits. A mention of this has been made in the previous section as well. The simulator time was slowed down on this account.

For investigating some control schemes where a process computer provides an overall control and is used to detect the faults and is programmed to take all the necessary correcting operations, the real time solution is a desirable feature. Generators nearest to the fault have to be provided with a fast responding voltage magnitude setting system.

A fully electronic modulator will be a suitable device. An heptode valve is conventionally used for this purpose, in which the mutual conductance (g_m) of the valve is controlled

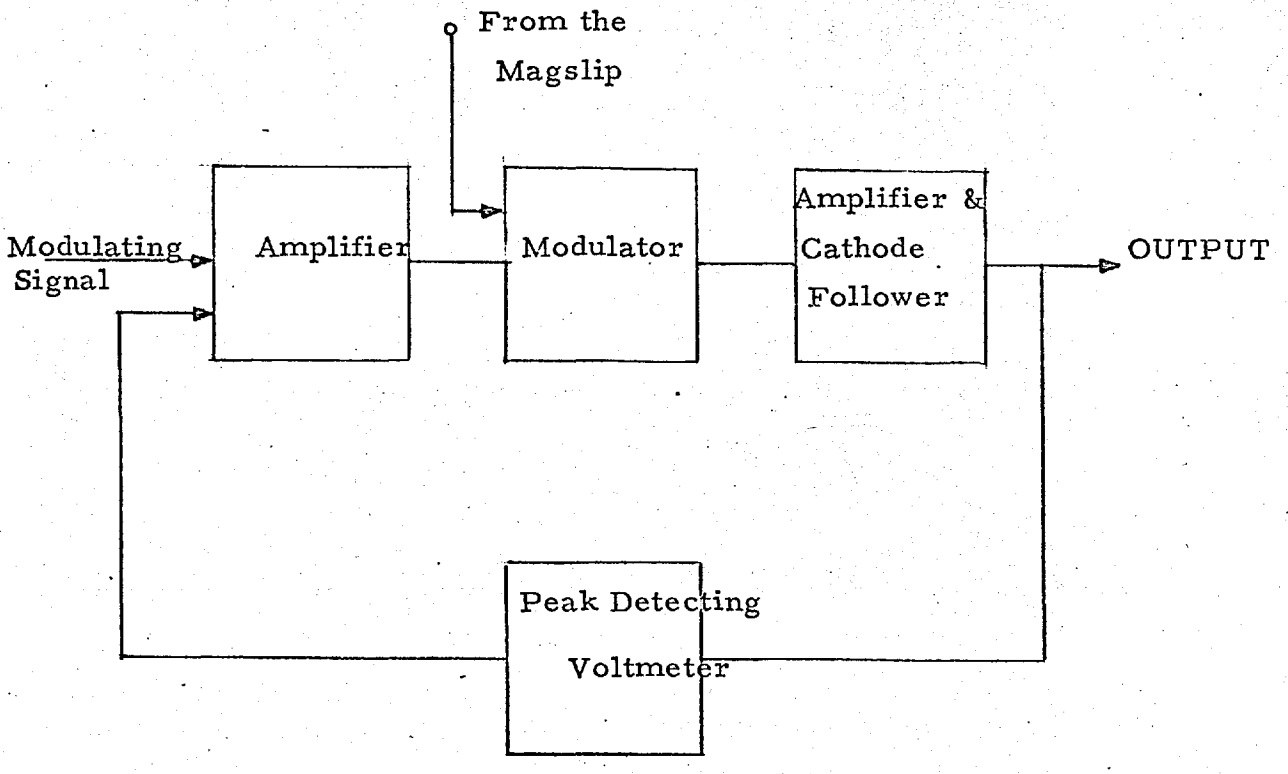

FIG : 6.1

SCHEMATIC OF ELECTRONIC

AMPLITUDE MODULATOR

by a signal on grid 3 and the wave to be modulated is applied to the normal grid. To minimise the effects of the non-linearities in the valve characteristics a modulating circuit is used in a feed back arrangement as shown in fig. 6.1 . The gain in the forward path should be as high as possible consistent with the stability requirements. If the distortion is still higher than 2 %, frequency selective circuits should be used in the plate circuit of the amplifier. These filters should be damped to avoide self-oscillations.

The modulating signal is obtained from the analogue computer in the same way as has been described in sections 4.1 , 4.2 and 4.3.

6.2.3 EXTENSIONS :-

After the damping characteristics have been correctly represented, the simulator should be extended to include more generator units to form a sub-system with one or two tie lines connecting it to the rest of the system. The merits of carrying out stability studies by simulation techniques will be more evident when comparison is made with a similar study on a digital computer. Organization of the system data and the programme, computational time and the training required for the development and the use of the computer programme should be compared with the relevent aspects of the simulator study.

Interconnection of the sub-system with the rest

can then be made to simulate the power-frequency characteristics of the system. This would require a generator unit which simply represents the governor droop and a time constant. Effect of controlling the power flow on the interconnection can then be studied.

6. 2. 4 LOAD REPRESENTATIONS :-

The next step in the power system simulation is to represent the local loads in the sub-system more accurately. Loads can have a profound effect on the damping of the system oscillations.

Synchronous motors are often a very small proportion of the total load but wherever there is a concentration of synchronous motors, these can be represented in exactly the same manner as the synchronous generators.

Loads of large metropolitan areas are of mixed type and exact information about the voltage and load characteristics can be obtained only by actual tests.

Three types of representations are often used during the stability study.

1. Constant Impedance.
2. Constant Power (Active & Reactive)
3. Constant Current (Active & Reactive Component

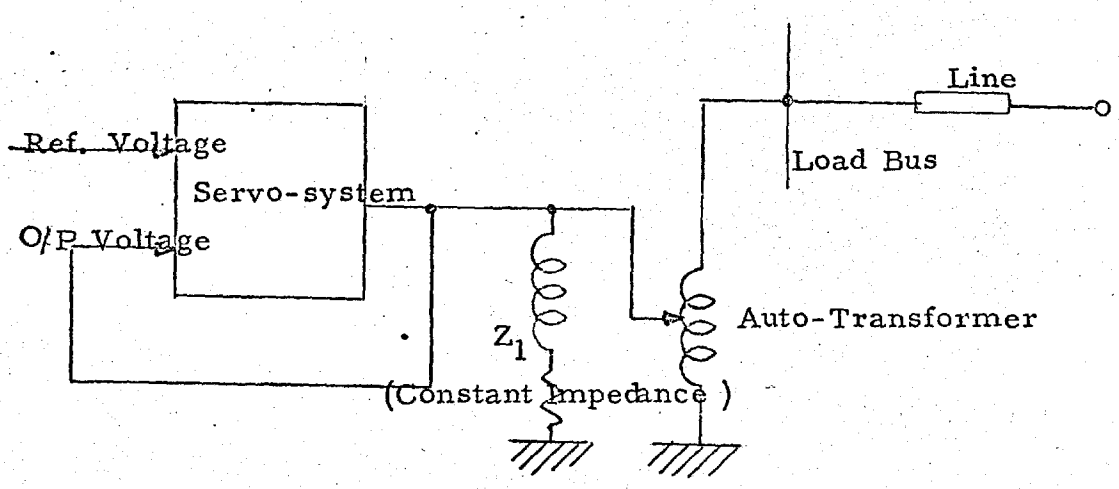

(a)

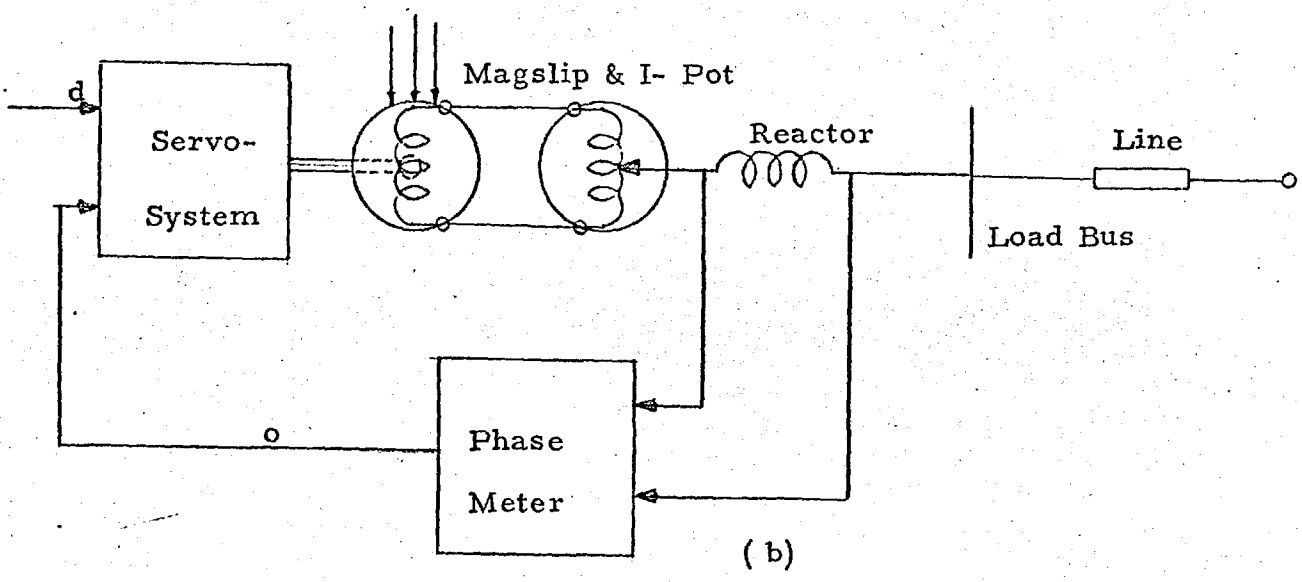

(b)

FIG : 6.2

(a) CONSTANT POWER

(b) CONSTANT CURRENT

The first method is the easiest to represent on the network analyser but gives very optimistic results as the power and reactive power both vary as the square of the voltage at the load bus.

The second method gives pessimistic results and absurd if the fault is near to the load bus. An auto-transformer of low losses can be used to keep the voltage across an impedance constant as shown in fig. 6.2. (a) . This method of representation can be used to achieve an initial power balance.

The third method of representation is the most realistic as the results of a few tests carried out show that active and reactive loads vary in direct proportion to the voltage. To achieve this automatically in the simulator , a high Q-inductor can be connected between the load bus and the generator unit (magslip and I-pot combination) and the phase angle difference between the voltages at the two ends can be kept constant by a servomechanism. The power $\frac{V_b \cdot V_1}{x} \cdot \sin \delta$ and reactive power $\frac{V_b \cdot V_1}{x} \cos \delta$ will vary as V_1 varies, as long as δ , the phase angle of the voltage across the load reactance, is kept constant by the servo-system.

If the load characteristics are known to follow any other law, function generators are needed to compute the

variation in V_b and δ to give the required values for P & Q.

6. 2. 5 INDUCTION MOTORS :-

Recently, large concentrations of induction motor loads, in the form of pumps in the oil fields and centrifugal plants in the nuclear fuel refining process, have appeared at certain points on the power systems.

Westinghouse engineers were the first to develop a method for including the induction motor transients in the system stability studies and this has been reported by Shankle and associates. (Ref. 23)

Theoretical developments of this method are not very rigorous (see discussion by Concordia on Ref. 23) and final equations for the induction motor transients are based on purely physical considerations.

Brereton, Lewis and Young (Ref. 82) have assembled and evaluated three different methods of representing induction motors and is an excellent reference work. A more recent paper by Lawrence and Stephenson (Ref. 83) contains a comprehensive bibliography of the studies in induction motor transients and covers various types of disturbances. The paper is primarily concerned with the transient characteristics of the induction motors, and many details are irrelevent when the significant effects of the induction motor loads are on the overall transient stability of the system are being studied.

In most system stability studies the transmission line network is considered to be in the steady state as also are the loads. It is also generally assumed that the frequency deviations are slow and the rotating machinery is capable of following these changes. With these assumptions accepted for the system in general, the stator electrical transients can be neglected when induction motors are included in a system stability study.

The effect of the stator transients is to produce a D. C. offset in the stator currents and fluxes when sudden disturbances take place in the stator circuits. The stator direct current and fluxes interacting with the rotor slip frequency currents produce pulsating torques near fundamental frequency and an average torque proportional to i^2. r losses is produced by the D. C. stator currents. The effect of these, as far as stability analysis is concerned, is usually minor.

(a) Representing Mechanical Transients only:-

The value of the ratio of the rotor time constant is, in certain cases, very small. In these cases, the induction motor representation is used to include only the mechanical transients. Also, in those cases where the motors are not completely interrupted from the supply, the rotor mechanical transients may alone be included.

When the short circuit or the open circuit comp-

lately interrupts the supply, both electrical and mechanical transients of the rotor should be included. Brereton's paper shows some guide lines when the motor and system parameters require the rotor electrical transients to be included.

When both the rotor and stator electrical transients can be neglected; the behaviour of the induction motor can be analysed using the familiar steady state equivalent circuit (fig. 6. 3) with the appropriate value of the reactance, resistance and slip. After the disturbance has been initiated the rotor resistive branch in the equivalent circuit has to be continuously adjusted. The power in this branch gives a measure of electrical torque developed by the motor. The difference between the load torque and the mechanical torque developed by the motor can be used to calculate the rotor slip but since the terminal voltage is also slipping the actual slip is obtained after subtracting the average system slip.

This simple representation will also require a considerable number of analogue computing elements.

The load characteristics are such that with the variation in slip the load torque will vary and therefore, a function generator is needed.

The electrical torque can be obtained by measuring power in the equivalent rotor resistance.

The difference between the load torque and the electrical torque has to be integrated and scaled for the inertia

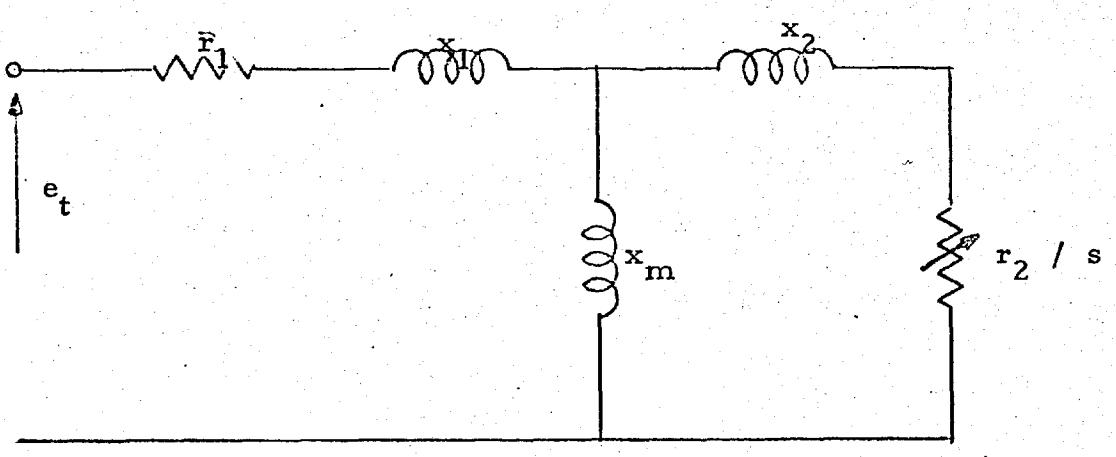

FIG : 6.3

INDUCTION MOTOR EQUIVALENT CIRCUIT

constant. This will give the nominal slip of the rotor.

The system slip has to be measured at the terminals of the induction motor equivalent circuit to obtain the actual slip. Since the frequency deviation is small, the phase difference of the terminal voltage has to be measured with respect to a fixed reference and differentiated to get the frequency deviation.

To compute (r_2 / s), a fuction generator is needed and to make this adjustment automatic a servo-mechanism is needed with two potentiometers ganged together. One of these will form the equivalent rotor resistance and the other will be needed for the feed back signal in the servo-mechanism.

If the simulator is working in real time the variations in the reactive branches of the equivalent circuit will also be an improvement in the induction motor simulator.

(b) Representing Rotor Mechanical and Electrical Transients :-

Induction motor transient equations neglecting the stator transients have been developed by Concordia (see discussion on Ref. 23) and Brereton. (Ref. 82)
The derivation is rigorous and the starting point is the idealised induction motor's differential equations referred to the synchronously rotating axes. The equations are;

$$\frac{d\vec{e'}}{dt} = -\frac{1}{T'_{do}} (\vec{e'} - j(x - x') \vec{i_1}) + j \vec{e'} (\omega - w)$$

$$\vec{i}_1 = \frac{\vec{e}_t - \vec{e'}}{(r_1 + j x')}$$

$$T_e = \vec{e'} \cdot \vec{i}_1$$

where

$\vec{e'}$ = Complex voltage proportional to rotor flux linkages (p. u.)

$\vec{i}_1$ = Complex stator current (p. u.)

$\vec{e}_t$ = Complex terminal voltage (p. u.)

$(\omega - w)$ = Negative of the rotor slip (rad/sec)

x = Open circuit reactance of the motor (p. u.)

x' = Blocked rotor reactance of the motor (p. u.)

T'_{do} = Open circuit time constant (sec)

On the network analyser the correct conditions of current and power are obtained by the equivalent network of fig. 6.4. The equivalent circuit is similar to that of a synchronous machine, except that the position of the vector e' is modified by the slip.

The electrical torque following the disturbance can be obtained by measurement with an electronic wattmeter and the nominal rotor slip determined from the difference in load torque and the motor electrical torque, but the change in e' (complex voltage proportional to the rotor flux linkages) seems almost impossible to compute on the analogue computer. A step-by-step method

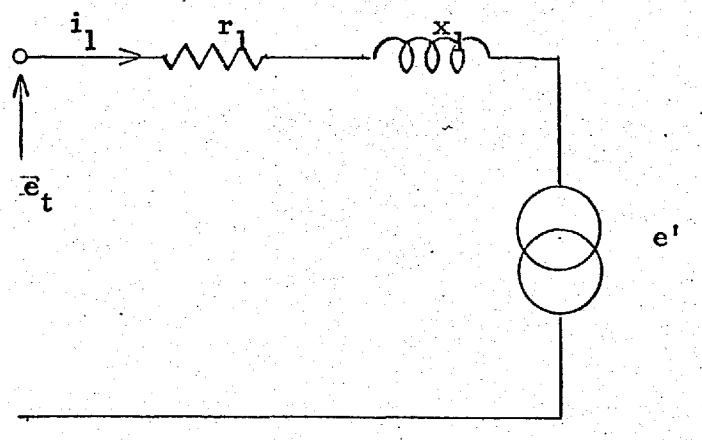

FIG: 6.4

INDUCTION MOTOR EQUIVALENT CIRCUIT

INCLUDING ROTOR ELECTRICAL TRANSIENTS

by Brereton (Ref. 23) could be easily adapted for use on a small digital computer. A digital computer can be supplied with information concerning the electrical torque, the resolved components of the terminal voltage with respect to $\vec{e}'$, and the rotor nomial slip from the network anlyser and the analogue computer, while the digital computer will process the change in e' which can be set by servomechanisms. These computations can be repeated once in 20 m-secs and will give an accuracy of better than 2 %.

6. 3. OTHER USES OF THE SIMULATOR : -

The simulator can be effectively utilized as a teaching and training aid, as a self balancing load flow analyser, and as a dynamic security assessor.

6. 3. 1 TEACHING AND TRAINING AID :-

With the aid of the simulator some fundamentals of power system stability analysis can be readily illustrated eg. elementary equations of power transfer, equal area criterion of stability and the action of the automatic voltage regulators in improving the machine transient stability limit.

With a display system and a control desk added to the system the simulator can be used as a training aid in load despatching and maintaining the frequency and the voltages. The development of the load units described in section 6. 2. 4 is only

to represent variations in load due to changes of the voltage on the load bus bar immediately following a disturbance, but when experiments on control have to be carried out load units similar to those discussed in Bain's model (Ref. 47) have to be developed in which the loads can vary according to a daily demand pattern.

6. 3. 2 SELF BALANCING LOAD FLOW ANALYSER ;-

For the load flow studies, the loads are represented following the method shown in fig. 6.2 (a), where a fixed impedance is connected between the auto-transformer wiper and the neutral bus, and the voltage reference settings are given to the servo for required P & Q . During the balancing period the servo-mechanisms will keep the load constant. Other known data is generation at some points which can be set as a D. C. level on the potentiometers in the generator simulators. If the generator terminal voltage is specified this could also be set on a potentiometer, but if this is not specified in the problem normal rated voltage can be set. The simulator can then be allowed to run as for the normal stability study. The unknown generation on some sets will take up the desired value to satisfy the demanded load.

During the period of self balancing the damping coefficients should be kept high to avoid the instability.

6. 3. 3 DYNAMIC SECURITY ASSESSOR :-

As mentioned in section 1. 3. 1 system security assessment is one of the tasks performed at the national control centre. Because of the complexity and the computer time required power flow over the supergrid network is obtained by solving the D. C. equivalent of A. C. network equations. Loss of one single or double circuit line is considered in estimating a new power flow pattern. Appropriate steps are taken if this loss will cause any line to be overloaded.

This method is serving C. E. G. B. very well because the transmission distances are not very large and the load density is such that synchronous instability is rarely heard of. Where the transmission distances are long and if the generating stations are not connected together through heavy load centres the disturbances in one part of the system can travel to other parts and can cause low frequency oscillations ultimately causing loss of some more lines.

In such cases, the simulator can be utilized as a security assessor. After the computer has predicted the load demand some hours ahead and allocated the generation for all sets in the system, this schedule can be used to set the initial conditions of power flow in the simulator. The voltages at the generator busses can be set as the normal rated values. The initial load balance will be achieved as described in the previous section.

The computer generally disregards the VAR flow and the voltage levels which can be readily checked on the simulator after the initial balance has been achieved.

The behaviour of the system following various types of disturbances such as short circuits, loss of line, or loss of generator can then be studied. If the system shows any instability, changes in the network configuration or the reallocation of the generation can be estimated and the studies follo ing the faults repeated. When a satisfactory pattern is achieved, the constraints in the computer can be changed for secure allocation and the computer will then control the out-put of the individual generating sets.

APPENDIX I

DEFINITIONS :

The Amplifier performance figures used in section 3.1.2 are defined from a black box representation of the differential amplifier (fig. i) and are as follows,

$$\text{Differential Mode Gain} = \frac{e_2 - e_2'}{e_1 - e_1'}$$

$$\text{Common Mode Gain} = \frac{e_2 + e_2'}{e_1 + e_1'}$$

$$\text{Inversion Gain} = \frac{e_2 - e_2'}{(e_1 + e_1')}$$

$$\text{Rejection Ratio} = \frac{\text{Differential Gain}}{\text{Inversion Gain}}$$

PERFORMANCE OF A SINGLE STAGE LONG TAIL PAIR DIFFERENTIAL AMPLIFIER :

The basic circuit is shown in fig. ii.

The equivalent circuit for a small signal input s is shown in fig iii.

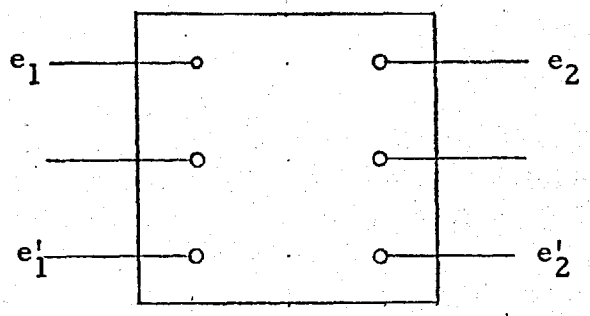

FIG: i DIFFERENTIAL AMPLIFIER AS A BLACK BOX

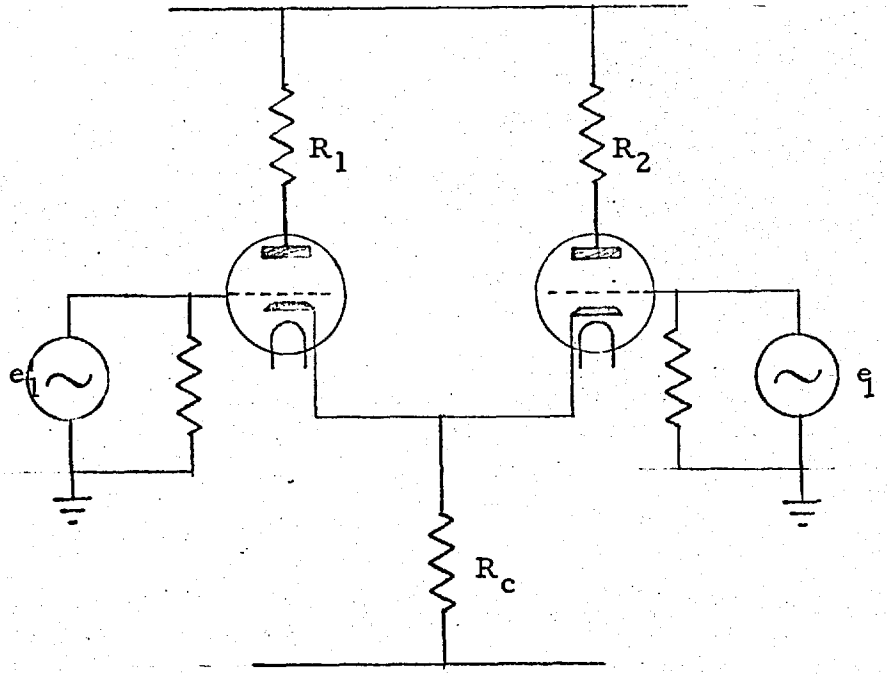

FIG (ii) SINGLE STAGE CATHODE COUPLED LONG TAIL PAIR

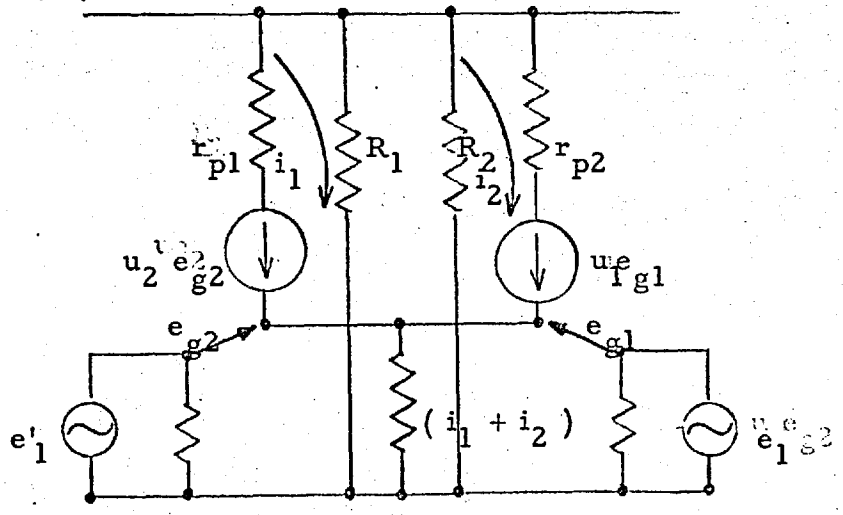

FIG : (iii) EQUIVALENT CIRCUIT

The following loop equations can be written from the equivalent ccircuit.

$$e_{g1} = e_1 - (i_{b1} + i_{b2}) R_c \quad \ldots\ldots (i)$$

$$e'_{g1} = e'_1 - (i_{b1} + i_{b2}) R_c \ldots\ldots\ldots (ii)$$

$$\mu e_{g1} = i_{b1} (r_{p1} + R_1 + R_c) + i_{b2} R_c \ldots iii$$

$$\mu e_{g2} = i_{b1} R_c + (r_{p2} + R_2 + R_c) i_{b2} \ldots iv$$

Substituting in eq=ns iii and iv the values of e_{g1} and e_{g2} from eq=ns i & ii .

$$\mu_1 e_1 - \mu_1 (i_{b1} + i_{b2}) R_c = i_{b1} (r_{p1} + R_1 + R_c) + i_{b2} R_c \quad \ldots\ldots\ldots v$$

$$\mu_1 e'_1 - \mu_2 (i_{b1} + i_{b2}) R_c = i_{b1} R_c + (r_{p2} + R_2 + R_c) i_{b2} \quad \ldots\ldots\ldots vi$$

Eq=ns v & vi can be written in the matrix form

$$\begin{bmatrix} \mu_1 e_1 \\ \mu_2 e'_1 \end{bmatrix} = \begin{bmatrix} r_{p1} + R_1 + (1+\mu_1) R_c & (1+\mu_1) R_c \\ (1+\mu_2) R_c & r_{p2} + R_2 + (1+\mu_2) R_c \end{bmatrix} \times \begin{bmatrix} i_{b1} \\ i_{b2} \end{bmatrix}$$

$$i_{b1} = \frac{\begin{vmatrix} \mu_1 e_1 & (1+\mu_1) R_c \\ \mu_2 e_1' & r_{p2} + R_2 + (1+\mu_2) R_c \end{vmatrix}}{\begin{vmatrix} r_{p1} + R_1 + (1+\mu_1) R_c & (1+\mu_1) R_c \\ (1+\mu_2) R_c & r_{p2} + R_2 + (1+\mu_2) R_c \end{vmatrix}} \quad \ldots\ldots\ldots \text{vii}$$

$$i_{b2} = \frac{\begin{vmatrix} r_{p1} + R_1 + (1+\mu_1) R_c & \mu_1 e_1 \\ (1+\mu_2) R_c & \mu_2 e_1' \end{vmatrix}}{\begin{vmatrix} r_{p1} + R_1 + (1+\mu_1) R_c & (1+\mu_1) R_c \\ (1+\mu_2) R_c & r_{p2} + R_2 + (1+\mu_2) R_c \end{vmatrix}} \quad \ldots\ldots\ldots\ldots \text{viii}$$

Denominator of (vii) & (viii) is abbreviated as D_z

$$\left| D_z \right| = \left[r_{p1} + R_1 + (1+\mu_1) R_c \right] \left[r_{p2} + R_2 + (1+\mu_2) R_c \right] - (1+\mu_1)(1+\mu_2) R_c^2$$

Consider $r_{p1} = r_{p2} = r_p$

$R_1 = R_2 = R$

$\mu_1 = \mu_2 = \mu$

for those terms containing the the sum or the product of these parameters,

$$\therefore \quad |D_z| = (r_p + R) \left[r_p + R + 2 (1 + u) R_c \right]$$

After i_{b1} and i_{b2} are known the output voltages can be very easily found,

$$e_2 = - i_{b1} R_1$$

$$e'_2 = - i_{b2} R_2$$

Now all the gain figures can be worked out.

DIFFERENTIAL MODE GAIN (BALANCED CONDITIONS)

If $e_1 = - e'_1$ and the circuit is balanced,

$$e_2 = - \frac{\mu e_1 \left[r_p + R + (1 + \mu) R_c \right] + \mu (1 + \mu) R_c e_1}{|D_z|}$$

$$= - \frac{\mu e_1 R \left[r_p + R + 2 (1 + u) R_c \right]}{|D_z|}$$

$$e'_2 = - \frac{- \mu e_1 \left[r_p + R + (1 + \mu) R_c \right] - \mu e_1 (1 + \mu) R_c}{|D_z|} . R$$

$$= - \frac{- \mu e_1 \left[r_p + R + 2 (1 + \mu) R_c \right]}{|D_z|} . R$$

$$e_2 - e'_2 = - \frac{2\mu e_1 R \left[r_p + R + 2(1+\mu) R_c \right]}{(r_p + R) \left[r_p + R + 2(1+\mu) R_c \right]}$$

$$\frac{e_2 - e'_2}{e_1 - e'_1} = - \frac{2\mu R}{r_p + R}$$

COMMON MODE GAIN : (BALANCED CONDITIONS)

If $e'_1 = e_1$

$$e_2 = \frac{- \left[\mu e_1 (r_p + R + (1+\mu) R_c) - \mu e_1 (1+\mu) R_c \right] R}{|D_z|}$$

$$e'_2 = \frac{- \left[\mu e_1 (r_p + R + (1+\mu) R_c - \mu e_1 (1+\mu) R_c \right] R}{|D_z|}$$

$$e_2 + e'_2 = \frac{- 2\mu e_1 (r_p + R) R}{(r_p + R) \left[r_p + R + 2(1+\mu) R_c \right]}$$

$$\frac{e_2 + e'_2}{e_1 + e'_1} = \frac{-\mu R}{r_p + R + 2(1+\mu) R_c}$$

This can be made very small if $R_c = \infty$

The drift in the amplifier due to poor stabilisation of of the supply rails is also minmized.

INVERSION GAIN :

$e_1' = e_1$ i.e the input is common mode, the differential mode out put will appear only when parameters μ, R and r_p for the two halves of the circuit.

$$\frac{e_2 - e_2'}{e_1 + e_1'} = \frac{-\left[\mu_1 R_1 r_{p2} - \mu_2 R_2 r_p + (\mu_1 - \mu_2)\left\{R_1 R_2 + R_c(R_1 + R_2)\right\}\right]}{(r_p + R)\left[r_p + R + 2(1+u)R_c\right]}$$

REJECTION RATIO :

$$\frac{\text{Differential Mode Gain}}{\text{Inversion Gain}} = \frac{\mu R}{(r_p + R)} \times \frac{(r_p + R)\left[r_p + R + 2(1+\mu)R_c\right]}{\mu_1 R_1 r_{p2} - \mu_2 R_2 r_{p1} + (\mu_1 - \mu_2)\left[R_1 R_2 + R_c(R_1 + R_2)\right]}$$

$$= \frac{\mu R \left[r_p + R + 2(1+\mu)R_c\right]}{\mu_1 R_1 r_{p2} - \mu_2 R_2 r_{p1} + (\mu_1 - \mu_2)\left[R_1 R_2 + R_c(R_1 + R_2)\right]}$$

$$= \frac{\mu R \left[r_p + R + 2(1+\mu)R_c\right]}{\mu_1 R_1 r_{p2} - \mu_2 R_2 r_p + (\mu_1 - \mu_2)(R^2 + R R_c)}$$

Dividing both the numerator and the denominator by R_c,

$$= \frac{\mu R \left[\frac{r_p + R}{R_c} + 2(1 + \mu) \right]}{\frac{\mu_1 R_1 r_p - u_2 R_2 r_p}{R_c} + (\mu_1 - \mu_2)(R^2 / R_c + R)}$$

If $R_c = \infty$

Rejection Ratio is

$$= \frac{2\mu R (1 + \mu)}{(\mu_1 - \mu_2) R} = \frac{2\mu (1 + \mu)}{(\mu_1 - \mu_2)}$$

$$= \frac{2\mu^2}{\Delta \mu}$$

REFERENCES

1. M. J. Short

The Conjoint use of a Network Analyser and Analogue Computer for studies of Automatic Governing and Regulating of Power Systems.

Ph. D. Thesis, University of London, 1965

2. H. E. Pulseford, P. F. Gunning

Developments in Power System Control.

Proc. I. E. E. , Vol. 114 - 1967.

3. E. D. Farmer, K. W. James, F. Moran and P. Pettit

The Development of Automatic Digital Control of a Power System from the Laboratory to a Field Installation.

I. E. E. Report on System Control Colloquium 1968.

4. P. Pettit

Digital Computer Programme for an Experimental Automatic Load Despatching System.

Proc. I. E. E. Vol. 115 -1968.

5. C. Brewer, Jennifer Frost & C. C. M. Parish

Control Room in an Experimental Load Despatching System for Power Supply Industry.

Proc. I. E. E. Vol 115, -1968.

6. E.D. Farmer

Stability and Noise Sensitivity of Digital Analogue Control System for the Automatic Loading of a Power System.

Proc. I.E.E. Vol. 115 - 1968.

7. F. Moran, D.K.S. Bain, J.S. Sohal

Development of the Equipment for the Loading of Turbo-Generators under Automatic Power System Control.

Proc. I.E.E. Vol. 115, - 1968.

8. F. Moran, D.R. Williams

Automatic Control of Power System Frequency by Machine Controllers.

Proc. I.E.E. Vol. 115 (A) -1968.

9. R. J. Alford

Micro-Machine Excitation System And Time Constant Regulator.

Imperial College Power System Report No. 49, 1963.

10. B. Adkins

Micro-Machine Studies at Imperial College.

Electrical Times, 7th July, 1960.

11. B. Adkins

System Developments by Models in U.S.S.R.

Electrical Times, 16th Jan. 1964.

12. D. B. Mehta, B. Adkins

Transient Torque and Load Angle of Synchronous Generator.

Proc. I.E.E., Vol. 107 A-1960.

13. P. Bharali, B. Adkins

Operational Impedances of Turbo-Generators with Solid Rotors.

Proc. I.E.E., Vol. 110 A , 1963.

14. A.S. Aldred and P.A. Doyle

Electronic Analogue Computer Study of Synchronous Machine Transient Stability.

Proc. I.E.E., Vol. 104 A, - 1956.

15. M. Riaz

Analogue Computer Representation of Synchronous Generators in Voltage Regulation Studies.
Trans. A. I.E.E., Vol. 75 III , - 1956.

16. Louiz V. Boffi, V. B. Haas,

Analogue Computer Representation of Alternators for Parallel Operation.
Trans. A.I.E.E., Vol 76 I , 1957.

17. G. Shackshaft

General Purpose Turbo-Alternator Model
Proc. I.E.E., Vol. 110 , -1963.

18. A. S. Aldred, G. Shackshaft

The Effect of Voltage Regulators on the Steady State and Transient Stability of Synchronous Generators.
Proc. I.E.E. Vol. 105 A , -1958.

19. A.S. Aldred

Electronic Analogue Computer Simulation of Multi-machine Power System Network.
Proc. I.E.E. Vol. 109 A , 1962.

20. J. B. Miles

Analysis of Overall Stability of Multi-machine Power System.

Proc. I. E. E., Vol. 109 A - 1962.

21. M. S. Dyrkacz, D. G. Lewis

A New Digital Transient Stability Programme

Trans. A. I. E. E., Vol. 78 III , - 1959.

22. M. S. Dyrkacz, C. C. Young, F. J. Maginniss,

A Digital Transient Stability Programme-- Including the Effect of Regulator, Exciters and Governor Response)

Trans. A. I. E. E., Vol. 79 III , - 1960.

23. D. F. Shankle, C. M. Murphy, R. W. Long , E. L. Harder

Transient Stability Studies I ---(Synchronous & Induction Machines)

Trans. A. I. E. E., Vol. 73 III , 1955.

24. C. M. Lane , R. W. Long, J. N. Powers

Transient Stability Studies II --- (Automatic Digital Computation),

Trans. A. I. E. E., Vol. 77 III , 1959.

25. R. J. Rindt, R. W. Long, R. T. Byerly

Transient Stability Studies III -- (Improved Computational Techniques)

Trans. A.I.E.E., Vol. 78 III , - 1960.

26. L. L. Freris, A. M. Sasson

Investigation of the Load Flow Problem.

Proc. I.E.E., Vol. 115 , - 1968.

27. D. W. Olive

New Techniques for the Calculation of the Dynamic Stability.

Trans. I.E.E.E. , PAS - 85 - (7)- 1966.

28. H. E. Lokay, R. L. Bolger,

Effect of Turbine- Generator Representation in System Stability Studies.

Trans. I.E.E.E., PAS -84, -- 1965.

29. K. Prabha shankar, W. Janischewsyj

Digital Simulation of Multi-machine Power System For Stability Studies.

Trans. I.E.E.E., PAS- 87, -- 1968.

30. J. E. Day, K. C. Parton

Generalised Computer Programme for Power System Analysis.

Proc. I. E. E., Vol. 112 - 1965.

31. W. D. Humpage, T. N. Saha.

Digital Computer Methods in Dynamic Response Analysis of Turbo-Generator Unit.

Proc. I. E. E., Vol. 114, 1967.

32. J. R. Mortlock

A Computer for Use in Power System Transient Stability Studies.

J. I. E. E. Vol. 25 II , -1948.

33. Watkins R. D.

The Development of Automatic Swing Curve Computer

M. Sc. Thesis, University of Manchester, -1952.

34. C. Adamson, L. Barnes , B. D. Nellist.

The Automatic Solution of Power System Swing Curve Equation.

Proc. I. E. E., Vol. 104 A , - 1957.

35. W. B. Boast, J. D. Rector

An Electronic Analogue Method for the Direct Determination of Power System Swing Curve

Trans. A. I. E. E. Vol. 70 , - 1950.

36. S. Kaneff,

A High Frequency Simulator for the Analysis of the Power System.

Proc. I. E. E., Vol. 100 II, 1953.

37. S. Kaneff

Dynamic Operation of the A. C. Network Analyser.

Proc. I. E. E., Vol. 102 A, 1955.

38. D. W. C. Shen, J. S. Packer,

Analysis of Hunting Phenomenon in Power System by means of Electrical Analogue.

Proc. I. E. E., Vol. 101 II, --1954.

39. D. W. C. Shen, S. Lisser,

An Analogue Computer for Automatic Determination of System Swing Curves.

Trans. A. I. E. E., Vol. 73 I , - 1954.

40. G. A. Bekey, F. W. Schott

Analyser Interconnection for Direct Determination of Power System Swing Curves.

Trans. A. I. E. E. , Vol. 73 I , 1954.

41. J. E. Van Ness

Synchronous Machine Analogue For Use with the Analyser.

Trans. AIEE, Vol. 73 , 1954.

42. Corless & Aldred

An Experimental Electronic Power System Simulator.

Proc. I. E. E. , Vol. 105 A , 1958.

43. J. L. Dineley

Study of Power System Transient Stability by a Combined Computer.

Proc. I. E. E., Vol. 107 III , - 1964.

44. Kusko & Heller

Computer for Automatizing Network Analyser Operation.

Trans. A. I. E. E. , Vol. 74 I , - 1955.

45. J.E. Van Ness, W.C. Peterson,

Use of Analogue Computer in Power System Studies.

Trans. A.I.E.E., Vol. 75 III, - 1956.

46. G.G. Richardson, T.C. Wane

Use of A.C. Network Analyser and Electronic Differential Analyser in the Study of Load Frequency Control.

Trans. A.I.E.E., Vol. 80 III, - 1961.

47. D.K.S. Bain,

Power System Model.

Proc. I.E.E. Vol. 114, - 1967.

48. R.E. Doherty, C.A. Nickle.

Synchronous Machines I & II

An Extension of Blondels Two Reaction Theory--

Steady State Power Angle Characteristic.

Trans. A.I.E.E., Vol. 45, 1926.

49. R.E. Doherty & C.A. Nickle

Synchronous Machine III

Torque - Angle Characteristic Under Transient Conditions.

Trans. A.I.E.E. Vol. 46 - 1927.

50. B. Adkins

The General Theory of Electrical Machines.

Book : Chapman & Hall - 1962.

51. R.H. Park

Two Reaction Theory of Synchronous Machines--I

Trans. A.I.E.E., Vol. 48 , 1929.

52. R.H. Park

Two Reaction Theory of Synchronous Machines --II

Trans. A.I.E.E. , Vol. 52, - 1933.

53. B. R. Prentice,

Fundamental Concept of Synchronous Machine

Reactances.

Trans A.I.E.E. , Vol. 86, 1937.

54. E.W. Kimbark

Power System Stability Vol. III

Book: John Wiley & Sons.

55. S.B. Crary

Power SystemStability Vol. II

Book : John Wiley & Sons.

56. J. Kettelus, E. Voipio

Network Damping and Synchronous Stability.

C.I.G.R.E. Conference Report --- 1956.

57. L.A. Stockdale

Servomechanism, Book: Pitman.

58. F.G. Helps

Data Transmission by Synchros

Electronic Engineering -- October, 1956.

59. W.S. Wood, J. Mc. Naull

A Simple Method of Recording Angular Acceleration.

The Engineer --March, 1962.

60. F. J. Sansom, H.E. Peterson, L.M. Warshawsky,

' MIMIC " -- A Digital Simulation Program.

SESCA International Memo 65-12, System Engineering Group, Wright -Patterson Airforce Base, Ohio, USA.

61. Notes From E.M.I. Laboratories.

Balanced Output Amplifiers of Highly Stable And Accurate Balance.

Electronic Engineering- Vol. 18, June 1946.

62. F. F. Offner

Balanced Amplifiers

Proc. I.E.E. , Vol. 35 , 1947.

63. D. H. Parnum

Transmission Factor of Differential Amplifier

Wireless Engineering, Vol. 27 , April, 1950

64. A, M. Andrew,

Differential Amplifier Design.

Wireless Engineering, Vol. 33, March, 1955.

65. D. W. Slaughter

Emitter Coupled Differential Amplifiers

I. R. E. Transactions on Circuit Theory, Vol CT 3, 1956.

66. R. D. Middlebrook, A. D. Taylor,

Differential Amplifier with Regulator Achieve

Stability, Low Drift.

Electronics, Vol. 34 , July, 1961.

67. P. J. Beneteu, E. Murari,

D. C. Amplifier using Transistors

Electronic Engineering, Vol 35, 1963.

68. D. R. Birt,

Self Balancing Push-Pull Circuits.

Wireless World, Vol. 66 , May-June, 1960.

69. C. Concordia.

The Differential Analyser as Aid In Power System Analysis.

CIGRE.--1950.

70. C. Adamson, A.M.S. El-Sarafi

Representation of Saliency on A.C. NetworkAnalyser.

Proc. I.E.E., Vol. 104 C , 1957.

71. A. W. Rankin

P.U. Impedances of Synchronous Machines. I & II.

Transactions A.I.E.E. , Vol. 64 , 1945

72. A.S. Aldred, G. Shackshaft

A Frequency Response Method for the Pre-determination of Synchronous Generator Stability.

Proc. I.E.E., Vol 107 C , 1960.

73. Jacovides L.J., B. Adkins,

Effect of Excitation Regulation on Synchronous Machine Stability

Proc. I.E.E , Vol. 113, 1966.

74. J. L. Dineley, E. T. Powner

Power System Governor Simulation

Proc. I.E.E., Vol. 111. 1964.

75. Rogazini

Sample Data Control, Book: McGraw Hill.

76. Thaler & Brown

Feed Back Control Systems.

Book: Mc Graw Hill.

77. F. Bussman, W. Casson

Results of Full Scale Stability Tests on the British 132 KV System.

Proc. I.E.E. , Vol. 105, 1958.

78. E. C. Scott, W. Casson, A. Chorlton , J. H. Banks

Multi-generator Transient Stability Performance under Fault Conditions.

Proc. I.E.E. , Vol 110 , 1963.

79. R. G. Harley

General Aspects of the Transient Stability,

Imperial College Power System Report No. 83.

80. R. A. Hore

Advanced Studies in Electrical Power System Design

Book, Chapman & Hall, 1966.

81. A. Ralston, S. Wilf.

Numerical Methods in Digital Computers.

Book: John Wiley , 1960

82. D.S. Brereton, D. J. Lewis, and C. C. Young.

Representation of Induction Motor Loads During Power System Stability Studies.

Trans. A.I.E.E. , Vol. 76 III, 1957.

83. P. J. Lawrence, J. M. Stephenson

Notes on Induction Motor Performance with a Variable Frequency Supply.

Proc. I.E.E. , Vol. 113 - 1966.